T

LE PAGE

1. Report No.	2. Government Accession No.	3
FHWA/TX-86/17+387-1		

4. Title and Subtitle	5. Report Date
A STRUCTURAL EVALUATION METHODOLOGY FOR PAVEMENTS BASED ON DYNAMIC DEFLECTIONS	July 1985
	6. Performing Organization Code
7. Author(s)	8. Performing Organization Report No.
Waheed Uddin, A. H. Meyer, W. Ronald Hudson, and K. H. Stokoe II	Research Report 387-1
9. Performing Organization Name and Address	10. Work Unit No.
Center for Transportation Research The University of Texas at Austin Austin, Texas 78712-1075	11. Contract or Grant No. Research Study 3-8-84-387
	13. Type of Report and Period Covered
12. Sponsoring Agency Name and Address Texas State Department of Highways and Public Transportation; Transportation Planning Division P. O. Box 5051 Austin, Texas 78763	Interim
	14. Sponsoring Agency Code

15. Supplementary Notes

Study conducted in cooperation with the U. S. Department of Transportation, Federal Highway Administration. Research Study Title: "Purchasing and Adapting a Falling Weight Deflectometer for Nondestructive Evaluation and Research on Rigid Pavement in Texas"

16. Abstract

A framework for structural evaluation of pavements based on dynamic deflections is presented. A self-iterative procedure has been developed to estimate insitu Young's moduli of pavement layers by using the approach of inverse application of layered elastic theory (ELSYM5) to obtain the best fit of a measured deflection basin. For asphalt pavements, a temperature correction procedure is presented for the asphaltic concrete moduli. Nonlinear strain-softening models are introduced and discussed to take into account nonlinear behavior of granular layers and subgrade. A self-iterative procedure has been developed to estimate nonlinear strain-softening moduli of these layers from Dynaflect deflection basins based on the concepts of equivalent linear analysis. An indication of the structural capacity of existing pavement is obtained from the remaining life analysis. Computer programs RPEDD1 (for rigid pavement) and FPEDD1 (for flexible pavements) are developed to evaluate dynamic deflection basins measured by the Falling Weight Deflectometer and Dynaflect. Guidelines are presented for applications and implementation of these computer programs, especially in rehabilitation design.

17. Key Words	18. Distribution Statement
rigid pavement, flexible pavement, dynamic deflections, deflection basin, Falling Weight Deflectometer, Dynaflect, Young's moduli	No restrictions. This document is available to the public through the National Technical Information Service, Springfield, Virginia 22161.

19. Security Classif. (of this report)	20. Security Classif. (of this page)	21. No. of Pages	22. Price
Unclassified	Unclassified	396	

Form DOT F 1700.7 (8-69)

A STRUCTURAL EVALUATION METHODOLOGY FOR PAVEMENTS BASED ON DYNAMIC DEFLECTIONS

by

Waheed Uddin
A. H. Meyer
W. Ronald Hudson
K. H. Stokoe II

Research Report Number 387-1

Purchasing and Adapting a Falling Weight Deflectometer for Nondestructive Evaluation and Research on Rigid Pavement in Texas
Research Project 3-8-84-387

conducted for

Texas State Department of Highways and Public Transportation

in cooperation with the
U. S. Department of Transportation
Federal Highway Administration

by the

Center for Transportation Research
Bureau of Engineering Research
The University of Texas at Austin

July 1985

The contents of this report reflect the views of the authors, who are responsible for the facts and the accuracy of the data presented herein. The contents do not necessarily reflect the official views or policies of the Federal Highway Administration. This report does not constitute a standard, specification, or regulation.

PREFACE

This report describes the research related to nondestructive evaluation of pavements conducted under Research Project 3-8-84-387, "Purchasing and Adapting a Falling Weight Deflectometer for Nondestructive Evaluation and Research on Rigid Pavements in Texas". This research project is being conducted at the Center for Transportation Research, The University of Texas at Austin, as part of tne Cooperative Highway Research Program sponsored by the State Department of Highways and Public Transportation and the Federal Highway Administration. A framework for structural evaluation based on dynamic deflections is presented in this report.

The authors gratefully acknowledge valuable discussions and contribution of Professor J. M. Roesset and Ko-Young Shao, a graduate student in the Department of Civil Engineering of The University of Texas at Austin. Gratitude is also expressed to Professor Thomas Sager of The University of Texas Business School for his constructive comments and critical review of statistical methods used in the research presented here. Thanks are due to Professor B. F. McCullough for his helpful suggestions and support during the course of this research. The authors are especially grateful to the staff of the Center for Transportation Research, who provided technical assistance and support. Appreciation is also extended to many students for assistance and cooperation, particularly Jeff Kessel, Soheil Nazarian, Victor Torres-Verdin, Alberto Mendoza, and Sheng-Huoo Ni. Thanks are also due to Messrs. Gerald Peck, Richard Rogers, Jerome Dalieden, Bob Mikulin, Ken Hankins, and others at the Texas SDHPT for their interest in and support of this research project.

Waheed Uddin
Alvin H. Meyer
W. Ronald Hudson
Kenneth H. Stokoe II

July 1985

LIST OF REPORTS

Report No. 387-1, "A Structural Evaluation Methodology for Pavements Based on Dynamic Deflections", by Waheed Uddin, A. H. Meyer, W. Ronald Hudson, and K. H. Stokoe II, presents the development of two computer programs, RPEDD1 and FPEDD1, for comprehensive structural evaluation of rigid and flexible pavements using dynamic deflection basin data, for use by Texas State Department of Highways and Public Transportation, July, 1985.

ABSTRACT

A framework for structural evaluation of pavements based on dynamic deflections is presented. A self-iterative procedure has been developed to estimate insitu Young's moduli of pavement layers by using the approach of inverse application of layered elastic theory (ELSYM5) to obtain the best fit of a measured deflection basin. For asphalt pavements, a temperature correction procedure is presented for the aspnaltic concrete moduli. Nonlinear strain-softening models are introduced and discussed to take into account nonlinear behavior of granular layers and subgrade. A self-iterative procedure has been developed to estimate nonlinear strain-softening moduli of these layers from Dynaflect deflection basins based on the concepts of equivalent linear analysis. An indication of the structural capacity of existing pavement is obtained from the remaining life analysis. Computer programs RPEDD1 (for rigid pavement) and FPEDD1 (for flexible pavements) are developed to evaluate dynamic deflection basins measured by the Falling Weight Deflectometer and Dynaflect. Guidelines are presented for applications and implementation of these computer programs, especially in rehabilitation design.

KEYWORDS: Rigid pavement, flexible pavement, dynamic deflections, deflection basin, Falling Weight Deflectometer, Dynaflect, material characterization, structural evaluation, Young's moduli.

SUMMARY

Nondestructive structural evaluation of pavements is important in selecting rehabilitation and reconstruction strategies in the project level pavement management process. The development of mechanistic overlay design procedures has resulted in research efforts for obtaining insitu material properties and evaluating structural capacity by analyzing NDT deflection data. This study was devoted to the mechanistic evaluation of dynamic deflection basins measured by a Dynaflect and a Falling Weight Deflectometer. Computer programs RPEDD1 (a rigid pavement structural evaluation system based on dynamic deflections) and FPEDD1 (a flexible pavement structural evaluation system based on dynamic deflections) have been developed in this study.

A review of published NDT evaluation procedures and existing practice of nonlinear characterization of granular materials and subgrade is also presented and their limitations are discussed. The analysis models developed in this study for use in RPEDD1 and FPEDD1 computer programs are summarized in the following.

(1) A self-iterative procedure to determine insitu moduli of pavement layers by matching theoretical and measured deflection basins through an inverse application of layered elastic theory. The pavement is assumed to behave as a layered linearly elastic system.

(2) A procedure for correcting the temperature sensitive asphaltic concrete (AC) modulus for flexible pavements by correcting the estimated AC modulus to the condition of the specified design temperature.

(3) A self-iterative procedure of equivalent linear analysis to obtain nonlinear strain dependent moduli for granular layers and subgrade if a Dynaflect deflection basin is being analyzed. This step is omitted for FWD deflection basin.

(4) Fatigue life prediction and subsequently remaining life analysis (if past traffic data is known) using appropriate fatigue equations.

Finally, guidelines are presented for plotting the results for visual evaluation, selection of design sections, and calculation of design moduli overlay design. Recommendations are also presented for future research related to field validation, developing generalized curves for nonlinear strain-sensitive models for unbound materials and subgrade.

IMPLEMENTATION STATEMENT

A structural evaluation system for pavements has been developed for the Texas State Department of Highways and Public Transportation (SDHPT). The system is comprised of self-iterative computer programs to evaluate dynamic deflection basin measured by such NDT devices as the Dynaflect and falling weight deflectometer. The computer programs RPEDD1 (for rigid pavements) and FPEDD1 (for flexible pavements) should be immediately implemented by SDHPT, as they will result in substantial savings in time and computational cost which is normally incurred using the existing evaluation procedures.

Guidelines presented in this study for application and implementation of the computer programs (especially regarding selection of design section and evaluation of insitu nonlinear design moduli for overlay design) should also be exposed to trial applications. When implemented, the framework of the structural evaluation system recommended in this study is envisioned to become an indispensable part of the overlay design systems used in Texas such as RPOD and RPRDS.

TABLE OF CONTENTS

CHAPTER 3. INTERPRETATION OF DEFLECTION DATA

CHAPTER 4. INSITU MATERIAL CHARACTERIZATION BASED ON DYNAMIC DEFLECTION DATA

CHAPTER 1. INTRODUCTION

BACKGROUND

Large sums of highway funds are currently devoted to maintenance, rehabilitation, and reconstruction of the nation's highway and road networks. Nondestructive structural evaluation of pavements is an important part of the pavement management process at the project level. Measuring surface deflection, which is essentially an elastic deformation of a pavement under a test load, has been generally preferred for the nondestructive evaluation of pavements. The deflection data are then analyzed to determine the structural adequacy of the pavement. Similarly, many overlay design procedures are based on empirical relationships which use a deflection parameter or employ mechanistic analysis involving calculation of insitu Young's moduli from deflection data. The ever growing demand for faster, easier to use, and mobile nondestructive testing (NDT) devices for pavement evaluation has resulted in the development of dynamic devices such as the Dynaflect, in 1960's (Ref 1), on commercial scale to replace the conventional time-consuming Benkelman Beam procedure. Because pavement materials do not exhibit ideal linear elastic behavior and pavement response is affected by the applied stress level, and rate and mode of loading, several other types of NDT devices such as the Road Rater (Ref 2) and the Falling Weight Deflectometer (Ref 3) have been developed. The empirical methods of structural evaluation are generally based on limiting deflection criterion, such as the Asphaltic Institute's procedure (Ref 4), which has been developed over several years by correlating pavement performance with Benkelman Beam rebound deflections. The development of commercially available dynamic NDT devices and increased research efforts towards applying a more rational and mechanistic approach for structural evaluation of pavement have resulted in (1) the measurement of deflection basins by recording more than one deflection measurement during the application of a test load and (2) the application of multilayered linear elastic theory for analyzing the measured

deflection basins to estimate insitu materials characterization of pavement layers and for subsequent overlay design by predicting critical strains and stresses in the pavement.

In a layered linear elastic model of a pavement (Fig 1.1), each layer can be characterized by its Young's modulus of elasticity (E) and Poisson's ratio. Reasonable values for Poisson's ratio can be assumed as it generally falls in a very narrow range for a specific material type. Also the pavement response is not sensitive to small variations in Poisson's's ratios. If the thickness information for each layer and its E-value are known, then, and a semi-infinite subgrade is assumed, a unique pavement response (surface deflections, stresses or strains) can be theoretically predicted. This is the basis of pavement design by the layered theory approach. However structural evaluation of a pavement starting from an NDT based dynamic deflection basin is a complex problem because of

(1) the non uniqueness of Young's moduli back-calculated from measured deflection basin, thickness, and Poisson's ratio information by applying layered elastic theory;
(2) errors and the time involved in the iterative process;
(3) error involved in assuming a semi infinite subgrade;
(4) errors due to possible variations in thickness of pavement layers;
(5) errors in back-calculated moduli due to the nonlinear behavior of granular layers and subgrade and if the magnitude of the test load is much smaller than the design equivalent single axle load;
(6) temperature effects on the modulus of the asphalt concrete surface layer for flexible pavements.

The Texas State Department of Highways and Public Transportation (SDHPT) presently uses a Dynaflect for nondestructive structural evaluation of pavements. However, a Falling Weight Deflectometer (FWD) has been acquired in this research study. It is another useful NDT device capable of applying heavier loads. This report describes the development of a system

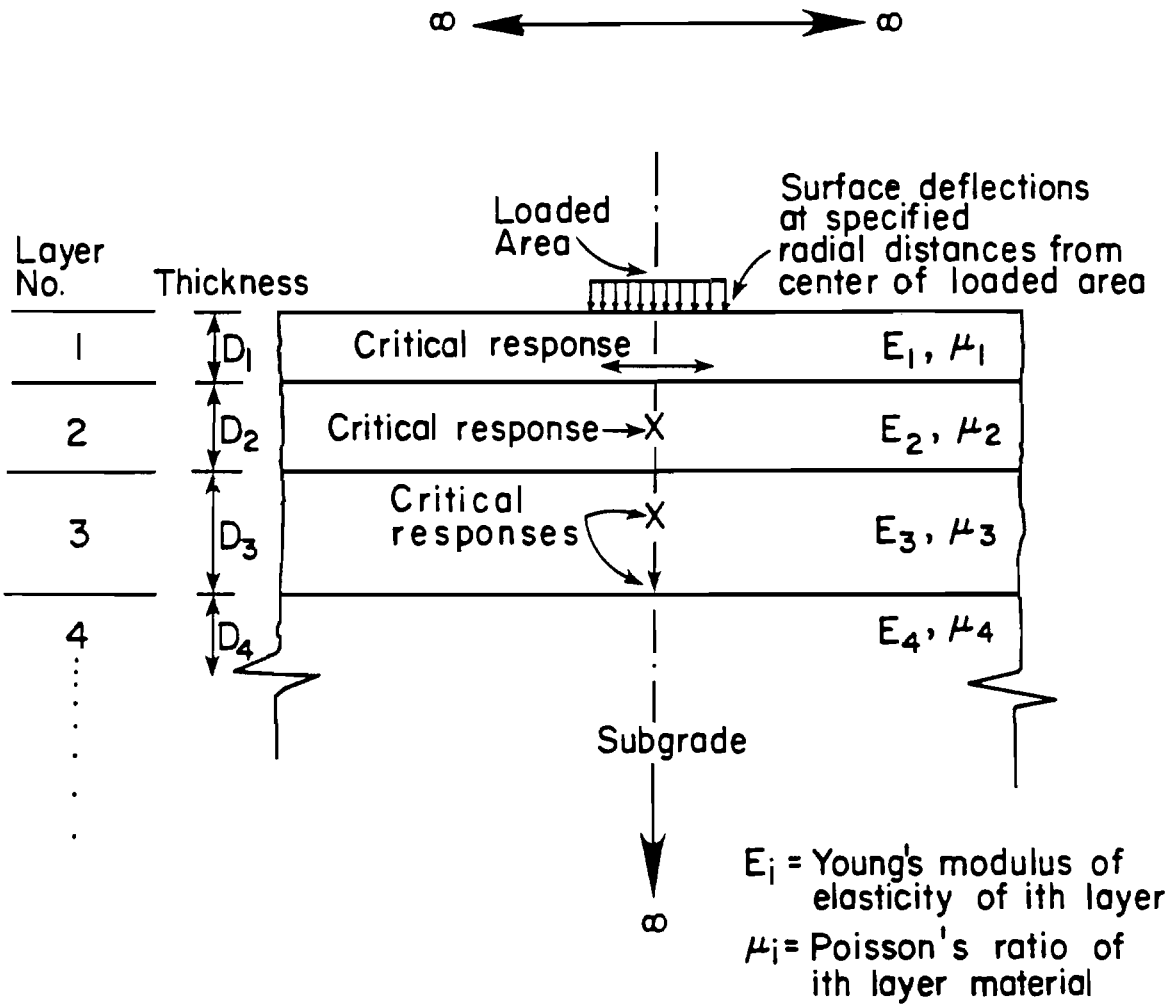

Fig 1.1. An idealized multilayer linearly eleastic pavement.

for the structural evaluation of flexible and rigid pavements based on dynamic deflection data obtained from the Dynaflect or FWD.

OBJECTIVES

The principal goal of this study is to develop computer based structural evaluation systems for pavements by analyzing NDT data for dynamic deflection basins. The following tasks constitute the objectives of this study.

(1) Review of existing practices for (a) interpretation of surface deflection data from NDT devices for the structural evaluation of pavements and (b) using dynamic deflection basins from the Dynaflect and Falling Weight Deflectometer for insitu material characterization of pavement layers.

(2) Development of self iterative computer models to determine Young's moduli of pavement layers from dynamic deflection basins based on

   (a) consideration of NDT data from the Dynaflect or Falling Weight Deflectometer and layered theory modelling of pavement;
   (b) investigations into input parameters that influence deflection basins;
   (c) consideration of a rigid bottom (rock layer) under a finite thickness of subgrade soil;
   (d) criteria for tolerances in deflections and moduli changes for accuracy and efficiency and the logic for convergence process;
   (e) routines for default values of some important input parameters; and
   (f) formulation of a methodology to ensure the uniqueness of estimated insitu moduli.

(3) Correction of insitu moduli for non linear behavior of granular layers and subgrade considering these factors:

   (a) a conventional approach to stress sensitivity and its limitations,

(b) the influence of shear strain amplitude on elastic moduli, and
(c) the concept of equivalent linear analysis for correction of insitu moduli of granular layers and the subgrade.

(4) Analysis of remaining life based on estimated insitu moduli of pavement layers.
(5) Development of separate computer programs for structural evaluation of rigid and flexible pavements, and example applications.
(6) Development of guidelines for implementation in existing overlay design systems.

SCOPE

The final products of research presented in this report on the development of a structural evaluation methodology for pavements based on dynamic deflections are two computer programs: RPEDD1 (for rigid pavements) and FPEDD1 (for flexible pavements). This report includes

(1) A discussion of dynamic deflection data measured by Dynaflect and FWD (Chapter 2);
(2) A review of current practices for the interpretation deflection data (Chapter 3);
(3) Development of a self iterative model to estimate insitu Young's moduli of pavement layers from dynamic deflection basins (presented in Chapter 4);
(4) Development of correction procedures for non linear behavior of granular layers and subgrade (Chapter 5);
(5) Development of a computerized structural evaluation system including remaining life analysis based on corrected insitu pavement moduli, guidelines to identify sections for consideration of overlays, selection of design sections, and recommendations on design modulus values (Chapter 6) enabling the user to obtain profiles of remaining life and the modulus of each pavement layer along the length of pavement;

(6) A description of RPEDD1 (Chapter 7); and

(7) A description of FPEDD1 (Chapter 8).

Finally Chapter 9 presents the summary, conclusions, and recommendations related to implementation and future work.

CHAPTER 2. DYNAMIC DEFLECTION DATA FROM NDT DEVICES

DYNAMIC DEFLECTION MEASUREMENT

Dynamic deflections are measured on the surface as the responses of a pavement under dynamic test loads. Dynamic force generators in Nondestructive testing (NDT) devices fall into two categories: (1) devices which generate steady state sinusoidal forces and (2) devices which produce transient impulse forces. In the first category, dynamic deflection is measured as peak-to-peak amplitude of the deflection signal. In the second case, the peak amplitude of a deflection signal is measured as dynamic deflection. References 5 and 6 present an excellent overview of several commercial and research NDT devices which generate dynamic deflection data. In this study only the Dynaflect and the Falling Weight Deflectometer (FWD) are considered for NDT evaluation of pavements.

DESCRIPTION AND OPERATING CHARACTERISTICS

A review of the description and operating characteristics of the Dynaflect and the Falling Weight Deflectometer is presented in the following sections.

Dynaflect

The Dynaflect, a light load NDT device, is described in this section.

Loading and Deflection Measuring System. A detailed description of the loading configuration and the deflection measuring system is given in Refs 1 and 7 and illustrated in Fig 2.1. The Dynaflect is a small two-wheel trailer which contains a dynamic force generator and deflection measuring system. The Dynaflect is towed by a light vehicle and travels on two pneumatic tired wheels at normal highway speed to and between test sections. The dynamic force is transmitted to the pavement by lowering two 4-inch-wide (16-inch-

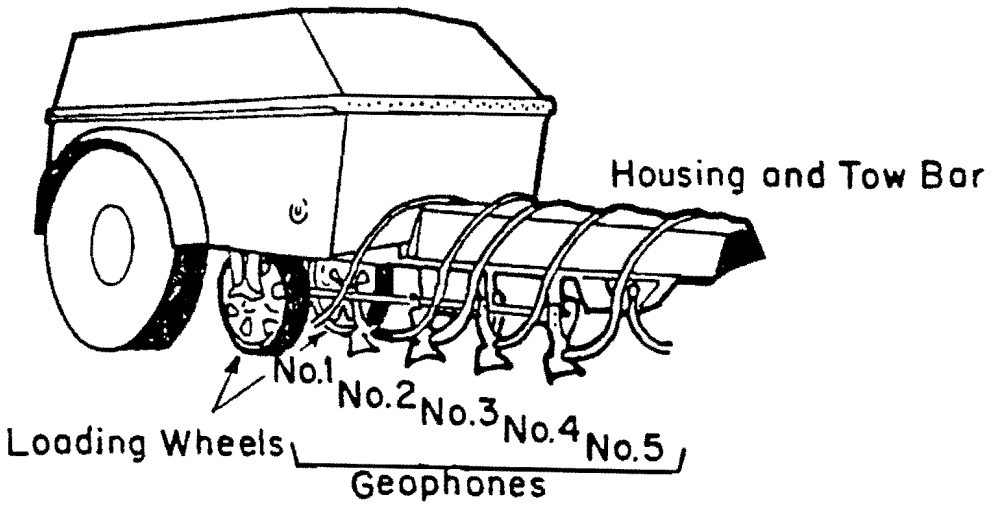

(a) The Dynaflect system in operating position.

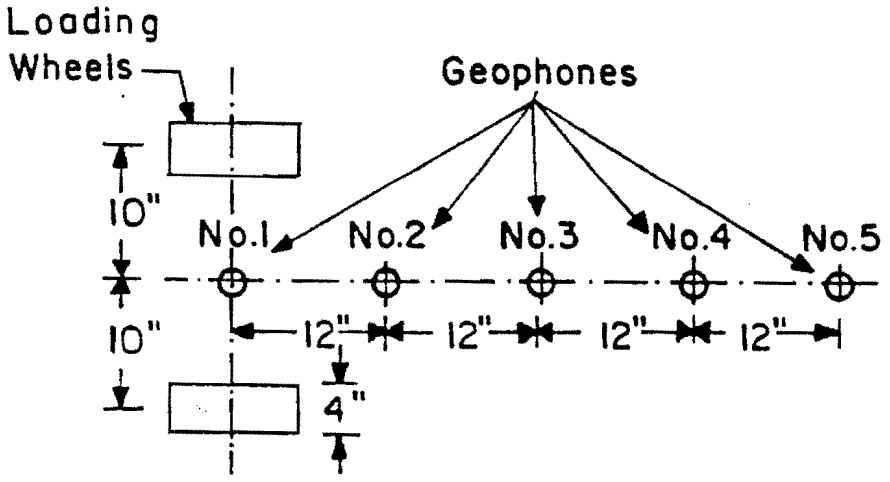

(b) Configuration of load wheels and geophones.

Fig 2.1. Configuration of Dynaflect load wheels and geophones in operating position (Ref 7).

outside-diameter) rubber-coated steel wheels. The operations control unit and a meter unit calibrated to read deflection are carried in the towing vehicle and the driver of the towing vehicle can also operate the Dynaflect. The operations control unit is hooked up to the power source of the towing vehicle.

The dynamic force generator employs two counter-rotating eccentric masses to generate steady state vibrations that are a sinusoidal function of time. The Dynaflect is operated at a fixed frequency of 8 Hz, which results in a 1,000-pound peak-to-peak magnitude of the vibratory force (Fig 2.2). Bush (Ref 6) reports results of a comparative study on four nondestructive vibratory devices. The findings related to the Dynaflect are that (1) the measured frequency was within 3 percent of the indicated frequency, 8 Hz, and (2) the peak-to-peak dynamic force of the Dynaflect was 4 percent below the measured force on rigid pavements. These findings show that the frequency and amplitude of the sinusoidal loading force of the Dynaflect are reasonably reliable. The loaded area under each steel tired wheel can reasonably be assumed as 3 sq. in. The force transmitted through each loading wheel is 500 pounds. In order to analyze the dynamic deflection basin, the loaded area is assumed to be circular.

Five equally spaced geophones are used to measure the dynamic deflection response of the pavement. Figure 2.1 shows the arrangements of the geophones. The geophones are velocity transducers which employ an inertial reference and give an output signal in volts. The peak-to-peak dynamic deflection is proportional to the output voltage of the geophone. Prior to testing, each geophone is calibrated at the driving frequency of 8 Hz so that, during the test, deflection can be recorded directly from the readout meter. Additional information about the characteristics of geophones can be found in Ref 5. The arrangement of five geophones for the Dynaflect provides half of a so-called deflection basin if the measured deflections under all sensors are plotted and joined by drawing a smooth curve. The Texas Transportation Institute (TTI) (Ref 8) investigated the effect of assuming peak-to-peak force to be a static load by measuring deflection basins while operating the Dynaflect at frequencies varying between 4 and 12 Hz at the same amplitude of dynamic force. The results showed that the vertical

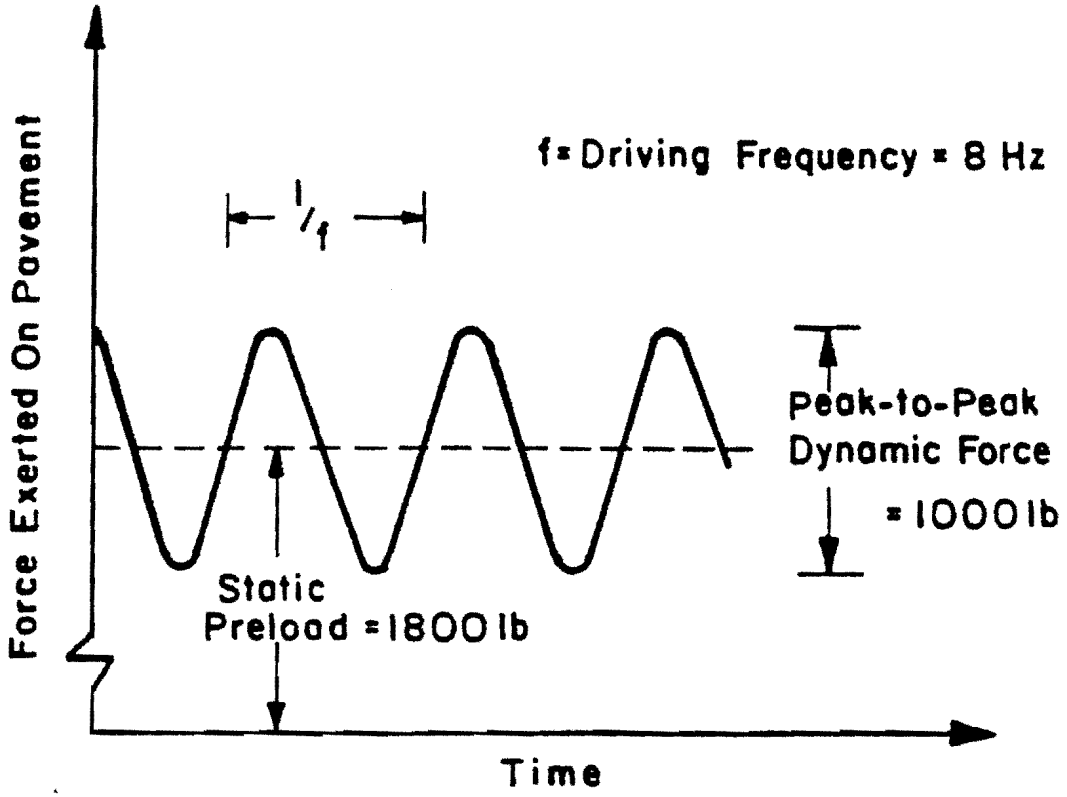

Fig 2.2. Typical dynamic force output signal of Dynaflect.

deflections measured at the surface are independent of the frequency in the range of 6 to 10 Hz. The Dynaflect deflections measured at the same location on two consecutive days have been found to repeat within close limits (Ref 1).

Test Procedure. The calibration of all five geophones is carried out every day prior to taking the Dynaflect to the test location. Geophones are placed in the calibrator unit, which provides a repetitive vertical motion of 0.005 inch at an operating frequency of 8 Hz. The calibrator unit is connected to the control unit. The sensor selector switch in the control unit is then switched to the position corresponding to geophone no. 1 and the respective sensitivity control is adjusted to obtain the correct deflection reading. The calibration procedure is repeated for each of the other geophones. The calibrator is disconnected from the control unit after all geophones are calibrated. The geophones are then refixed on their bases and connected to the draw-bar of the Dynaflect. The draw-bar is raised and the towing vehicle tows the Dynaflect on its pneumatic tired wheels to the marked test location. The sequence of operations for routine digital Dynaflect measurements is as follows (Ref 7).

(1) The Dynaflect is positioned so that geophone no. 1 (midway between the two solid steel wheels) rests over the marked location.
(2) The Dynaflect trailer is raised onto its solid wheels.
(3) The dynamic force generator is switched on and the frequency is adjusted to 8 Hz.
(4) The geophone bar is lowered to the surface of the pavement.
(5) The voltage output of each geophone is read on the digital readout meter directly in milli-inches of vertical deflection at the pavement surface and recorded by the operator. (The procedure for the analog type unit will be slightly different).
(6) The geophone bar is raised and the dynamic force generator is switched off and the Dynaflect is towed on its solid wheels to the next location in the same test section.

Falling Weight Deflectometer

General principles of Falling Weight Deflectometer testing are presented in this section.

Loading and Deflection Measuring System. Basically a FWD applies an impulse load by dropping a known mass from a predetermined height as illustrated in Fig 2.3. The mass falls on a foot plate connected to a rigid base plate by rubber buffers which act as springs. The properly designed mass configuration and springs are very important to achieve the desired peak stress, shape, and duration of the FWD force signal. The force can theoretically be calculated using the following relationship:

$$P = (2 \cdot g \cdot h \cdot m \cdot k)^{\frac{1}{2}} \qquad (2.1)$$

where

P = peak force, pounds-force
g = acceleration due to gravity, feet/second^2
h = height of drop of the mass, feet
m = mass of FWD, pounds and
k = spring constant.

However, in routine FWD testing, peak force is measured by a load cell. The Danish version of the FWD has been studied in detail by comparing the results with a moving wheel load, as described by Bohn et al (Ref 3). The Swedish version of FWD employs a two-mass system and reportedly (Ref 9) gives a smoother shape to the force signal. Tholen et al (Ref 10) describe good agreement of FWD and moving wheel load deflections. Typical FWD dynamic deflection signals (as reported in Ref 3) are illustrated in Fig 2.4(a). The same figure also shows measured deflection signals under a moving wheel load, indicating that the FWD test response resembles a moving wheel load response. The duration of the FWD deflection signal is around 25 m-seconds, somewhat smaller than the duration of the deflection signal under a moving wheel load. The comparisons of stresses and strains as reported by Bohn et al (Ref 3) are

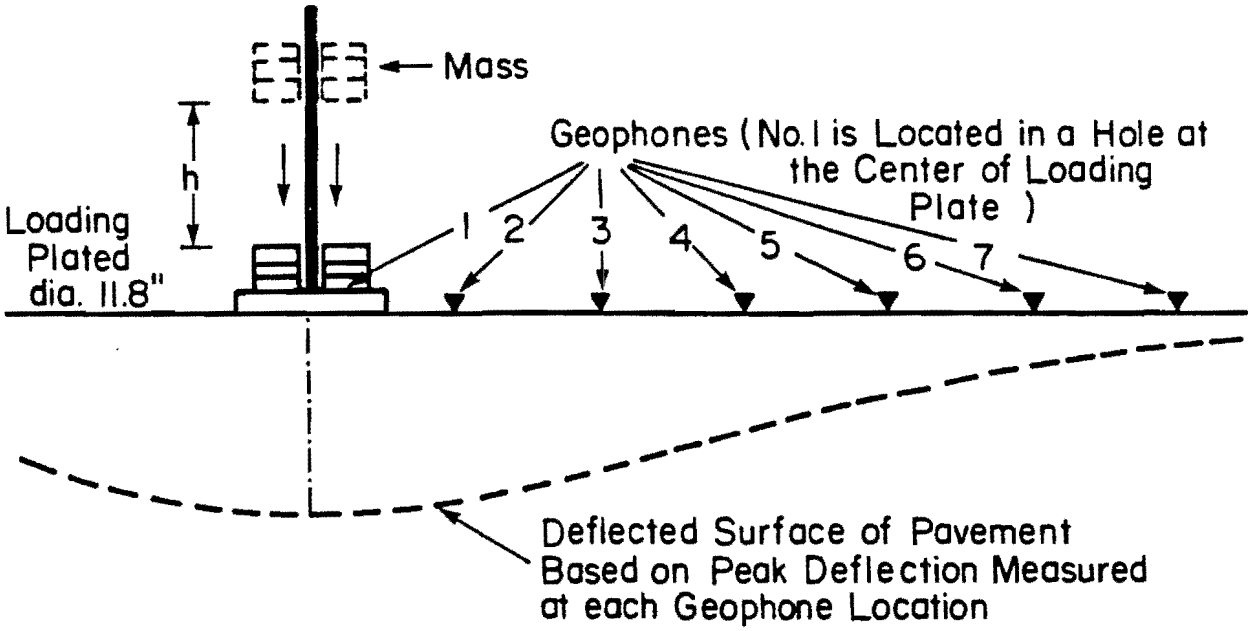

(a) FWD in operating position

(b) Load-time history of FWD on pavement surface

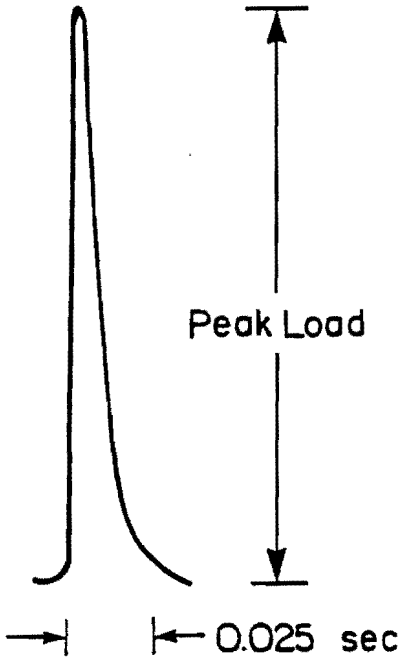

Fig 2.3. Principle of a Falling Weight Deflectometer, FWD test.

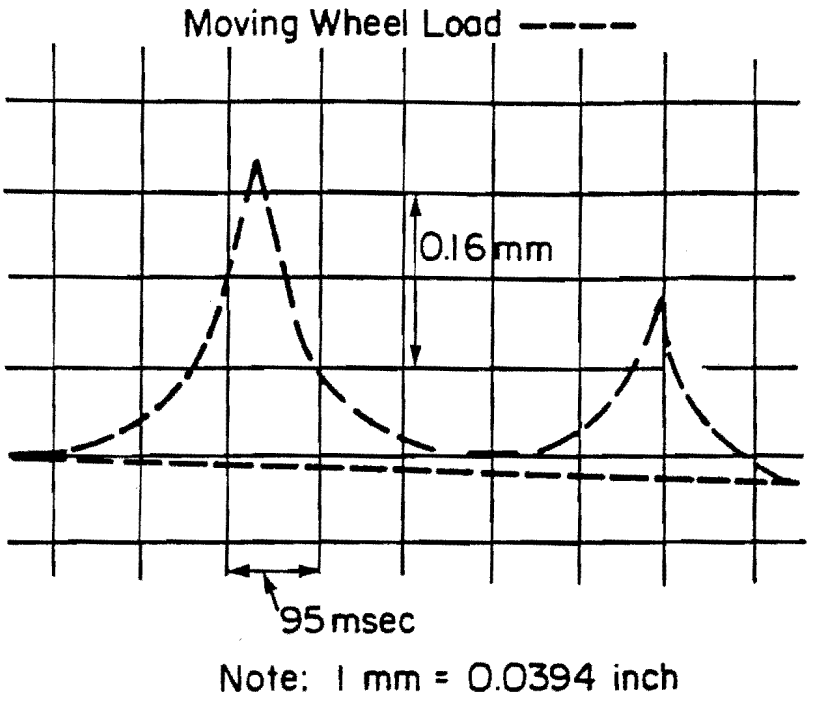

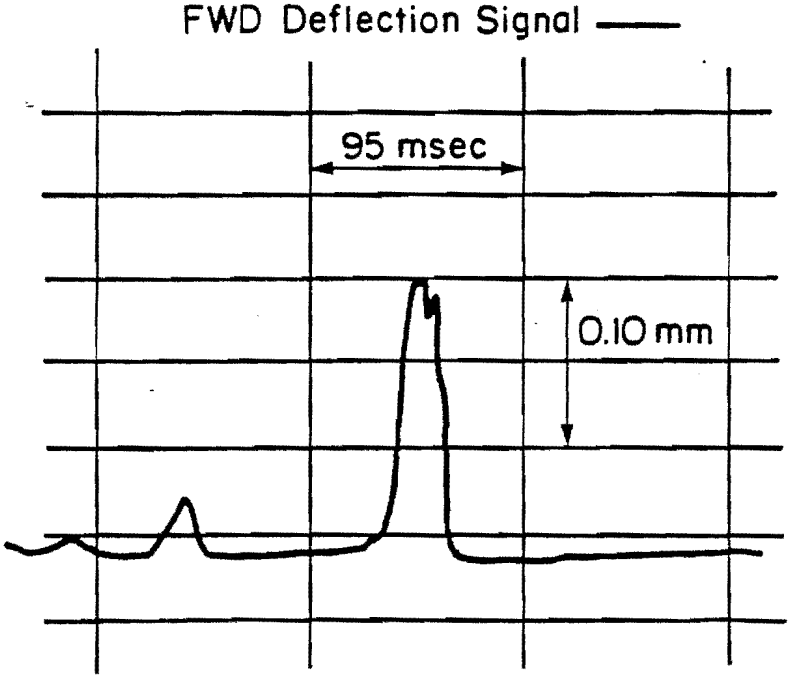

Fig 2.4(a). Typical deflection-time history records (Ref 3).

illustrated in Fig 2.4(b). The capability of the FWD to apply a variable load both in the low load and overload ranges may be a useful feature for structural evaluation of pavements. In the last couple of years, many agencies in the U. S. have acquired FWD units and have used them for structural evaluation and insitu material characterization of pavements and also for load transfer and void detection studies on rigid pavements (Ref 11). A comparative field study was made in Texas with the FWD and the Dynaflect for rigid and flexible pavements (Ref 12); dynamic deflections of the FWD were measured by geophones. A comparative study of the FWD with the Road Rater has been reported in Illinois (Ref 13). Bush (Ref 6) describes laboratory checks on the accuracy of force signals and geophone outputs and field comparisons of FWD and other NDT devices, which are summarized in Table 2.1.

The Danish version of the FWD is currently marketed in the U. S. by Dynatest as the Model 8000 Dynatest Falling Weight Deflectometer (Ref 14). The Swedish version of the FWD is being marketed as the KUAB Falling Weight Deflectometer by S.E.I. (Ref 15). The Texas State Department of Highways and Public Transportation has acquired one unit of the model 8000 Dynatest Falling Weight Deflectometer (referred to as FWD in this report). Figure 2.5 illustrates the FWD in operating position. The configurations of load and deflection measuring sensors to be used in this study are described in the following section.

Model 8000 Falling Weight Deflectometer

Description and Operating Characteristics. The material presented here is based on the information provided in Ref 14. The FWD is a trailer mounted device which can be towed by any standard passenger car or van at highway speed. The total weight of the impulse generating device and the trailer does not exceed 2,000 pounds. The transient pulse generating device is the trailer mounted frame capable of directing different sets of mass configurations to fall from a preset height, perpendicular to the surface. This gives the capability to produce a wide range of peak force amplitudes, as indicated by Eq 2.1, where peak force can be changed by varying mass

--- Moving Wheel Load, 5 tons (10,000 lb) at 38.3 km/h (23.8 mph)

—— Falling Weight Deflectometer (150 kg mass at a drop height of 40 cm)

1 cm = 0.394 in.

1 kg = 2.20 lb

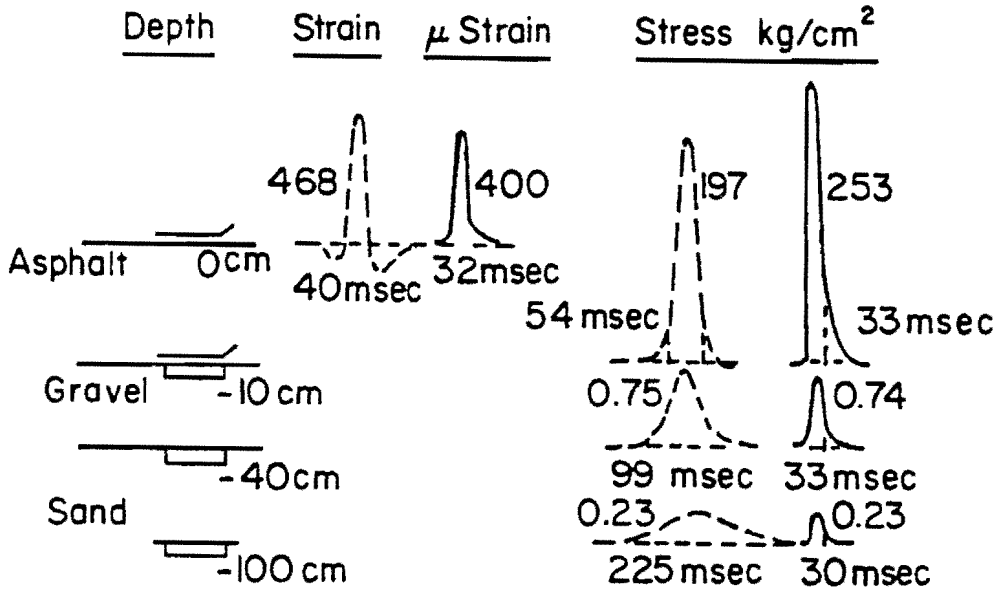

Fig 2.4(b). Typical records of stress-time history and strain-time history at different depths in a pavement (Ref 3).

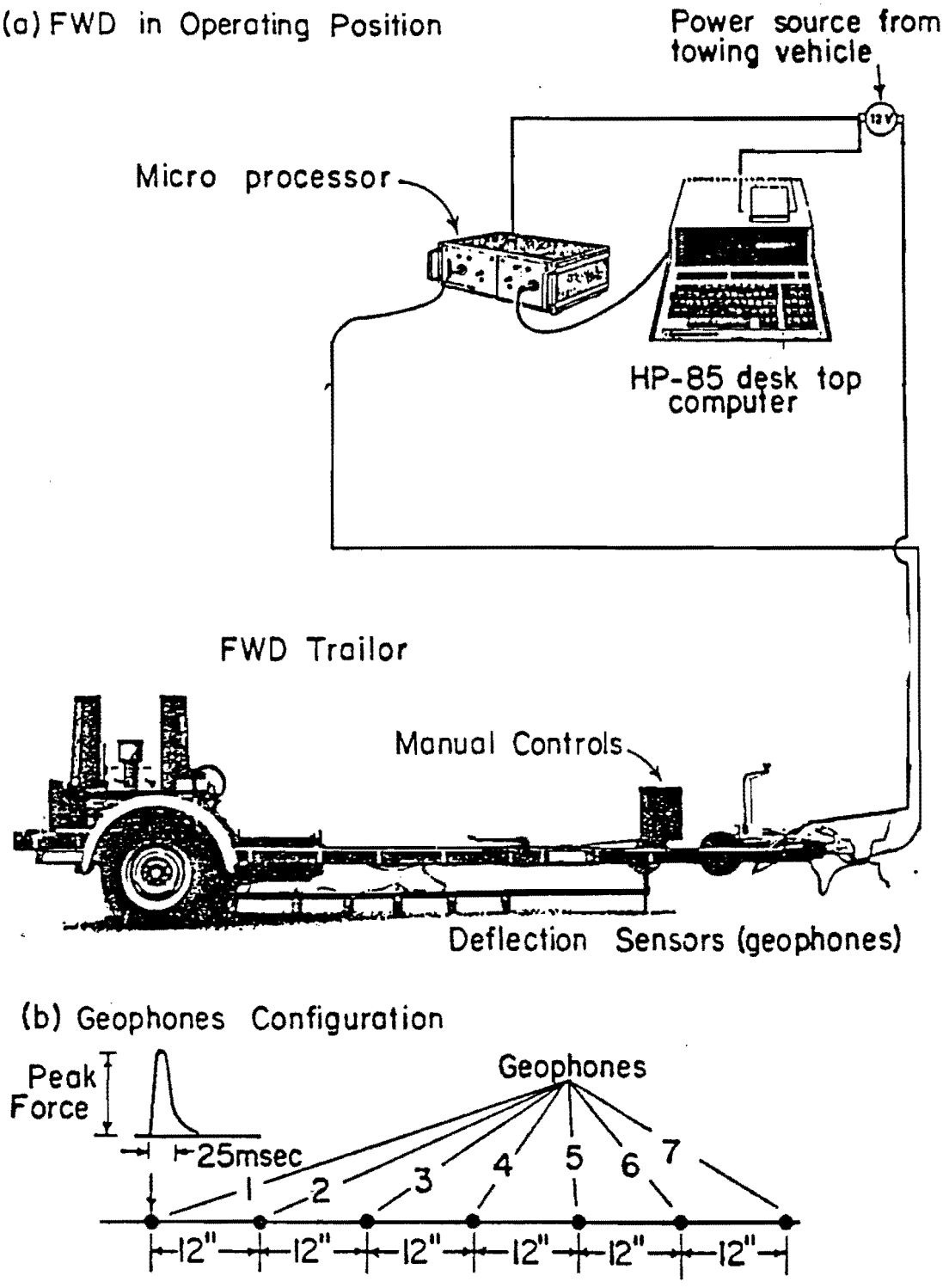

Fig 2.5. Illustration of Model 2000 FWD.

TABLE 2.1. SUMMARY OF ACCURACY CHECKS ON MEASUREMENTS OF DYNAMIC FORCE AND DEFLECTION SIGNALS

Accuracy Check of Deflection Signal from Velocity Transducers	
Device	Percent Error at Operating Frequency
Dynaflect	5.5
FWD	5.1

Accuracy Check of Amplitude of Dynamic Force Signal	
Device	Percent Error
Dynaflect	
Rigid Pavements	- 4.2
Flexible Pavements	-12.9
FWD	- 5.4

and/or height. (In the older models, a fixed mass was used, as described in Refs 3, 12, and 13.) The assembly consists of the mass, the frame, loading plates, and a rubber buffer, which acts as a spring. The operation of lifting and dropping the mass on the loading plate is based on an electro-hydraulic system.

The falling weight/buffer subassembly is furnished so that four different configurations of mass can be employed. All four mass configurations produce a transient reproducible load pulse of approximately a half-sine wave and 25 to 30 m-seconds in duration. The drop weights are constructed so that the falling weight/buffer subassembly can be quickly and conveniently changed between falling masses. The buffers are constructed so as to clearly indicate which drop weight configuration they accompany. Each of these falling weight/buffer combinations is so constructed as to be capable of releasing the weight from a variable height, such that different peak loads for the four specified masses are producible in the following ranges:

Falling Weight	Peak Loading Force
110 lb	1,500 - 4,000 lbf
220 lb	3,000 - 8,000 lbf
440 lb	5,500 - 16,000 lbf
660 lb	8,000 - 24,000 lbf

For routine testing, a loading plate 11.8 inches (300 mm) in diameter is used. The mass guide shaft is perpendicular to the road surface in the measuring mode as well as the transport mode. The system includes a load cell capable of accurately measuring the force that is applied perpendicular to the loading plate. The force is expressed in terms of pressure. The load cell can be removed for calibration.

The system provides at least seven separate deflection measurements per test. One of the deflection sensing transducers (geophones) measures the deflection of the pavement surface through the center of the loading plate, while the six remaining transducers can be positioned along the raise/lower

bar, up to 7 feet from the center of the loading plate. All deflection sensing transducer holders are spring loaded, insuring good contact between the transducers and the surface being tested. An extension geophone bar is provided to measure deflection on the other side of the load plate. This facilitates load transfer studies on jointed rigid pavements. The unit is capable of testing in the long distance towing position by simply lowering the loading plate/mass/seismic detector bar subassembly to the pavement surface with controls located within the towing vehicle. The trailer is also equipped with a hand pump so that the loading plate/mass/seismic detector bar subassembly can be raised for removal of the equipment from the roadway in an emergency, for example, if the electro-hydraulic system fails. The electronic registration equipment is operated by a nominal 12 volt DC power supply taken from the towing vehicle. The system includes a Hewlett-Packard Model 85 Computer, which features a cassette tape recording/playback, CRT display and a thermal printer for recording data from field testing and keyed-in site identification information. All operations of testing are done from the key board of the computer.

Test Procedure. The routine test procedure is briefly described here.

(1) The FWD trailer is towed on its rubber tires to the test location. The trailer is positioned on the pavement such that the marked test location is directly below the center of the loading plate.
(2) Necessary connections are made to hook up to the battery. The processing equipment and HP-85 computer which are carried in the towing vehicle are turned on.
(3) The mass configuration is selected using the guide lines given in the earlier section and secured in place.
(4) A test sequence is identified and programmed from the HP-85 keyboard (site identification, height and number of drops per test point, etc.). When the operator enters a "run" command, the FWD loading plate/buffer/geophone bar assembly is lowered to the pavement surface. The weight is dropped (e.g., 3 times) from the

pre-programmed height and the plate and bar assembly are raised again.

(5) A beep signal indicates that driving to the next test location is allowed. The test sequence described in Step 4 lasts approximately one minute.

(6) The measured set of deflection data (peak values of geophone responses) are displayed on the HP-85 CRT screen for direct visual inspection.

(7) If the operator does not enter a "skip" command within a pre-programmed time, the deflection data is stored on the HP-85 magnetic tape cassette together with the peak force magnitude and site identification information. The data are also printed using the thermal printer.

GRAPHICAL PRESENTATION OF DYNAMIC DEFLECTION DATA

Dynaflect Deflection Basin

Peak-to-peak dynamic deflections measured by the array of five geophones in a Dynaflect test generally represent half of the deflection basin as illustrated in Fig 2.6 (Refs 7, 16, and 17). The other half of the basin is a mirror image of the measured half. As discussed in a later section, deflection basins are characterized by various parameters which are functions of the deflection values of one or more geophones. For this purpose and for comparing dynamic deflection data of the Dynaflect with the dynamic deflection data of other NDT devices, deflection basins have been plotted as shown in Fig 2.6 (for example Ref 12). However when the Dynaflect loading is modelled in a layered theory analysis such as used for Chevron's or the ELSYM5 programs (Refs 7, 16, and 18), the theoretical deflection responses are computed at the five geophone locations by specifying their radial distances from the center of one loading wheel. The radial distances are 10.0, 15.6, 26.0, 37.4 and 49.0 inches respectively, with the first sensor at 10.0 inches, as illustrated in Fig 2.7. This rational approach to plotting the Dynaflect deflection basin (Fig 2.7) provides better interpretation of

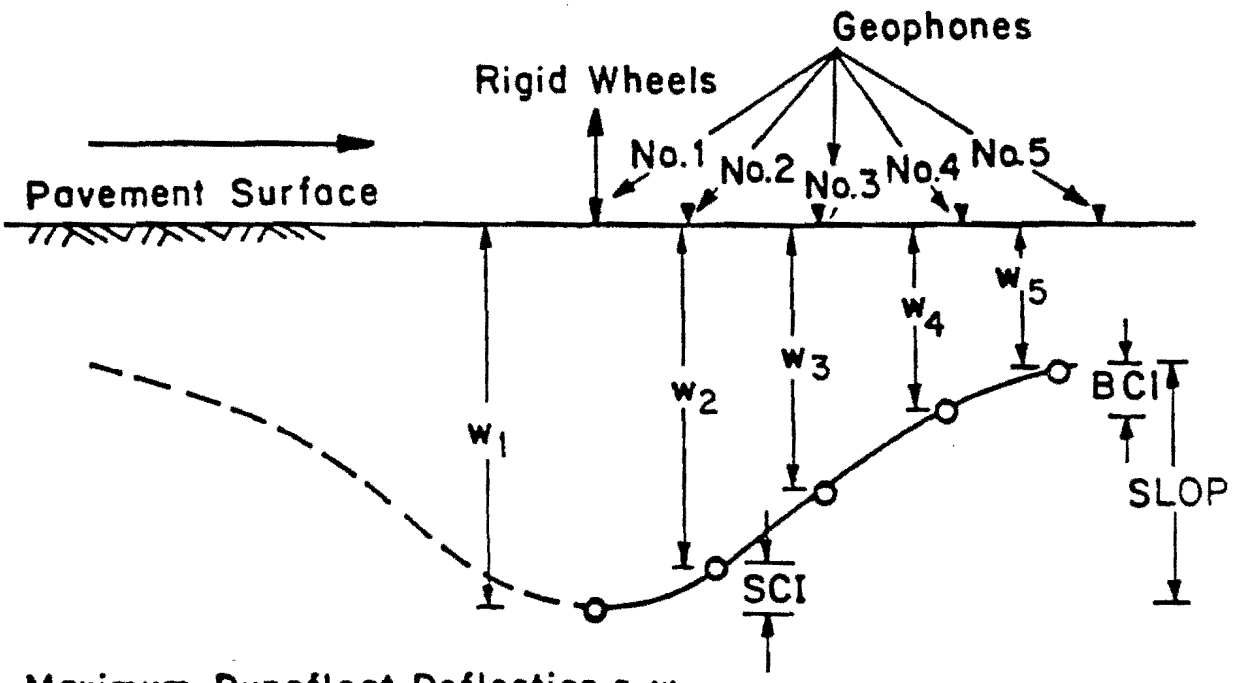

Maximum Dynaflect Deflection = w_1

Surface Curvature Index, SCI = $w_1 - w_2$

Base Curvature Index, BCI = $w_4 - w_5$

Spreadibility, % = $100(w_1+w_2+w_3+w_4+w_5)/(5w_1)$

Basin Slope, SLOP = $w_1 - w_5$

Fig 2.6. Typical Dynaflect deflection basin.

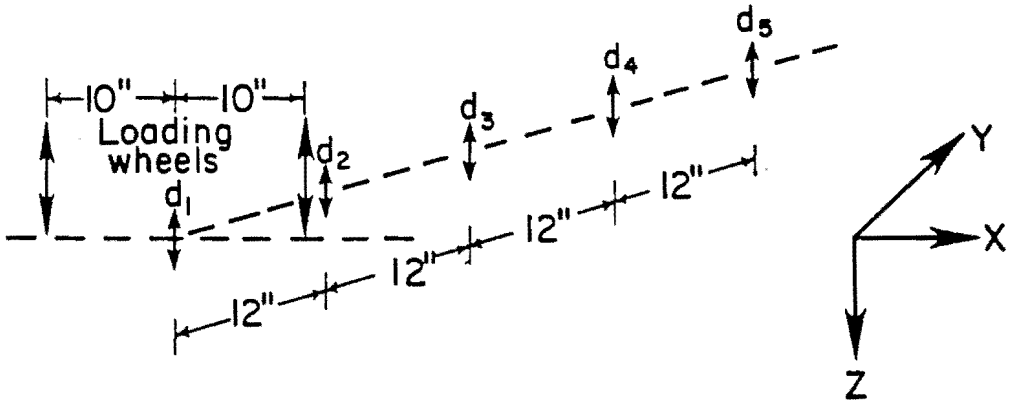

Configuration of Dynaflect loading and deflection measurements (d_1, d_2, d_3, d_4, d_5 are peak to peak deflections at radial distance of 10.0, 15.6 26.0, 37.4, 49.0 inches from each loading wheel)

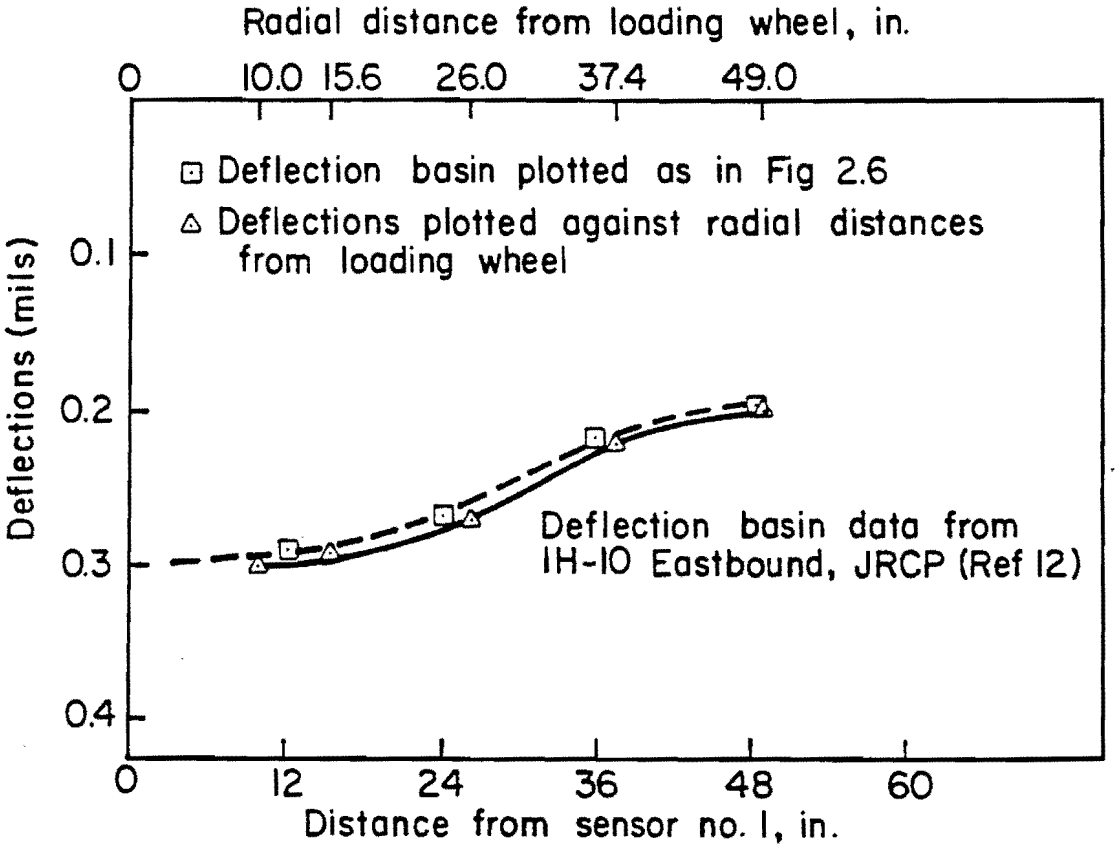

Fig 2.7. Graphical illustration of Dynaflect deflection basin adopted in this study.

the deflection basin and is used in this study. The plotting of the Dynaflect deflection basin in this way is especially useful in making comparisons with an FWD deflection basin.

A commonly used basin parameter for structural evaluation is deflection measured at geophone no. 1, also termed as Dynaflect maximum deflection, DMD (Ref 17). This could be misleading as for some pavement the maximum Dynaflect deflection may not be midway between the loading wheels (location of geophone no. 1). This observation is illustrated in Fig 2.8 by plotting the theoretical Dynaflect deflection basins computed using the layered theory program, ELSYM5. For the stiff rigid pavement case (deflections shown by circles), maximum deflection occurs at the geophone no. 1 location, i.e., midway between the two loading wheels. This happens because a stiff pavement spreads the load over a large area and the use of the principle of superposition results in the largest deflection midway, due to the additive effect of deflections produced by loads on the two loading wheels. On the other hand, for a weaker flexible pavement (deflections shown by triangles) maximum deflection occurs at the center of the loading wheel. However, for other NDT devices, such as the FWD, a deflection basin plotted with the relative positions of the sensors from sensor no. 1 coincides with the deflection basin plotted using radial distances from the center of the loading plate. In that case the maximum deflection basin will occur at sensor no. 1, which is in the center of the loading plate. Therefore in this study, Dynaflect deflection basins are plotted using the radial distance of the sensors from the center of the loaded area as the abscissa.

FWD Deflection Basin

Figure 2.9 illustrates a FWD deflection basin computed for a rigid pavement using the FWD configuration shown in Fig 2.5. The radial distances of seven sensors are on the abscissa and the ordinates are in terms of normalized deflections. FWD deflections are normalized with respect to the 1,000-lbs peak force, as given by following expression:

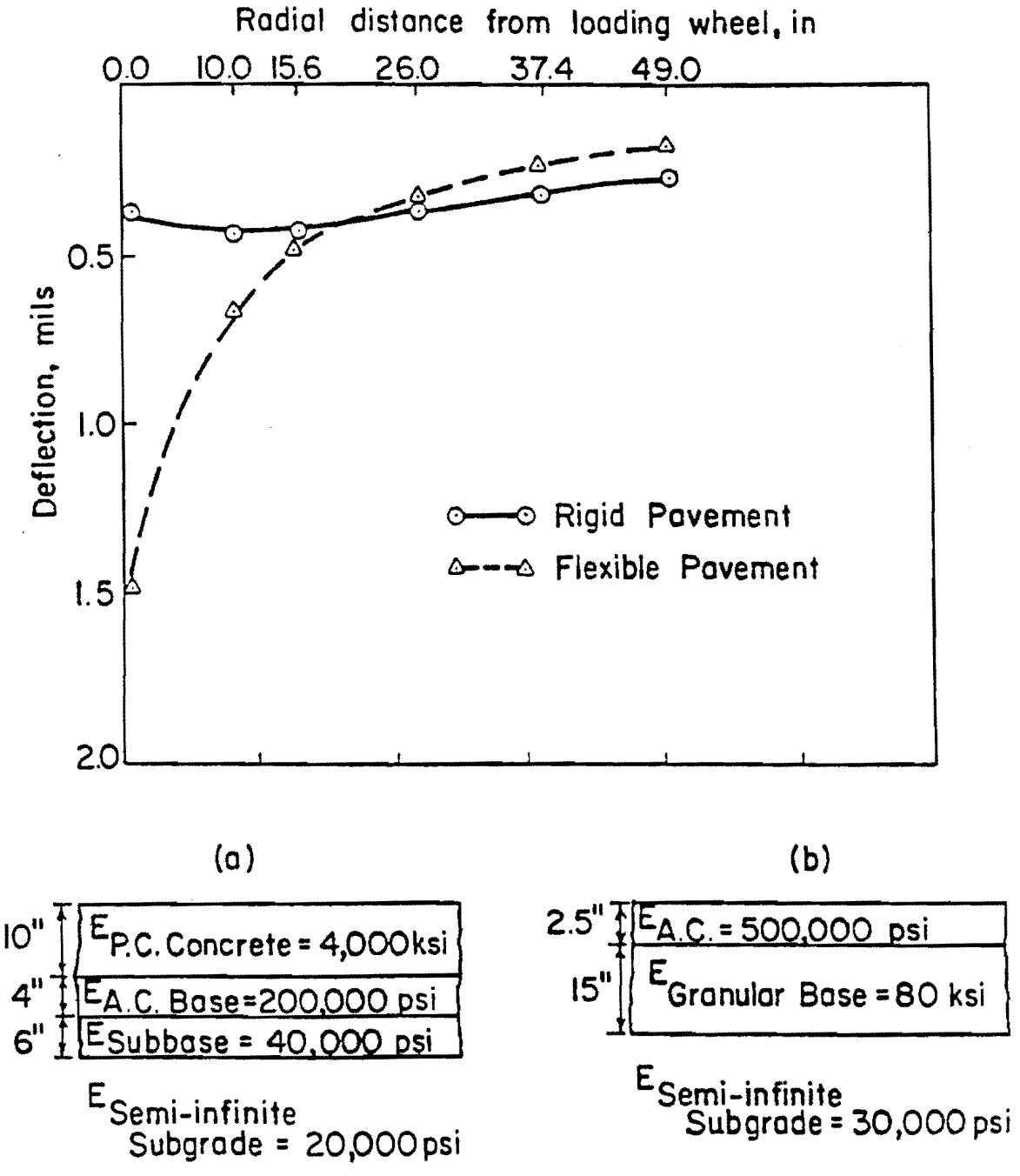

Fig 2.8. Theoretical deflection basins under Dynaflect loading for a very stiff and a weak pavement.

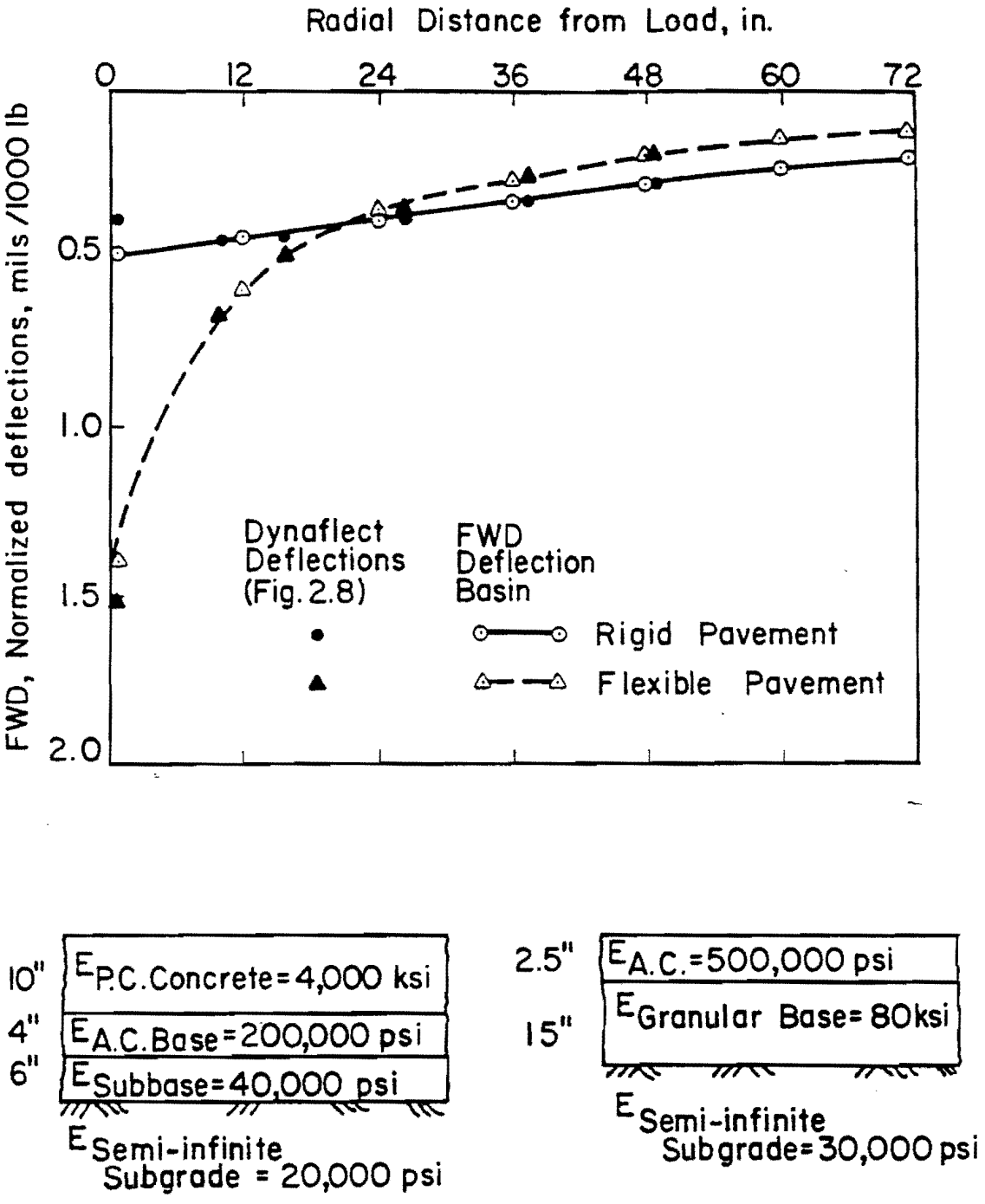

Fig 2.9. Theoretical deflection basins under FWD loading for a very stiff and a weak pavement.

$$W'_{R_i} = W_{R_i} \times \left(\frac{1000}{P_{FWD}}\right) \qquad (2.2)$$

where

W'_{Ri} = normalized deflection, at the radial distance, R_i,

W_{R_i} = FWD deflection measured at the radial distance, R_i at the peak force of P_{FWD},

P_{FWD} = peak force on the FWD loading plate at which deflections are measured or theoretically calculated.

The above method of plotting FWD deflection basins makes it convenient to compare FWD deflections at different levels of peak force as well as with a Dynaflect deflection basin. It is pointed out that, even for a pavement behaving as a perfectly linear elastic system and assuming that dynamic loads are equal to corresponding static loads used in the analysis, the theoretical Dynaflect deflection basin may not coincide with the FWD basins plotted using normalized deflections, as illustrated in Fig 2.9. This discrepancy is a result of the effect of the size of the loaded area on the pavement response.

SUMMARY

This chapter presents a review of procedures for dynamic deflection measurement by NDT methods with the Dynaflect and Falling Weight Deflectometer. The model 8000 FWD acquired by the Texas State Department of Highways and Public Transportation is described in detail. Graphical presentation of dynamic deflection data is made by plotting a deflection basin. The radial distance of the deflection sensors from the load is to be used as the abscissa. For the FWD deflection basin, normalized deflections are used as ordinates.

CHAPTER 3. INTERPRETATION OF DEFLECTION DATA

This section presents a brief review of existing practices of analysis and the application of deflection data, including empirical procedures to estimate structural adequacy and overlay design, mechanistic interpretation and insitu material characterization. Consideration is also given to other factors which influence the analysis of a deflection basin for the structural evaluation of pavements.

EMPIRICAL AND BASIN PARAMETER BASED PROCEDURES

Limiting Deflection Criteria

Traditionally, pavement evaluation and overlay design have been based on criteria of allowable deflections and empirical relationships developed from field studies of maximum deflection and pavement performance. For example, the Asphalt Institute procedure is based on empirical relationships between Benkelman beam rebound deflections and traffic data from inservice pavements (Ref 4). Similar procedures were developed by other user agencies. These procedures are summarized in Refs 17, 19, and 20. Overlay thickness requirements are determined from nomographs developed from these empirical relationships which can reduce deflection below the limiting deflection criterion. Later correlation studies made between results from other NDT devices, such as the Dynaflect (Refs 1 and 4), enable these nomographs to be used. These empirical methods are based solely on local experience and therefore limited in useful applications. Maximum deflection is indicative of total pavement response and alone it cannot lead to the evaluation of structural integrity and material characterization of different pavement layers. It can be shown that two different pavements can have the same value of maximum deflection but different Young's moduli of layers if the measured deflection basins are of different shapes. A summary of limiting deflection criteria adapted by different agencies is presented by Majidzadeh (Ref 17).

Use of Deflection Basin Parameters

Basin Parameters. Deflection basins measured by NDT devices, such as the Dynaflect, Road Rater, and FWD, have been characterized by different parameters which are functions of deflection values at one or more sensors. A summary of widely used deflection basin parameters and their sources is presented in Table 3.1. Figure 2.6 illustrates Dynaflect maximum deflection (DMD), surface curvature index (SCI), base curvature index (BCI), spreadability (SP), sensor no. 5 deflection (W5), and basin slope (SLOP), which have been used for the Dynaflect deflection basin (Refs 17, 22, and 23). Recently Road Rater and FWD deflection basins have been characterized by area and shape factors, F_1 and F_2 (Ref 13), as presented in Fig 3.1 and Table 3.1. If spreadability, SP, is calculated for Road Rater (Table 3.1), then area can be related to SP by the following relationship (Ref 13):

$$\text{Area} = 0.24\ SP(\%) - 6\ (W_2 + W_3)/W_1 \qquad (3.1)$$

where W_1, W_2, and W_3 are deflections at sensors 1, 2, and 3.

Deflection ratio (W_R) has been widely used with agencies and researchers using FWD. Tangent slope, TS is another parameter proposed for defining basin shape (Ref 28). This parameter is defined in Table 3.1 and illustrated in Fig 3.2. A curve is fitted through the measured deflections to describe the deflected surface. This function is then solved simultaneously with the equation of a straight line, the tangent (Fig 3.2). Tangent slope is then calculated by finding the slope of the line joining the point of maximum deflection and the tangent point.

Deflection basin parameters have been used for three major applications: (1) for diagnostic checking of the structural conditions of pavements based on field experience; (2) to relate to critical pavement response and subsequently to axle load applications; and (3) to calculate insitu Young's

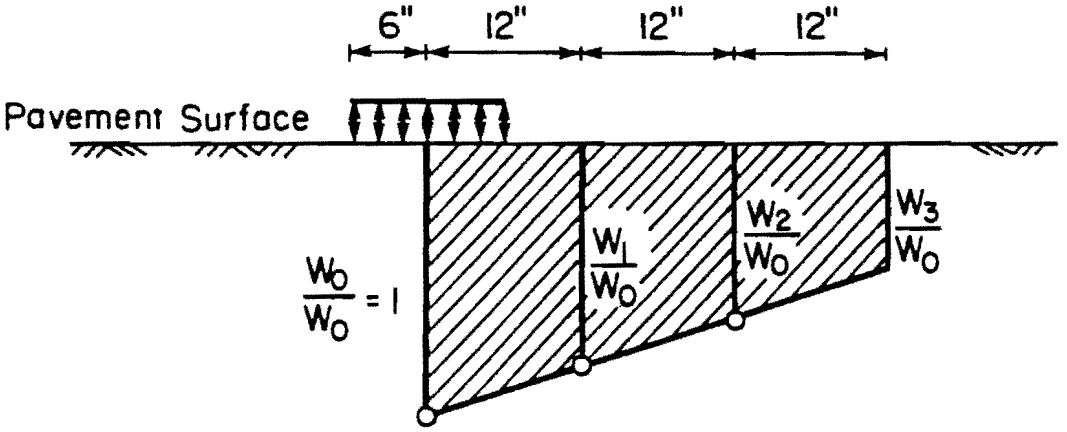

$(W_0, W_1, W_2, W_3$ are measured Deflections)

$$\text{Area (inch)} = 6\left(1 + 2\frac{W_1}{W_0} + 2\frac{W_2}{W_0} + \frac{W_3}{W_0}\right)$$

Fig 3.1. Illustration of AREA, a deflection basin parameter defined for Road Rater (Ref 13).

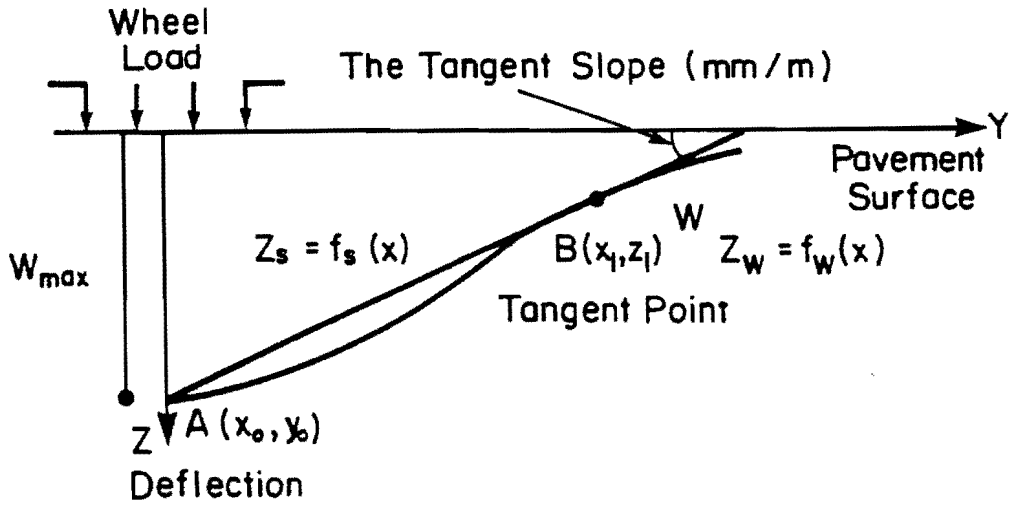

Fig 3.2. Illustration of the deflection basin parameter, tangent slope (Ref 28).

TABLE 3.1. SUMMARY OF DEFLECTION BASIN PARAMETERS

Parameter	Definition[1]	NDT Device[2]	Reference
Dynaflect maximum deflection, DMD	$DMD = W_1$	Dynaflect	(17)
Surface curvature index, SCI	$SCI = W_1 - W_2$	Dynaflect, Road Rater model 400	(17) (21)
Base curvature index, BCI	$BCI = W_4 - W_5$	Dynaflect	(17)
Spreadibility, SP	$SP = \frac{\sum_{i=1 \text{ to } 5} W_i}{5\ W_i} \times 100$	Dynaflect	(17, 22)
	$SP = \frac{\sum_{i=1 \text{ to } 4} W_i}{4\ W_i} \times 100$	Road Rater model 2008	(13)
Basin slope, SLOP	$SLOP = W_1 - W_5$	Dynaflect	(23)
W5	$W5 = W_5$	Dynaflect	(23)
Radius of Curvature, R	$R = \frac{r^2}{2\ W_m\left(\frac{W_m}{W_r} - 1\right)}$	Benkelman Beam	(24)

(continued)

TABLE 3.1. (CONTINUED)

Parameter	Definition[1]	NDT Device[2]	Reference
Deflection ratio, Q_r	$Q_r = \frac{W_r}{W_o}$	FWD Benkelman Beam	(25, 26) (27)
Area (inch), A	$A = 6\left(1 + 2\frac{2}{W_1} + 2\frac{3}{W_1} + \frac{4}{W_1}\right)$	Road Rater model 2008	(13)
Shape factors, F_1, F_2	$F_1 = (W_1 - W_3)/W_2$	Road Rater model 2008	(13)
	$F_2 = (W_2 - W_4)/W_3$		
Tangent Slope, TS	$TS = \frac{W_m - W_x}{x}$	None	(28)

[1] W = deflection; subscripts: 1, 2...5 = sensor locations,
0 = center of load
r = radial distance
m = maximum deflection
x = distance of tangent point from the point of maximum deflection

[2] The NDT device for which deflection parameter was originally defined.

moduli. The first two categories of applications are briefly reviewed in the following section. The third application, i.e., calculation of insitu elastic moduli is discussed in a later section.

Application and Limitations. Dynaflect deflection basin parameters have been studied and a set of limiting criteria for DMD, SCI, and BCI has been proposed for rating the structural condition of a pavement (Ref 13). SCI is believed to be a measure of basin curvature near the center of a deflection basin and therefore is used as an indicator of structural integrity of the pavement surface layer where layer thickness, stiffness (Young's modulus of elasticity), and defects and discontinuities, such as joints and cracks, are the primary factors influencing SCI values. However Taute et al (Ref 23) found from Dynaflect deflection data obtained on rigid pavements in Texas that SCI is typically a very small value and therefore not suitable for correlating with upper layer stiffness. The Dynaflect data collected on rigid pavements in another research study (Ref 12) support this finding about SCI. Taute et al (Ref 23) therefore defined basin slope (Table 3.1) and correlated it with the Young's modulus of the concrete layer. Spreadability and area can be considered as a function of overall pavement stiffness and an indicator of its ability to distribute load. Deflection ratio and radius of curvature parameters are used to estimate insitu pavement moduli. The tangent slope parameter, as reported in Ref 28, has been used with theoretical deflection basins.

Deflection basin parameters have also been related to critical response of pavement and to design life of pavements. Figure 3.3(a) presents the relationship between maximum tensile strain and SCI values based on Road Rater deflection data (Ref 21) on asphalt pavements. Figure 3.3(b) illustrates the relationship between tensile strain and radius of curvature calculated from Benkelman beam deflection data on asphalt pavements. Finally Fig 3.3(c) illustrates the relationship between the tangent slope and design life based on a theoretical study (Ref 28).

A major application of deflection basin parameters is to estimate insitu Young's moduli of the pavement layers which will be reviewed in a later section. In many cases the shape of the deflection basin has been idealized but, as illustrated in Fig 3.4, wide variation in the shape of measured

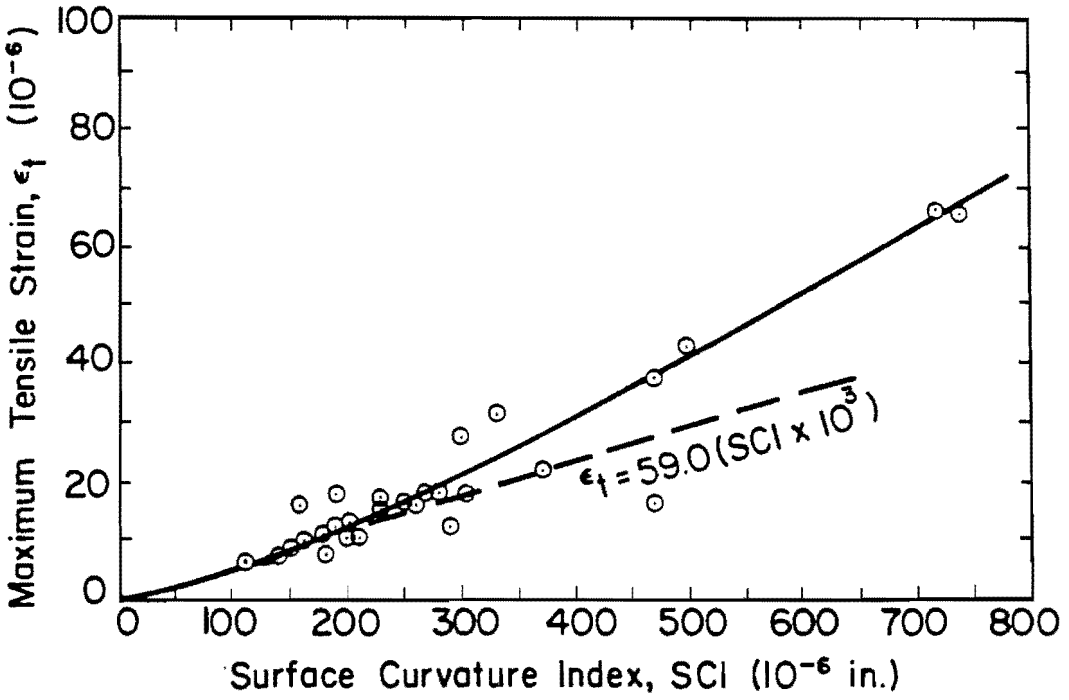

Fig 3.3(a). Relationship between maximum tensile strain and surface curvature index of Road Rater deflection basin (Ref 21).

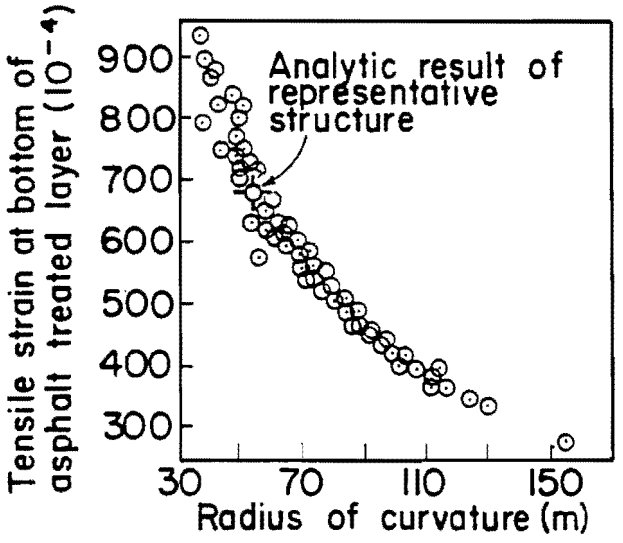

Fig 3.3(b). Relationship between tensile strain and radius of curvature (Ref 24).

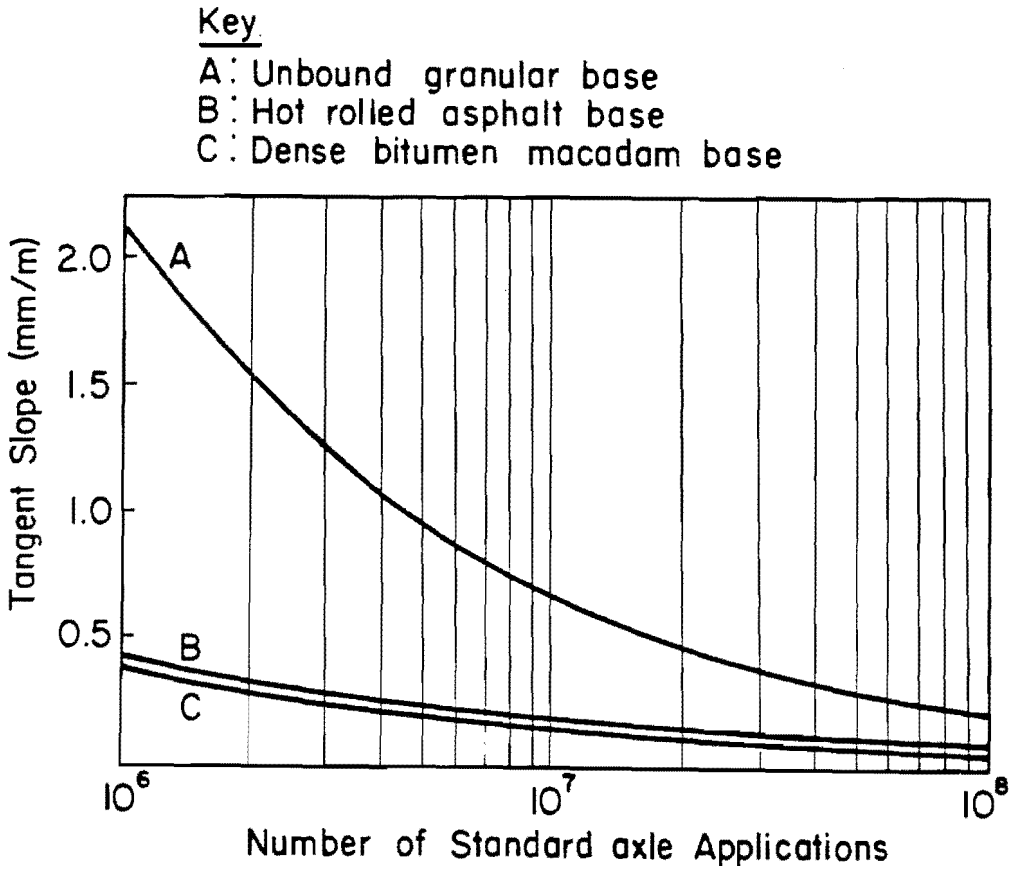

Fig 3.3(c). The tangent slope values for typical RN29 structures (Ref 28).

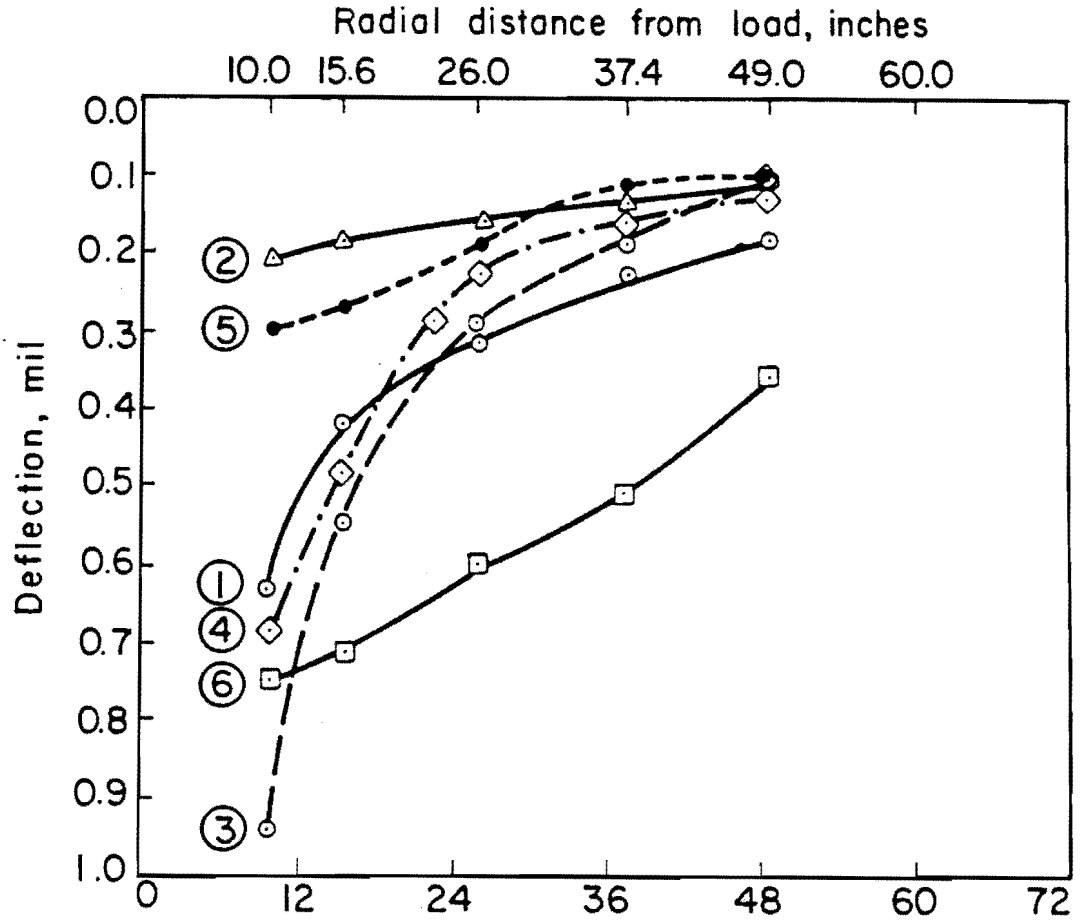

①	②	③	④	⑤	⑥
2.5 in AC	10 in CRCP	3 in AC	13.15 in AC	9.2 in AC	10.5 in AC
15 in Flexible Base	6 in Cement Treated Base	4 in Gran. Base	4 in Gran. Base	7 in Gran. Base	6 in Cement Treated Base
Semi-infinite Subgrade	Semi-infinite Subgrade	Semi-infinite Subgrade	Semi-infinite Subgrade	Semi-infinite Subgrade	Semi-infinite Subgrade
(Ref 66) Hwy 183 NB Austin, TX	IH10/EB ST. 1511 +38 Aug. 1984 Columbus, TX	(Ref 19) American Fork to Main St., ST. 5, Utah	(Ref 19) Coalville to Echo Jct., ST. 1, Utah	(Ref 19) Spanish Fork to Provo, ST. 9, Utah	(Ref 19) Dead River, ST. 1, Arizona

Fig 3.4. Examples of variations in deflection basin shapes (Dynaflect).

deflection basins can be expected. Using basin parameters makes the analysis of deflection data for pavement evaluation easier and simpler, but it may cause the loss of vital information about structural properties of pavement layers which can possibly be extracted from the interpretation of whole deflection basin.

ANALYTICAL MODELS FOR MECHANISTIC INTERPRETATION OF DEFLECTION BASIN

In this section several theoretical models used to analyze deflection data for structural evaluation/insitu material characterization of deflection data are reviewed. A model is selected for use in the development of the structural evaluation system described later in this study.

Mechanistic Modelling of Pavement Structure

In modelling the mechanistic behavior of a pavement structure, following input and response parameters must be considered:

(1) input - load/traffic variables, pavement characteristics and materials properties, environment, locations where responses are required; and

(2) response - stresses, strains, and deflections at preselected locations.

The required materials input for pavement design are based on the constitutive laws established for an idealized theoretical and deterministic structural response model. The materials are characterized from laboratory tests, and pavement response is predicted from theoretical analysis under certain assumptions (Fig 1.1). The calculated responses are unique. The constitutive equations for the simplest idealized system are based on linear elasticity. In the real world, pavement materials generally exhibit non linear characteristics. The viscoelastic approach can be used to model time dependent response of a pavement. Figure 3.5 illustrates basic principles of

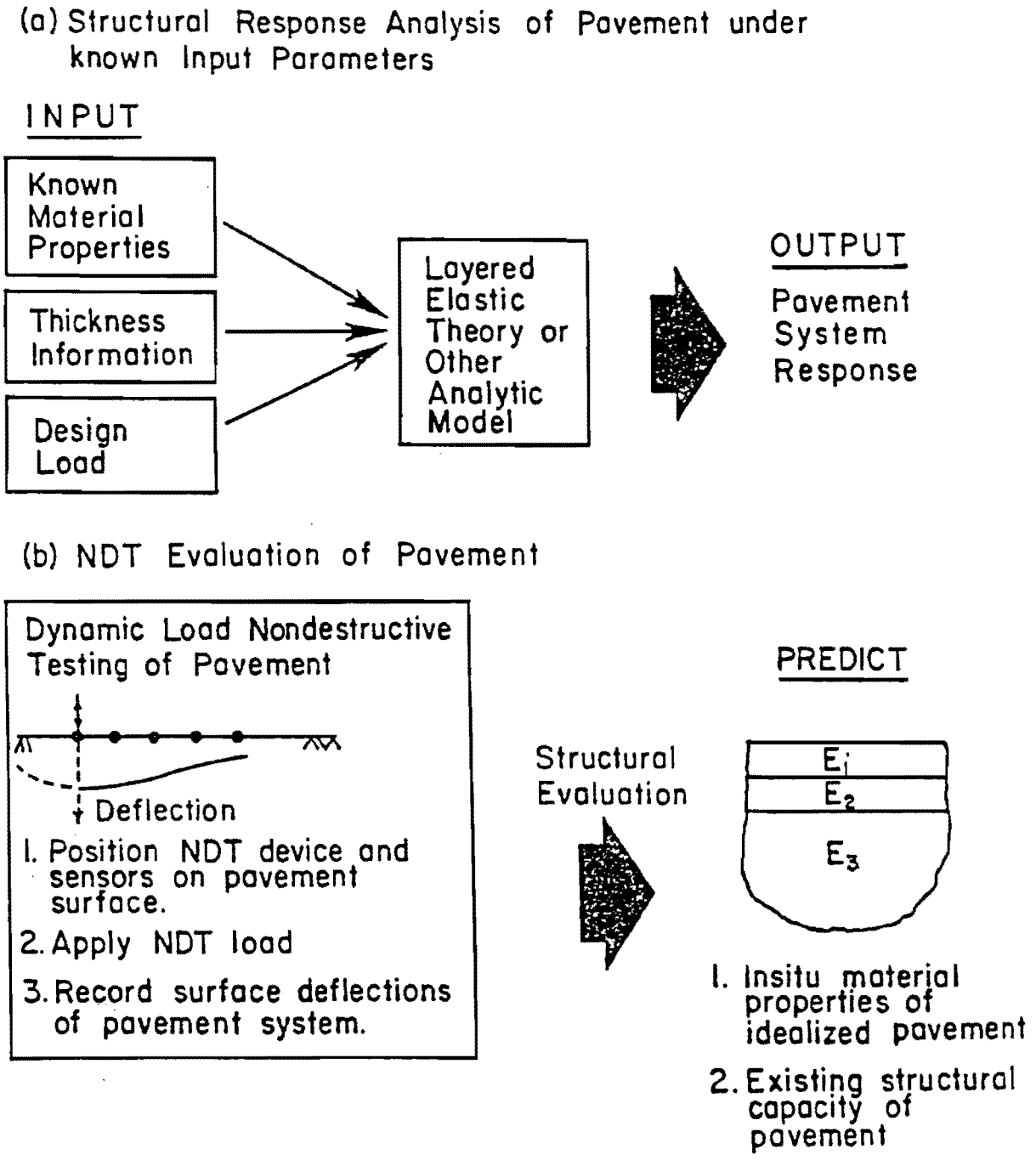

Fig 3.5. Principles of structural response analysis and structural evaluation of pavements based on NDT data.

these constitutive laws considered in the development of structural response models for pavements. Linear viscoelastic theory has been used to develop the structural response model (Ref 29) but has not found wide application due to its complexity, and because more laboratory parameters are required to characterize any pavement material. Linear elastic approach requires the least numbers of parameters to characterize pavement material. These are Young's modulus of elasticity (E) and Poisson's ratio (μ).

In applying the linear elastic approach, solutions for structural analysis of pavements have been developed using plate theory or layered theory. Plate theory is used for the analysis of rigid pavements only. Dr. Westergaard's solutions (Ref 30) for stresses are based on a pavement model consisting of a finite thickness of plate resting on springs which represents behavior of subgrade. The physical model and discrete element analysis made by Hudson and Matlock (Ref 31) provide the ability to analyze the effects of pavement discontinuities and partial loss of support on pavement response. The two-layer model (a pavement layer resting on a semi-infinite subgrade) analyzed by Burmister (Ref 32) was a major breakthrough in the structural analysis of flexible pavements. Before this work, Bousinessq's theory of loading an elastic half space was the best theory available for design of pavements (Refs 33 and 34). Burmister (Ref 32) also formulated a three-layer system. Later other researchers solved the three-layer problem for the complete state of stresses and strains. Computerized versions of multilayer elastic theory, such as ELSYM5 (Ref 18), Shell's BISAR (Ref 35), etc., solve a generalized multilayered system allowing consideration of more than one load. These programs consider only homogeneous material in each layer. Finite element theory has also been used to develop computer programs based on plate theory and layered theory. Finite element theory also permits variation of Young's modulus, E, with depth. Haas and Hudson (Ref 36) present a summary of published works on the comparison of measured and calculated pavement responses. Only static loading is considered in all the structural response models discussed above while specifying design load input.

So far, a review has been made of structural response models which are used to predict pavement response under known input parameters of loading and

material properties for a pavement structure. In the case of structural evaluation of dynamic deflection data from NDT devices, attempts are made to predict pavement structural capacity and material characterization from the measured pavement response (Fig 3.5). This is a more complex task in view of the following considerations.

(1) The response is measured under a dynamic test load which is generally different from the magnitude and loading made of the design wheel load.
(2) The measured response is a dynamic deflection basin but static deflections are predicted from the structural response models.
(3) The material characterization input parameters derived from the NDT data are then used in place of laboratory derived parameters to determine the structural capacity of the pavement or for overlay design.

Mechanistic Models for NDT Evaluation

This section deals with a review of theoretical models used for the analysis and interpretation of NDT data.

Elastic Layered Theory. The most widely used analytical procedures for mechanistic interpretation of deflection basin measure on flexible pavements are based on multilayered linear elastic theory. As shown in Fig 3.6, the layered model of an existing pavement can be used for insitu characterization of materials in each layer. Later this information can be used again in the layered theory computations to estimate the pavement's load carrying capacity and for overlay design. McCullough (Ref 37) has shown the application of layered theory for overlay design of rigid pavements. Seeds et al (Ref 38) used a combination of layered theory and plate theory solutions to develop a design system for rigid pavement rehabilitation. Application of layered theory for insitu material characterization for a deflection basin requires estimation of only one unknown parameter, Young's modulus of elasticity, E of each layer. Poisson's ratio (μ) can be assumed from the literature as any

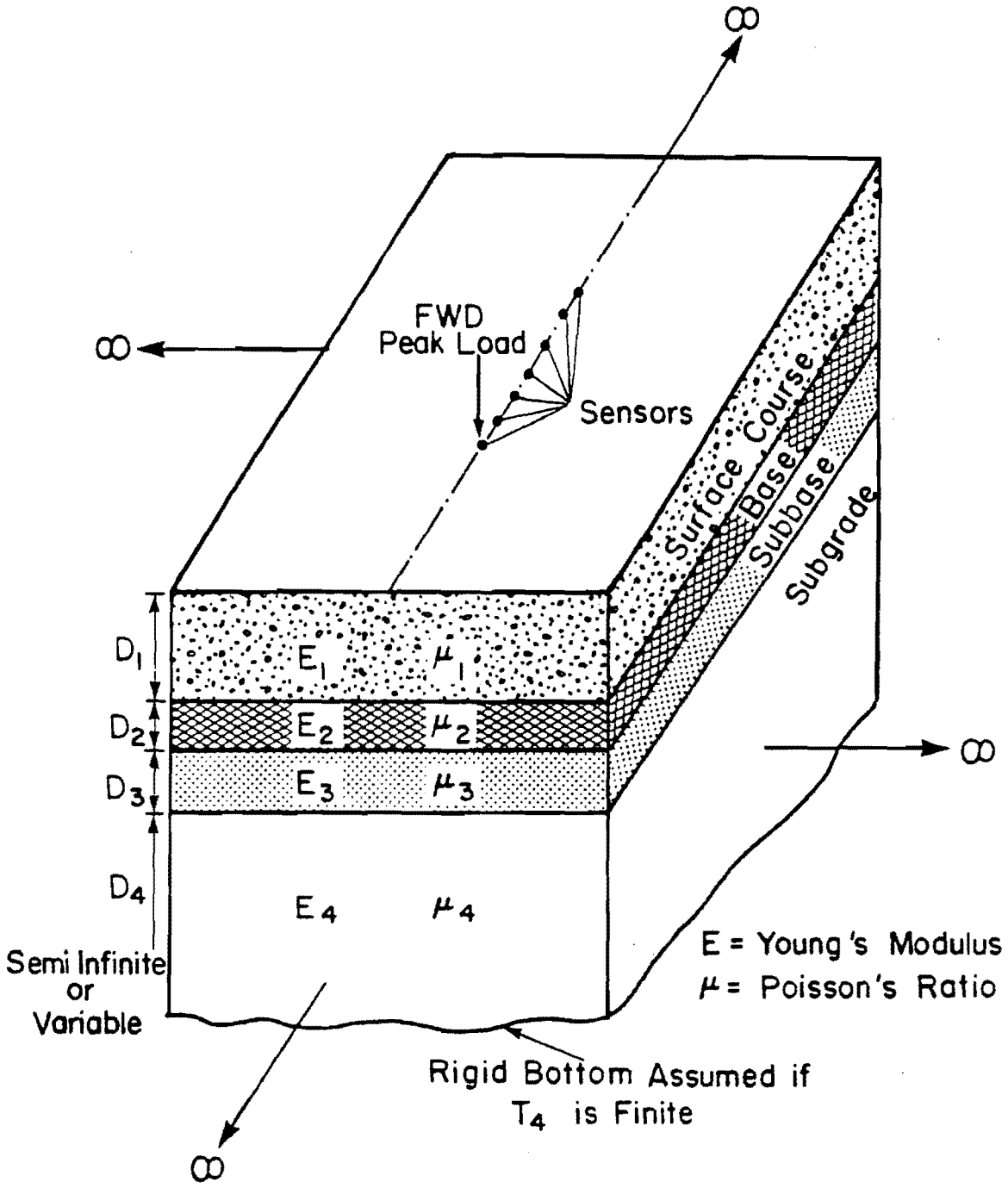

Fig 3.5. Multilayer linearly elastic model of pavement.

small variations in μ does not have any significant effect on pavement response. The following assumptions are made in layered theory solutions.

(1) The material in each layer is linear elastic, homogeneous, and isotropic.
(2) The layers overlying the elastic half space are weightless, and are finite in thickness but are infinite in the horizontal plane.
(3) Uniform static load is applied on a circular area of the surface.
(4) Inertia effect is neglected.
(5) The boundary conditions are as follows:

   (a) Layers are in continuous contact. There is no normal stress outside the loaded area at the top of the surface layer, and it is free from shearing stress.
   (b) For the elastic half space, stresses and displacement are assumed to approach zero at a very large depth.
   (c) Full friction is generally assumed at each interface, i.e., vertical stress, displacement, and shear stress are assumed to be continuous across the interface.
   (d) An important assumption is that horizontal strains across an interface are equal.
   (e) Temperature effect is neglected.

Layered theory solutions are based on axisymmetric condition; therefore the principle of superposition is applied to determine the effect of more than one load. Dynamic load or vibrations are not handled by layered theory. Therefore some researchers have used simplified dynamic models for interpretation of dynamic deflection data. Some of these procedures are briefly reviewed in the following section.

Application of Dynamic Models. The simplest dynamic model of a pavement structure is represented by a single degree of freedom system (SDOF) as illustrated in Fig 3.7. This spring-mass-dashpot system with forced vibrations is treated in text books on vibrations (for example, Ref 39). This dynamic model allows consideration of inertia effect and vibratory

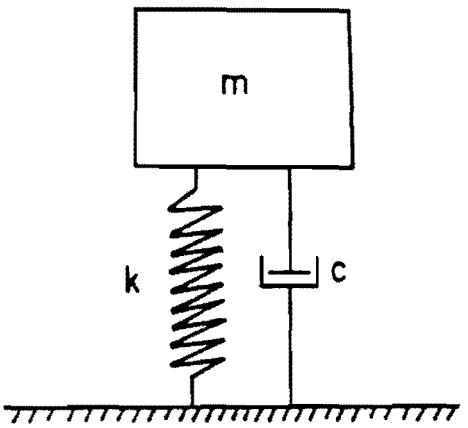

m = Mass = $\frac{\text{Weight}}{g}$

k = Spring stiffness

c = Damping constant

Fig 3.7. Principle of single degree of freedom system.

force. Researchers (Refs 40 and 41) have used principles of vibration theory to evaluate dynamic deflection data. There are two approaches used in making the tests with steady state vibrators: (1) the load-sweep method developed at WES (Ref 42) and (2) the frequency-sweep method developed by Yang (Ref 41).

Load-sweep tests are conducted on a preselected frequency (generally 15 Hz) over a range of dynamic loads and a dynamic stiffness modulus (DSM) is calculated by dividing amplitude of the dynamic force by the corresponding dynamic deflection. DSM is an indication of structural integrity of the pavement subgrade system and has been correlated with the performance (Ref 42). Subgrade modulus can also be found from this test, using the analytical procedure described by Weiss (Ref 40).

In the frequency-sweep approach, pavement is tested at fixed amplitude of dynamic force at a wide range of driving frequencies, from well below the primary resonant frequency to several times higher. An equivalent modulus, E_C is then computed from the dynamic deflection frequency data. Both methods provide a measure of resistance to pavement deformation under vibratory loads but two severe limitations in these approaches are recognized: (1) the arbitrary criteria for preselecting a fixed frequency, or a fixed dynamic force level, and (2) the inability to estimate the structural integrity of each pavement layer. As information about material properties of individual pavement layer can not be extracted, the mechanistic approach to use layered theory for pavement design can not be effectively applied.

Research is also being carried out in applying a time-dependent transfer function theory (Ref 43) to analyze pavement behavior under an impulse load representing a moving wheel load.

Excitation of a pavement surface by steady state vibrations or a transient load generates disturbance in a pavement subgrade system. Another rational and a true mechanistic approach to analyzing this problem is the application of the theory of stress wave propagation in layered elastic media. Further discussion of such dynamic analysis is made in a later section in this chapter.

DERIVATION OF YOUNG'S MODULI FROM DEFLECTION BASIN

A review of existing procedures to estimate Young's moduli from a deflection basin using layered theory is presented in the following sections.

Earlier Work, and Graphical and Nomograph Based Procedures

Scrivner et al (Ref 44) in the early 70's presented a procedure to determine moduli of a one-layer pavement resting on elastic half space based on Burmister's work (Ref 32). The method relied on matching deflections measured at two points one foot apart with theoretical deflections. For the rigid pavements, the distance between the points was increased to two feet. A graphical technique was later developed by Swift (Ref 45) to determine elastic moduli of a two-layer pavement by fitting a measured Dynaflect deflection basin. Cogill (Ref 46) presented a computer program based on a set of simultaneous equations to determine Young's moduli from a surface deflection basin. Coefficients of the equations were obtained from layered theory computations.

Various deflection basin parameters (Table 3.1) have been correlated to pavement moduli based on layered theory computations, and graphical and nomograph-based procedures using basin parameters have been developed, generally for a two or three-layer pavement model. Vaswani (Ref 22) used spreadability (SP) and maximum deflection to develop nomographs for the evaluation of moduli. Majidzadeh (Ref 17) developed graphs to determine subgrade modulus from W5, the sensor 5 deflection of the Dynaflect. Majidzadeh (Ref 17) also developed series of nomographs to estimate moduli of a composite pavement layer and the elastic half space by using DMD, SP, and W5, the Dynaflect deflection basin parameters. Koole (Ref 47) used the deflection ratio, Q_r, obtained from FWD data to prepare a series of graphs to determine subgrade and asphaltic concrete moduli if the base modulus is known. Another graphical technique using Q_r (Ref 27) has been prepared to determine moduli ratios and the subgrade modulus based on two layered theory and Benkelman Beam data. The Road Rater basin parameter, area, and maximum deflection have been used with a finite element program to prepare a series

of nomographs to determine moduli of three-layer flexible pavement (Ref 13). Taute et al (Ref 23) presented nomographs to determine moduli of a three-layer rigid pavement from the Dynaflect basin parameters SLOP and W5.

All the graphical procedures discussed so far are of limited use as

(1) They are developed for a specific NDT device.
(2) Layered theory or any other structural model's computations used to develop these procedures are based on specific ranges of moduli of pavement layers. This factor is often neglected when a user applies these types of nomographs to practice.
(3) They are limited to two or three layers and a particular pavement type.
(4) In general the bottom layer is assumed to be semi-infinite which can result in a large over-estimation error in the subgrade modulus if a rock layer actually exists at a shallow depth as shown, in Fig 3.8.

Inverse Application of Layered Theory

Background. Irwin (Ref 48) presented an iterative procedure for applying layered theory in reverse order by changing the modulus value in each iteration until a best fit of predicted and measured basins is obtained. The moduli in the best fit iteration represent insitu moduli. This approach is very promising as it can be applied to a multilayered flexible or rigid pavement. Uddin et al (Ref 7) used this approach to determine insitu moduli of rigid pavements considering a subgrade of semi-infinite as well as finite thickness. Figure 3.9 illustrates a flow diagram of this procedure. In the past few years a number of self iterative computer programs have been developed using this approach; they are reviewed in the following section.

Self Iterative Procedures. Findings of a literature search on published self iterative procedures are summarized in Table 3.2, which presents titles of computer codes, origins, applicability, and sources. Anani and Wang (Ref 49) developed a self iterative computerized procedure to determine insitu moduli of a four-layer flexible pavement by obtaining a best fit of

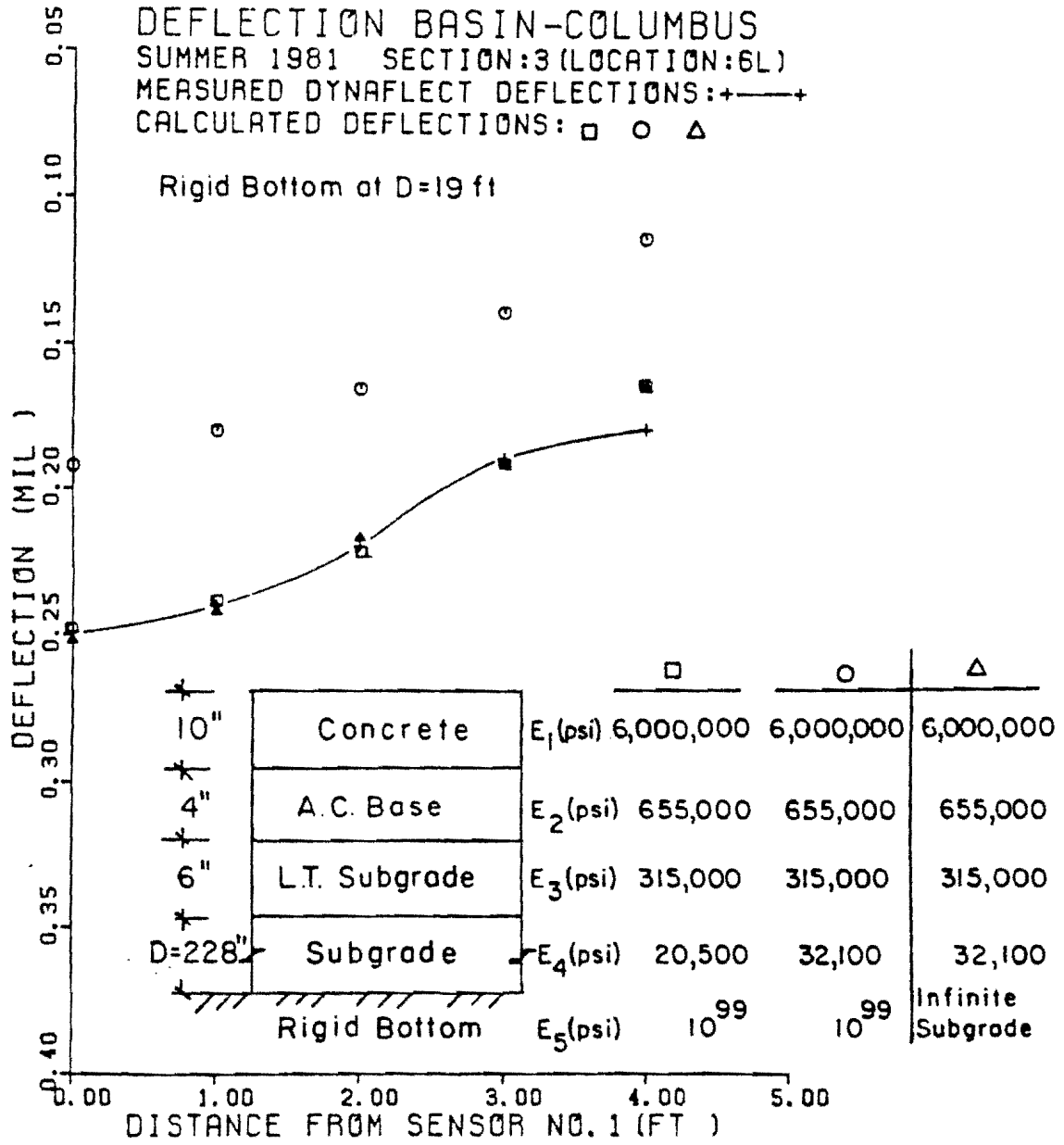

Fig 3.8. Reduction in subgrade modulus assuming a rigid bottom at some finite depth (Ref 7).

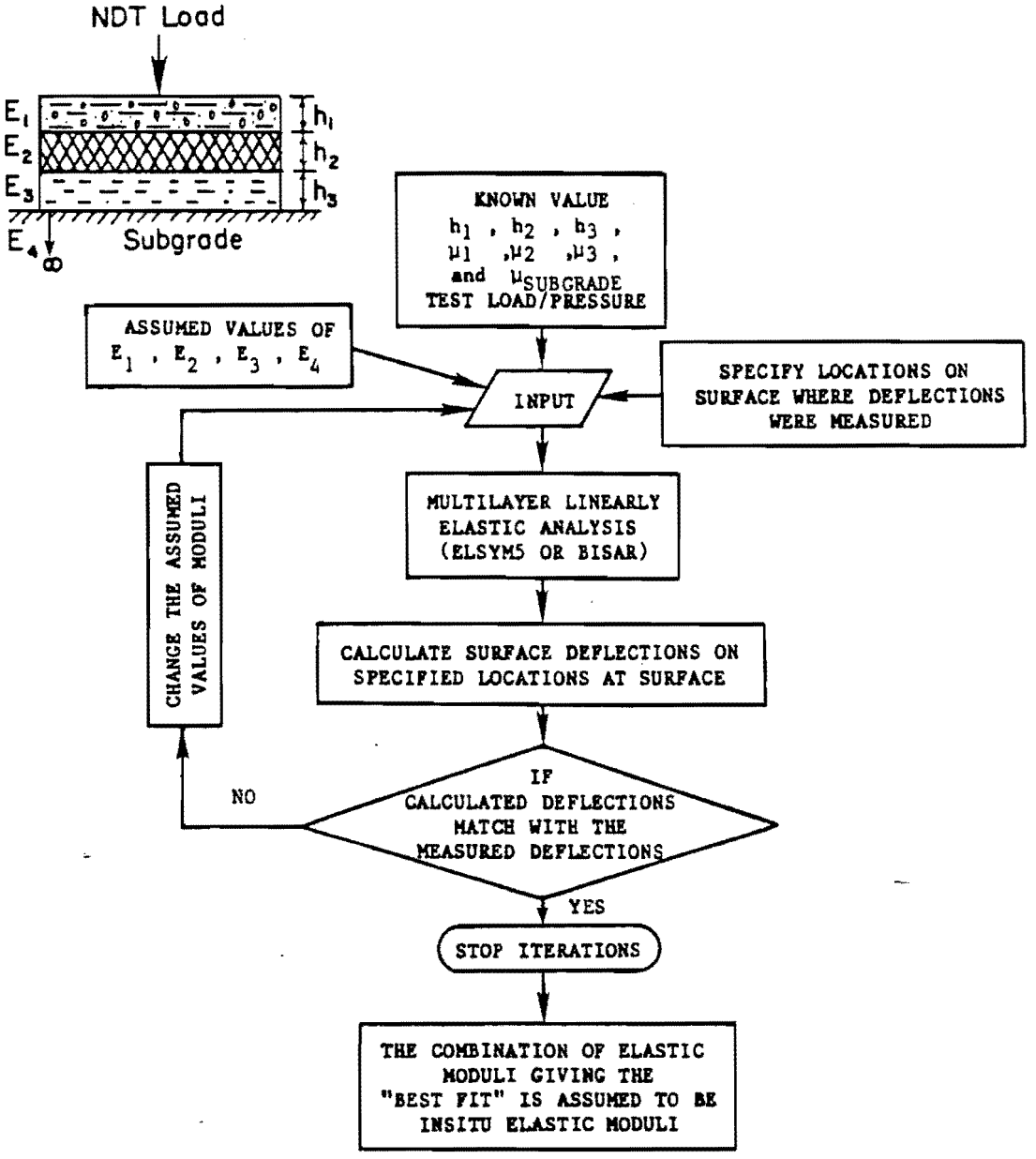

Fig 3.9. Simplified flow diagram of derivation of insitu Young's moduli based on dynamic deflection basin data.

TABLE 3.2. SUMMARY OF SELF-ITERATIVE PROCEDURES FOR EVALUATION OF PAVEMENT MODULI FROM DEFLECTION BASINS

Procedure Title	Source	Pavement Model[1] (n=no. of layers)	Layered Theory Program for Analysis	NDT Method	Input[2]	Output
*	Anani and Wang, 1979 (Ref 49)	4-layers flexible	BISAR	RR400	W_i i=1 to 4	E_1, E_2, E_3, E_4
ISSEM4	Sharma and Stubstad, 1980 (Ref 50)	4-layers flexible	ELSYM5	FWD	W_i i=variable	E_1 to E_4 for 4-layer input
CHEVDEF[3]	Bush-WES, 1980 (Ref 51)	4-layers (Not to exceed number of deflections) flexible	CHEVRON	RR2008	W_i i=1 to maximum 4 (i=1+n)	E_j j=1 to n
OAF	FHWA, 1981 (Ref 52)	3 or 4-layers flexible	ELSYM5	Dynaflect RR FWD	W_i i=variable	E_j j=1 to 3 or (overlay thickness)
OAR[4]	FHWA, 1983 (Ref 53)	Rigid n = *	ELSYM5	Dynaflect RR FWD	W_i i=variable	E_j j=1 to n (overlay thickness)
INVERSE	Hou, 1977 (Ref 54)	n = *	CHEV5L	*	W_i i=variable	E_j j=1 to n
*	Tenison-NMSHD, 1983 (Ref 55)	3-layers flexible	CHEVRON's n-layer	RR-2000	W_i i=1 to 4	E_j j= 1 to 3
RPEDD1[5]	Uddin et al, 1984	3 or 4-layers rigid	ELSYM5	Dynaflect FWD	W_i i=1 to 5 or i=1 to 7	E_j j=1 to 3 or 4
FPEED1[5]	Uddin et al, 1984	3 or 4-layers flexible	ELSYM5	Dynaflect FWD	W_i i=1 to 5 or i=1 to 7	E_j j = 1 to 3 or 4 (remaining life)
BASFIT**	Seeds and Tsute, 1981 (Ref 7)	8 layers (flexible/rigid	LAYER8	Dynaflect	W_i**	**

[1] Semi-infinite subgrade assumed in input.

[2] Thickness, Poisson's ratio, initial seed modulus of each layer (except the thickness of bottom layer) are required input allowable ranges of moduli are also required.

[3] Can be easily modified to handle other NDT devices.

[4] Detailed review has not been made of this reference.

[5] These procedures are developed in the present study.

[6] Not known or unavailable.

** Interactive computer program that allows the user to enter changes in moduli and obtain theoretical deflections (another modified version, BASFT2 has been developed recently, which allows the user to enter measured deflections and plot measured and theoretical deflection basins at the end of each trial and also handles finite thicknesses of subgrade).

deflection basin measured by Road Rater model 400. The method employs successive corrections in moduli starting from the fourth sensor reading and the modulus of the fourth layer (the semi-infinite subgrade). The initial set of moduli are to be assumed by the user. Once all four moduli are corrected, the first iteration is completed. Correction factors are derived from an earlier sensitivity analysis on the effect of moduli changes on deflections. The procedure is valid only for Road Rater model 400 and four-layer flexible pavements with semi-infinite subgrades. Moreover, the the effects of the nonlinear behavior of subgrade and granular layers on back calculated moduli are not considered in the procedure. It is reported (Ref 49) that unique results can be obtained but a literature search in pavement related publications could not find examples (other than those reported in Ref 49) of the field application and validation of this procedure. In general 30 iterations are needed to converge the moduli values according to Ref 49. In other words, BISAR is used 120 times to calculate theoretical deflections for a four-layer pavement. For the test facility (Ref 49), deflection basins measured on only one test section were analyzed individually, but the computation cost is prohibitatively expensive if a large number of basins are to be analyzed. Therefore, for other test sections, only an average deflection basin for one set of data was calculated from the mean deflection values at each sensor and analyzed to determine insitu moduli. However, development of this procedure was a major step towards insitu material characterization as it uses a mechanistic approach to applying layered theory and does not rely on empirical procedures or nomographs.

The self iterative procedure ISSEM4 described by Sharma and Stubstad (Ref 50) is based exclusively on a FWD deflection basin. The computer program handles four-layer flexible pavement, uses ELSYM5 to calculate structural response, and is designed for evaluation of stress dependent moduli. The importance of analyzing an individual deflection basin is realized by Sharma an Stubstad (Ref 50). The derived insitu stress-dependent moduli are claimed to be unique to the accuracy allowed in the iterative procedure. The criterion for uniqueness is reportedly (Ref 50) that there must be one or more deflection readings per structural layer and placed as

outlined in the paper. The reproducibility of derived moduli under the assumption of different levels of initial assumed moduli is not reported in Ref 50. This procedure has been used on flexible pavements only.

A computer program, CHEVDEF, was developed at WES (Ref 51) to analyze deflections basin measured by Road Rater model 2008. The procedure uses Chevron's layer program to calculate deflections when an initial set of moduli and their acceptable ranges are given. The self iterative procedure is based on determining a set of moduli which could minimize errors between predicted and measured deflections. The number of layers handled by this program should be one less than the number of deflection sensors. Examples of field applications are reported for flexible pavements (Ref 51). However the input requirements are generalized, and therefore a deflection basin from any other NDT device, such as the Dynaflect, could be analyzed by this procedure and it could be used for rigid pavement. The last layer of subgrade is assumed to be semi-infinite. Nonlinear behavior of granular layers and subgrade is not considered in this procedure but the output includes stresses, strains, and deflections at the center of the granular layers and at the top of the subgrade.

The recently developed computerized overlay design procedure for flexible pavements, OAF-FHWA (Ref 52), has an option for deriving insitu moduli from a deflection basin measured by NDT devices, such as the Dynaflect, the Road Rater (the model which applies load through two steel columns), and the Falling Weight Deflectometer. ELSYM5 is used to calculate structural response in this program which also assumes a semi infinite subgrade. To determine insitu moduli for (1) a three-layer pavement, a best fit of basin parameter SP, sensor one deflection, and sensor 2 or sensor 3 deflection is used, or (2) a four-layer case, SP and the first 3 sensors deflections are used. The moduli determined from matching deflections are corrected to derive stress dependent moduli by considering gravity stress and non-linear behavior of granular layers and subgrade. To validate the self iterative procedure of the OAF program for uniqueness of the derived stress dependent moduli, a desirable method is to measure deflection basins on a test section using the Dynaflect, Road Rater and Falling Weight Deflectometer

at the same time. Insitu stress-dependent moduli determined from deflection basins of these NDT methods should agree within reasonable tolerance and also compare favorably within laboratory derived moduli or moduli determined from wave propagation techniques. The field applications cited in Ref 52 are based on the analysis of individual deflection basins but lack any study such as outlined above to check the uniqueness of the derived moduli. Very recently tne OAR-FHWA program (Ref 53) has been developed for overlay design of rigid pavements. It also evaluates insitu moduli from deflection basins. Details are not available at this time.

Hou (Ref 54) describes a self iterative computer program INVERSE, developed at the University of Utah, Salt Lake City, Utah, to evaluate insitu moduli from measured deflection basins. The method employs a least squares minimization of errors between deflections computerized by the CHEV5L layered program and the measured deflection basin successive approximation process is used to change moduli in the iterative procedure. Examples are presented for flexible pavements. No other published material on field applications of this program could be found. The proposed deflection analysis program of tne New Mexico State Highway Department (Ref 55) is also a self iterative program based on tne principles of the procedure of Wang and Anani (Ref 49) described earlier. It is designed to analyze deflection basins measured by model 2000 Road Rater on the three-layer flexible pavements. Moduli of pavement layers are obtained when best fit of a set of three deflections measured at 1, 2 and 3 feet away from tne center of tne loading plate is achieved with tne deflections computed by Chevron's n-layer program. Nonlinear behavior of the granular layer and the subgrade is not considered in this version of the deflection analysis program.

The features of the self iterative procedures outlined above are summarized in the following

(1) With the exception of the OAF program, procedures were developed to analyze deflection basin of only one specific type of NDT device.
(2) Procedures are limited to either three or four-layer pavements, except OAF, which can handle both types of pavement.

(3) Computer programs based on multilayered linear elastic theory are used in these procedures to compute theoretical deflections. Anani and Wang use BISAR, whereas ELSYM5 is used in OAF and ISSEM4 procedures, and Chevron's n-layer programs are used in all other procedures.

(4) Generally these procedures are designed to handle only flexible pavements.

(5) Semi-infinite subgrade is assumed in nearly all procedures. Existence of a rigid layer at a finite thickness of subgrade influences pavement responses. This influence is not applicable on stresses, but could be very significant on surface deflections. Effects of considering a rigid bottom or a rock layer at a finite depth of subgrade on computed deflections and derived moduli are not addressed in the development of these methods.

(6) Effects of nonlinear behavior of granular layers and subgrade on derived moduli are not considered in most of these procedures with the exception of OAF and ISSEM4.

(7) All procedures need extensive field applications in order to validate and calibrate if necessary their convergence processes and to check the uniqueness of the derived moduli.

(8) All these procedures are user dependent as far as the effect of initial assumed moduli on the convergence process is concerned.

(9) Dynamic aspects of the dynamic deflection data and the effect of the loading mode are ignored in all the above procedures. Further discussions related to this topic are presented in the following section.

DYNAMIC ANALYSIS OF NDT DATA

Introduction

The discussion presented here is applicable to all NDT devices which generate dynamic deflections, including steady state vibratory devices, such as the Dynaflect, and impulse devices, such as the FWD. Dynamic loading on a

pavement surface causes disturbance in pavement-subgrade system. If the pavement-subgrade system is assumed to be linearly elastic then a true dynamic analysis of this problem is possible by the application of the theory of stress wave propagation in layered elastic media (Ref 56). This approach is in use in seismic analysis of earthquakes by geophysicists and geotechnical engineers and also in structural dynamics area. Details of the theoretical background can be found in Refs 56 and 57. The concepts are summarized in Ref 58. A brief outline is presented in this section. Wave motion created by a disturbance in a homogeneous and isotropic elastic half space is described by three types of waves: (1) compression (P) wave, (2) shear (S) wave, and (3) Rayleigh (R) wave. P and S waves are also called body waves, as they travel inside the body of the medium whereas R waves travel near the surface. Figure 3.10 illustrates the particle motion relative to the direction of wave propagation. Shear wave has two components, S_v, the vertical component, and S_h, the horizontal component. The amplitudes of R waves attenuate very rapidly with depth. The attenuation of energy associated with these waves is caused by geometric and material damping (Ref 57). The propagation of the three types of waves away from a vertically vibrating surface is shown in Fig 3.11. In a layered medium, the wave front becomes very complicated because of reflection, refraction, and polarization of waves (Refs 56 and 57). The basic concepts related to only elastic half spaces for the evaluation of material properties from propagation velocity are discussed here. P wave velocity (V_p) and S wave velocity (V_s) are related to elastic properties of material by the following expressions:

$$V_P = (M/\rho)^{\frac{1}{2}} \qquad (3.2)$$

and

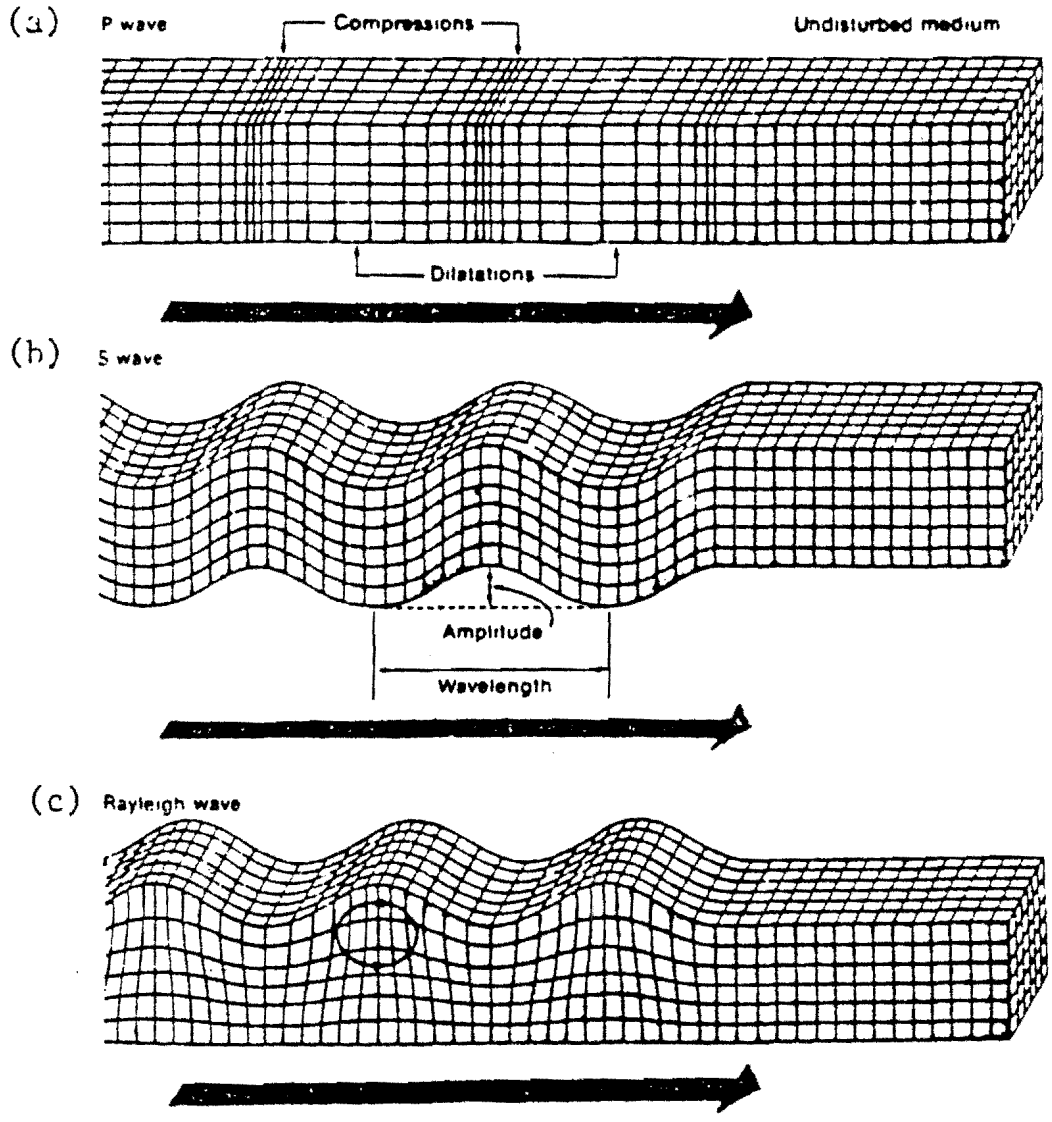

Fig 3.10. Forms of wave motion in an elastic half-space (Ref 61).

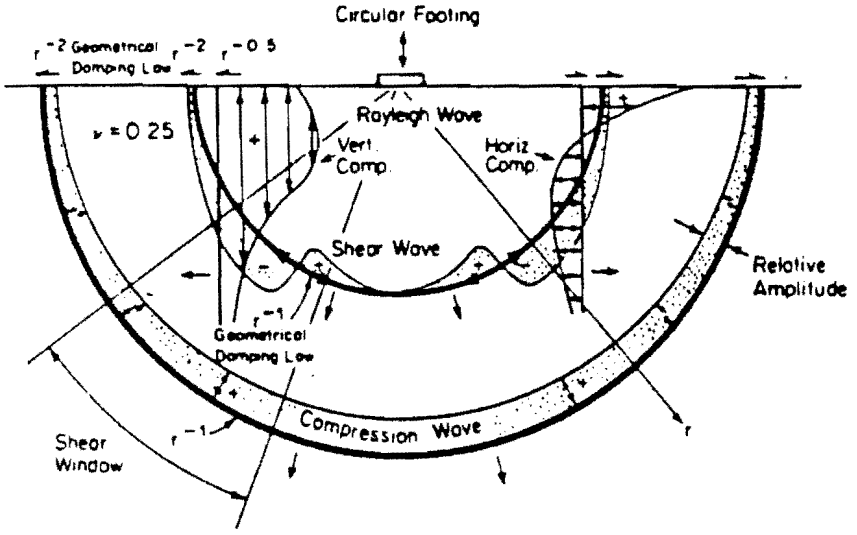

(a) Distribution of waves from a vertically vibrating footing on a homogeneous, isotropic, elastic half-space

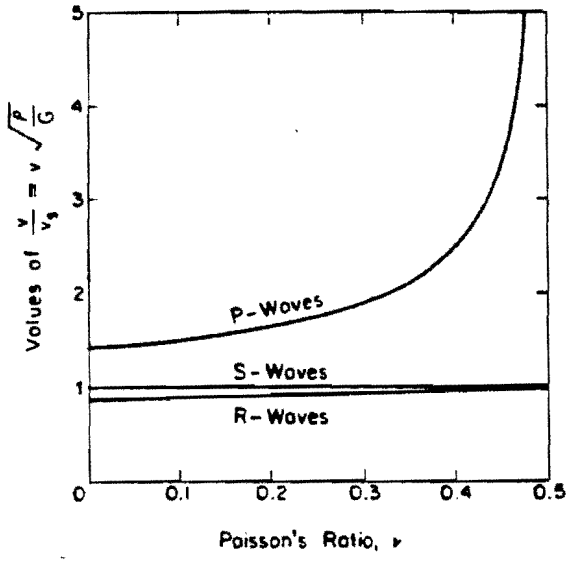

(b) Relationship between Poisson's ratio and wave velocities in an elastic half-space

Fig 3.11. Propagation of waves in an elastic half-space.

$$V_s = (G/\rho)^{\frac{1}{2}} \tag{3.3}$$

where

M = constrained modulus of elasticity,

G = shear modulus, and

ρ = mass density = $\frac{\text{unit weight}}{\text{acceleration due to gravity}}$

Using the relationships between elastic parameters, M, G, E, and Poisson's ratio (μ) it can be shown that

$$E = \rho (1 + \mu) (1 - 2\mu) V_p^2/(1 - \mu) \tag{3.4}$$

and

$$G = \rho(1 - 2\mu)V_s^2 / \left[2(1 - \mu)\right] \tag{3.5}$$

The conventional experimental procedure for evaluating pavement moduli from steady state vibrations is based on developing a dispersion curve where Rayleigh wave velocity, V_R, is plotted against L_R, the wavelength of the R wave (Ref 59). The following relationship is used in this procedure to calculate V_R by measuring L_R:

$$V_R = f L_R \tag{3.6}$$

where

f = frequency of excitation.

Equation 3.6 is equally valid for V_p, L_p, and V_s, L_s. Nazarian and Stokoe (Ref 58) use Eq 3.6 and the spectral analysis of a surface wave generated by an impulse source to measure the frequency content and wavelength associated with each frequency to determine V_R. Once V_R is known, E can be found from the following equation:

$$E = 2(1 + \mu)\ P\ V_s^2 \qquad (3.7)$$

as $V_R \approx 0.9\ V_s$.

The experimental procedures to determine pavement moduli basically use the fundamental relationships discussed above.

Research is currently in progress at The University of Texas at Austin (Ref 60) to develop a dynamic model for determining structural response under dynamic NDT tests, as discussed briefly in the following section.

Dynamic Analysis for Steady State NDT Data

A detailed treatment of the dynamic model (Ref 60) is out of the scope of this study. At the present time, the model is being continually improved and calibrated. The formation is capable of giving complete structural response under harmonic loading at a specific fixed frequency or a transient response under an impulse load. The basic assumption is that, in each horizontal layer, the material is homogeneous, isotropic, and linearly elastic. The basic principles used in formulating and solving the wave equation in the simple model are: (1) coupled P and S_v waves can be considered as R waves in the x-z direction and (2) the S component of the shear wave can be treated as a Love wave (Ref 56) in the y-direction. (In the more detailed model being developed at present, these assumptions are no longer made and all different forms of waves are properly accounted for.)

The coordinates system is shown in Fig 3.12. Stresses and displacement are assumed continuous at the interfaces. Displacements are considered to be linear between the top and bottom of a layer. The problem is solved for a displacement which can be differentiated to obtain strain, and Hooke's law is then applied to calculate stresses. The input includes E, μ, and the thickness of each layer, unit weights of materials, the excitation frequency, and the boundary condition at the bottom of the subgrade layer. Wave velocities are calculated internally in the program.

The flexible pavement illustrated in Fig 3.13 has been analyzed for various thicknesses of the subgrade, ranging from 10 feet to infinity. The Dynaflect loading and geophone configuration was modelled in the dynamic analysis. Typical results are presented in Figs 3.14 to 3.19.

Figure 3.14 illustrates the theoretical dynamic deflection basin at an assumed frequency of zero Hertz for a 110 feet deep subgrade which corresponds to a static loading condition. The same figure also shows the static deflection basin calculated by using ELSYM5. The basins are virtually same. Variations of ratio of dynamic amplitude at 8 Hz and static deflection are illustrated in Figs 3.15 to 3.19, for subgrade depths ranging from 10 feet to 110 feet. For this analysis, static deflections were calculated using ELSYM5 with the input data shown in Fig 3.13. These figures illustrate that at a depth of subgrade to rock layer of 35 feet, large dynamic deflection are predicted by the dynamic analysis. The same ratios have been plotted versus depths of subgrade in Fig 3.20 for each geophone location. The 5th geophone, which is often used to characterize subgrade modulus (Ref 23), also shows the highest ratio at 35 feet. At sensor 1, the effect is less pronounced. This analysis indicates that if, at 35 feet depth, a rock layer exists, the Dynaflect will record higher deflections, and the use of a static analysis will result in errors in back-calculated moduli. The self iterative program FPEDD1 (developed and described in the present study) was used to back calculate insitu moduli from the theoretical dynamic deflection basins using the input data of Fig 3.13. The back-calculated moduli are summarized in Table 3.3. As anticipated, significant errors in all back-calculated moduli occur at depths of 20 and 35 feet.

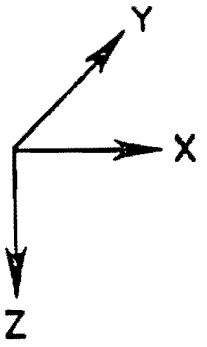

Fig 3.12. Coordinate system assumed in the dynamic analysis.

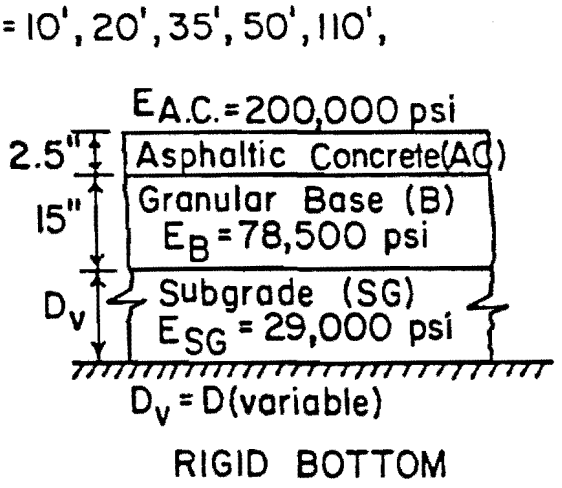

Fig 3.13. Flexible pavement used in the dynamic analysis.

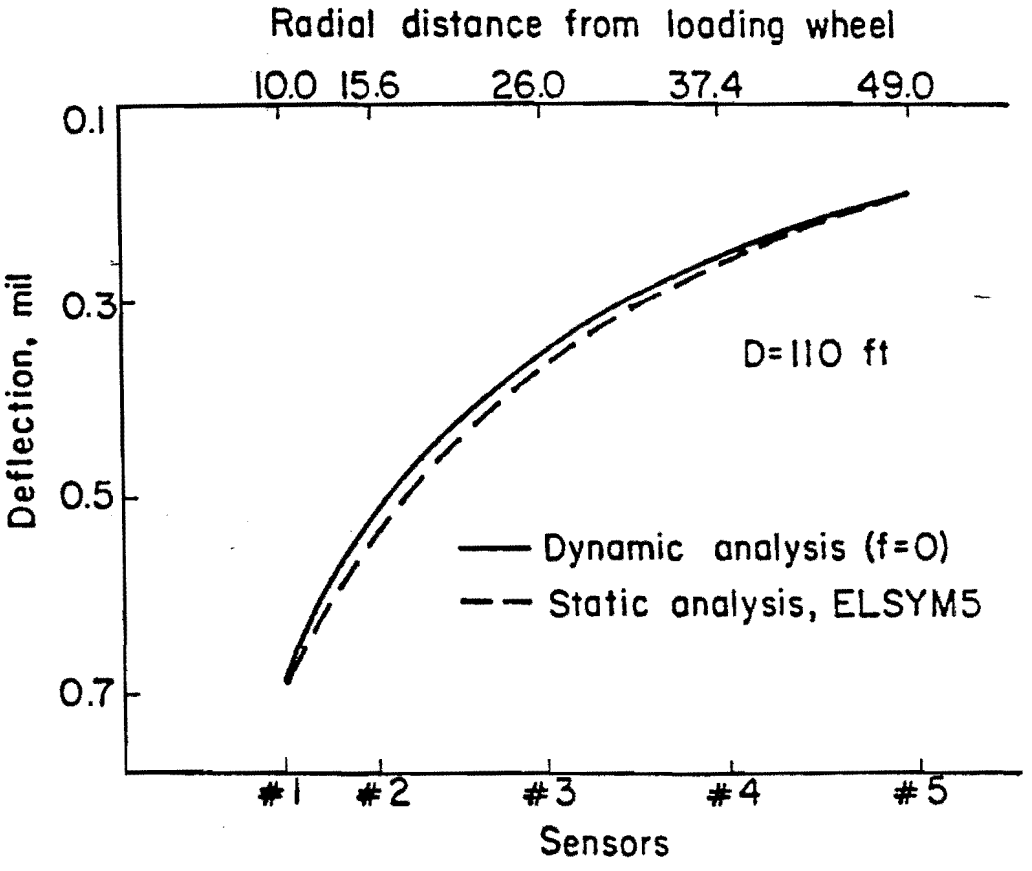

Fig 3.14. Comparison of theoretical Dynaflect deflection basins calculated using dynamic and static analysis.

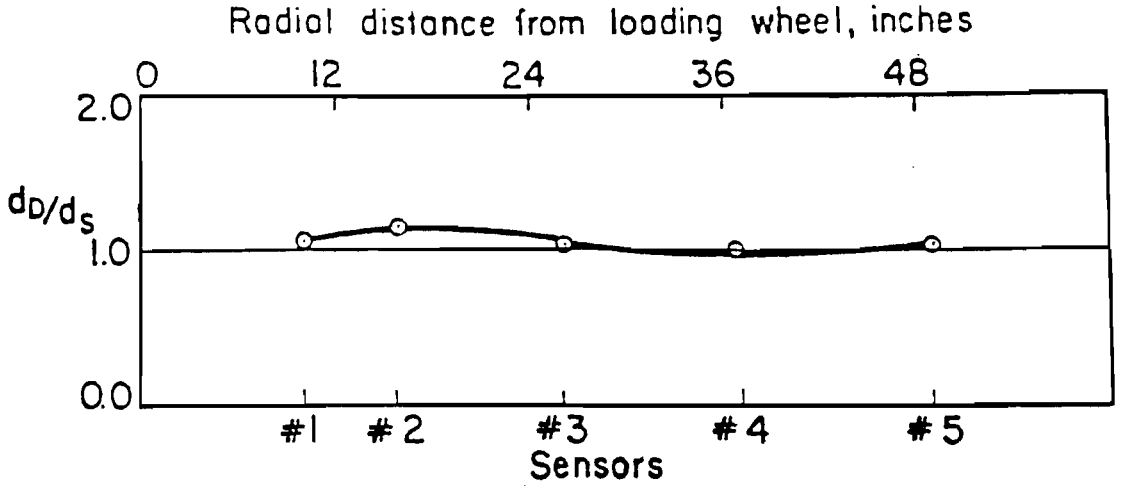

Fig 3.15. Plot of d_D/d_s corresponding to the locations of Dynaflect sensors for D = 10 feet.

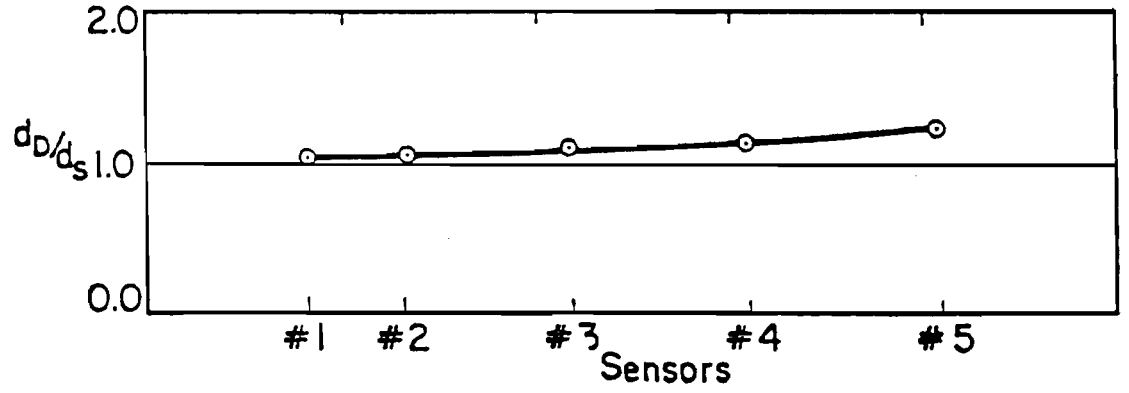

Fig 3.16. Plot of d_D/d_s corresponding to the locations of Dynaflect sensors for D = 20 feet.

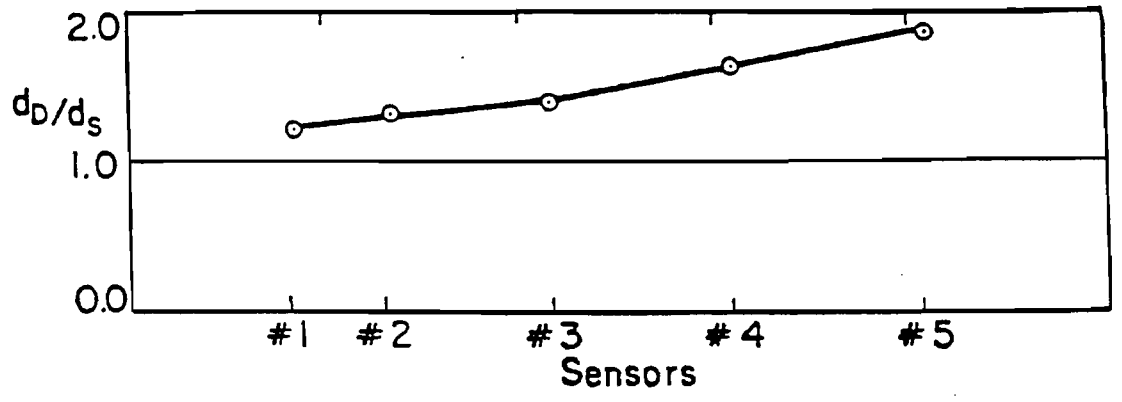

Fig 3.17. Plot of d_D/d_s corresponding to the locations of Dynaflect sensors for D = 35 feet.

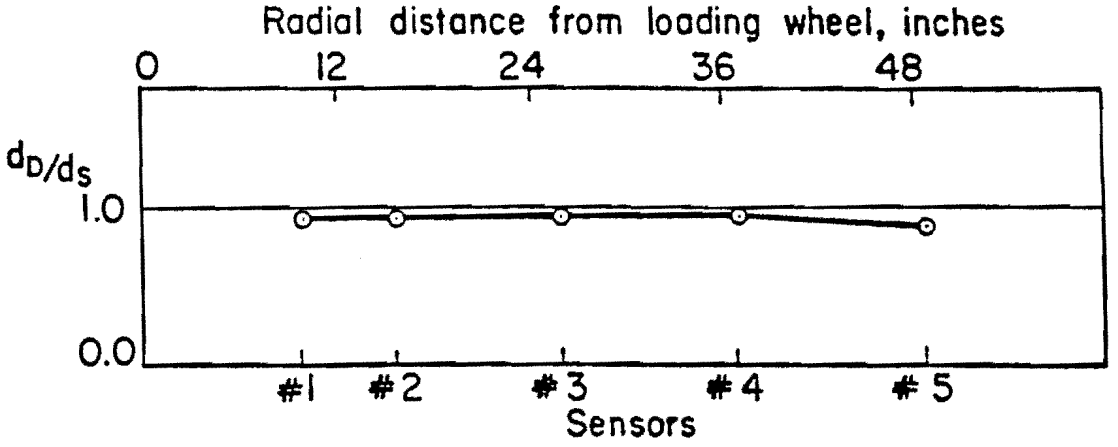

Fig 3.18. Plot of d_D/d_s corresponding to the locations of Dynaflect sensors for D = 50 feet.

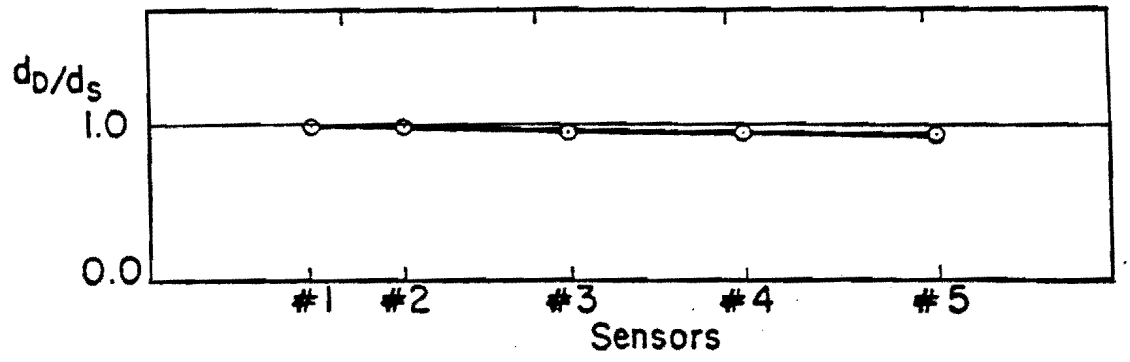

Fig 3.19. Plot of d_D/d_s corresponding to the locations of Dynaflect sensors for D = 110 feet.

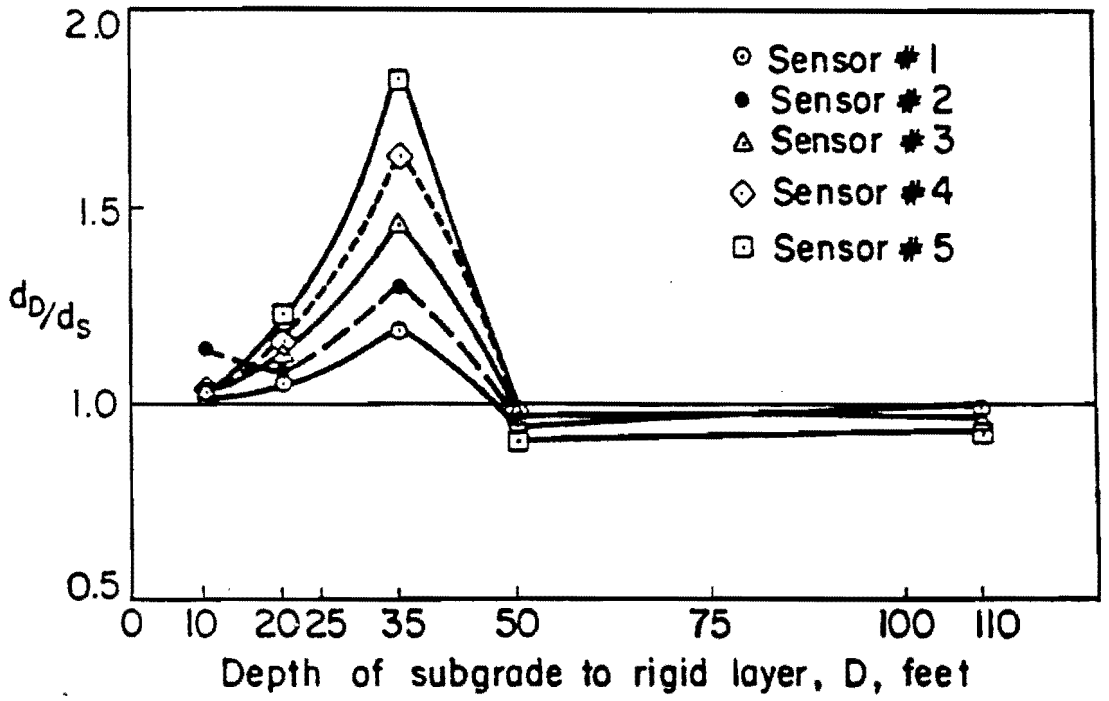

Fig 3.20. Plot of d_D/d_s versus D corresponding to locations of Dynaflect sensors.

TABLE 3.3. MODULI DERIVED FROM THEORETICAL DEFLECTION BASINS BASED ON DYNAMIC ANALYSIS

Depth of Subgrade, D	E_{AC}, psi		E_{BASE}, psi		E_{SG}, psi	
	Calculated	Error*	Calculated	Error*	Calculated	Error*
10 Feet	200,000	0%	65,096	-17.1%	27,943	-3.6%
20 Feet	285,833	+42.9%	69,558	-11.4%	23,927	-17.5%
35 Feet	295,366	+47.7%	53,252	-32.2%	17.751	-38.8%
50 Feet	200,000	0%	78,500	0%	32,164	+10.9%
110 Feet	200,000	0%	78,500	0%	30,817	+ 6.3%
Original Moduli	200,000 psi		78,500 psi		29,000 psi	

*Error = $\frac{\text{Original Modulus - Calculated Modulus}}{\text{Original Modulus}} \times 100$

By looking at wave motion induced by the Dynaflect, long wavelengths result due to the low excitation frequency. For typical subgrade soils (assuming nondispersive medium), half wavelengths will be more than 35 feet. Such a long wavelength decreases attenuation (relative to shorter wavelengths). Also, the effect of pavement layers existing near the surface will be practically negligible on wave attenuation. This discussion leads to the conclusion that peak-to-peak vibratory force of the Dynaflect can be approximated as a pseudo static load, and the corresponding peak-to-peak dynamic deflections can be treated as static deflections. Therefore, it is reasonable to apply a static analysis using layered elastic theory to analyze Dynaflect deflections. This discussion is also supported by the results of the dynamic analysis described earlier if we know that there is no rigid or rock layer at some critical depth. This critical depth can be approximated as 1/4 to 1/2 of the wavelength of the P wave in the subgrade soil (Ref 60).

Dynamic Analysis of FWD

A transient impulse on a pavement surface can excite a wide range of frequencies. If the frequency content is known, the dynamic analysis discussed in the preceding section, can be applied for each frequency level, and the principle of superposition can be used to determine dynamic response (Ref 60). In an earlier study reported by Scott et al (Ref 61), field measurements were made on the dynamic response of the FWD. A simplified approach to calculate the predominant frequency excited by the FWD is to represent the FWD load by the idealized load-time history, as illustrated in Fig 3.21(a). Assuming a harmonic waveform as shown in Fig 3.21(b), the period, T, of the wave is approximately 50 seconds. Frequency, f, being the inverse of T, can be taken as 20 Hz. From the time-history and auto power spectra for the FWD, Scott et al (Ref 61) found that the predominant frequency excited by the FWD was 20 or 21 Hz. Comparisons of FWD theoretical dynamic deflection basins with static basins calculated by layered theory analysis (such as described for the Dynaflect in Figs 3.15 to 3.20) are not available at the present time. Further research is warranted in this area.

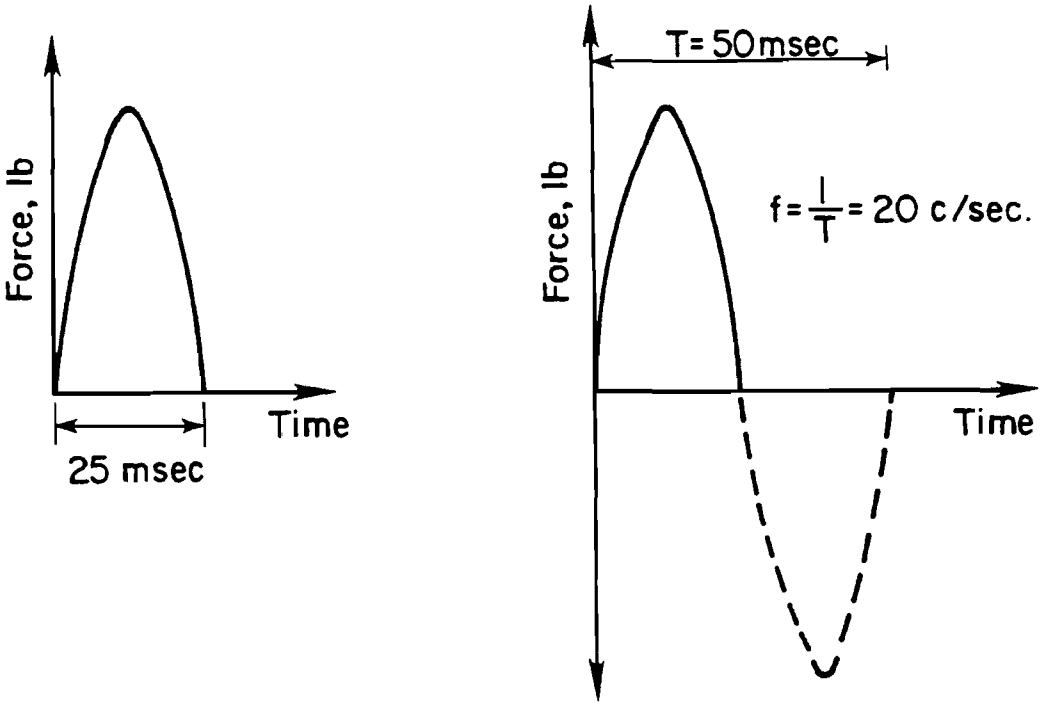

Fig 3.21. Idealized load-time history of FWD for determination of predominant frequency.

A very simplified dynamic analysis of the FWD is to examine the behavior of waves propagating in a hypothetical column under the loading plate. Results of a preliminary study using an idealized load-time history of the FWD on a homogeneous and isotropic elastic half space is presented in Appendix A. The model was used to generate deflection-time histories and the distribution of vertical stress in the medium under an impulse. An important and interesting finding is that the theoretical vertical stress distribution and deflection-time history under an FWD pulse are similar to measured signals of the FWD as illustrated in Fig 2.4.

It can be seen that until the present time not much attention was paid to developing dynamic analysis procedures using the wave propagation for the interpretation of dynamic NDT data of pavements. Dynamic analysis of dynamic deflection data involves the use of research performed in seismic analysis and structural dynamics areas. A very brief discussion of this topic was presented above to emphasize the need for further research in this area. In the meantime, layered elastic theory provides the best approach to modeling pavement behavior for interpretation of NDT data.

SUMMARY

This chapter presents a literature review of analytical procedures for interpretation of dynamic deflection data generated with NDT devices. Various deflection basin parameters are defined and their applications and limitations were discussed. Available analytical models for analyzing pavement behavior were briefly described. The mechanistic models commonly used for evaluation of NDT data were reviewed. Next, procedures to derive Young's moduli of pavement layers from dynamic deflection data were reviewed; they include use of graphs and nomographs based on basin parameters and self iterative procedures involving the inverse application of layered elastic theory. Concepts of dynamic analysis of NDT devices such as the Dynaflect and FWD using the stress wave propagation approach were also briefly presented. It has been concluded that the layered elastic theory can be

effectively used to analyze the dynamic deflection basins for insitu material characterization of a pavement-subgrade system.

CHAPTER 4. INSITU MATERIAL CHARACTERIZATION BASED ON DYNAMIC DEFLECTION DATA

INTRODUCTION

General

Nondestructive testing of pavements is performed by measuring dynamic deflection basins, which is an important part of the inservice monitoring of pavements at the project level of the pavement management process. In those places where pavement management concepts are still not in practice, dynamic deflection basins must still be measured before any major rehabilitation program is planned. In each case the data are collected for specific purposes using established procedures of the user agency. For example, Uddin et al (Ref 62) identified the following purposes for which Dynaflect deflection data are collected on rigid pavements:

(1) insitu material characterization,
(2) void detection studies,
(3) load transfer studies across joints and cracks, and
(4) reflection cracking analysis prior to placing flexible overlays.

The positioning of the Dynaflect on the pavement depends on the purpose for which deflection data are to be evaluated later. Keeping in view the main objectives of this study, i.e., structural evaluation, the research presented in this document is directed towards mechanistic interpretation of the dynamic deflection basins measured for the purpose of insitu material characterization. The specific procedures pertaining to positioning of the NDT device on the pavement, testing sequence, sample size and frequency of tests, replication requirements, time and season of testing, and any necessary correction or adjustment applied to raw data are not addressed in

this study. The reader is referred to the established practice or the recommended testing procedures in Ref 62.

Dynamic deflection basins measured for the purpose of insitu material characterization are analyzed to derive insitu Young's moduli of pavement layers which is the first step in a structural evaluation system. The second step is to correct moduli of the pavement material which exhibit nonlinear benavior or temperature sensitivity. The majority of the existing evaluation procedures stop here, and further application of the derived moduli is left to the user's discretion. In order to develop a comprehensive structural evaluation system in this study, additional analyses will be incorporated for (1) calculation of critical stress or strain, (2) estimation of fatigue life using the critical response, and (3) determination of remaining life of the pavement. Plots of remaining life and pavement moduli with distance along the pavement can then be used to identify areas which need an overlay and to calculate design moduli value. The insitu Young's moduli are used for overlay design using recently developed mechanistic procedures for overlay design. An important concept used in this study is to treat every deflection basin on an individual basis for analysis. This chapter is devoted to the first step in the structural evaluation system, i.e., development of a self iterative model to derive insitu pavement moduli.

Computer Program for Structural Response Calculations

Several existing and operational structural response models were reviewed in Chapter 3. Layered elastic theory programs were found to be the most powerful method for analyzing deflection basins as well as for any subsequent overlay design. The possible limitation of not considering a dynamic loading mode in a solution based on layered theory is also discussed in the last section of Chapter 3. At the present state of our knowledge layered theory programs are the most suitable means for mechanistic interpretation of dynamic deflection basins for all practical purposes. A number of computer programs based on layered elastic theory are available to researchers (Table 3.2). Computer programs ELSYM5 (Ref 18) and BISAR (Ref 35) were accessible for use in this study for the development of a structural

evaluation system. Figure 4.1 illustrates the comparison of theoretical deflection basins predicted for the Dynaflect loading and the geophone configuration. A basin predicted by ELSYM5 is shown in solid lines and broken lines represent BISAR predictions for rigid pavement. The predicted deflections match very closely except under the loading wheel, where BISAR slightly over predicts. For a flexible pavement, comparison of predicted basins is shown in Fig 4.2. For all practical purposes, the slight difference between the predictions from these two programs can be ignored as neither of the two models can predict exact behavior of a pavement. Previous experience using these two programs at The University of Texas at Austin indicates that (1) input data manipulation is easier with ELSYM5, (2) in general ELSYM5 is more efficient, faster, and less expensive in computational cost than BISAR, and (3) ELSYM5 can be easily adopted as a subprogram. BISAR has additional capabilities such as handling more than five layers, horizontal loads, and variable friction at layer interfaces. For the purpose of this study, ELSYM5 can handle the requirements related to layers, vertical loads, locations of responses, and rock layer which are considered in this study. Therefore, ELSYM5 has been selected as the subprogram based on layered elastic theory for use in the development of a structural evaluation system. In addition, some of the preliminary work related to parametric studies on variables affecting Dynaflect deflection basins and generation of deflection basins based on factorial designs to develop simplified predictive equations for moduli was performed using LAYER8 and its interactive version BASFT2 (described in Ref 7). The deflection basins predicted from ELSYM5, LAYER8, and BASFT2 are virtually the same.

PARAMETERS INFLUENCING DEFLECTION BASIN

Parametric studies were carried out to evaluate (1) the effect of the rate of change of the input parameter on a deflection basin and (2) the input parameters which show very significant influence on the deflection basin.

	Young's Modulus (psi)
10 in. P.C. Concrete	4,000,000
4 in. A.C. Base	200,000
6 in. Subbase	40,000
Semi-infinite Subgrade	20,000

Radial Distance from load (in.)	F W D Deflections (mils/lb)		Radial Distance from load (in.)	DYNAFLECT Deflections (mils)	
	ELSYM5	BISAR		ELSYM5	BISAR
0.0	0.49	0.49			
12.0	0.44	0.44			
24.0	0.39	0.39	10.0	0.45	0.46
36.0	0.33	0.33	15.6	0.43	0.43
48.0	0.29	0.29	26.0	0.38	0.38
60.0	0.24	0.24	37.4	0.33	0.33
72.0	0.21	0.21	49.0	0.28	0.24

Fig 4.1. Comparison of responses from ELSYM5 and BISAR for a rigid pavement.

	Young's Modulus (psi)
2.5 in A.C. Surfacing	500,000
15.0 in Flexible Base	80,000
Semi-infinite Subgrade	30,000

F W D			DYNAFLECT		
Radial Distance from load (in.)	Deflections (mils/lb)		Radial Distance from load (in.)	Deflections (mils)	
	ELSYM5	BISAR		ELSYM5	BISAR
0.0	1.25	1.25			
12.0	0.60	0.60	10.0	0.67	0.67
24.0	0.36	0.36	15.6	0.49	0.50
36.0	0.26	0.26	26.0	0.34	0.34
48.0	0.19	0.19	37.4	0.25	0.25
60.0	0.15	0.15	49.0	0.19	0.19
72.0	0.13	0.13			

Fig 4.2. Comparison of responses from ELSYM5 and BISAR for a flexible pavement.

Young's Moduli of Pavement Layers

The basin fitting procedure for deriving insitu moduli basically relies on making appropriate changes in an initial set of assumed moduli through a number of iterations. Studies were therefore made to find out suitable rates of change in each modulus which can be related to the discrepancies in calculated and measured deflections. This was accomplished by assuming a typical pavement structure of known properties and then varying one of the E values while keeping the other E's fixed at their original values. First the E value was doubled and a deflection basin was calculated then another basin was compured with the E value reduced to half of its original value. During this parametric study for a pavement structure, all other input parameters, such as thicknesses and Poisson's ratios, were fixed.

Rigid Pavements. One of the objectives of this study is to develop structural evaluation procedures applicable to dynamic deflection basins measured either by Dynaflect or FWD. All the deflection basins referred to in these sections are theoretical and pavement is assumed to be a linearly elastic system. Therefore in general, the FWD deflection basin (plotted using a deflection normalized with respect to a 1000-lb peak load as discussed in Chapter 2, Fig 2.9) coincides with the corresponding Dynaflect deflection basin, as illustrated in Fig 4.3 for a three-layer pavement. A parametric study has been reported by Uddin et al (Ref 7) to investigate the influence of the rate of change of E's on theoretical Dynaflect deflection basins. The rigid pavement structure and initial input data used in that study are shown in Fig 4.4. E_1, E_2, E_3, and E_4 are Young's moduli of elasticity for the surface concrete layer, asphaltic concrete base, lime-treated subbase, and subgrade. In the first part of the study (Ref 7) a semi infinite subgrade was assumed. The findings summarized by Uddin et al are stated below.

(1) An increase in the previous value of the elastic modulus of any layer is accompanied by a decrease in the calculated deflections of all sensors. Also, a decrease in the original value of the elastic

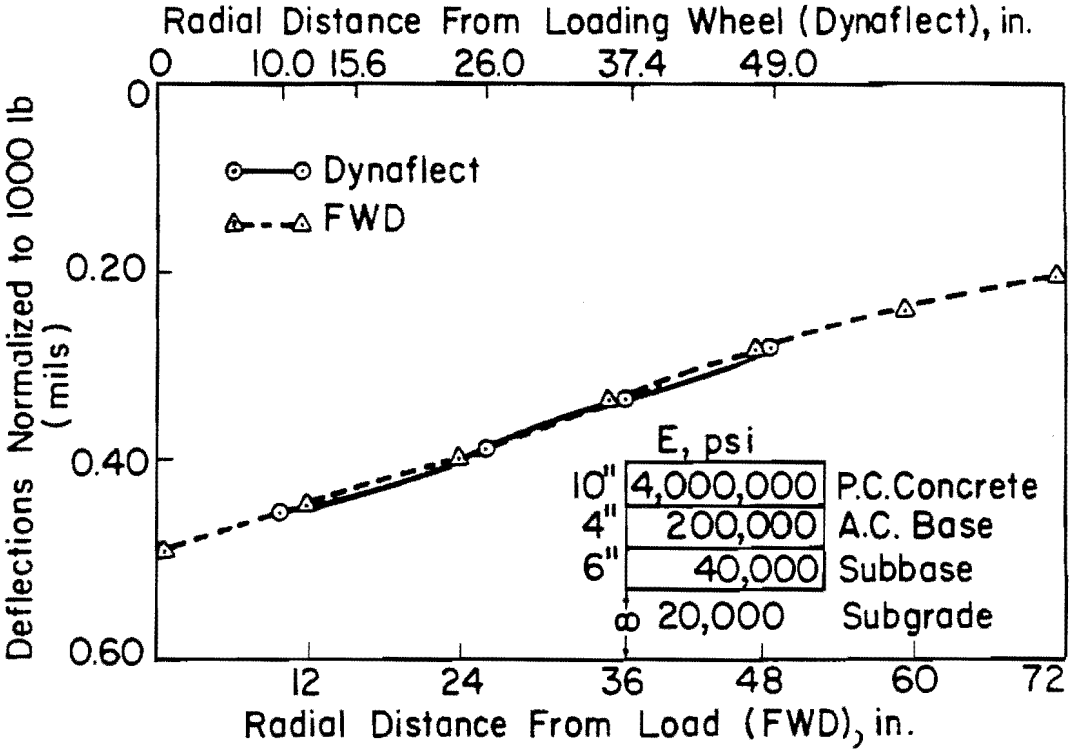

Fig 4.3. Theoretical deflection basins of Dynaflect and FWD.

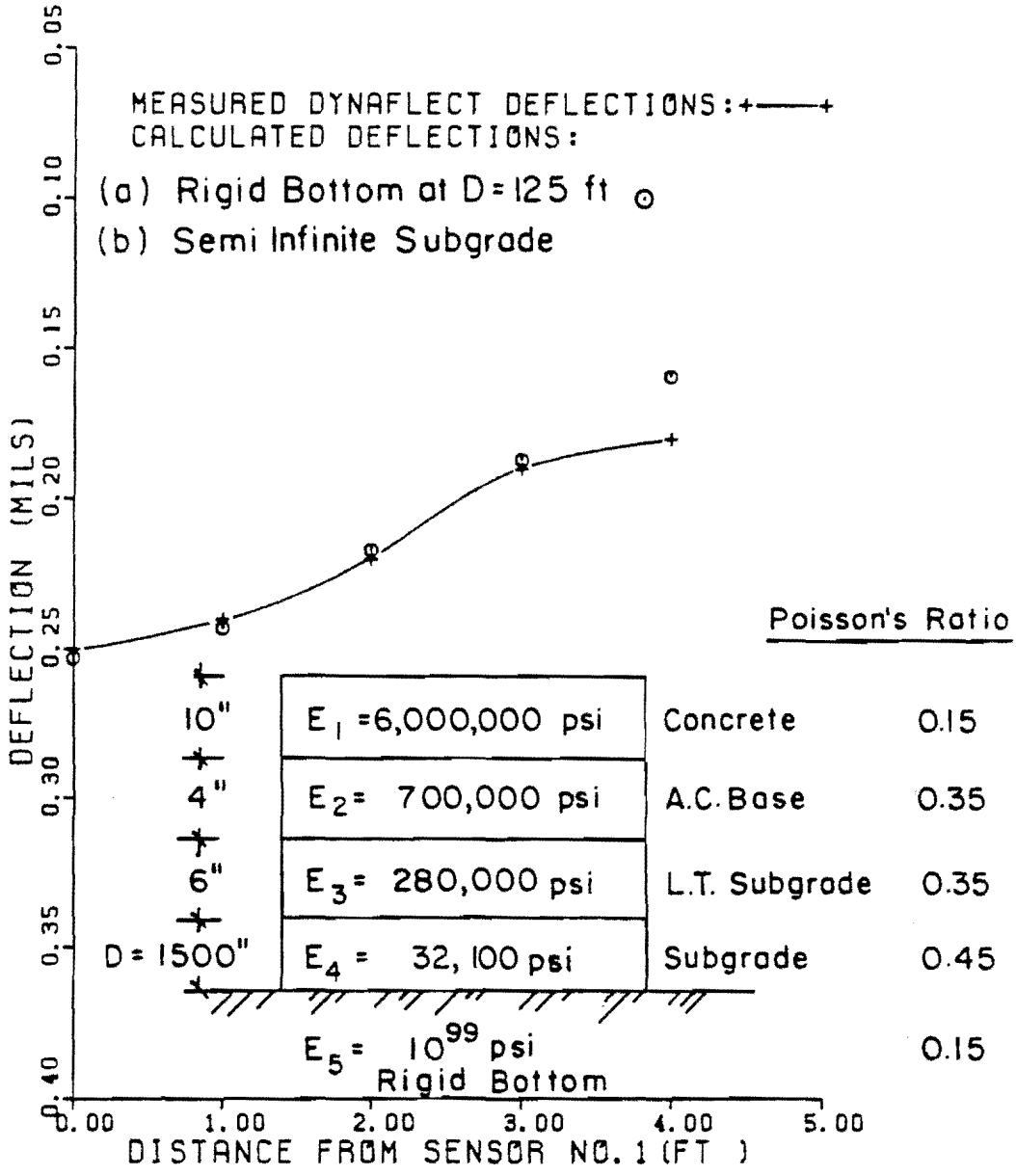

Fig 4.4. The back calculated Young's moduli (case of rigid bottom under 125 ft. of natural subgrade).

modulus of any layer is associated with a corresponding increase in the deflections of all sensors.

(2) Any increase or decrease in any of the elastic moduli, E_1, E_2, and E_3 shows a corresponding but opposite change in the calculated deflections. However any change in E_4 is accompanied by a relatively higher percent decrease or increase in the calculated deflections.

(3) In all cases the relative change in the calculated deflections (due to a change in an elastic modulus) is not the same for all sensors. In general sensors closer to the load exhibit the largest change and the farthest sensor exhibits the least change.

(4) The calculated Dynaflect deflection basins corresponding to changes in elastic modulus of each layer, reveal the following:

   (a) If E_4 is increased by 100 percent (an increase of 32,100 psi), the deflection at sensor 5 is reduced by 46 percent and the deflection at sensor 1 is decreased by 37 percent from the original value. Therefore E_4 can be used to match sensor 5 deflection or vice versa.

   (b) For this pavement structure, a change in E_1 affects the deflection at sensor 1 more than that at sensor 5. For example, if E_1 is decreased by 50 percent, the calculated deflections at sensors 1 and 2 are increased by 14 and 10 percent respectively, whereas the deflection at sensor 5 is increased by only 4 percent. Therefore E_1 can be effectively used for matching sensors 1 and 2 deflections.

   (c) The deflection basin is the least sensitive to changes in E and E_3.

Similar observations were made for a parametric study when a finite subgrade 1500 inches thick was assumed. The following conceptual relationship is based on the results of the study described above:

$$\Delta E_i \approx f(\Delta d_j) \tag{4.1}$$

where ΔE_i represents a predicted change in the present value of the modulus of the i^{th} layer and Δd_j stands for a discrepancy between the original deflection and its present value corresponding to the j^{th} sensor where j can take any value (s) from 1 to 5 for the Dynaflect or 1 to 7 for the FWD. For a four-layer rigid pavement and Dynaflect testing, the following approximate relationships are conceptually formed:

$$\Delta E_4 \simeq f(\Delta d_5) \tag{4.2}$$

$$\Delta E_3 \simeq f(\Delta d_1, \Delta d_k) \tag{4.3}$$

$$\Delta E_2 \simeq f(\Delta d_1, \Delta d_k) \tag{4.4}$$

$$\Delta E_1 \simeq f(\Delta d_1) \tag{4.5}$$

where k stands for all intermediate sensors. In the case of FWD, Δd_5 in Eq 4.2 can be replaced by Δd_6. Equation 4.2 can be used to predict appropriate change in the modulus of the subgrade layer from the discrepancy observed in the farthest sensor (more than 4 feet away from the load). The high correlation between the sensor 5 deflection of the Dynaflect and the subgrade modulus has been used by Taute et al to predict the subgrade modulus (Ref 23). As was found earlier, the deflection basin is relatively insensitive to changes in the moduli of intermediate layers; therefore, it is

very difficult to arrive at unique values of E_2 and E_3. This is also obvious from Eqs 4.3 and 4.4. Additional checks are to be provided to ensure obtaining reasonable moduli values of intermediate layers. If the discrepancy in the first sensor is very large as compared to the intermediate sensors, then the relationship in Eq 4.5 can be used to correct surface concrete modulus before proceeding to the moduli of intermediate layers. The most significant parameter influencing a deflection basin is the subgrade modulus.

Flexible Pavement. A parametric study was also made to investigate the effect of the rate of change of Young's moduli on deflection basin. The flexible pavement used in the study is shown in Fig 4.5 with the material properties and thickness information. The normalized deflection basin of the FWD and the Dynaflect deflection basin calculated for this pavement are shown in Fig 4.6. The FWD configuration with 10,000 lb of peak force was assumed in these parametric studies. FWD deflections at the locations of seven sensors are shown by triangles. Theoretical deflections at Dynaflect sensor locations are plotted with circles. The two theoretical deflection basins virtually coincide, which is expected as the pavement is being analyzed assuming a linear system. Therefore it is reasonable to extend the inferences deduced from these studies of theoretical Dynaflect deflection basins to FWD.

The methodology used in the parametric study to see the effect of the rate of change of moduli in the case of flexible pavement (Fig 4.5) is the same as described in the preceding section for rigid pavement. Results are plotted in Fig 4.7(a) to (d). It is observed that the deflection basin is very sensitive to E_4, the subgrade modulus. This finding is the same for rigid pavement. Any change in any modulus causes a corresponding change in deflections, which is opposite in sign. Changes in the moduli of the top two layers are reflected mostly in sensors closer to the load, which are the first 2 sensors for Dynaflect. For the FWD, the first three sensors will show the effect of changing E_1 and E_2. Comparing the effects of equal amount of increase or decrease in E_1 and E_2; E_2 causes a relatively higher variation in the sensor 1 (Dynaflect) deflection (about 11-13 percent) as compared to

	Young's Modulus (psi)	Poisson's ratio
6 in. A.C. Surfacing	400,000	0.35
8 in Stabilized Base	100,000	0.35
12 in. Subbase	45,000	0.40
Semi-infinite Subgrade	20,000	0.45

Fig 4.5. Flexible pavement structure used in the parametric studies.

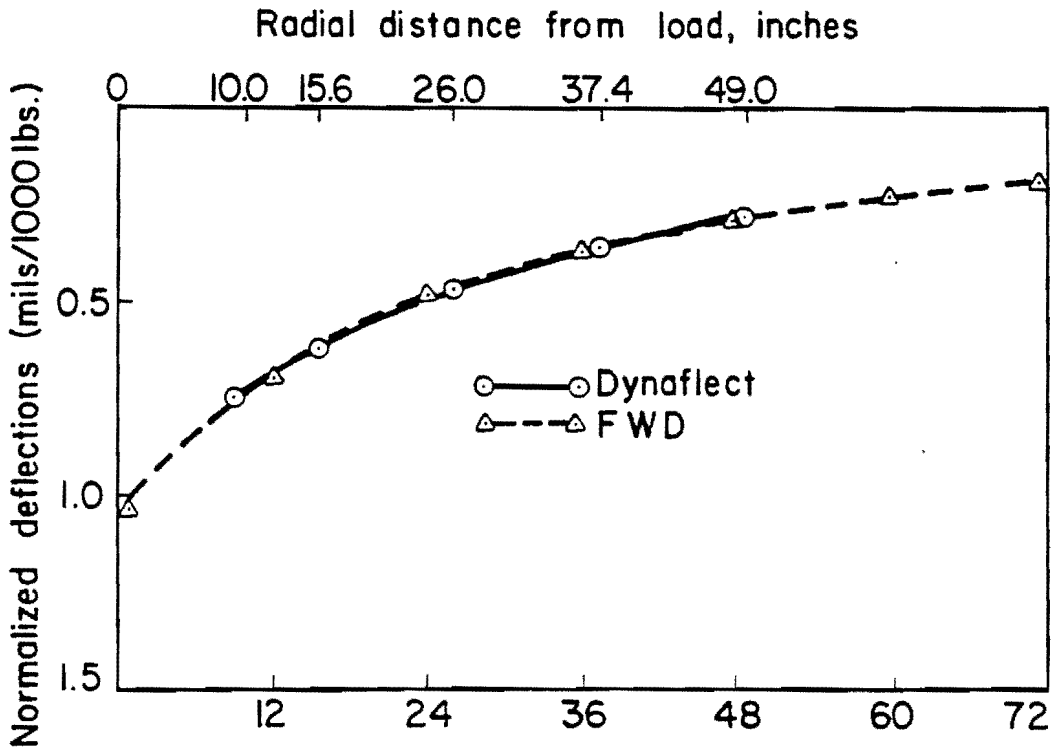

Fig 4.6. Theoretical deflection basins for the flexible pavement shown in Fig 4.5.

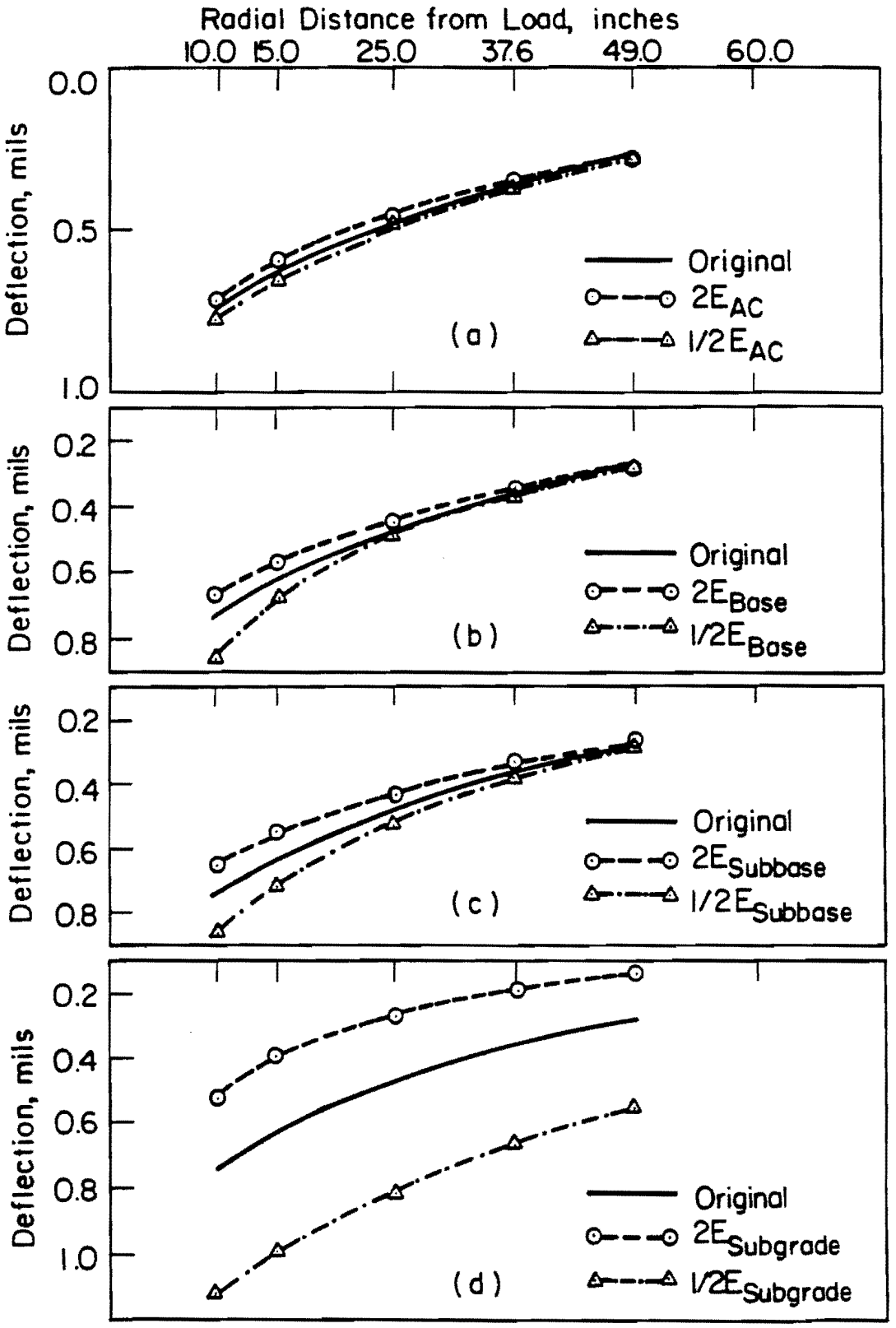

Fig 4.7. Effect of rate of change of moduli on theoretical Dynaflect deflection basins for the flexible pavement illustrated in Fig 4.5.

the change (4-5 percent) caused by the new E_1. These plots also indicate the following:

(1) Deflection at the farthest sensor (more than 4 feet from the load) is insensitive to any changes in E_1, E_2, or E_3. Therefore any discrepancy in the deflection of the farthest sensor can be attributed to a variation in E_4, or, in other words,

$$\Delta E_4 = f(\Delta d_5) \qquad (4.6)$$

The various terms have been defined earlier.

(2) The sensor 4 deflection for the Dynaflect (this corresponds to sensor 4 in FWD model 8000) is very sensitive to any change in E_3 or E_4. Assuming E_4 corresponds to the corrected value according to Eq 4.6, then a change in E_3 can be considered a function of a appropriate change in sensor 4. Therefore,

$$\Delta E_3 = f(\Delta d_4) \qquad (4.7)$$

Figure 4.7(a) to (d) also illustrates the merit of using 5 sensors (with the radial distance of the 5th sensor exceeding 4 feet) to establish the deflection basin. An FWD deflection basin with seven sensors (a maximum radial distance of 6 feet) is even better for identifying deflections away from loads which are sensitive to the moduli of lower layers.

(3) As noted earlier, deflections at the first three Dynaflect sensors are significantly sensitive to changes in E_1 and E_2.

Or

$$\Delta E_2 \simeq f(\Delta d_j) \tag{4.8}$$

and

$$\Delta E_1 \simeq f(\Delta d_j) \tag{4.9}$$

where j represents all the first three Dynaflect sensors.

However a change in E_2 causes nearly twice as much change in deflections at sensors 1 and 2 as caused by an equal change in E_1. Therefore, at first E_2 can be predicted by the deflection at the Dynaflect second sensor and sensor 1 can solely be related to E_1. The guidelines developed in these comparative studies will be utilized later in the self iterative model for deriving insitu moduli from dynamic deflection basins.

Poisson's Ratios of Pavement Layers

Poisson's ratio of each layer is another input parameter required in layered theory calculations for a theoretical deflection basin. Poisson's ratios of typical pavement materials are known to vary within very narrow ranges. Typical values of Poisson's ratios are presented in Table 4.1. Small deviations from the tabulated values do not cause significant differences in calculated deflections. It is also customary in the pavement design field to assume the established values for normal pavement materials and soils and not to make any measurements. However it is pointed out that pavement response is significantly affected by variations in Poisson's ratios

TABLE 4.1. RECOMMENDED VALUES OF POISSION'S RATIO FOR DIFFERENT PAVEMENT MATERIALS (REFS 38, 62)

Material Type	Range of Poisson's Ratio	Recommended Value
Portland cement concrete	.15 - .20	0.15
Asphaltic concrete	.25 - .35	0.35
Cement stabilized base	.20 - .30	0.30
Asphalt stabilized base	.25 - .35	0.35
Unbound granular base	.20 - .50	0.40
Granular subgrade	.30 - .50	0.40
Clayey or silty subgrades	.40 - .50	0.45
Lime treated subgrade		0.40

(especially of soils and granular material) in any dynamic analysis based on wave propagation (Refs 57, 58, 61).

Thickness Information for Pavement Layers

Thickness is an another important input parameter for layered theory computations. Thin pavements result generally in higher deflections, as compared to relatively thicker pavements. In the prediction of critical responses for pavement design and in the iterative procedure for deriving insitu moduli from measured pavement responses; the thickness input for layered theory computations is assumed to be exactly the same as the design thickness or insitu thickness. Parametric studies were made to investigate the sensitivity of theoretical Dynaflect deflection basins to variations in the thickness of pavement layers. The basic approach used in these studies is the same as that applied in the studies on the effect of the rate of change of a modulus value, described earlier. The effect of discrepancies in thickness on calculated deflections was studied by varying the original thickness of a layer by a factor of 2 or 1/2 while keeping all other input data fixed at original levels. This approach will facilitate estimating the effect of the rate of change of thickness of a layer in terms of percent variations in theoretical deflections. A semi-infinite subgrade was assumed in the thickness studies using Dynaflect loading. However the findings can be equally applied to normalized deflection basins of the FWD.

Rigid Pavements. The rigid pavement structure used in this parametric study is illustrated in Fig 4.8. The initial input information and the calculated Dynaflect deflection basin are also shown in the same figure. The results are summarized in Table 4.2. Graphical illustrations of the sensitivity of deflections to variations in a layer thickness are presented in Fig 4.9(a) to (c). The following observations are based on the results of this study:

(1) Any increase in thickness is reflected by a decrease in the calculated deflection at all sensors.

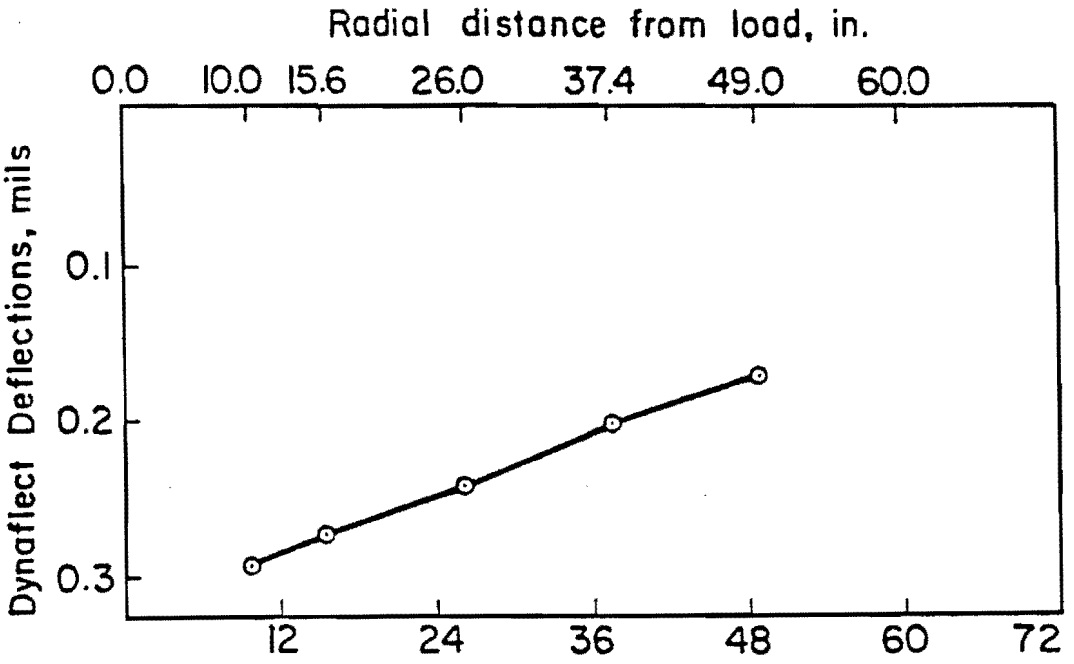

	Young's Modulus (psi)	Poisson's Ratio
10 in P.C. Concrete	4,000,000	0.15
4 in A.C. Base	500,000	0.35
6 in Lime treated	150,000	0.40
Semi-infinite Subgrade	32,500	0.45

Fig 4.8. The rigid pavement structure used in thickness study.

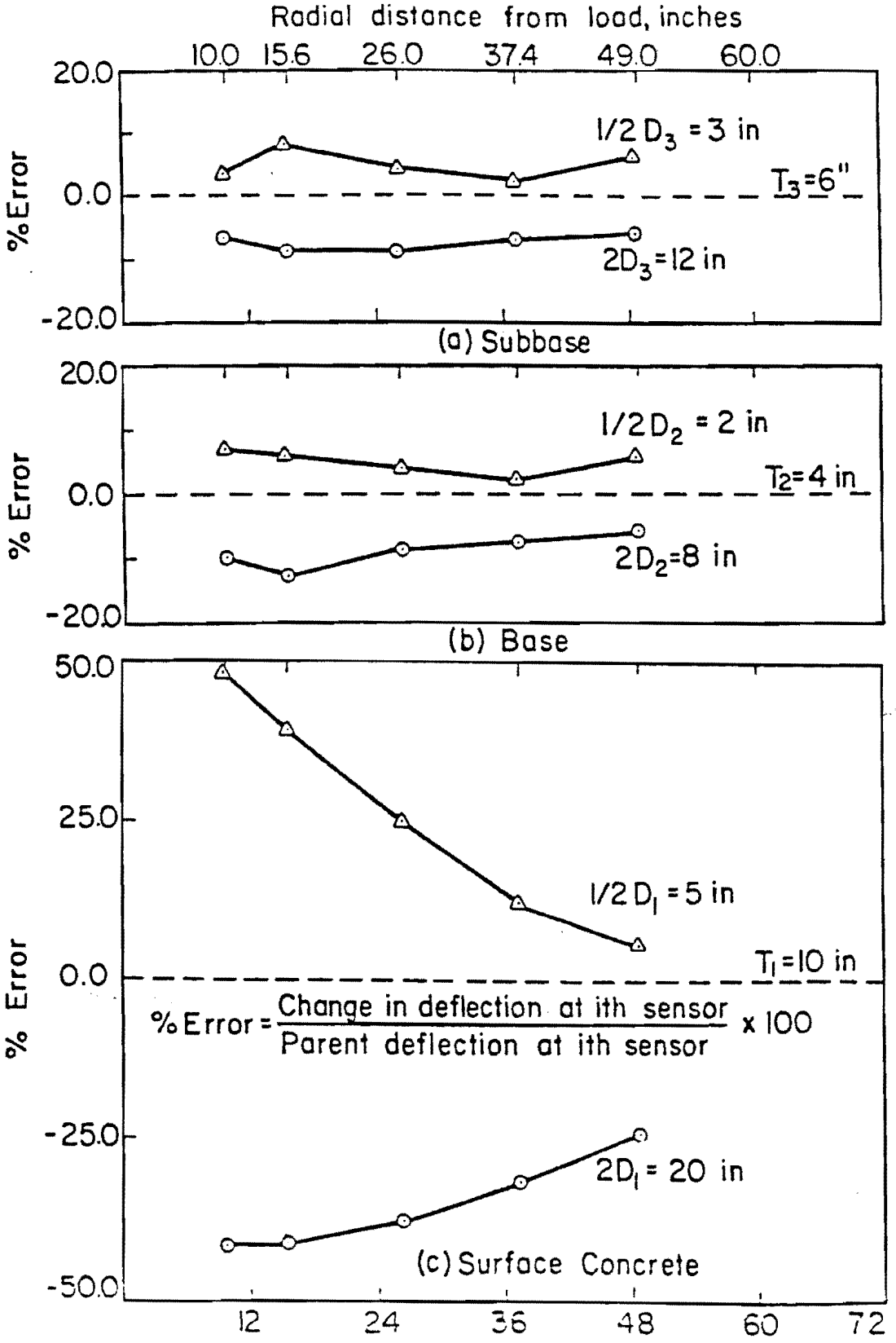

Fig 4.9. Effect of variations in thickness of pavement layers on theoretical Dynaflect deflections using rigid pavement of Fig 4.8.

TABLE 4.2. SUMMARY OF PARAMETRIC STUDY ON THICKNESS - RIGID PAVEMENT (DYNAFLECT LOADING)

E_1; D_1=10 in.	D_1=20 in.	D_1= 5 in.				
E_2; D_2= 4 in.			D_2=8 in.	D_2= 2 in.		
E_3; D_3= 6 in.					D_3= 12 in.	D_3= 3 in.
E_4, Semi-infinite Subgrade						

Sensor No.	Deflection, mils	Deflections, mils		Deflections, mils		Deflections, mils	
1	0.29	0.17 (-41.4%)	0.63 (+48.2%)	0.26 (-10.1%)	0.31 (+6.9%)	0.27 (-6.9%)	0.30 (+3.4%)
2	0.27	0.16 (-41.6%)	0.38 (+38.7%)	0.24 (-12.4%)	0.29 (+5.8%)	0.25 (-8.87%)	0.28 (+8.0%)
3	0.24	0.15 (-37.5%)	0.30 (+25.0%)	0.22 (- 8.3%)	0.25 (+4.2%)	0.22 (-8.3%)	0.25 (+4.2%)
4	0.20	0.14 (-31.7%)	0.23 (+12.2%)	0.19 (-7.3%)	0.21 (+2.4%)	0.19 (-7.3%)	0.21 (+2.4%)
5	0.17	0.13 (-23.5%)	0.18 (+ 5.9%)	0.16 (-5.9%)	0.18 (+5.9%)	0.16 (-5.9%)	0.18 (+5.9%)

E_1 = 4,000,000 psi (PC Concrete) E_2 = 5000,000 psi (AC Base)
E_3 = 150,000 psi (Stabilized Subbase) E_4 = 32,500 psi (Subgrade)

(Figures in parenthesis represent percent deviation from the deflections computed for the parent pavement structure.)

(2) The discrepancies observed in calculated deflections do not show any linear relationship with the rate of change of the thickness of a layer. In other words, the discrepancy in deflections caused by an increase in the thickness of the layer is not the same as that resulting from an equal reduction in the original thickness of that layer. This is particularly true for sensors close to the load.

(3) In general, sensors closer to the load (the first two sensors of the Dynaflect) are more sensitive to variations in thickness. Considering the same rates of change of thickness of all the top three layers, the surface layer shows the most significant influence on the relative discrepancies of deflections of these sensors.

Therefore, it can be concluded that a discrepancy in the thickness of the surface concrete layer will result in relatively large errors in the theoretical deflections as compared to the effect of variations in the thickness of intermediate layers.

Flexible Pavements. The flexible pavement and its input data used in the thickness study are shown in Fig 4.5. The procedure of varying the thickness of each of the top three layers of this four-layer pavement was the same as described above for the rigid pavement. The resulting calculated Dynaflect deflection basins are summarized in Table 4.3. The results of this study are essentially similar to conclusions (1) to (4) made for the rigid pavement case. Additionally it is observed that the sensor 5 deflection is insensitive to $\pm$ 100 percent variations in thickness of the surface asphaltic concrete layer and the influence on sensor 1 deflection is less pronounced compared to the influence of variations in the thickness of the surface concrete layer (of rigid pavement).

DEVELOPMENT OF A SELF ITERATIVE MODEL FOR CALCULATING INSITU YOUNG'S MODULI

The basic approach to deriving insitu moduli based on fitting a dynamic deflection basin by applying successive corrections in the initially assumed

TABLE 4.3. SUMMARY OF PARAMETRIC STUDY OF THICKNESS - FLEXIBLE PAVEMENT (DYNAFLECT LOADING)

E_1; D_1= 6 in.	D_1=12 in.	D_1=3 in.				
E_2; D_2= 8 in.			D_2=16 in.	D_2=4 in.		
E_3; D_3=12 in.					D_3=24 in.	D_3=6 in.
E_4; Semi-infinite Subgrade						

Sensor No.	Deflection, mils	Deflections, mils		Deflections, mils		Deflections, mils	
1	0.75	0.57 (-24.0%)	0.85 (+13.3%)	0.61 (-18.7%)	0.85 (+13.3%)	0.68 (-9.3%)	0.80 (+6.7%)
2	0.62	0.50 (-19.3%)	0.60 (+ 9.7%)	0.51 (-17.8%)	0.69 (+11.3%)	0.56 (-11.3%)	0.67 (+8.1%)
3	0.47	0.41 (-12.8%)	0.49 (+4.2%)	0.40 (-14.9%)	0.50 (+6.4%)	0.42 (-10.6%)	0.50 (+6.3%)
4	0.36	0.34 (- 5.5%)	0.37 (+2.8%)	0.33 (-8.3%)	0.37 (+2.8%)	0.33 (-8.3%)	0.37 (+2.8%)
5	0.28	0.28 (0.0%)	0.28 (0.0%)	0.27 (-3.6%)	0.28 (0.0%)	0.27 (-3.5%)	0.29 (+3.6%)

E_1 = 400,000 psi (AC Surface) E_2 = 110,000 psi (Stabilized Base)

E_3 = 45,000 psi (Granular Subbase) E_4 = 20,000 psi (Subgrade)

(Figures in parenthesis represent percent deviation from the deflections computed for the parent pavement structure.)

moduli and layered theory computations is discussed in this section. A self iterative procedure could be developed after consideration of certain assumptions related to input parameters and output response, establishing tolerances in deflections, moduli, criterion of acceptable limits for moduli, and consideration of the finite thickness of the subgrade. This section is devoted to a detailed description of the self iterative model developed in this study.

Assumptions

A set of simplified assumptions are necessary to validate the application of layered theory for determining insitu moduli from a deflection basin. The assumptions can be separated into two groups:

(1) The first assumptions are inherent with the use of layered linear elastic theory to calculate pavement structural response. These are related to material properties, thickness information, and boundary conditions, as described earlier in detail in Chapter 3 in the section on mechanistic models for NDT evaluation.

(2) The second group of assumptions are required for application of layered theory to analyze the NDT data of a pavement in existing condition as listed below:

   (a) The existing pavement is considered to be a layered linearly elastic system. Therefore, the principle of superposition is valid for calculating pavement response due to more than one load.

   (b) The peak-to-peak dynamic force of 1000 lbs of the Dynaflect is modelled as two pseudo static loads of 500 lb. each uniformly distributed on circular areas (167 lb./sq in. on each circular area). The peak dynamic force of the FWD is assumed to be equal to a pseudo static load uniformly distributed on a circular area with a radius 5.9 inches (i.e., the radius of the FWD loading plate).

(c) The thickness of each layer is assumed to be known and exact. All layers are assumed to be in perfect contact, parallel to each other, and extending to infinity in the horizontal plane. For rigid pavements, the deflection basin is to be measured with the loading in the midspan position between joints or transverse cracks (as recommended by Ref 62) and far enough from pavement edge to satisfy this assumption.

(d) The theoretical static deflections are assumed to be the same as measured dynamic deflections (i.e., peak-to-peak deflection of the Dynaflect and peak value of the FWD deflection signal).

(e) The subgrade is to be characterized by assigning an average value to its modulus of elasticity.

Methodology

Procedure of Successive Correction. The review of existing self iterative procedures (Table 3.2) and findings of the parametric studies described earlier in this chapter have resulted in the formulation of a self iterative methodology for determining a set of Young's moduli of pavement layers based on a best fit of measured deflection basin within reasonable tolerances. The methodology relies on generating theoretical deflection basins using ELSYM5 and changing the initial values of assumed moduli through a procedure of successive correction in order to obtain a best fit of the measured deflection basin. The discrepancies in theoretical and measured deflections have been related to required corrections in the preceding values of moduli. The correction procedure is designed to handle deflection basins of the Dynaflect and FWD. A conceptual treatment of the procedure of successive correction is presented below:

$$ERR_j = DEFM_j - DEF_j \qquad (4.10)$$

and

$$ERRP_j = 100\ (ERR_j/DEFM_j) \qquad (4.11)$$

where the subscript j refers to deflection sensors (j = 1 to 5 for the Dynaflect; j = 1 to 7 for the FWD),

$DEFM_j$ = deflection measured at the j^{th} sensor,
DEF_j = deflection calculated at the j^{th} sensor,
ERR_j = error in measured and calculated deflection at the j^{th} sensor, and
$ERRP_j$ = percent error in measured and calculated deflection.

To start with, deflections are calculated from the initial input values of moduli referred to as seed moduli in this study. The first cycle of iterations is equal to the number of layers in the pavement. In each set, the first iteration is made to correct the subgrade modulus, ELSYM5 is then called to calculate theoretical deflections. The procedure of successive correction to the modulus of the next upper layer and use of ELSYM5 to calculate theoretical deflections is continued until moduli of all layers have been checked for correction. Then another cycle starts from the subgrade layer. The relationship used in the procedure of successive correction is given below in the generalized form:

$$ENEW_i = E_i\ (1.0 - CORR_i \times ERRP_k \times 0.5) \qquad (4.12)$$

where

$ENEW_i$ = corrected value of Young's modulus of the i^{th} layer,

E_i = value of Young's modulus of the i^{th} layer in the previous iteration (in the first iteration, it is the seed modulus),

$CORR_i$ = correction factor (for the i^{th} layer) applied to the discrepancy in measured deflection and calculated deflection, and

$ERRP_k$ = discrepancy in calculated (based on E_i's) and measured deflections of the k^{th} sensor(s) in terms of percent error as calculated in Eq 4.11.

Only half of the discrepancy in measured and calculated deflections is meant to be removed by applying appropriate correction to the corresponding modulus value. The correction factors ($CORR_i$'s) have been based on the parametric studies described earlier concerning the influence of the rate of change of moduli on deflection basins. A set of three correction factors is used in the self iterative procedure for rigid pavement. A separate set of three factors has been selected for flexible pavements. These correction factors are presented in Table 4.4. $CORR_1$ is the correction factor for the modulus of the surface layer; $CORR_M$ is for all intermediate layers and $CORR_L$ is assigned for the subgrade layer. A number of additional measures are implemented in the self iterative model to ensure efficiency, reliability, and accuracy of the finally derived moduli, which are discussed in the next section. Iterations are stopped whenever one of the following occurs.

(1) permissible tolerance in the maximum absolute discrepancy among calculated and measured deflections is exceeded,

(2) any correction in a modulus value causes the discrepancies in calculated and measured deflections to increase. This is an important criterion to ensure that the solution is not going in the wrong direction.

(3) the allowable maximum number of iterations is exceeded.

TABLE 4.4. CORRECTION FACTORS FOR USE IN THE PROCEDURE OF SUCCESSIVE CORRECTION (FOR BASIN FITTING ROUTINES)

PAVEMENT TYPE	PROGRAM	CORRECTION FACTORS		
		CORR1[1]	CORRM[2]	CORRL[3]
RIGID	PREDD1 (Subroutine BASINR)	0.050	0.100	0.015
FLEXIBLE	FPEDD1 (Subroutine BASINF)	0.150	0.180	0.019

[1]For correction in the modulus of surface layer.

[2]For correction in the moduli of intermediate layers.

[3]For correction in the modulus of subgrade.

Algorithm of Self Iterative Model. A simplified flow diagram of the self iterative procedure for determining insitu Young's moduli from the deflection basin is illustrated in Fig 4.10. The procedure was initially developed and evaluated for the analysis of a four-layer pavement model as discussed below. Later the algorithm was modified to handle a three-layer pavement model. Basic steps followed in the algorithm are described below.

(1) Input: Number of layers; type of base/subbase material (granular or stabilized); NDT device type (FWD or Dynaflect); data related to FWD peak force and size of loading plate; measured deflections in mils (corresponding to 5 sensors for the Dynaflect and 6 or 7 sensors for the FWD); information related to each layer, such as thickness, Poisson's ratio, initial seed modulus, maximum and minimum permissible values of modulus; maximum number of iterations; tolerances related to discrepancies in deflections and change in a modulus values.

(2) Default Parameters: All tolerances are provided with default values. The default maximum number of iterations is 10. Additionally, default procedures are provided for seed moduli and permissible ranges of moduli of different pavement material. The provision of default values of seed moduli is an important step of the self iterative model developed in this study and contributes a significant improvement over other previously reviewed self iterative procedures. It helps to reduce the number of iterations required for convergence of the iterative procedure and ensures a unique set of moduli. The validity of uniqueness will be dealt with in a separate section.

(3) If the original flexible pavement is of three layers, the program creates an additional layer from the top 6 inches of the last layer. However, throughout the program, checks are provided to obtain the same moduli for the third and fourth layers. The same Poisson's ratios are assigned to both layers.

(4) If the user wishes to consider an arbitrary rock layer under a finite thickness of subgrade, that is possible through a default procedure.

(5) Before starting iterations, all the initial seed moduli and the ranges of modulus of each layer are checked to ensure that these remain

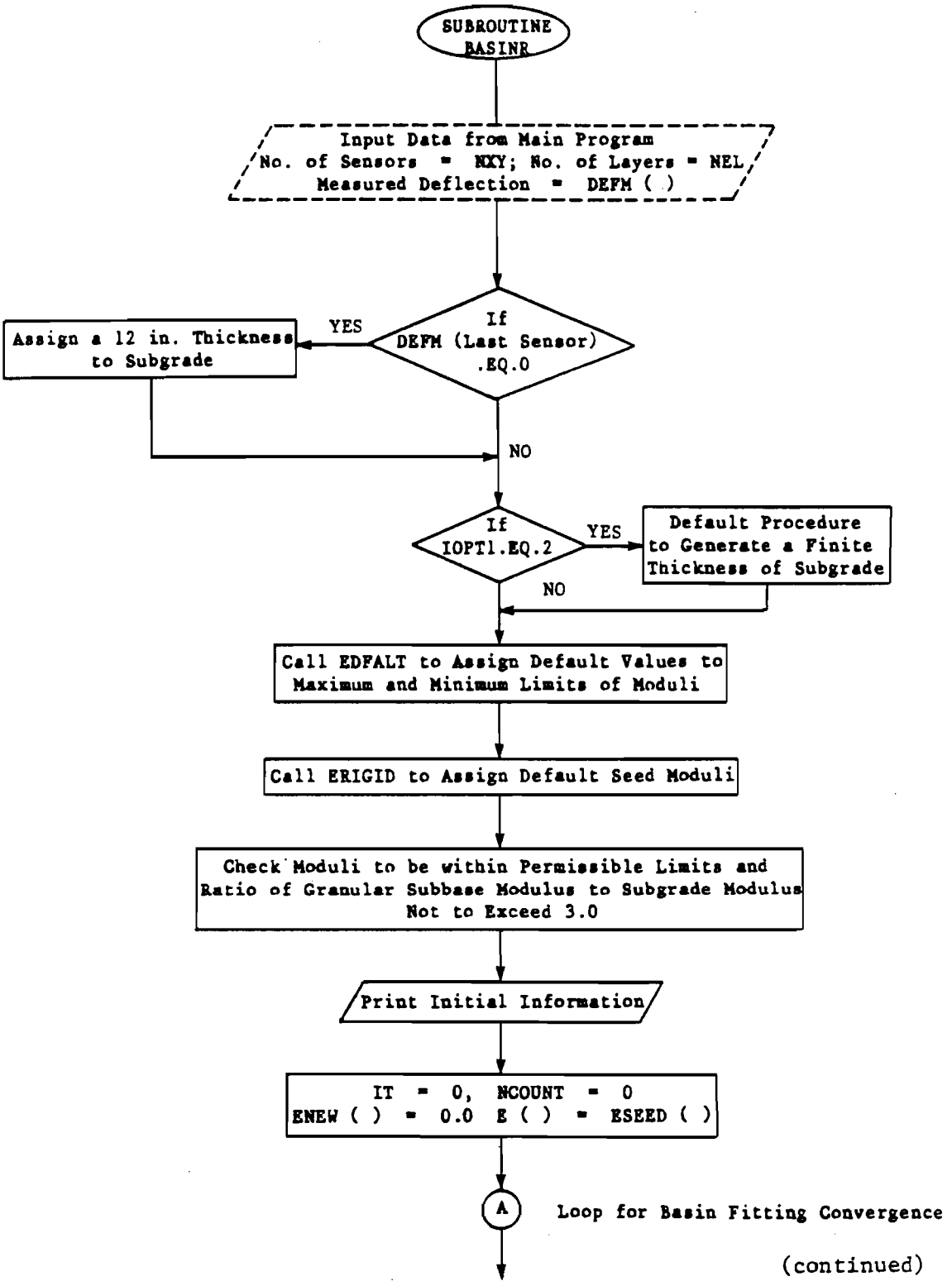

Fig 4.10. Simplified flow diagram of BASINR (for rigid pavement evaluation program RPEDD1).

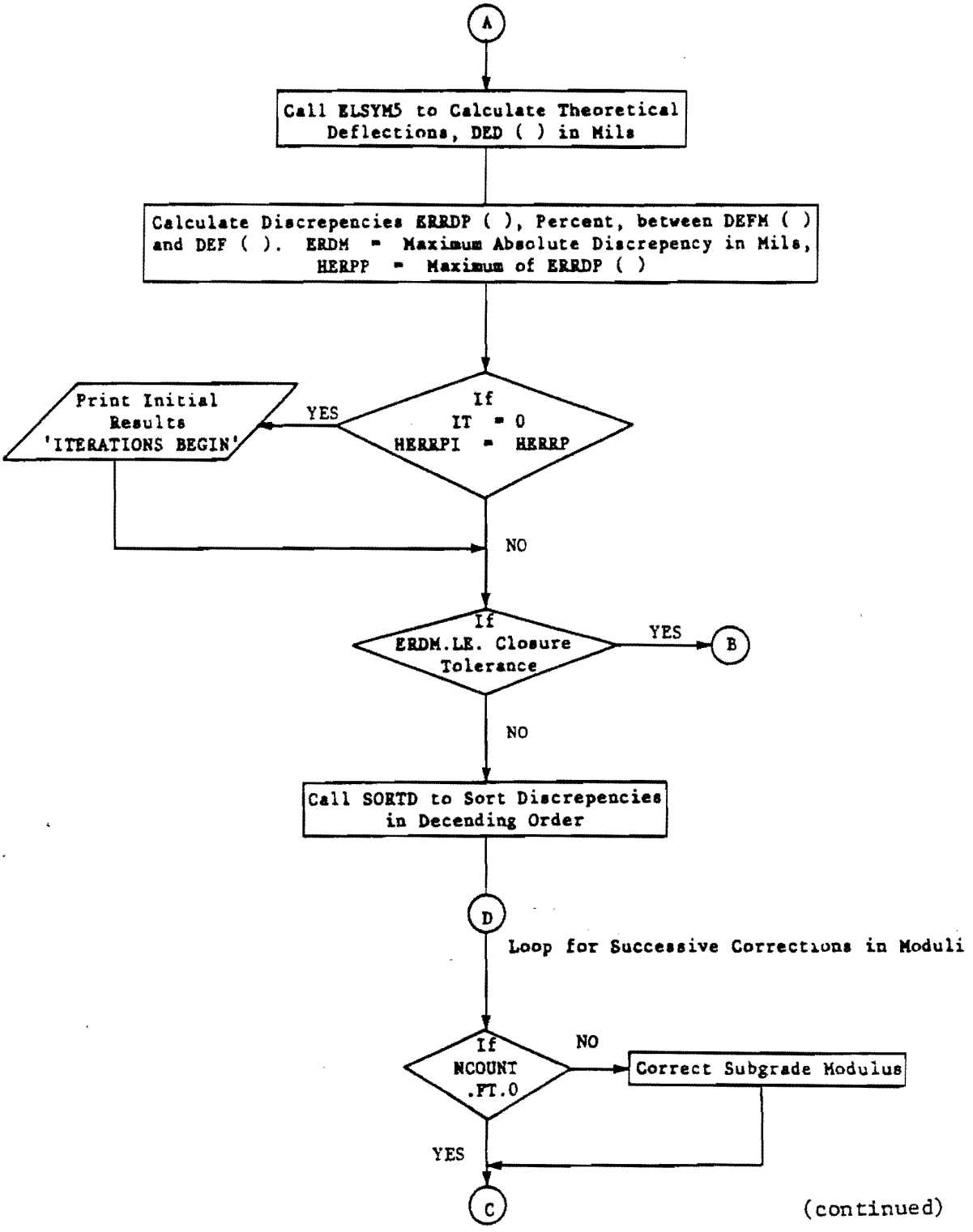

Fig 4.10. (continued).

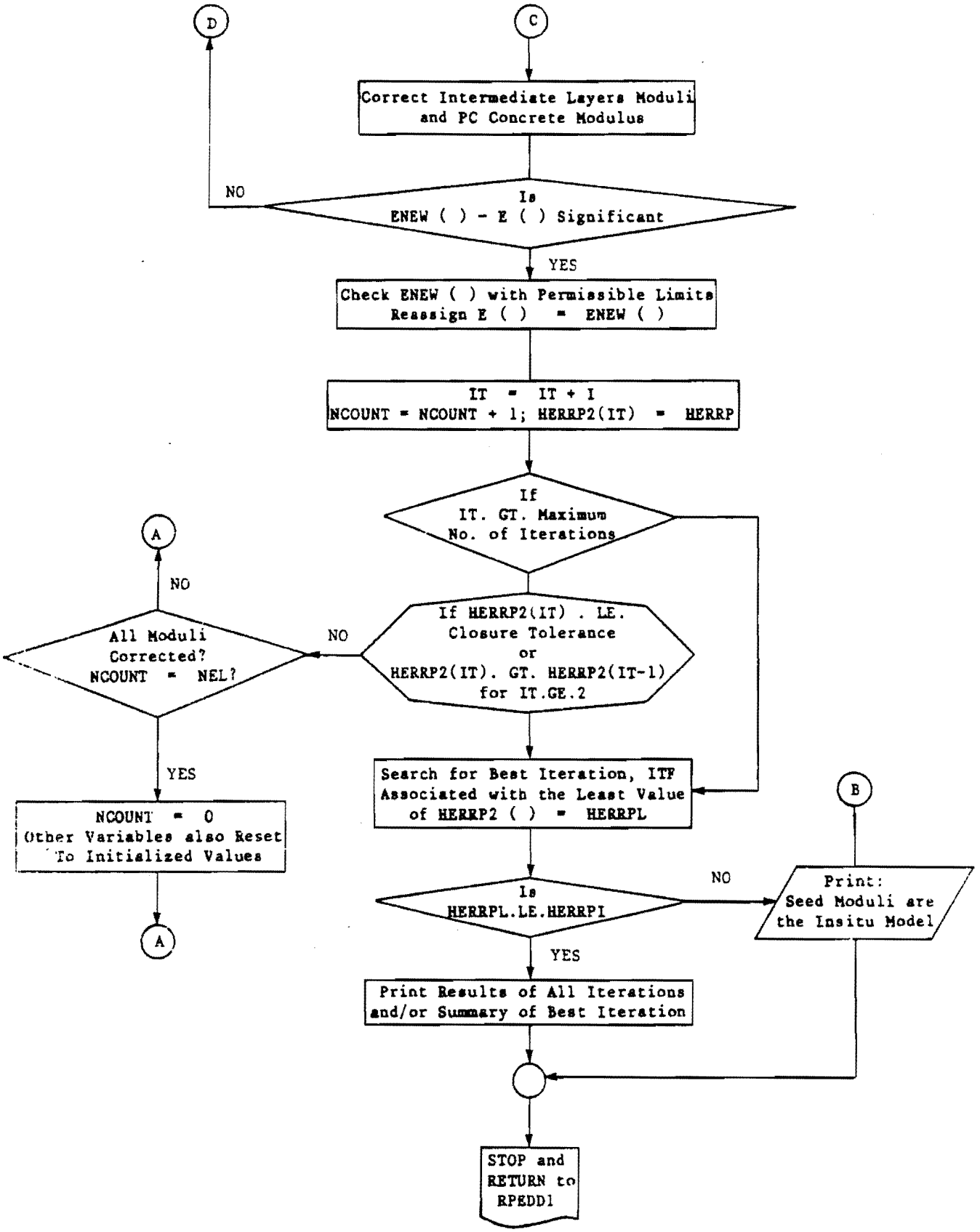

Fig 4.10. (continued)

witnin permissible limits. All the input and initial information are then printed.

(6) NCOUNT and IT (iteration number) are initialized with zero values. NCOUNT is a flag to restart successive corrections from subgrade modulus.

(7) ELSYM5 is called to calculate deflections corresponding to sensor locations of the measured deflections. The calculated deflections are converted into mils.

(8) The discrepancies in measured and calculated deflections (Eqs 4.10 and 4.11) are computed. The percent maximum absolute discrepancy (HERRP) is also calculated. The initial seed moduli, theoretical deflections, measured deflections and corresponding value of HERRP are also printed. If the maximum absolute difference in calculated and measured deflection, ERDM, is equal to or less than the corresponding tolerance (the default value is 0.05 mils) then the program does not attempt any iterations and assumes seed moduli as the insitu moduli and skips to step 20. Otherwise iterations are started.

(9) Using a subroutine, SORTD, the computed discrepancies are sorted in a decreasing order. The subroutine used after the correction of the subgrade modulus to identify the layer for which the modulus is to be corrected.

(10) If NCOUNT is zero, correction is applied to the subgrade modulus. If NCOUNT is a positive value, corrections will be applied to moduli of the upper layer. Equation 4.12 is used to obtain the new modulus value. The order of correcting modulus values is from the bottom layer to the top. The sorted values of discrepancies (Step 9) are used to select the discrepancy related to an appropriate sensor location for use in Eq 4.12.

(11) If the difference in the new modulus value and the value used in the preceding ELYSM5 computation is equal to or less than a specified tolerance (it may have one of three values: TOLR31, TOLR32, or TOLR33) then the new modulus value is reset to the old modulus value and the program returns to step 10 to continue successive correction of the modulus of the next layer. Otherwise the program proceeds to step 12.

(12) The new moduli are checked for the permissible maximum and minimum limits. The modulus of the granular subbase layer is checked so as not to exceed the subgrade modulus by a factor of 3. A check is also made in a four-

layer pavement to ensure that the modulus of the granular base layer does not exceed the modulus of the lower stabilized subbase layer.

(13) An iteration number is assigned by adding one to the previous value of IT. NCOUNT is also increased by one. If the iteration number is greater than the allowable number of iterations, the program stops the iterative procedure and proceeds to step 17.

(14) If the maximum calculated discrepancy, HERRP, is equal to or less than the specified tolerance (1.5 percent), then iterations are stopped and the program skips to step 17. The program also skips to step 17 if the HERRP calculated in step 8 in the previous two iterations are compared and one of the following is observed: (a) The HERRP calculated now is equal to or exceeds its previously calculated value, or (b) the difference between the two HERRP values is relatively insignificant. This step is used to improve efficiency in the iterative procedure. Program also skips to step 17 if there is no change in the moduli from their values in the preceding iteration.

(15) Logical variables are used to enable correction in the previously uncorrected modulus in a cycle of four-iterations. If the cycle is not completed, the program goes to step 7 to complete this iteration. Otherwise, all the logical variables and NCOUNT are reset to the initialized values and then the program proceeds to step 7 to start a new cycle of iterations.

(16) Successive corrections are continued until iterations are stopped due to the constraint of a maximum number of iterations or completion of convergence as dictated by closure tolerances.

(17) Iteration number IT is reduced by 1.

(18) The program searches the best iteration based on the lowest discrepancy in deflection, HERRP.

(19) The estimated moduli, calculated and measured deflections, and the HERRP corresponding to the best iteration (step 18) are printed. An option in input provides a printout of the results of all the iterations. If the seed moduli are the best solution then program proceeds to step 21; otherwise it goes to the next step.

(20) If HERRP of the best iteration exceeds 10 percent then another complete cycle of iterations is attempted using estimated insitu moduli as the new seed moduli. In this case, the program goes to step 6 after completing this new cycle of iterations, the program goes to step 22.

(21) The program gives the message that the seed moduli are the best estimate of the insitu moduli.

(22) The self iterative procedure is stopped.

The self iterature model is included in the computer program on the structural evaluation system for rigid pavements as a routine named BASINR and BASINF in the computer program for the evaluation of flexible pavement.

Different Criteria and Tolerances Used in the Self Iterative Model

Acceptable Ranges of Moduli. The acceptable ranges of moduli of different pavement materials are important input and the user should enter them. It ensures that the derived moduli will be within reasonable limits. The default values assume very wide ranges and have been selected from a limited review of published data. The default values are presented in Table 4.5.

Tolerances for Moduli. These tolerances (TOLR31, TOLR32, and TOLR33) are employed to avoid any unnecessary ELSYM5 calculations based on corrected moduli values if there is no significant difference from the theoretical deflections of a preceding iteration (used in step 11 of the self iterative model). TOLR31 is for the modulus of the surface layer. TOLR32 is used for checking moduli of intermediate layers and TOLR33 is for the subgrade layer. The basic approach used in sensitivity analyses to establish these tolerances was to determine the maximum percent change in the modulus of a pavement layer which will result in insignificant changes (less than 2 percent) in the calculated deflection of typical four-layer pavements. The variation in one modulus value was made in increments of one percent (starting from one percent to 10 percent) for layers above the subgrade. During the sensitivity analysis of one layer, moduli of other layers were kept at fixed initial levels. Because deflections are very sensitive to any change in the subgrade

TABLE 4.5. DEFAULT VALUES FOR MAXIMUM AND MINIMUM RANGES OF MODULI OF PAVEMENT LAYERS (SUBROUTINES EDFALT)

MODULI		RIGID PAVEMENTS	FLEXIBLE PAVEMENTS
E_1	Maximum	6,500,000 psi *(5,000,000)	1,110,000 psi * (100,000)
	Minimum	2,000,000 psi *(1,000,000)	80,000 psi * (50,000)
E_2	Maximum	2,000,000 psi	** 300,000 psi *** 90,000
	Minimum	50,000 psi	** 80,000 psi *** 25,000
E_3	Maximum	500,000 psi	** 250,000 psi *** 70,000
	Minimum	30,000 psi	** 25,000 psi *** 20,000
E_4	Maximum	70,000 psi	70,000 psi
	Minimum	5,000 psi	10,000 psi

* Default values to be assumed when ICON1 = 1 is entered in input (badly cracked surface layer).

** Stabilized layer.

*** Granular material.

modulus a comparatively small increment was used in the sensitivity analysis for the subgrade modulus. The tolerances established from these studies for use in the self iterative model are presented in Table 4.6.

Closure Tolerances for Deflections. Two types of closure tolerances are specified in the self iterative model to obtain convergence in the deflection basin fitting process. TOLR1 is to check the maximum value (ERDM) of all the absolute differences between measured and calculated deflections before every iteration. The default value assigned to TOLR1 is 0.05 mils, as described earlier in step 8 of the algorithm.

TOLR2 is a percent type tolerance to check the maximum (HERRP) of absolute differences at all sensors calculated using Eq 4.11. TOLR2 is used to stop iterations such as in step 14 of the algorithm described earlier. The default value of TOLR2 is 1.5 percent.

Additional Checks. As mentioned in step 12 of the algorithm described earlier, for the case of a granular layer over the subgrade, the modulus of the granular layer is checked before each iteration so as not to exceed three times the value of the subgrade modulus. This criterion is based on the work of Heukelom and Klomp (Ref 63).

The correction factors used in the successive correction procedure are valid for all discrepancies ($ERRP_j$) in deflections below certain upper limits. For the farthest sensor this limit is 70 percent, and for other sensors it is 10 percent. Special provision is provided in the self iterative procedure to reduce the calculated discrepancy so that it does not exceed the appropriate upper limit before making any correction to the previous value of a modulus.

The default value of the maximum number of iterations is 10. The limited application with the programs developed in this study indicates that generally a solution is reached in less than 10 iterations if the seed moduli are not drastically far from actual values, especially if default seed moduli are used. If a user observes a larger discrepancy in matching the deflection based on derived moduli and iterations are stopped due to the constraint of the maximum number of iterations, then it is advisable to increase this constraint to 15 iterations. However, it is recommended that the limits of

TABLE 4.6. TOLERANCES TO ACTIVATE CHANGES IN MODULI (FOR USE IN BASIN FITTING SUBROUTINES)

PAVEMENT TYPE	PROGRAM	TOLERANCES IN MODULI		
		TOLR31	TOLR32	TOLR33
RIGID	RPEDD1 (Subroutine BASINR)	4.0%	3.0%	0.05%
FLEXIBLE	FPEDD1 (Subroutine BASINF)	4.0%	2.0%	0.10%

Note: TOLR31 is used for E_1 (Young's modulus of surface layer).
TOLR32 is used for intermediate layers.
TOLR33 is used for subgrade modulus.

all the other tolerances, i.e., TOLR1, TOLR2, TOLR31, TOLR32 and TOLR33, not be increased from their default values.

Consideration of Rigid Bottom

Background. The semi-infinite thickness of subgrade is an inherent assumption in the use of layered theory to calculate a deflection basin. The presence or assumption of a rock layer at some finite depth necessitates consideration of a rigid bottom instead of a semi-infinite subgrade because it can significantly affect the deflection basin (Fig 4.11). Ignorance of this condition may result in significant errors in moduli derived from deflection basins, as shown by Taute et al (Ref 23) in Fig 4.12. A rigid bottom has not been considered in the development of many self iterative procedures. Uddin et al (Ref 62) have recommended a procedure for consideration of a rigid bottom if no information is available about any rock layer under a finite subgrade. The ELSYM5 computer program assumes a semi-infinite subgrade if no value for the thickness of the last layer is entered in the input. ELSYM5 can also handle a rigid bottom if a finite thickness of subgrade is specified in the input along with the interface condition. In the self iterative model of this study, a full friction (FF) condition has been assumed at the interface of subgrade and the bottom rigid layer.

Case of Known Thickness of Subgrade. If the thickness of the subgrade overlying a rock layer is known from design/construction records and other evidence or from SASW tests (Ref 58), then its value should be entered in the input of the structural evaluation programs of this study. A rigid bottom with an FF interface condition is then assumed by the program internally.

Case of Unknown Thickness of Subgrade. This condition is undoubtedly more common in NDT data. The error involved in overpredicting deflections due to the assumption of a semi-infinite subgrade is very obvious. Some researchers, such as Wiseman et al (Ref 27), have considered using an arbitrary depth of subgrade to the rigid layer. The approach recommended by Uddin et al (Ref 62) is utilized in this study to develop a default procedure for estimating a reasonable depth of the subgrade over a rigid bottom. The default procedure is activated by an option in the input if desired by the

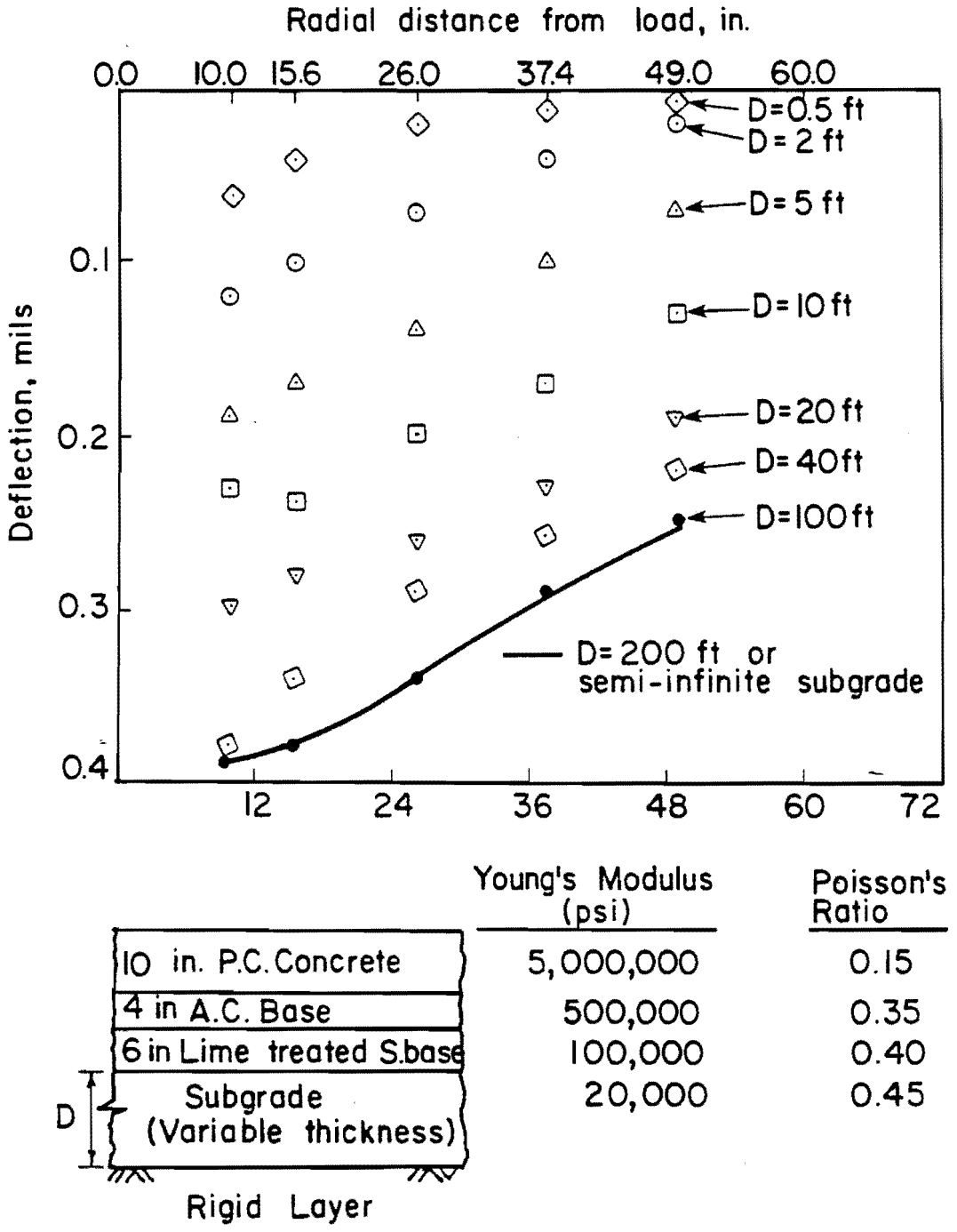

Fig 4.11. Effect of the presence of a rigid layer at varying depths on theoretical Dynaflect deflection basins.

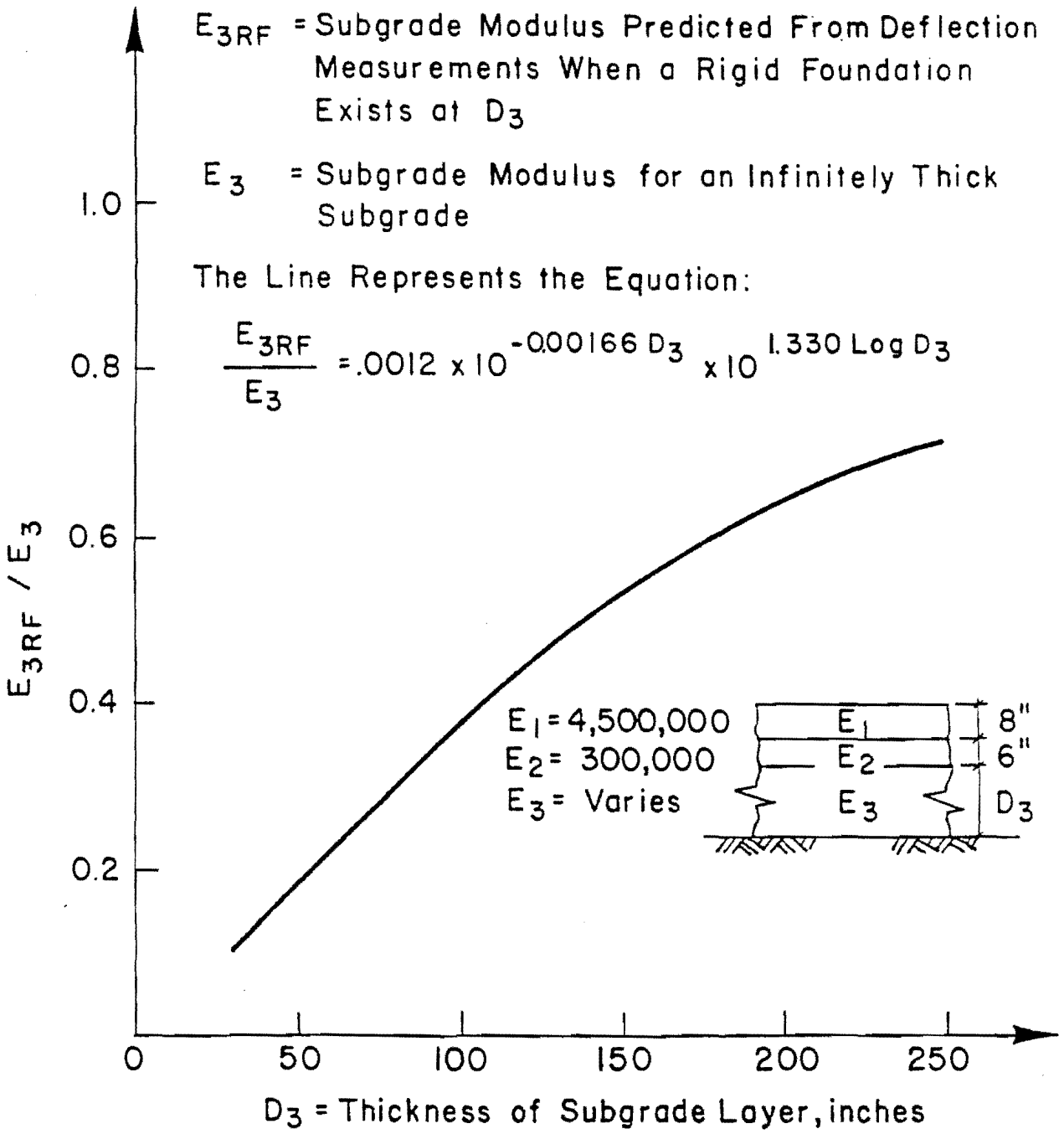

Fig 4.12. The reduction in subgrade modulus predicted using deflection measurements when the subgrade is supported by a rigid foundation depth D_3 (Ref 23).

user. The approach is based on concepts from wave propagation theory and dynamic analysis elaborated in the later part of Chapter 3.

In the first step of the default procedure used in this study, an estimate of the subgrade modulus (ENAT) is made from the predictive relationships based on the measured deflection at a location far from the test load. These relationships are presented in Table 4.7. The step-by-step procedure is described in the following.

(1) An initial estimate of the Young's modulus of the subgrade, ENAT, is made.

(2) The constrainted modulus of elasticity of the subgrade (M), is calculated using the following relationship (as discussed in Chapter 3):

$$M = \left[ENAT \cdot (1 - \mu)\right] / \left[(1 + \mu) \times (1 - 2\mu)\right] \quad (4.12)$$

(3) The mass density, ρ , of the subgrade soil is calculated from the unit weight of the soil.

(4) The wavelength of the P-wave, L_p, is then calculated using the following relationship:

$$L_p = \frac{\sqrt{M/\rho}}{f}$$

where

f = frequency of the driving force (8 Hz for the Dynaflect and for the FWD; the predominant frequency

TABLE 4.7. PREDICTIVE EQUATIONS FOR SUBGRADE MODULUS, E_{SG}

PAVEMENT TYPE	NDT DEVICE	EQUATIONS	R^2
RIGID	DYNAFLECT	$E_{SG} = -2637.155 + 119.65703 * (R_5/W_5)$	0.981
	FWD	$LOG_{10} = 5.55310 - 1.12294 * LOG_{10} (R_6 \times W_6)$	0.984
FLEXIBLE	DYNAFLECT		
	(a) Stabilized Base	$LOG_{10} (E_{SG}) = 2.6088 - 0.90216 * LOG_{10} (R_5 \times W_5)$	0.950
	(b) Granular Base	$LOG_{10} (E_{SG}) = 2.5366 - 0.95488 * LOG_{10} (R_5 \times W_5)$	0.973
	FWD		
	(a) Stabilized Base	$LOG_{10} (E_{SG}) = 5.38214 - 0.95433 * LOG_{10} (R_6 \times W_6)$	0.995
	(b) Granular Base	$LOG_{10} (E_{SG}) = 5.43902 - 0.1400 * LOG_{10} (R_2 \times W_2) - 0.8734 * LOG_{10} (R_5 \times W_5)$	0.999

R_i is the radial distance of i^{th} sensor from test load.

W_i is the measured deflection at i^{th} sensor.

can be taken as 20 Hz, as discussed in Chapter 3 and illustrated in Fig 3.21.)

(5) The thickness of the subgrade is then assumed to be half of L_p. This criterion has been based on discussions presented in Chapter 3 related to dynamic analyses.

Handling of Zero or Close to Zero Deflections. If the deflection measured at the farthest sensor (e.g., sensor 5 of the Dynaflect, located at a radial distance exceeding 4 feet from the loading wheels) are zero, or less than 0.1 mils, it is indicative of a rock layer. Dynaflect deflection basins measured on a pavement built on a rock fill layer over bed rock in Austin support this discussion. One such deflection basin is illustrated in Fig 4.13. The self iterative model in this study handles such cases internally by assigning a 12-inch thick subgrade over a rigid layer.

UNIQUENESS OF ESTIMATED INSITU MODULI

Background

A severe limitation, which can also be a major criticism, is that insitu Young's moduli derived by fitting a measured deflection basin may not be unique. This section deals with this aspect and the measures adapted in the present study to achieve a unique set of moduli. Insitu moduli determined from a deflection basin measured on a two-layered pavement can be unique if the subgrade modulus is first determined by matching the deflection measured at the farthest sensor. Deflections measured at other sensors are then matched by iterating with the modulus of the top pavement layer. The final modulus of the surface layer will also be a unique value. However, in the case of a three or four-layer pavement, more than one combination of moduli can be used to generate theoretical deflection basins which will match the measured deflection basin within reasonable closure tolerances. An example of the non uniqueness is illustrated in Fig 4.14 for a four-layer rigid pavement.

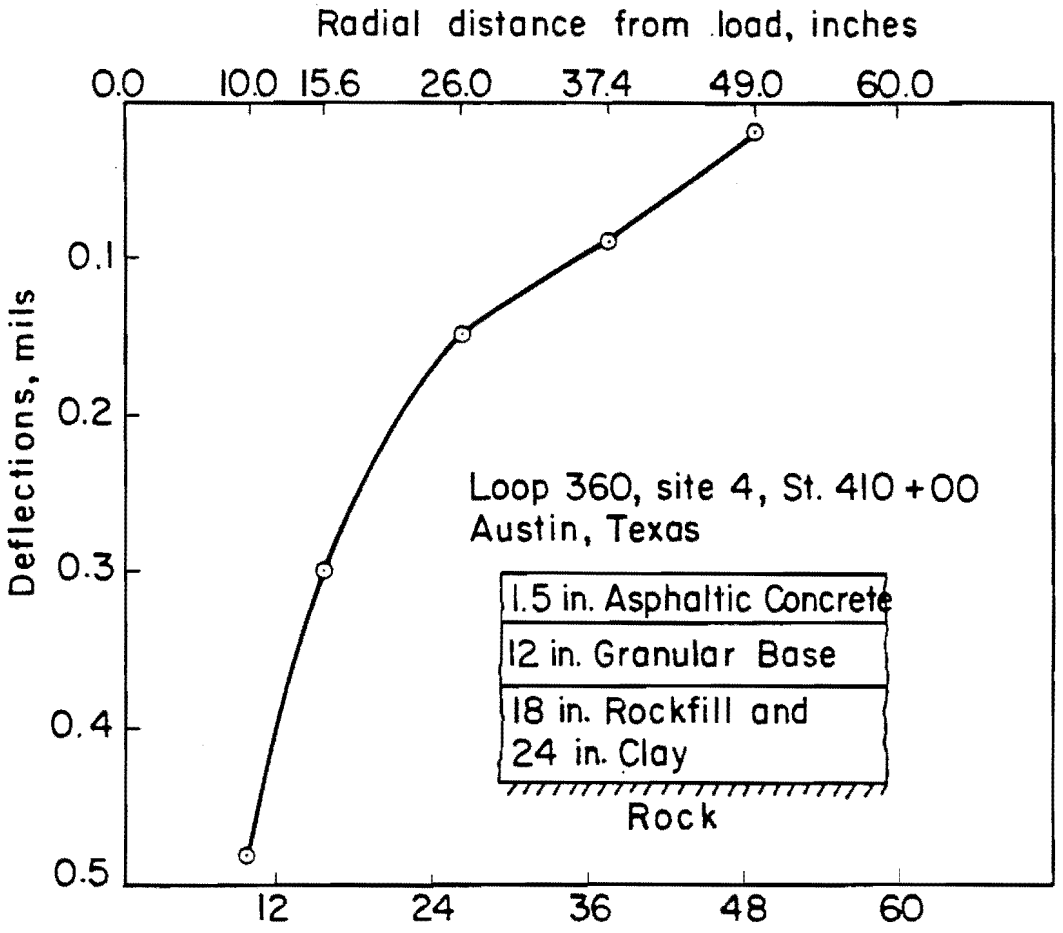

Fig 4.13. Example of a measured Dynaflect deflection basin with a 0.02 mils deflection at sensor 5.

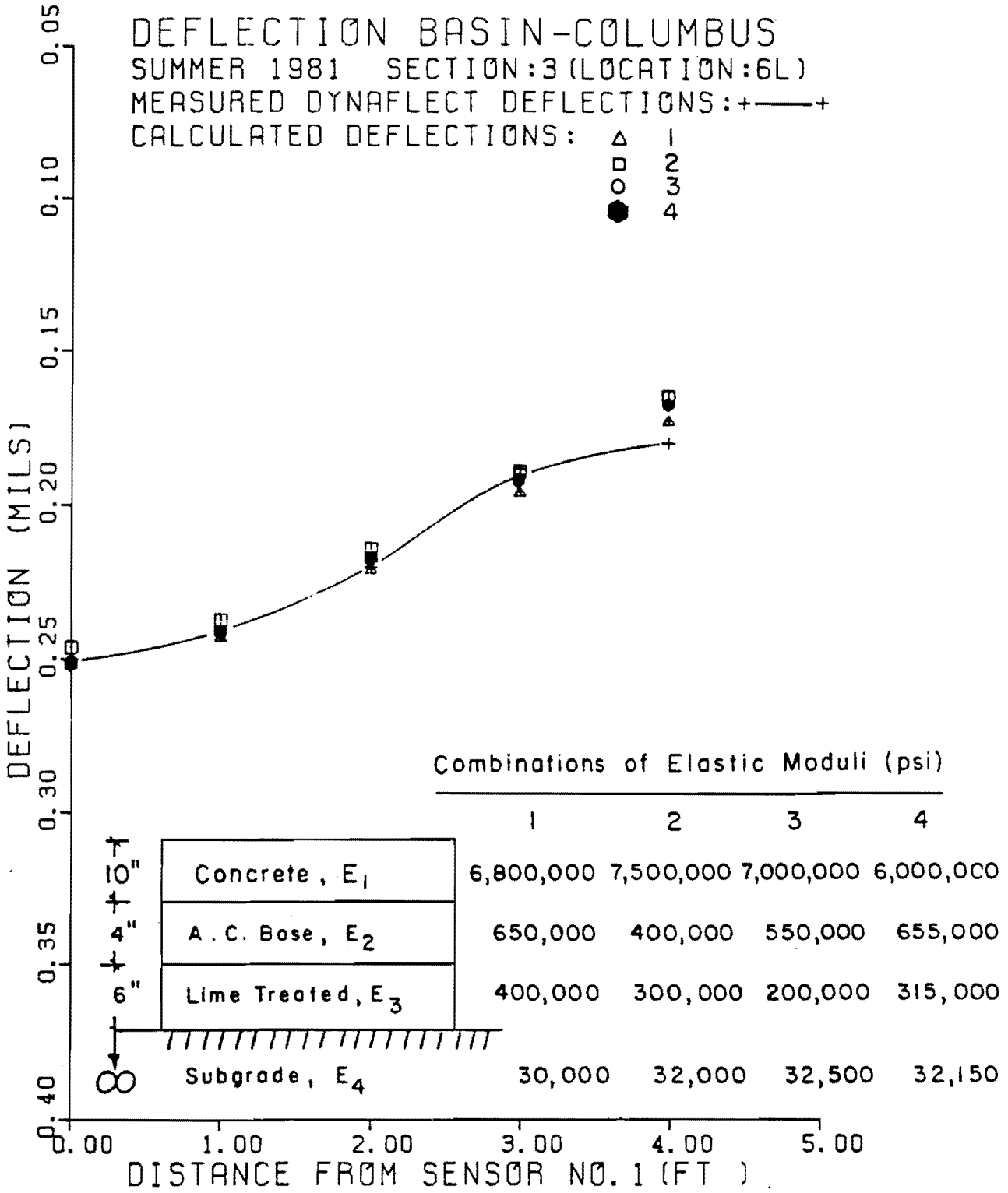

Fig 4.14. Deflection basin fitting results which illustrate possible non-uniqueness of moduli (Ref 7).

From discussions on the parametric study of moduli presented earlier in this chapter, a unique value of the subgrade modulus can be obtained from the deflection measured at the farthest sensor (e.g., sensor 5 in the Dynaflect and senor 6 or 7 of the FWD) using a relationship such as Eq 4.2. The margin of error in the derived subgrade modulus will be essentially negligible if the thickness of the subgrade is appropriately modelled in the input of the self iterative procedure. This leaves us with the moduli of upper pavement layers. If the initial seed moduli are very close to the actual values then generally a reasonably unique solution can be easily reached within a reasonable margin of error. The approach used in this study is that, if relationships are developed which can be used to predict seed moduli from measured deflections, then any guess work in seed moduli will be eliminated. Furthermore, if only one unique set of seed moduli is generated by the program internally using the input data, then the moduli derived by the self iterative model will also be unique within an acceptable margin of error. Several predictive relationships for seed moduli are used in the default procedure of the self iterative models developed in this study.

Development of Default Procedures for Seed Moduli

Figure 4.15 illustrates a simplified flow diagram of the procedure used in this study to develop predictive relationships for incorporation in the default procedure for seed moduli. An outline of the methodology is presented below.

Methodology. The methodology used in the development of the procedure for default seed moduli is shown in Fig 4.16. Deflections at all sensor locations used in the NDT method are computed by layered elastic theory using moduli (E), and thicknesses of layers (D) and specifying the radial distances R of sensors from the test load. Numerous combinations of E's and D's are used at fixed values of R's and Poisson's ratios (μ) to predict deflections (W) at all sensor locations. Now, using regression techniques, predictive relationships can be developed from the statistical fit to predict E's from known values of D's and W's at all sensors as illustrated in Fig 4.16.

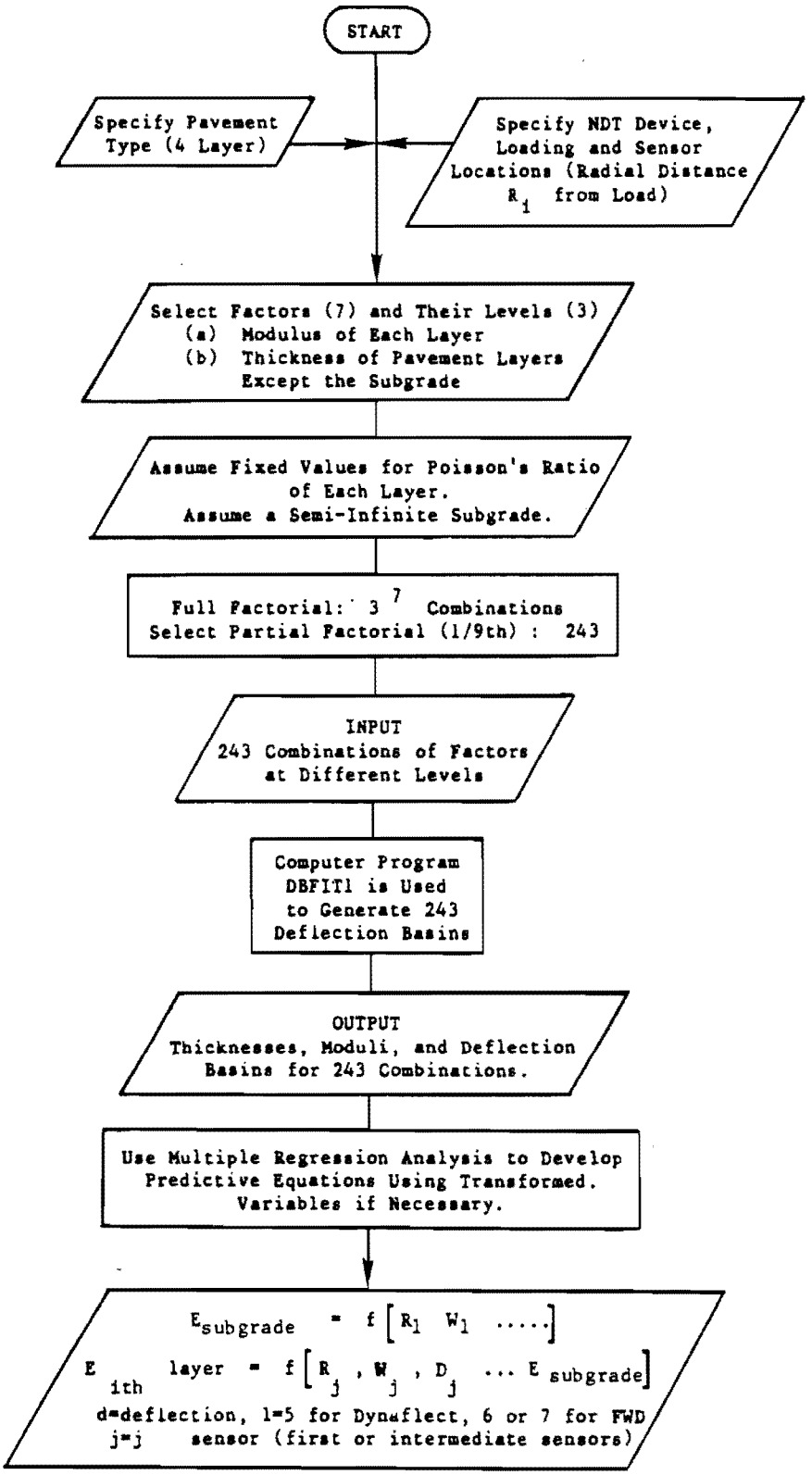

Fig 4.15. A conceptual flow diagram for developing predictive equations for seed moduli.

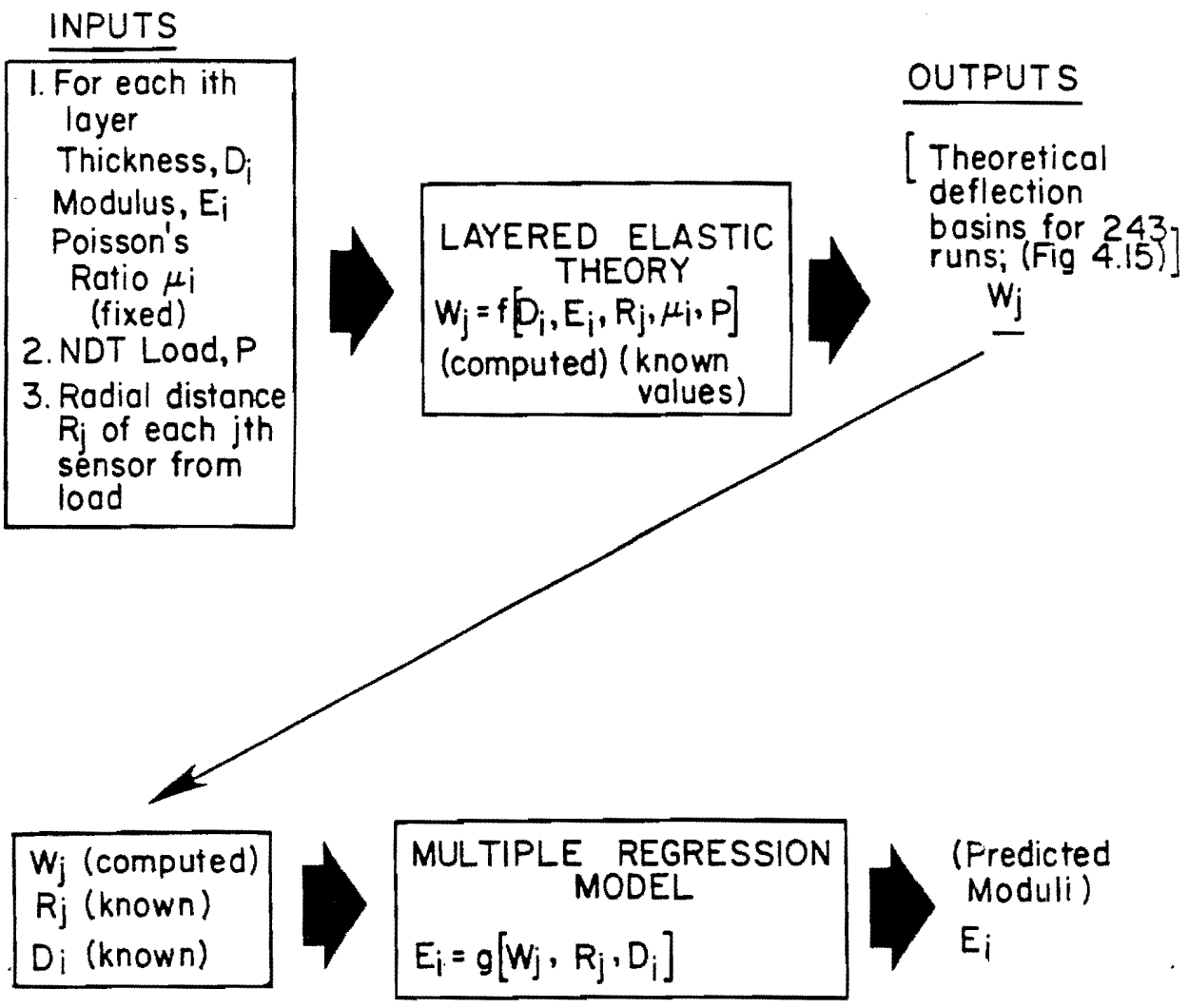

Fig 4.16. A conceptual illustration of methodology for predicting moduli from deflection basin and thickness data.

Fractional Factorial Designs. The first step of the methodology described above is to use layered elastic theory to generate theoretical deflection basins using a set of factors, such as D's and E's, at preselected levels. Factorial design is a statistical technique of experiment design which enables the user to investigate simultaneously effects of all factors and their interactions on responses (deflections at preselected locations). A full factorial design can be prohibitively costly to run if factors are large in number. A fractional factorial plan enables the user to select a fraction of all possible factorial combinations. In this study, a 1/9th replicate of a 3^7 factorial design described by Connor and Zelen (Ref 64) is selected to generate deflection basins (using 7 factors at 3 levels). This replicate results in 243 runs of layered theory computations. Table 4.8 presents a summary of the seven factors (thickness, D, of each of three pavement layers and the modulus, E, of each layer) and the selected three levels of each factor. This plan is designed for a four-layer rigid pavement (Fig 4.17) assuming a semi-infinite subgrade. Further discussion on factorial design and a summary of 1/9 fractional replicate designs for flexible and rigid pavements are presented in Appendix B. The selected levels of factors (Table 4.8 and Appendix B) are based on engineering experience.

Layered Theory Computations. A driver program, DBFIT1, was used to facilitate calling LAYER8 for computation of the deflection basin in each of 243 runs of each fractional factorial plan. Theoretical deflections computed by LAYER8 and ELSYM5 are identical. Separate runs were made for the Dynaflect and the FWD. Fig 4.18 illustrates a simplified flow diagram of computer program DBFIT1. The details are presented in Appendix B. A semi-infinite subgrade was assumed in all runs and Poisson's ratios were based on Table 4.1. The surface deflections were computed at all radial distances, R's corresponding to sensor locations.

Computations for deflections were made for the three experimental plans, which are summarized below.

(1) A rigid pavement plan for which factors and levels are presented in Table 4.8. An important assumption made in the selection of moduli

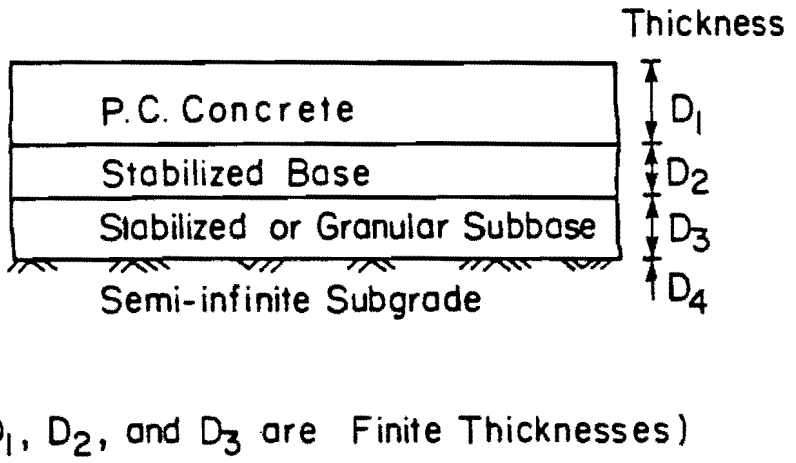

Fig 4.17. Rigid pavement structure assumed in the fractional design.

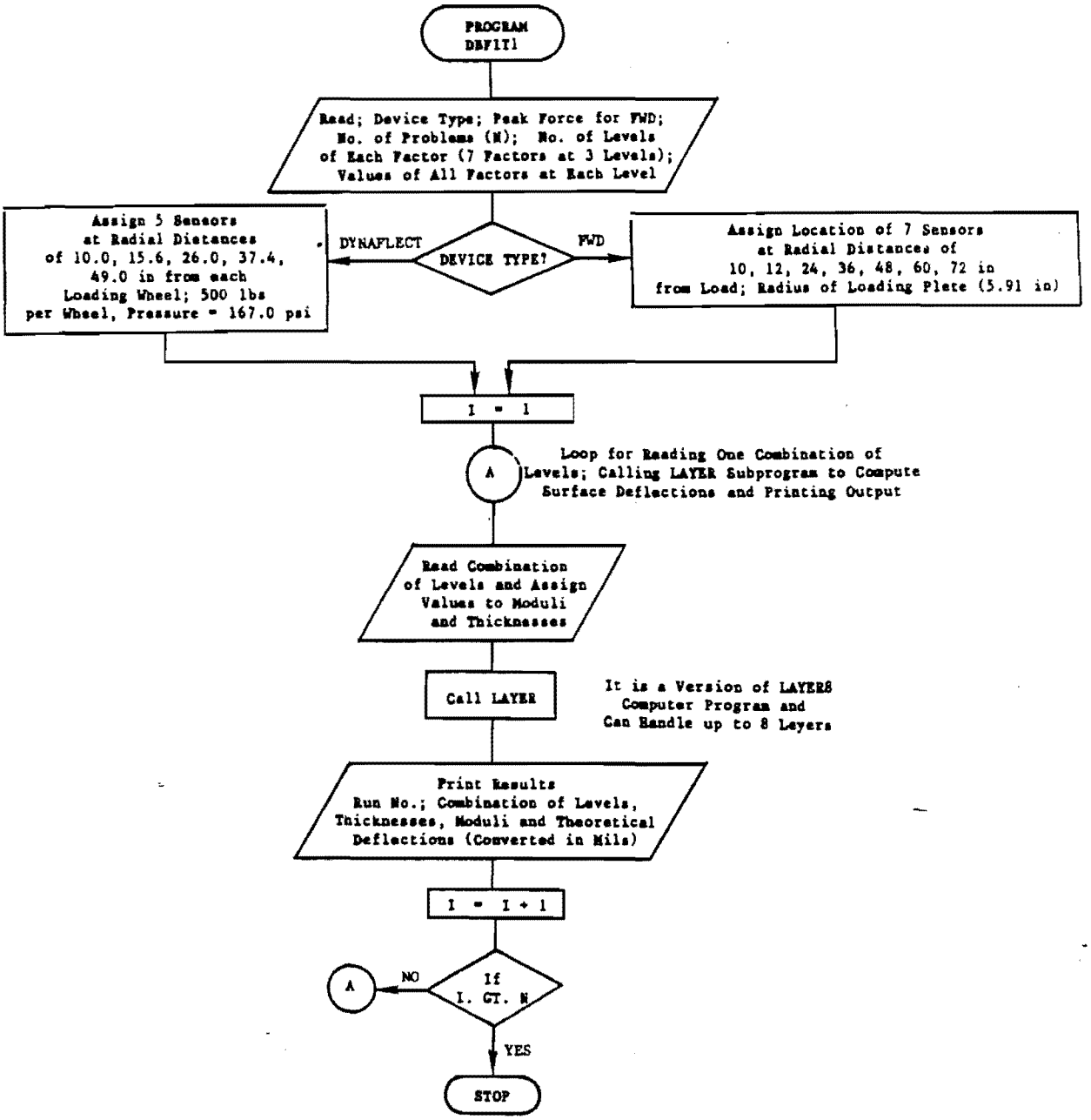

Fig 4.18. Simplified flow chart of program DBFIT1.

TABLE 4.8. FRACTIONAL FACTORIAL DESIGN TO GENERATE DEFLECTION BASIN DATA FOR DEVELOPMENT OF MODULI-PREDICTIVE EQUATIONS - RIGID PAVEMENTS (FOR DYNAFLECT AND FWD)

	FACTORS						
LEVELS	W_1 (in.)	W_2 (in.)	W_3 (in.)	E_4 (psi)	E_3 (psi)	E_2 (psi)	E_1 (psi)
Low	8	0	6	5,000	30,000	100,000	2,000,000
Medium	10	4	9	15,000	150,000	500,000	4,000,000
High	13	8	12	45,000	450,000	1,000,000	6,000,000
[Semi-Infinite Subgrade in All Cases]	PC Concrete Thickness	Base Thickness	Subbase Thickness	$E_{Subgrade}$	$E_{Subbase}$	E_{Base}	$E_{PC\ Concrete}$

Full Factorial = 3^7

1/9th Fractional Factorial = 3^5 = 243 combinations

levels is that base layer (Fig 4.17) is of a stabilized material. Base and subbase layers are intermediate layers and their low and high levels cover a very wide range. This approach is not unreasonable as deflection basins of rigid pavements are relatively insensitive to wide variations in the moduli of intermediate layers.

(2) A fractional factorial plan for flexible pavements with stabilized base layers (see Appendix B for levels of the seven factors).

(3) A fractional factorial plan for flexible pavements with granular base layers for which details are given in Appendix B.

Development of Predictive Equations for Moduli. This is the third step of the methodology described above. The multiple regression technique was used to develop predictive relationships. An overview of the multiple regression technique as applied to deflection data has been presented elsewhere (Ref 7). At first, multivariate regression analyses were made where the multivariate responses are the deflection predicted by layered theory, and the independent variables are D's and E's using the results generated in one of the experimental plans described in the preceding section. The resulting regression equations showed poor correlation coefficients. Therefore, a study was done to find a suitable transformation. The evidence that deflections at different radial distances, R's, from the load are unique for a pavement (also supported by layered theory) was used to attempt regression using transformations of multivariate deflection results. Details about these analyses are presented in Appendix B. Results from the experimental plan number (for the Dynaflect) is referred to in the following discussion. The transformation used in this case is

$$RDEF_j = f(DEF_j, R_j) \qquad (4.14)$$

where DEF is the theoretical deflection at j^h sensor.

Multivariate regression analyses (Ref 65) using the transformed response variable produced equations with high values of coefficient of multiple determination, R^2 (above 0.90). The equations are of the following form:

$$\overline{RDEF_j} = f_1(E_i, D_{i-1}) \qquad (4.15)$$

where

i = number of layers in the pavement and
all other terms have been defined earlier.

In the case of the Dynaflect, a set of five simultaneous equations resulted from Eq 4.15. D_{i-1} refers to thicknesses of all pavement layers excluding the subgrade. In the process of analyzing a deflection basin, thicknesses D's are known and E's are the only unknown. RDEF's are also known. Therefore, for a four-layer pavement, any four of five simultaneous equations can be solved to determine four unknown E's. Theoretically, any four equations should give same E's. But when this procedure was used in the self-iterative program to calculate default seed moduli, it was found this approach does not give a unique result. Moduli calculated from one set of equations were not the same as moduli computed from another combination of four equations. Therefore the conceptual model presented in Fig 4.16 was tried. A univariate multiple regression technique was used to develop equations with a single E as the response variable and thicknesses (D) and RDEF's as predictor (independent) variables. Various transformations were used in order to achieve high R^2 values. The resulting equations for rigid and flexible pavements are presented in detail in Appendix B. For Dynaflect deflections generated by the rigid pavement plan, one of the equations for subgrade modulus was simplified by removing all independent variables except $RDEF_5$, which corresponds to the fifth sensor of the Dynaflect. Figure 4.19 illustrates a plot of calculated and actual values of subgrade moduli. This

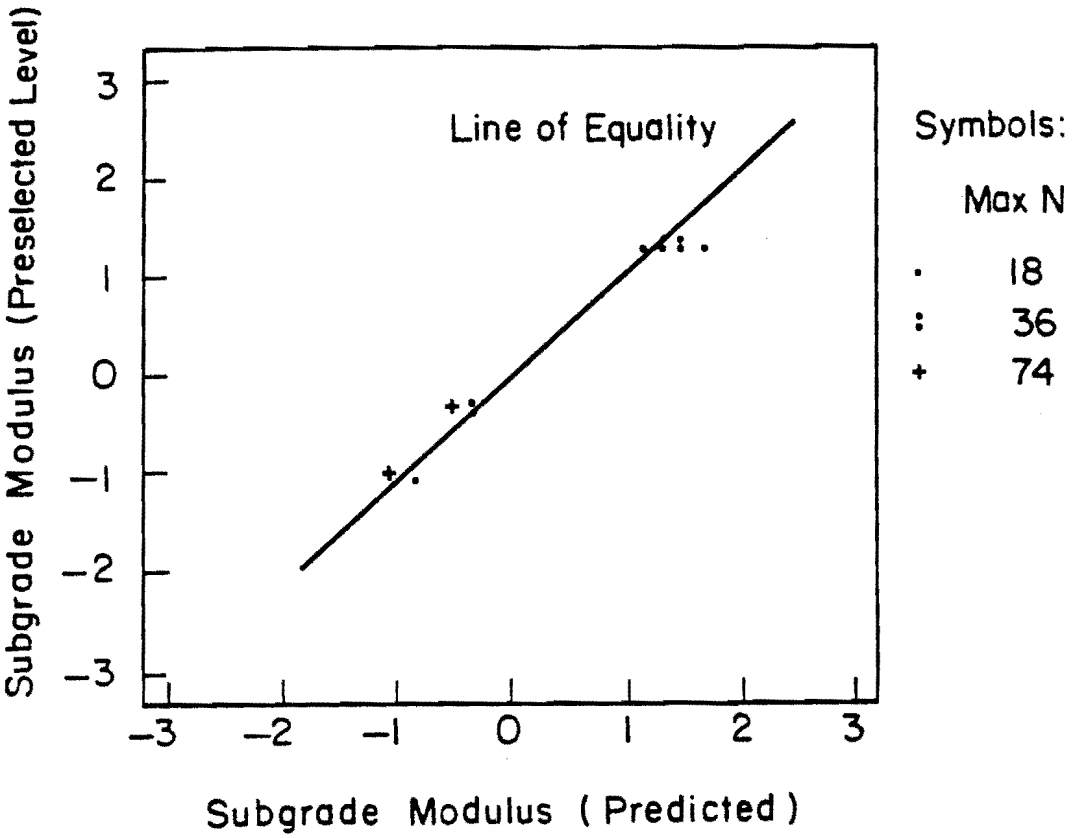

Fig 4.19(a). Standardized scatter plot - rigid pavement factorial (case of Dynaflect).

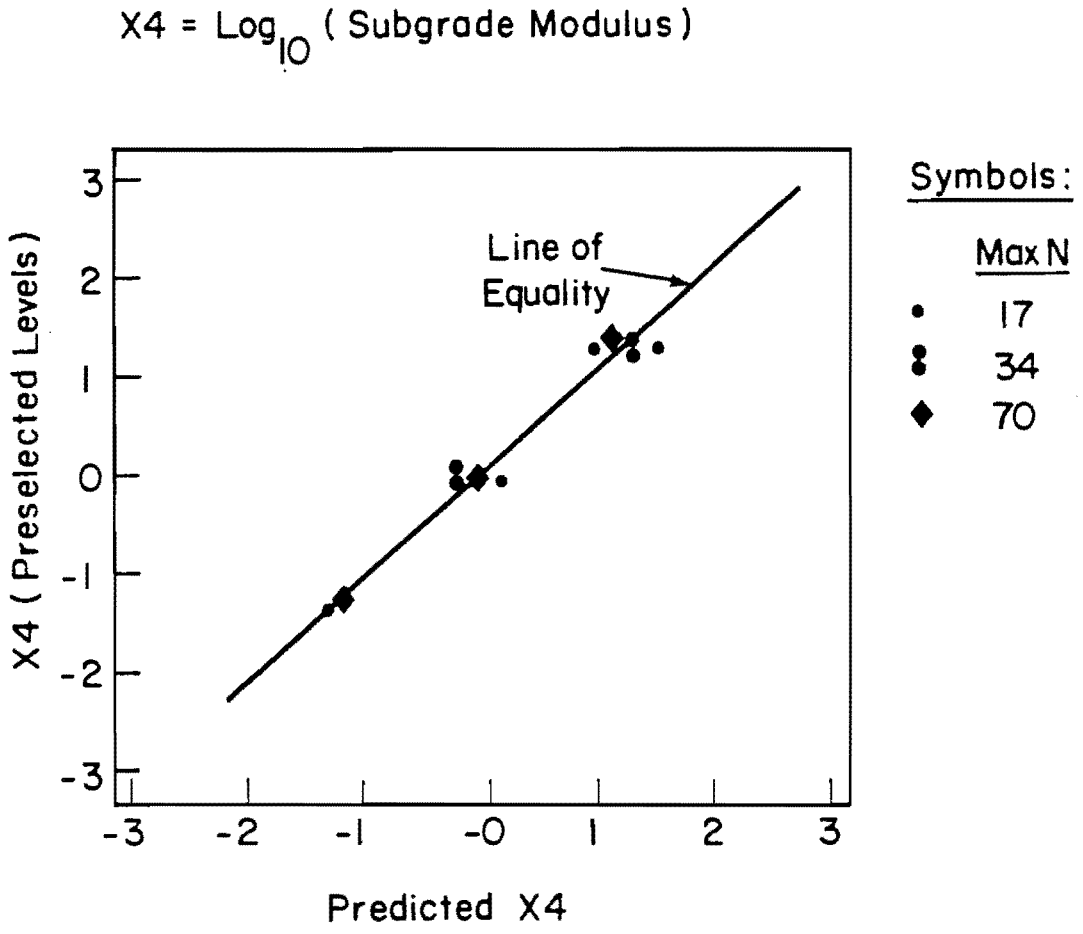

Fig 4.19(b). Standardized scatter plot - rigid pavement factorial (case of FWD).

equation and similar equations for flexible pavements were used in the self-iterative models for the default procedure of assigning a finite depth of the subgrade over a rigid bottom. The generalized form of regression equations (Appendix B) developed for calculation of default seed moduli is

$$E'_1 = c + g\,(DEF_j, R_j) + h\,(D_{i-1}) \qquad (4.16)$$

where

E'_1 = transformation of Young's modulus E of the i^{th} layer (i can have any one value from 1 to 4).

c = a constant term.

All other terms have been defined earlier.

Appendix B provides a summary of all regression equations developed in this study for use in default procedures of seed moduli.

Evaluation of Default Seed Moduli. In this section a few examples of the predictions of default seed moduli are presented. Different rigid and flexible pavements with assumed known moduli used in these examples are presented in Fig 4.20. The same figure also illustrates Dynaflect deflection basin generated by layered theory computations (using BASFT2). The deflections and thicknesses were plugged into the input of programs developed for self-iterative models with routines for default seed moduli. The predicted default seed moduli are presented in Table 4.9. It can be seen that in general the predicted moduli are not too far from the actual moduli. This approach of default seed moduli offers distinct advantages:

(1) Guess work is eliminated in assuming initial seed moduli in the self-iterative procedures.

(2) As default seed moduli are not drastically different from actual moduli, fewer iterations will be needed for convergence.

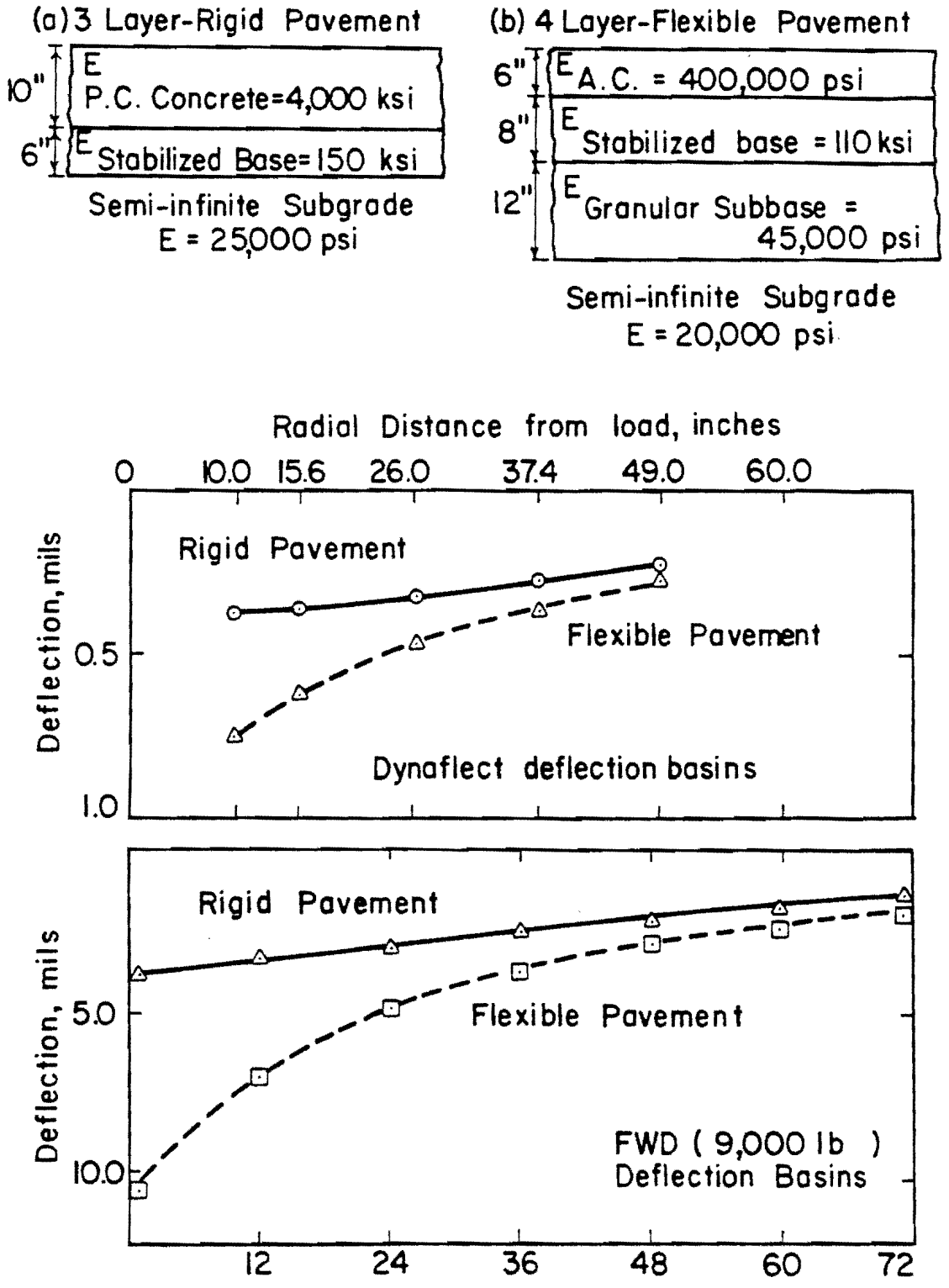

Fig 4.20. Theoretical deflection basins generated for a rigid pavement and a flexible pavement.

TABLE 4.9. EXAMPLES OF PREDICTED SEED MODULI (FOR PAVEMENT SHOWN IN FIG 4.20)

(a) RIGID PAVEMENTS (PROGRAM RPEDD1 - SUBROUTINE ERIGID)

	PREDICTED SEED MODULI (psi)		
LAYERS	DYNAFLECT	FWD	TRUE YOUNG'S MODULI (psi)
PC Concrete	3,862,250	5,108,699	4,000,000
Stabilized Base	196,214	109,973	150,000
Subgrade	24,278	23,915	25,000

(b) FLEXIBLE PAVEMENTS (PROGRAM FPEDD1 - SUBROUTINE EFLEX)

	PREDICTED SEED MODULI (psi)		
LAYERS	DYNAFLECT	FWD	TRUE YOUNG'S MODULI (psi)
AC Surface	321,833		400,000
Stabilized Base	100,020		110,000
Granular Subbase	70,550		45,000
Subgrade	23,517		20,000

(3) The derived insitu moduli will represent a unique combination of moduli within allowable tolerances used in the self-iterative model for deriving insitu moduli from a deflection basin.

Recommended Procedure to Determine Unique Insitu Young's Moduli

(1) Determine thicknesses of pavement layers at the test location. The thickness of the concrete layer in rigid pavements and the thickness of the aspnaltic concrete layer in flexible pavements is particularly important. Core thickness data should be used wherever available. The thickness profile can also be determined from SASW tests (Refs 58, 66), which is a nondestructive method based on wave propagation.

(2) If exact information is unavailable about the thickness of the subgrade and rock layer is not believed to exist, then the default procedure for the depth to a rigid bottom should be used. It generally results in a better fit of the deflection basin.

(3) Acceptable limits for maximum and minimum values of the modulus of each layer should be specified by the user. Poisson's ratios are also entered by the user.

(4) Enter the zero values input of the initial seed moduli. However, it is suggested that the user input the surface modulus if he or she has some confidence in it. Computer programs based on the self-iterative models will generate default seed moduli using appropriate equations for the pavement type. After the iterative procedure is completed, the derived insitu moduli will present a unique combination of pavement moduli.

EVALUATION OF THE SELF-ITERATIVE MODEL

The concepts, methodology, and description of the self-iterative models have been presented in preceding sections. Subprograms BASINR (for rigid pavement) and BASINF (for flexible pavement) are the first stages of computer

programs for structural evaluation developed in this study. Applications of the self-iterative models to evaluate reproducibility and uniqueness, efficiency, and accuracy of the convergence process, and usefulness of capability to consider a rigid bottom are presented in this section.

Reproducibility and Uniqueness

This part of the study is based on theoretical deflection basins generated by layered theory for pavements of assumed known properties. The theoretical deflection basins are input in all cases presented here. If default seed moduli are not opted, the insitu moduli determined from the analysis of a deflection basin will be dependent upon the user-supplied initial seed moduli. Reproducibility is the capability of the self-iterative procedure to derive sets of insitu moduli within reasonable agreement disregarding variations in the user-supplied seed moduli. Pavement structures used in this study and theoretical deflection basins are presented in Fig 4.21. Variations in seed moduli and their effects on derived insitu moduli are presented in Tables 4.10 and 4.11. The insitu moduli determined on the basis of user dependent seed moduli are reproducible but are also associated with varying margins of error. It should be realized, however, that a reasonable reproducibility does not guarantee that the derived moduli are also unique.

The same tables also present unique sets of insitu moduli derived on the basis of default seed moduli. It can be seen that errors in the uniquely derived moduli are very small, especially for subgrade and surface moduli, which have greater influence on pavement response as compared to intermediate moduli (particularly for rigid pavements).

Efficiency and Accuracy of Convergence Process

Efficiency of the self-iterative model is judged from the number of iterations required to converge to the final solution. The iterations required in deriving insitu moduli for examples discussed in the preceding section are also presented in Tables 4.10 and 4.11. It can be seen that the self-iterative programs are very efficient as the iterations never reach a

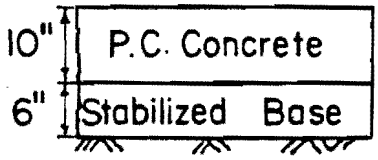

	"True" Young's Modulus (psi)	Poisson's Ratio
P.C. Concrete	4,000,000	0.15
Stabilized Base	150,000	0.35
Semi-infinite Subgrade	25,000	0.45

Data	FWD (9000 lb. peak force)							Dynaflect				
Radial distance from Load (inch.)	0	12	24	36	48	60	72	10.0	15.6	26.0	37.4	49.0
Theoretical Deflection (mils)	3.84	3.42	2.97	2.52	2.13	1.79	1.52	0.38	0.36	0.32	0.27	0.23

Fig 4.21. Rigid pavement structure used in the reproducibility study.

TABLE 4.10. SUMMARY OF MODULI DETERMINED BY ANALYZING FWD DEFLECTION BASIN (RIGID PAVEMENT CASE)

Young's Moduli (psi)				Theoretical Deflections (mils)		
Modulus	PC Concrete	Stabilized Base	Subgrade	Sensor No.	'True'	Predicted
"True'	4,000,000	150,000	25,000	1	3.84	3.82
Default Seed	4,000,000	109,973	23,915	2	3.42	3.42
				3	2.97	3.01
Low Input	2,500,000	90,000	20,000	4	2.52	2.59
Predicted (Iteration 3)	4,561,000	192,500	23,200	5	2.13	2.20
				6	1.79	1.87
				7	1.52	1.59

(continued)

TABLE 4.10. (CONTINUED)

Young's Moduli (psi)				Theoretical Deflections (mils)		
Modulus	PC Concrete	Stabilized Base	Subgrade	Sensor No.	'True'	Predicted
High Input	5,000,000	300,000	30,000	1	3.84	3.91
Predicted (Iteration 3)	3,367,000	159,000	25,620	2	3.42	3.47
				3	2.97	2.97
				4	2.52	2.48
				5	2.13	2.06
				6	1.79	1.72
				7	1.52	1.43

TABLE 4.11. SUMMARY OF MODULI DETERMINED BY ANALYZING DYNAFLECT DEFLECTION BASIN (RIGID PAVEMENT CASE)

Young's Moduli (psi)				Theoretical Deflection (mils)		
Modulus	PC Concrete	Stabilized Base	Subgrade	Sensor No.	'True'	Predicted
'True'	4,000,000	150,000	25,000	1	0.38	0.38
Default Seed	3,862,251	196,214	24,278	2	0.36	0.36
				3	0.32	0.32
Low Input	2,500,000	90,000	20,000			
				4	0.27	0.28
Predicted (Iteration 4)	4,887,000	229,400	22,310	5	0.23	0.24

(continued)

TABLE 4.11. (CONTINUED)

Young's Moduli (psi)				Theoretical Deflections (mils)		
Modulus	PC Concrete	Stabilized Base	Subgrade	Sensor No.	'True'	Predicted
High Input	5,000,000	300,000	30,000	1	0.38	0.37
				2	0.36	0.35
Predicted (Iteration 2)	3,818,000	217,200	24,920	3	0.32	0.31
				4	0.27	0.26
				5	0.23	0.22

double digit number. The programs are, of course, highly efficient if the user knows dynamic moduli of one or more pavement layers from SASW or other tests. It is suggested that if the modulus of the surface layer is roughly known, it can be entered in the input of the seed moduli. This approach will result in improved efficiency and reliability.

The accuracy of the convergence process is judged by HERRP (the maximum percent discrepancy in calculated and measured or input deflections among all sensor locations). The calculated and input deflection basins are plotted in Fig 4.22. Additional examples based on field dynamic deflection basins are presented in Figs 4.23 and 4.24.

Usefulness of Rigid Bottom Consideration

Consideration of a rigid bottom can considerably improve the efficiency and accuracy of the convergence process and the reliability of the derived moduli. Fig 4.25 illustrates this point where a deflection basin predicted assuming 50 feet of subgrade has been analyzed. It can be seen that the analysis with the assumptions of a semi-infinite subgrade results in large errors in predicted insitu moduli, as compared to the insitu moduli predicted using 50 feet of subgrade overlaying a rigid layer.

Another example is presented in Fig 4.26 where prior knowledge of the presence of a rock layer at a shallow depth was available. The Dynaflect deflection basin was measured on a flexible pavement site in Austin. This example also illustrates how the computer programs handle a small deflection value (less than 0.1 mil) at the last sensor of the NDT device.

TEMPERATURE CORRECTION FOR FLEXIBLE PAVEMENT

All asphalt-bound materials in pavements exhibit temperature sensitivity. Temperature correction of deflections measured on asphalt pavements is recommended by the Asphalt Institute (Ref 4). Asphaltic concrete modulus derived from a deflection basin using the self-iterature model described above represents the insitu modulus value at the test temperature. For pavement analysis and overlay design, an asphaltic concrete

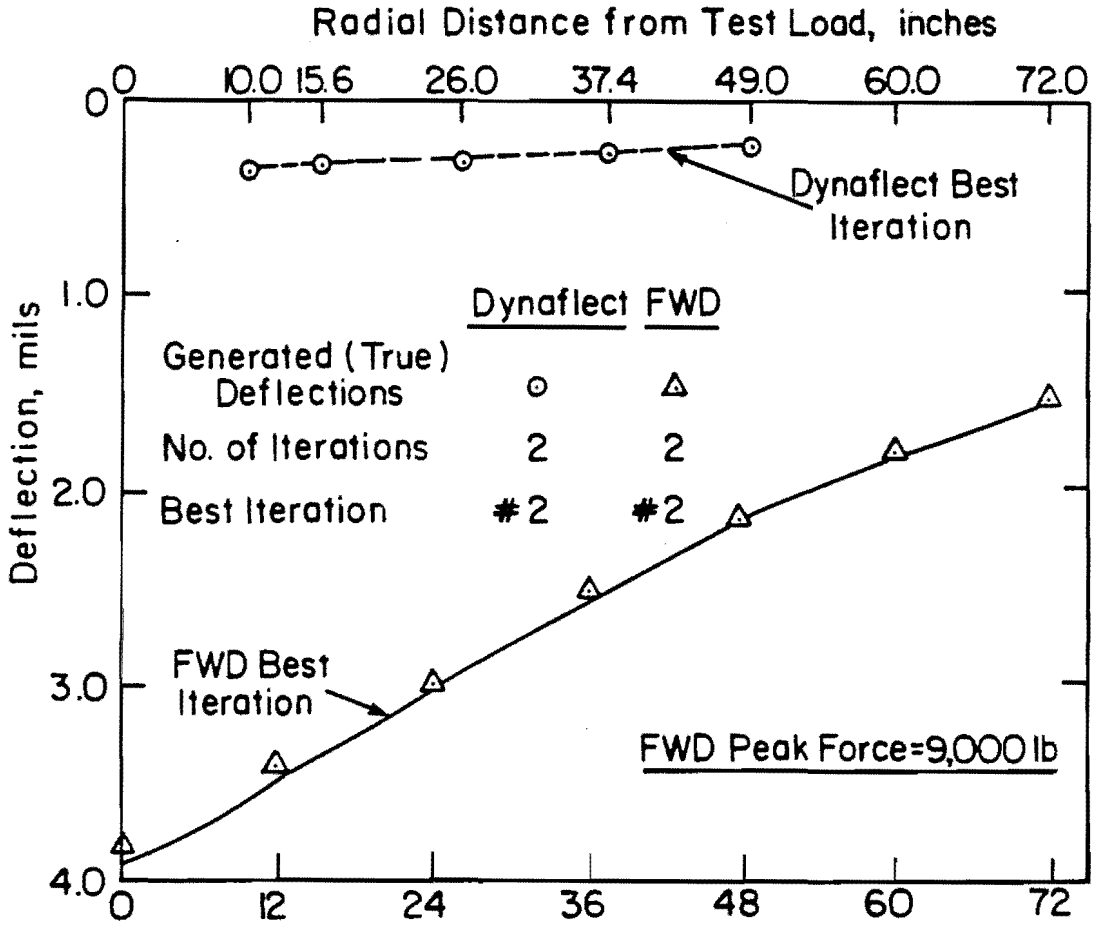

	True Moduli (psi)	Input Seed Moduli (psi)	Predicted Young's Moduli (psi)	
			Dynaflect Basin	FWD Basin
PC Concrete	4,000,000	0	3,862,000	4,000,000
Stabilized Base	150,000	0	249,300	150,000
Subgrade	25,000	0	23,300	23,920

Fig 4.22. "True" and predicted deflection basins for the rigid pavement shown in Fig 4.21.

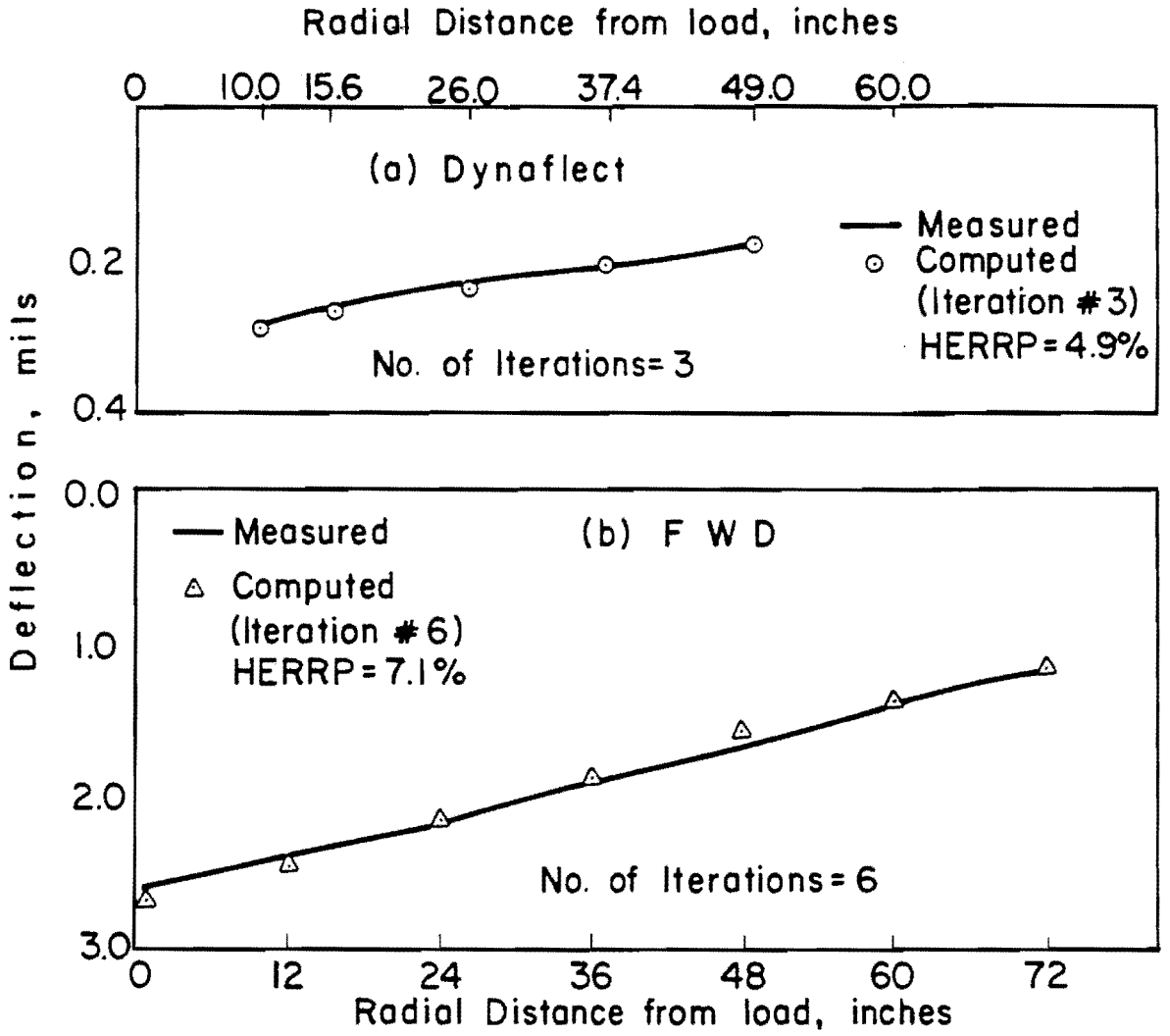

IH-10 (EB) East of Columbus, Texas

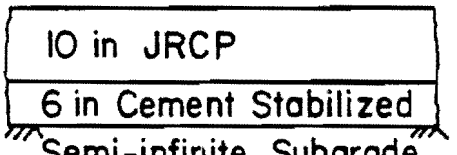

Young's Moduli (psi)	Dynaflect	FWD
10 in JRCP	5,398,000	5,500,000
6 in Cement Stabilized	500,000	500,000
Semi-infinite Subgrade	31,030*	32,820

(*Uncorrected subgrade modulus)

Fig 4.23. Example application of the self-iterative deflection basin fitting procedure (Program RPEDD1) for a rigid pavement.

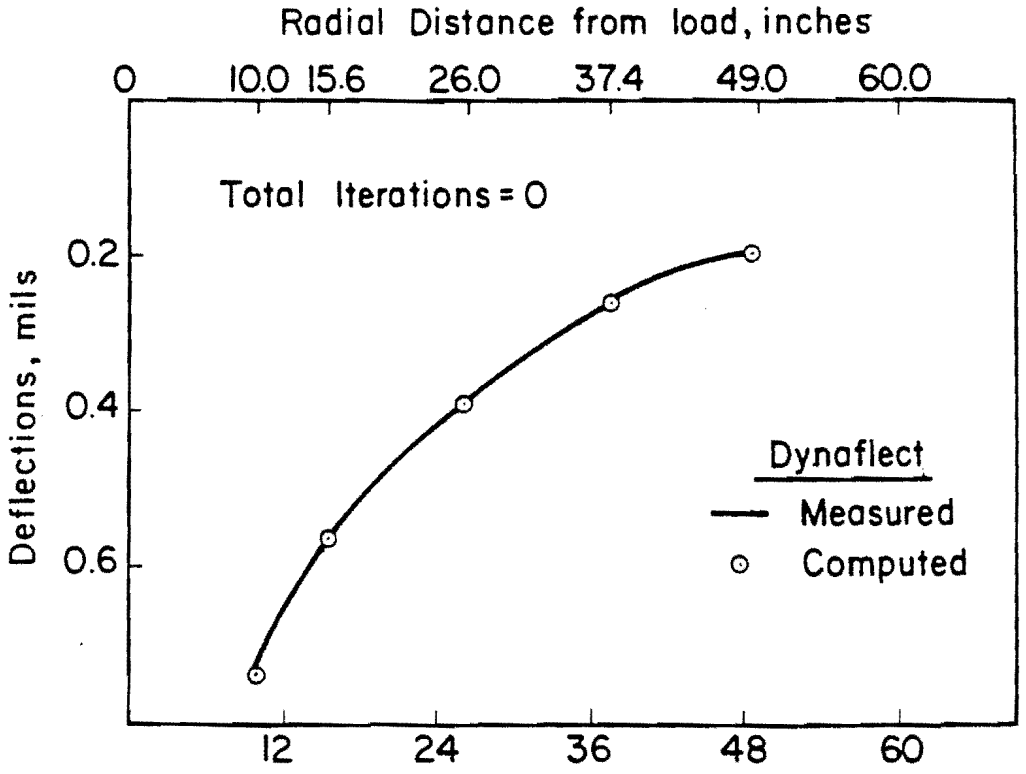

IH-40 (WB) Oklahoma
June 1984
Test Temperature=95°F

	Young's Modulus (psi) Input Seed	Predicted
4.5 in A.C. Surface	0	292,900
8.0 in. Bituminous Base	0	112,900
Semi-infinite Subgrade	0	28,280*

(*Uncorrected subgrade modulus)

Station 02 miles (site 3)
(Courtesy of A.R.E.)

Fig 4.24. Example application of the self-iterative deflection basin fitting procedure (Program FPEDD1) for a flexible pavement.

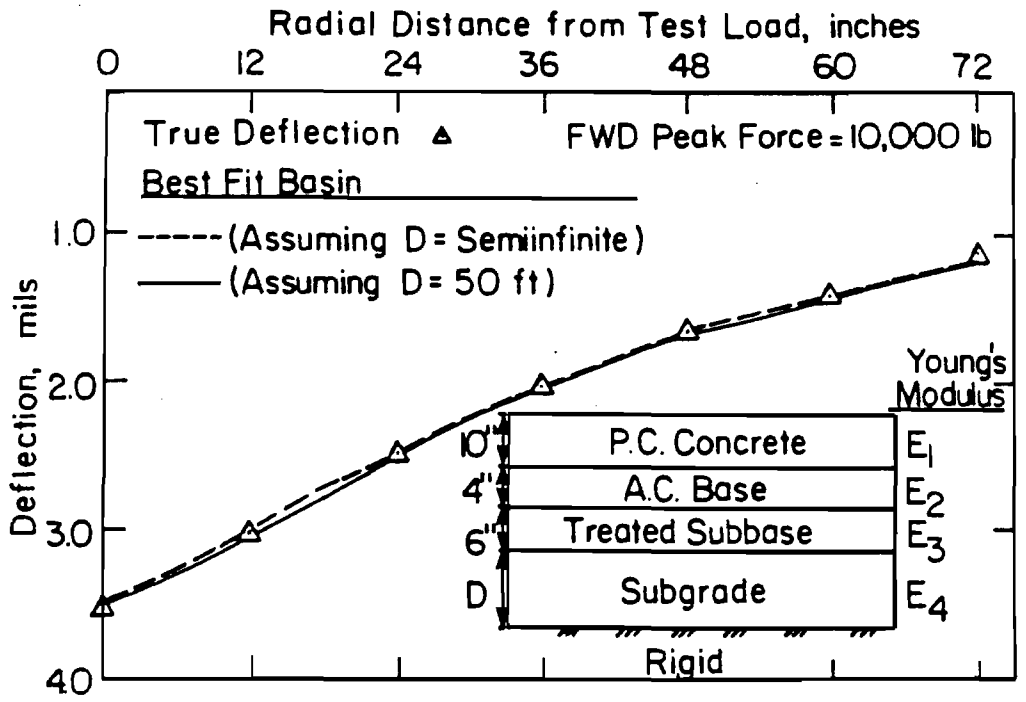

Young's Moduli	True	Input Seed	Predicted (Iteration #2)	Percent Difference	HERRP (Percent)
E_1 (psi)	4,000,000	0	3,085,000	-22.9	2.98
E_2 (psi)	400,000	0	273,100	-31.7	
E_3 (psi)	100,000	0	129,000	+29.0	
E_4 (psi)	30,000	0	34,610	+15.4	

(a) D = Semi-infinite subgrade (no. of iterations 2)

Young's Moduli	True	Input Seed	Predicted (Iteration #2)	Percent Difference	HERRP (Percent)
E_1 (psi)	4,000,000	0	3,921,000	-2.0	3.72
E_2 (psi)	400,000	0	430,000	+7.5	
E_3 (psi)	100,000	0	129,000	+29.0	
E_4 (psi)	30,000	0	28,850	- 3.8	

(b) D = 50 ft subgrade (no. of iterations 2)

Fig 4.25. A theoretical FWD deflection basin generated to study rigid bottom consideration.

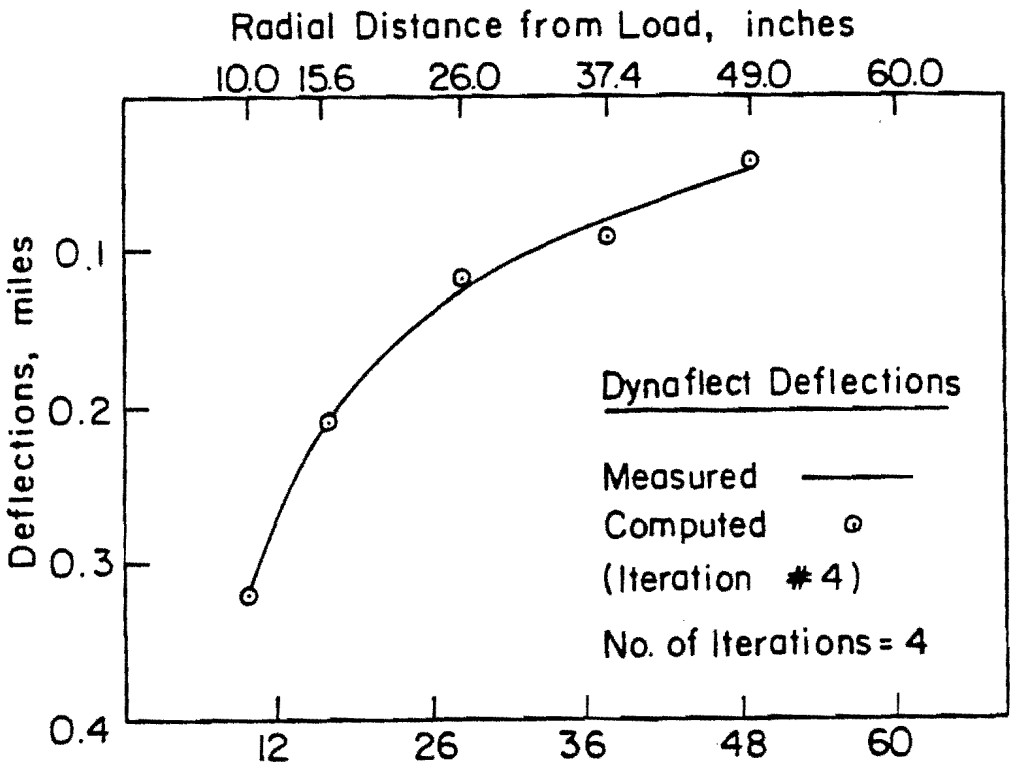

Pavement		Young's Moduli (psi)		
Loop 360 SB (Site #3) St. 404 + 52 (May 1983)	Poisson's Ratio	Input Seed	Predicted	Corrected for Nonlinearity*
1.5-in. AC Surfacing	0.35	0	407,000	--
12.0-in. Flexible Base	0.40	0	100,000	55,300
20-ft Subgrade (17.5 ft Rockfill and Clay) Overlying Bedrock	0.45	0	70,000	50,030

* Procedure for determining nonlinear moduli of granular base and subgrade material is discussed in Chapter 5.

Fig 4.26. Prediction of insitu moduli for a flexible pavement with known depth of subgrade to rock using flexible pavement evaluation program FPEDD1.

modulus at the design temperature is used. In this section, a procedure is described for use in the structural evaluation methodology to estimate the asphaltic concrete modulus, corrected to the design temperature.

Reference Temperatures

Asphalt-bound material is sensitive to temperature and loading frequency. Therefore, its resilient modulus determined in the laboratory is also referred to as dynamic stiffness. However, analysis of the dynamic deflection basin provides Young's modulus of elasticity of the asphaltic concrete layer at the test temperature. The test temperature, T_t, can be estimated using graphical solution (Ref 67) which utilizes the previous five-day mean temperature history at the test site to estimate the test temperature. Worked examples of this procedure are presented in Refs 4 and 52. An alternative approach is to use the computerized procedure of Shahin and McCullough (Ref 68) based on the theory of conduction of heat in an elastic mass. Uddin et al (Ref 7) revised Shahin and McCullough's computer program to predict temperatures in concrete pavements. This approach utilizes daily climatological data and material properties to predict hourly temperature at any depth. Appendix I presents a listing of computer program FTEMP for prediction of test temperatures at the middepth of the asphaltic layer in a flexible pavement.

Design temperature, T_d, is the temperature to which asphaltic concrete stiffnesses should be referenced for the design of pavements. T_d can be taken as the mean annual air temperature. A design temperature of 70°F has been recommended in the FHWA-ARE overlay design procedure (Ref 69); it is the default value to be used in this study.

Correction Procedure

A simplified flow diagram of subroutine TEMPTF for temperature correction of the asphaltic concrete modulus is illustrated in Fig 4.27. This procedure is essentially based on the approach used in the FHWA-RII overlay design method (Ref 19) for flexible pavements. The following

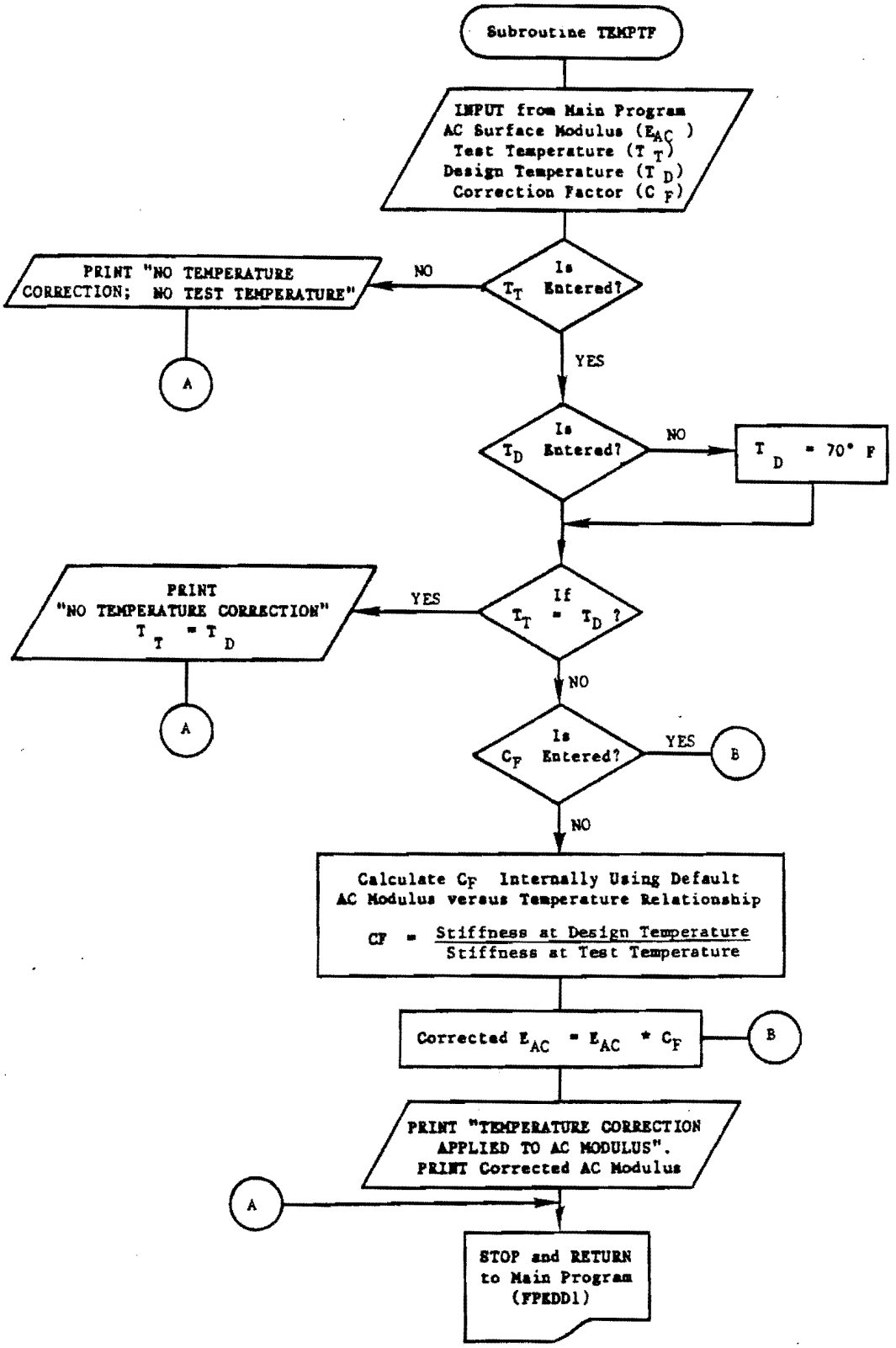

Fig 4.27. Simplified flow diagram of subroutine TEMPTF.

expression is used to obtain the corrected modulus, E1COR, at the design temperature:

$$E1COR = E_1 * CF \qquad (4.17)$$

where

E_1 = insitu modulus derived from the self-iterative analysis of the deflection basin at the test temperature and

CF = correction factor.

The correction factor is calculated from the following relationship:

$$CF = \frac{E1D}{E1O} \qquad (4.18)$$

where

E1D = stiffness of the asphalt mix at the design temperature, T_d, and

E1O = stiffness of the asphalt mix at the test temperature, T_t.

E1D and E1O are to be obtained from the laboratory M_R test (such as described in Refs 69 and 70). Figure 4.28 (taken from Ref 19) illustrates some typical temperature M_R relationships. It is assumed that the insitu asphalt stiffness has a temperature M_R - relationship parallel to the laboratory derived curve for the same asphalt mix. If CF is not entered by the user, the subroutine described here uses a default temperature M_R curve which is taken from Ref 19 (as illustrated in Fig 4.28) to calculate CF. Correction is skipped if the test and design temperatures are identical. If a pavement is old and badly cracked, then it will be unreasonable to use a

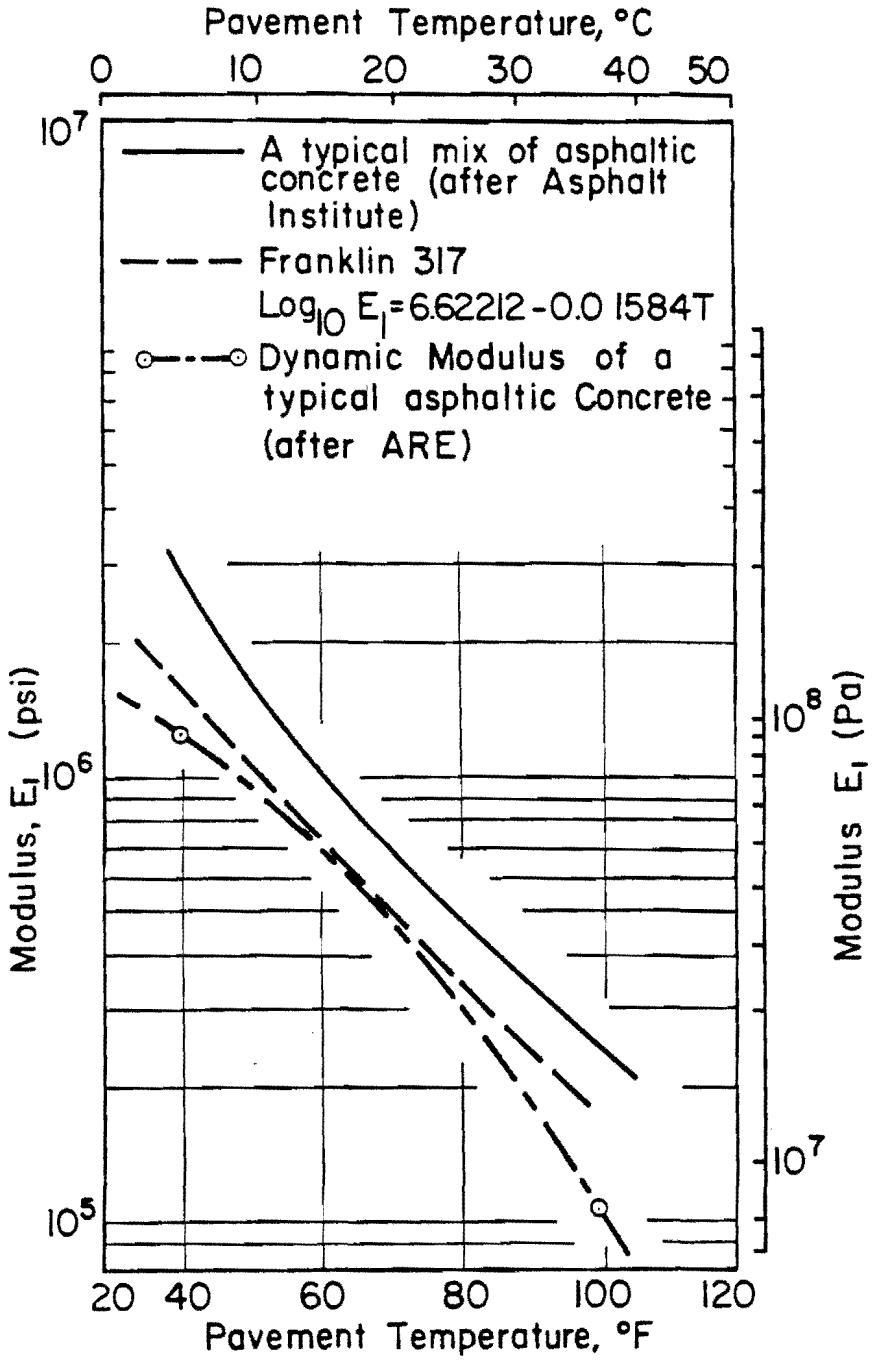

Fig 4.28. Modulus temperature relationships for several asphaltic concretes (Ref 19).

laboratory curve for temperature sensitivity. Due to the aging effect, asphalt stiffness will be only slightly sensitive to temperature changes. In this case, an option is used in the structural evaluation program for flexible pavements (Chapter 8) to omit any correction of the derived insitu asphaltic concrete modulus. Temperature correction is applied after making corrections to the moduli of the granular layers and subgrade for nonlinear behavior.

SUMMARY

The methodology of insitu material characterization from the analysis of a dynamic deflection basin was developed in this chapter. A self-iterative model has been developed to derive the insitu Young's moduli of pavement layers. The model is applicable to a three or four-layer pavement for analyzing Dynaflect or FWD dynamic deflection data. A procedure of successive correction has been developed for the self-iterative model to derive insitu moduli. The correction procedure is based on parametric studies to investigate the sensitivity of a deflection basin to the rates of change in moduli and thicknesses. The procedure is also capable of handling a finite thickness of a subgrade with a rigid bottom. Different criteria and tolerances used for an efficient and reliable convergence process are also developed and discussed in this chapter. A procedure using default seed moduli developed and recommended to achieve uniqueness of insitu moduli was also presented in this chapter. The self-iterative computer subprograms (BASINR for rigid pavement and BASINF for flexible pavement, as described in Chapters 7 and 8) were then used to derive insitu moduli for a number of example problems to evaluate uniqueness, efficiency and accuracy of convergence processes.

Finally, it is recognized that the insitu asphaltic concrete modulus derived from the self-iterative analysis of asphalt pavement represents the stiffness of asphaltic concrete at pavement test temperature. A temperature correction procedure (subroutine TEMPTF) is described which is used to correct the insitu asphaltic concrete modulus to a specified design

temperature. In summary, this chapter is concerned with the development of the first stage of a structural evaluation system based on dynamic deflection basins.

CHAPTER 5. NONLINEAR BEHAVIOR OF SUBGRADE AND GRANULAR MATERIALS IN PAVEMENT SUBLAYERS

BACKGROUND

Insitu moduli of elasticity derived from the static analysis of a deflection basin by the self-iterative procedure using layered elastic theory do not necessarily predict exact behavior of pavement materials under traffic loads. Discrepancies generally exist when predicted behavior for design load is compared with measured response. Pavement moduli are based on the assumption that pavement materials follow the constitutive law of linear elasticity. In the real world these materials do not show exact linear elastic behavior. However, when we are dealing with such materials as concrete, stabilized materials (using cement, lime, or asphalt as stabilizing agents), and asphaltic concrete (taking into account temperature dependency), linear elasticity is usually a good assumption. Therefore, insitu Young's moduli of these materials determined from deflection basins (Chapter 4) can be used for pavement analysis and design with layered elastic theory without causing any significant errors in predictions of pavement response. However, it has long been recognized that granular layers (base/subbase layer) and the subgrade exhibit nonlinear behavior (Refs 69, 70, 71, 72, 73, 74, 75). Therefore, in the laboratory material characterization procedures resilient modulus, M_R, rather than Young's modulus of elasticity is measured. Repeated load triaxial compression tests are used to characterize nonlinear response of these materials. A typical load pulse applied on the specimen is illustrated in Fig 5.1. The duration of the load pulse is typically 0.1 second followed by a rest period of varying duration (Ref 36). Stress and strain are measured after the specimen is conditioned by applying a number of load repetitions. The stress-strain response is generally curvilinear. LVDT (linear variable differential transformer) transducers are used to measure the resilient deformation. M_R, modulus of resilient deformation, is then calculated as a secant modulus using the following relationship:

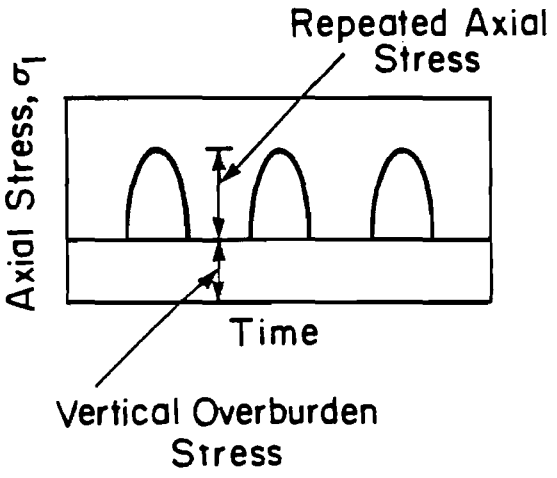

Fig 5.1. Stress state in repeated load triaxial test (Ref 74).

$$M_R = \frac{\sigma_d}{\varepsilon_r} \qquad (5.1)$$

where

σ_d = repeated deviator stress, psi,

ε_r = resilient axial strain, in/in.

M_R is analogous to Young's modulus of elasticity. The deviator stress can be as low as 1 psi and as high as 64 psi (Ref 69). Typical relationships of M versus repeated deviator stress are presented in Fig 5.2.

Nonlinear relationships for M_R of granular and fine-grained materials are reviewed in this chapter. The stress-sensitivity concept and its limitation are also reviewed. The problems involved in using laboratory-derived M_R relationships to correct deflection-basin-based insitu moduli are discussed. An equivalent linear analysis approach is developed using the published research work on dynamic response of granular and fine-grained material. Finally, a self-iterative computerized procedure is described which can be used to correct insitu moduli derived from dynamic deflections for design load conditions.

STRESS SENSITIVE NONLINEAR MATERIAL CHARACTERIZATION

Nonlinear stress-sensitive models for the moduli of granular layers and subgrade are presented in this section.

Granular Materials

Concept. Seed et al (Ref 71), Hicks (Ref 72), Smith and Nair (Ref 75), and other investigators have looked into various factors influencing M_R of unbound granular materials (used for base and subbase layers) and into the

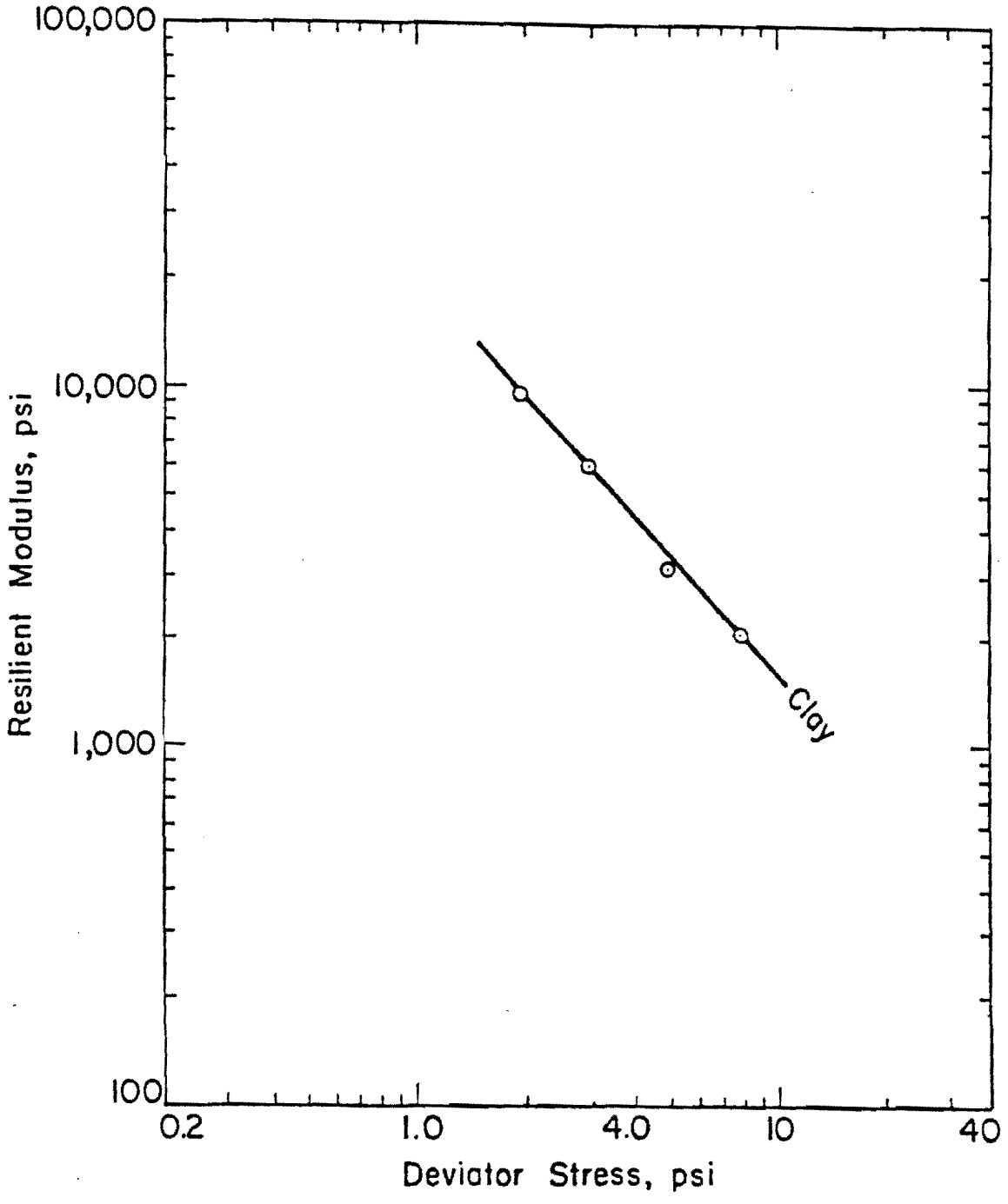

Fig 5.2. Relationship between resilient modulus and deviator stress for typical clay soils (Ref 69).

application of M_R in pavement design and analysis. The most significant factor which influences M_R is confining pressure. The simplest and most widely used nonlinear model for resilient modulus, M_R, of granular materials is presented below:

$$M_R = K_1 \theta^{K_2} \qquad (5.2)$$

where

K_1 = material constant,
K_2 = material constant, and
θ = bulk stress (sum of principal stresses σ_1, σ_2, and σ_3).

The relationship (5.2) is illustrated conceptually in Fig 5.3. Circles present the data points and, on a log-log scale, this relationship is a straight line with K_1 and K_2 being regression constants. Granular materials therefore exhibit so-called stress stiffening behavior. K_1 and K_2 are greatly influenced by the type of material, degree of saturation, and density of the specimen. Rada and Witczak (Ref 76) have summarized published data of 271 M_R tests on a variety of granular materials, including sand gravels, crushed stone, crushed limestone, soil-aggregates blends, etc. Figure 5.4 (taken from Ref 76) shows K_1 and K_2 values (using Eq 5.2) from these tests plotted on a log-log scale. A trend of increasing K_1 with decreasing K_2 can be observed from this plot. One observation related to these data is that there is a significant scatter in laboratory M_R results.

Applications. The laboratory M_R-bulk stress relationship (Eq 5.2) has been applied to correct insitu Young's moduli of granular layers as it allows the consideration of nonlinear behavior (Refs 13, 19, 50, 77, 78). In this approach, layered-elastic theory is applied in an iterative procedure. Figure 5.5 illustrates a simplified flow diagram of this procedure. Principle stresses are computed in the granular layer under a design load

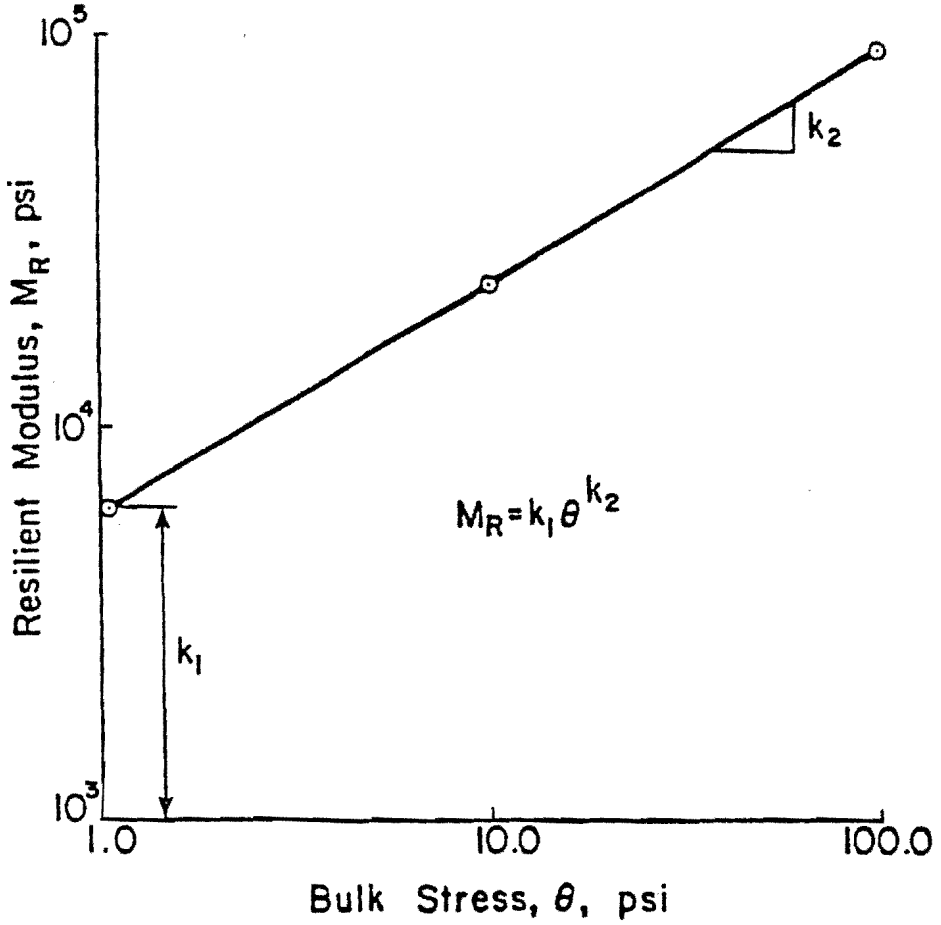

Fig 5.3. A conceptual illustration of M_R versus bulk stress relationship for granular materials.

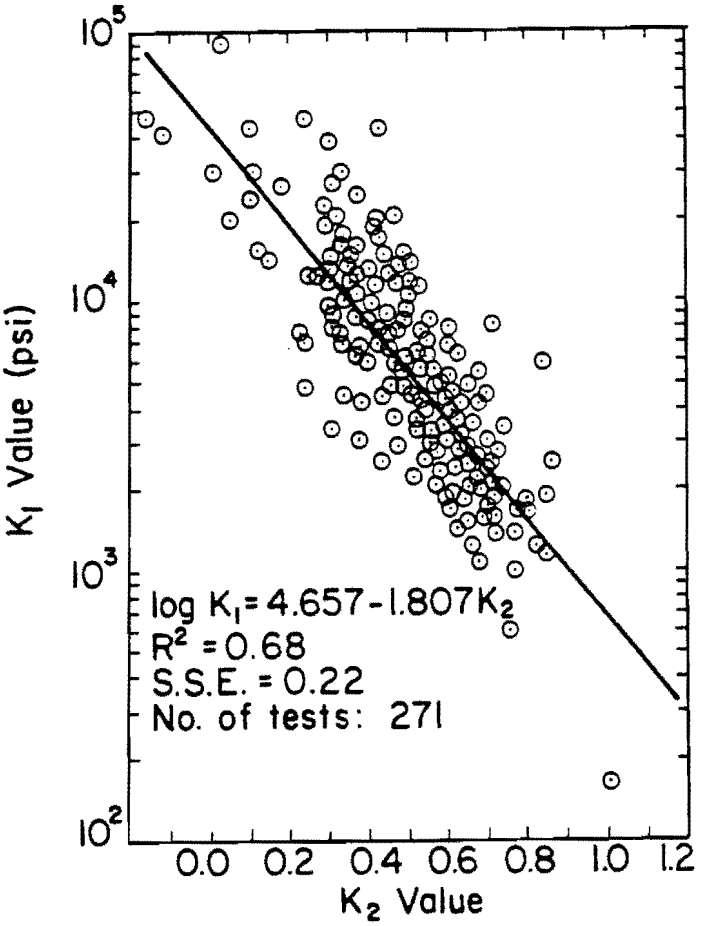

Note: A wide range of materials are included in these data; e.g., crushed stone, gravels, soil-aggregate mixture, lime rock, sand gravels, sands, crushed gravel, slag and silty sand, etc.

Fig 5.4. K_1 - K_2 relation of M_R test results on granular materials (Ref 76).

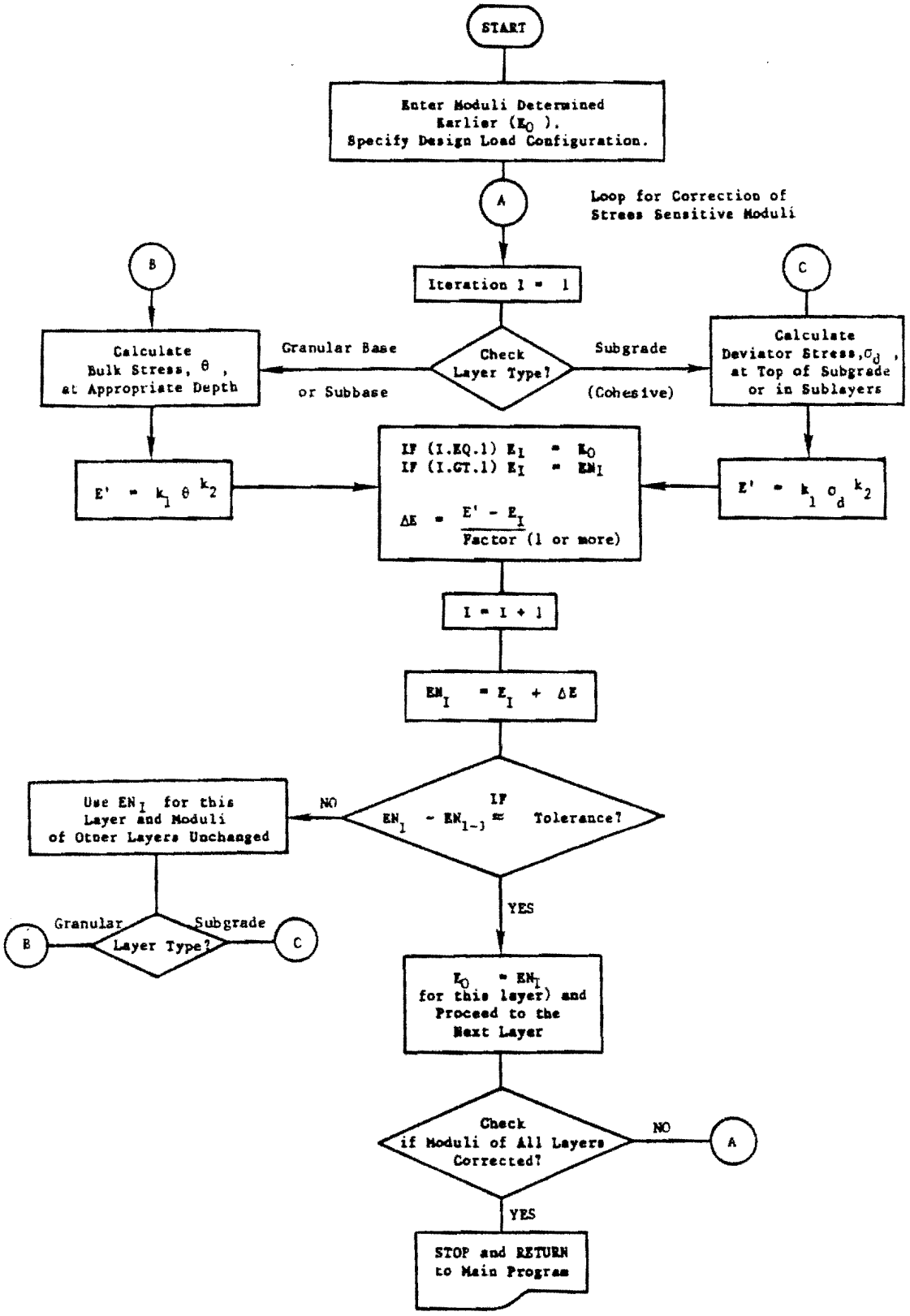

Fig 5.5. A conceptual flow diagram of an iterative procedure to determine non-linear stress sensitive moduli.

condition in order to compute bulk stress, which is subsequently used in Eq 5.2 to obtain the M_R value. This value is then compared to the initial insitu modulus derived from the deflection basin. If the two values are not within a specified tolerance, the new modulus is used to compute stresses. The iterative procedure is continued until a reasonable convergence is obtained in modulus values.

In applying layered theory or finite element solutions, a granular layer can be divided into more than one sublayer, and a variation in the corrected moduli with depth in the granular layer is obtained. The effect of stress changes in the horizontal direction is generally ignored, which is not unreasonable, as shown by Seed et al (Ref 71).

Fine-Grained (Subgrade) Materials

Concept. M_R values are greatly influenced by the level of the repeated deviator stress, σ_d (Ref 69). A conceptual illustration is shown in Fig 5.6. Unlike that of granular materials, the influence of confining pressure is less pronounced. A log-log plot exhibiting a linear relationship between σ_d and M_R is shown in Fig 5.7 and presented by the following expression:

$$M_R = K_1 \sigma_d^{K_2} \qquad (5.3)$$

where K_1 and K_2 are material constants.

K_1 and K_2 are material constants which depend on physical properties of soil and are different from K_1 and K_2 of Eq 5.2. Lower M_R values are associated with a higher level of deviator stress. This behavior is also referred to as stress softening behavior and is considered to represent the nonlinear behavior in the subgrade modulus (Refs 69, 77, 79).

Application. Nonlinear subgrade behavior is taken into account by correcting the insitu modulus using the relationship of Eq 5.3 (developed in the laboratory) through an iterative procedure of using layered theory or

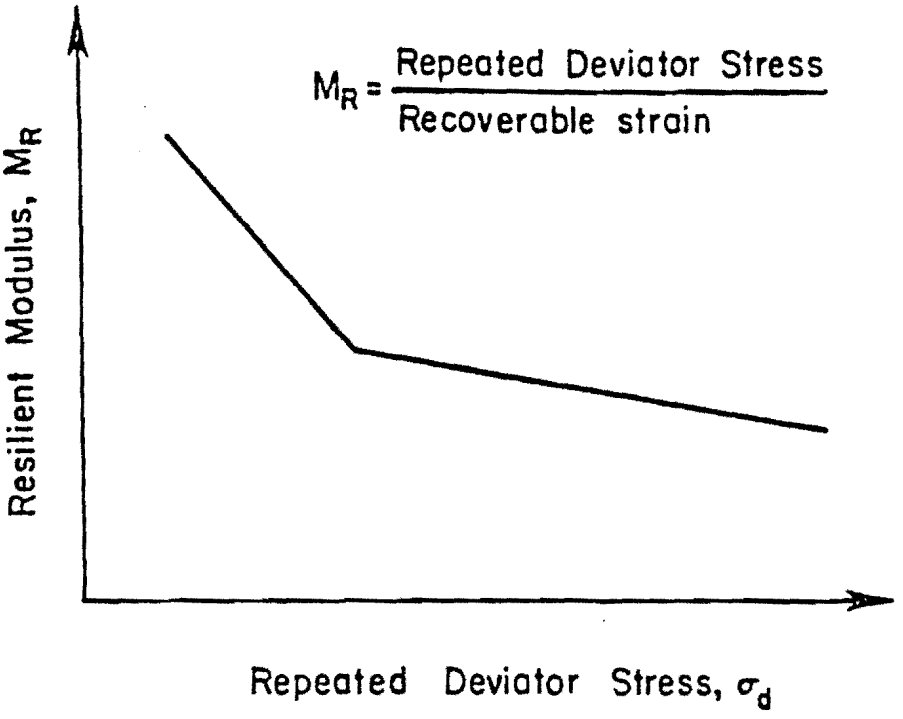

Fig 5.6. A conceptual illustration of M_R versus σ_d relationship for typical subgrade soil.

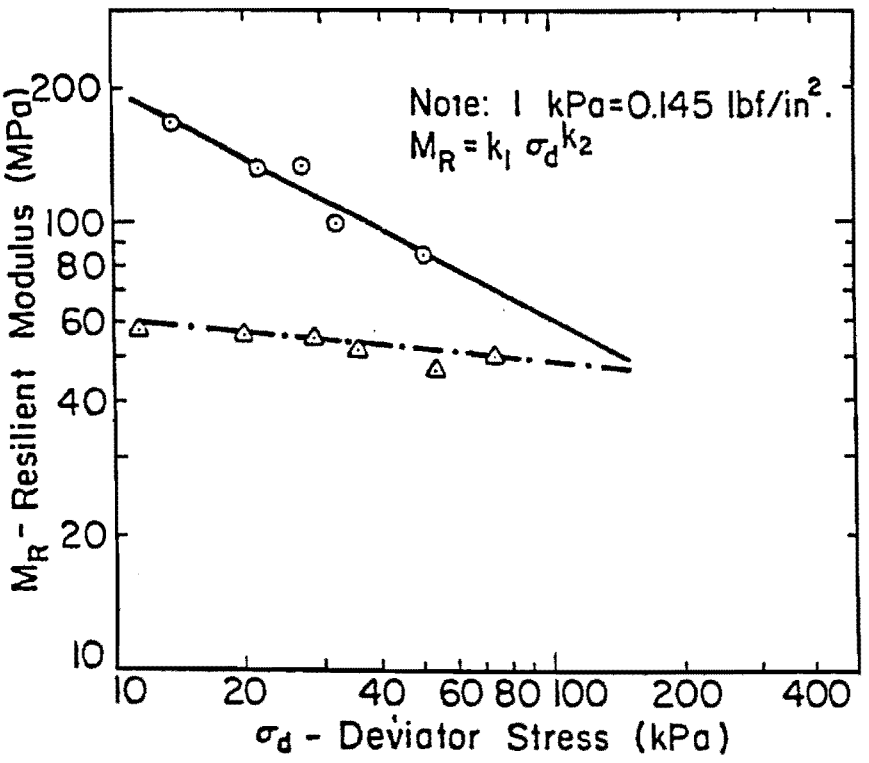

⊙ Indonesian Soil
ω=27.2% γ_d=95.6 pcf
ω_L=41% ω_p=25% I_p=16%
A-7-6 CL
$M_R = 631{,}877\,\sigma_d^{-.506}$ (Metric)
$(34{,}500\,\sigma_d^{-.506})$ (U.S. Units)

△ Maryland Route 97 Soil
ω=17.6% γ_d=106.2 pcf
ω_L=30% ω_p=27% I_p=3%
A-4(0) SM
$M_R = 76{,}042\,\sigma_d^{-.099}$ (Metric)
$(9110\,\sigma_d^{-.099})$ (U.S. Units)

Fig 5.7. Typical nonlinear modulus results of subgrade soils on log-log scale.

finite element programs to converge to a corrected nonlinear subgrade modulus (Refs 13, 19, 50, 51, 78, 80). The iterative procedure is illustrated in Fig 5.5. Recognizing the importance of the variation of the modulus in the vertical direction due to its dependence on deviator stress, nonlinear moduli of several layers in the subgrade are generally computed as illustrated in Fig 5.8. It has not been shown that for an NDT loading condition a homogeneous subgrade (depending on the uniformity of subgrade soils) does not result in significant errors (Ref 78). A summary of published data on K_1 and K_2 of Eq 5.3 as reviewed in Ref 79 is presented in Table 5.1. It was also found (Ref 79) that K_1 increases and K_2 decreases with an increase in dry density or a decrease in moisture content. To predict stress-dependent subgrade moduli from the NDT based insitu modulus of the subgrade, the laboratory M_R relationship is assumed to be known.

Limitations

The stress-sensitivity approach to characterizing nonlinear moduli of granular layers and subgrade from deflection basin-based insitu moduli and laboratory M_R relationships has a number of limitations and discrepancies. A discussion of these and a review of related research is presented below.

Stress Parameters Used in Non-Linear Models. Commonly used stress parameters in nonlinear models discussed above are bulk stress, θ , for the granular layers and deviator stress, σ_d , for fine-grained (subgrade) materials which are defined below:

$$\theta = \sigma_1 + \sigma_2 + \sigma_3 \qquad (5.4)$$

$$\sigma_d = \sigma_1 - \sigma_3 \qquad (5.5)$$

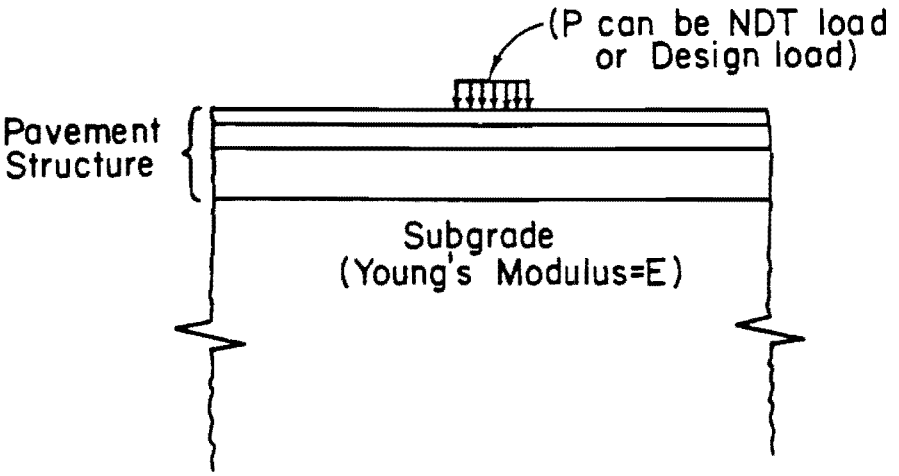

(a) Pavement behaving as an ideal linearly elastic system

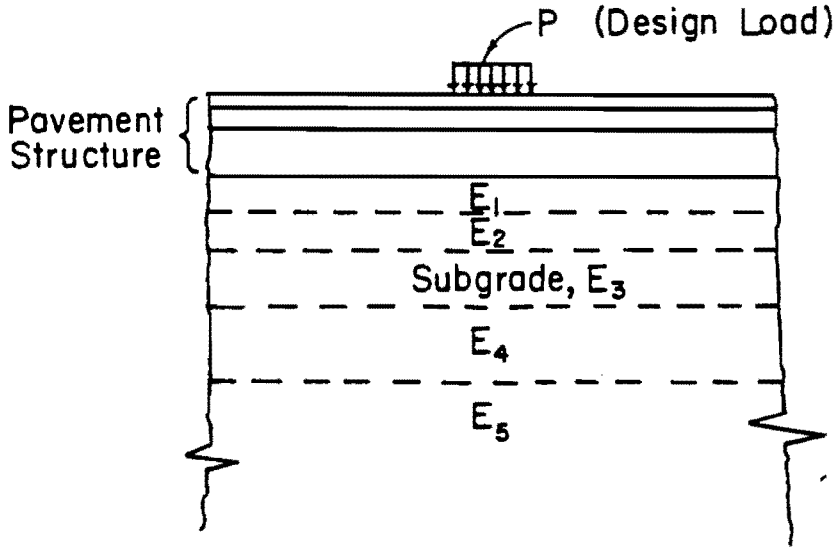

(b) Nonlinear characterization of subgrade modulus

Fig 5.8. Pavement models for subgrade characterization.

TABLE 5.1. SUMMARY OF k_1, k_2 PARAMETERS FOR TYPICAL SUBGRADE SOILS (REF 79).

	San Diego Study		Illinois Study		Maryland Study	
Parameter	K_1	K_2	K_1	K_2	K_1	K_2
Mean	60.6 kips/in^2	-0.37	16.5 kips/in^2	-0.42	47.7 kips/in^2	-0.51
SD	89.3 kips/in^2	0.264	8.3 kips/in^2	0.156	37.8 kips/in^2	0.290
Coefficient of Variance (%)	147	71	51	37	79	57
Range	5.0 to 684 kips/in^2	-1.17 to 3.93	3.0 to 34.0 kips/in^2	-0.74 to -0.17	8.0 to 125.0 kips/in^2	-1.13 to -0.004
Total no. of samples	79		39		19	

These definitions are not unique. Other definitions or stress parameters used by different researchers are presented here

(1) Nonlinear models of granular materials:

(a) Definitions of bulk stress, θ, also depend on testing conditions in the laboratory, as illustrated in Fig 5.9 (Ref 75).

(b) $$M_R = K_1 (\sigma_3)^{K_2} \qquad (5.6)$$

where σ_3 is confining pressure.

(c) Mean normal stress, P, has also been used in place of θ or σ_3.

$$P = \frac{1}{3}\left[\sigma_1 + 2\sigma_3\right] = \theta/3 \qquad (5.7)$$

(2) Nonlinear models of cohesive subgrade:

Stress parameters used in nonlinear models are based on the triaxial state of stress. Bulk stress, θ, is invariant in the sense that it can be defined either in terms of principal stresses (triaxial state of stresses) or normal stresses. However, the stress parameter, σ_d, used in the non-linear model of a cohesive subgrade will be influenced by the way it is calculated. The following definitions have been summarized in Ref 19 (in addition to Eq 5.5):

(a) $$\sigma_d = \sigma_z - \sigma_r \qquad (5.8)$$

where z and r denote symbols for vertical and radial directions.

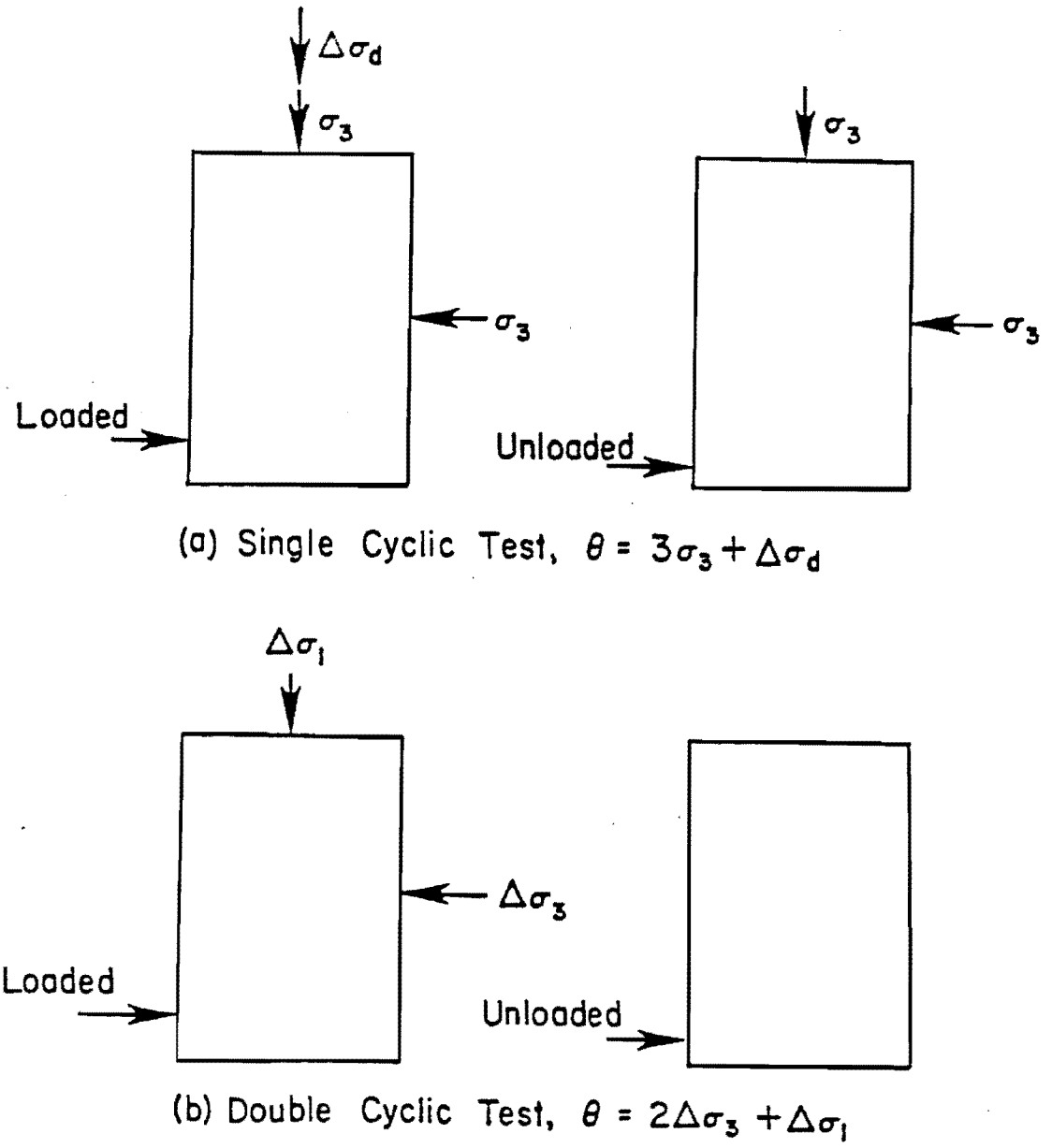

Fig 5.9. Comparison of stress conditions in repeated load triaxial tests (Ref 75).

$$(b) \quad \sigma_d = \sigma_z - \frac{1}{3}(\sigma_x + \sigma_y + \sigma_z) \qquad (5.9)$$

$$(c) \quad \sigma_d = \sigma_z - \frac{1}{2}(\sigma_x + \sigma_y) \qquad (5.10)$$

This equation is identical to Eq 5.5 for the triaxial test condition.

(3) Consideration of gravity stresses:

In applying laboratory M_R relationships to determine nonlinear stress-dependent moduli from insitu linear moduli, stresses are calculated from layered theory computations. Layered theory assumes a weighless medium. Recognizing the contribution of the stress component on an element in a sublayer due to overburden pressure, procedures have been developed which consider gravity (self-weight) stress in addition to the stress due to design load to determine nonlinear moduli (Refs 13, 19, 77, 78). Static preload of NDT devices is also considered by Ref 19, in computation of gravity stress. However, D'Amato and Witczak (Ref 78) have shown in a study of insitu granular layer moduli that non consideration of static preload does not result in any significant error in the non-linear moduli.

Development of Tensile Stress. For certain combinations of pavement moduli, layered elastic theory predicts tensile stresses in granular sublayers (Ref 19, 77). Incorporation of overburden stresses in computation of bulk stress by layered theory has not reportedly resulted in elimination of tensile stress (Ref 77). Moreover, if θ is less than one psi, an unreasonably low nonlinear modulus will be obtained using such relationships as Eq 5.2 (Ref 19). To overcome this problem, different approaches have been proposed by researchers. The simplest approach is to set σ_x and σ_y to zero in the following relationship:

$$\theta = \frac{1}{3}\left[\sigma_z + \sigma_y + \sigma_x\right] \qquad (5.11)$$

However, this approach will result in erroneous moduli as discussed in Ref 19. The approach used by Majidzadeh and Ilves (Ref 19) is to use Eq 5.2 for all cases where the computed value of is equal to or greater than one psi and to use the following expression (Eq 5.12) if computed is less than one psi.

$$E \text{ (nonlinear modulus)} = K_1(0.99 + 0.01\theta) \qquad (5.12)$$

In other words, if the θ is less than one psi, then the modulus of the granular layer is essentially treated as stress independent. This approach is somewhat arbitrary. A more rational and theoretically based method for nonlinear characterization of granular material has been advocated by Stock and Brown (Ref 77); it utilizes a failure criterion of stress in a variant ratio, q/p, where p has been defined earlier in Eq 5.3 and q is expressed as the following (Ref 77):

$$q = (1/\sqrt{2})\left[(\sigma_1 - \sigma_2)^2 + (\sigma_2 - \sigma_3)^2 + (\sigma_3 - \sigma_1)^2\right]^{\frac{1}{2}} \qquad (5.13)$$

The relationship of Eq 5.2 is used for all cases where q/p is equal to or below 1.0. A different nonlinear modulus relationship is used for all values

of q/p between 1.0 and 2.2. Stock and Brown recommend an arbitrarily chosen low value of the modulus (3MPa) for q/p equal to or exceeding 2.2, which is the selected limiting value at failure. Other researchers have used an effective principal stress ratio, σ_1/σ_3 , as a failure criterion. The above discussions on nonlinear characterization of granular materials led to the conclusion that the use of current laboratory characterization procedures to obtain non-linear modulus from the insitu modulus derived by analyzing a deflection basin is somewhat questionable.

Validation of Applying Laboratory M_R Relationships for InSitu Nonlinear Material Characterization. Current procedures which evaluate nonlinear moduli from a deflection basin have the inherent assumption that laboratory derived M_R relationships are valid for the insitu state of stresses. As discussed earlier, K_1 and K_2 parameters are influenced by degree of saturation, water content, and density, which are not always simulated in laboratory tests. A discrepancy may also arise from using total stresses instead of effective stresses in computation of stress parameters in stress-dependent nonlinear models if the material is not in a dry state. The conventional state of stress in the triaxial repeated load test does not truly represent the actual state of stress on an element in the pavement. Horizontal variability in moduli of actual pavement layers is ignored in applying laboratory M_R relationships for nonlinear characterization. Maree et al (Ref 80) reported a comparison of M_R relationships obtained in the field with the laboratory M_R relationships. The nonlinear moduli in the field were determined by measuring the resilient deflection at different wheel loads in different layers and then applying the ELSYM5 computer program (Ref 18) in an iterative procedure. Laboratory and field values of nonlinear moduli of granular and subgrade layers were compared and a shift factor was determined. It was concluded by Maree et al (Ref 80) that conventional triaxial tests overestimate the modulus of granular material and that a shift factor of 0.3 to 0.5 needs to be applied to their test data.

A notable contribution has been made by Witczak and his coresearchers (Refs 78, 81) in recognizing the discrepancy in the current laboratory procedure for nonlinear characterization of granular materials. In the Road Rater study (Ref 78), comparisons are based on mean values of deflections,

tnicknesses, and moduli in each test section. Moduli of different layers of flexible pavement in every test section were obtained by appropriate laboratory tests. Deflection basins were measured by the Road Rater. Granular layers and the subgrade were characterized by nonlinear stress dependent moduli of forms of Eqs 5.2 and 5.3. Theoretical deflections predicted by using the Chevron NLAYER (layered elastic theory) program were consistently found to be two to four times the dynamic deflections measured by the Road Rater, as illustrated in Fig 5.10. The discrepancy between measured deflections (d_m) and predicted deflections (d_p) was attributed to underestimation of resilient moduli of granular layers determined from the nonlinear model of Eq 5.2. A new expression has been used by D'Amato and Witczak (Ref 78) by modifying the nonlinear M_R model of granular layers as given below:

$$M_R = K'_1 K_1 \theta^{K_2} \qquad (5.14)$$

Where the K'_1 factor is a multiplier required to obtain a deflection ratio, R_d, of 1.0 (i.e., $d = d$). The K'_1 factor was obtained only for sensor 1 deflections (located midway between the Road Rater loading plates) by using assumed values of K'_1 and iterative layered theory computations until the condition of $d_p = d_m$ was observed. The K'_1 factor was then considered to be analogous to the K_2 factor used by Seed and Idriss (Ref 82) in their expression of shear modulus used for dynamic response analyses. Based on the shear modulus-shear strain relationship in the dynamic response analysis (Ref 81), D'Amato and Witczak (Ref 78) found the K'_1 factor to be an inverse function of maximum shear strain. This study clearly demonstrate that recent research related to dynamic/seismic response analysis in geotechnical engineering can provide a rational approach towards nonlinear characterization of unbound layers under current dynamic NDT methods used for pavement evaluation.

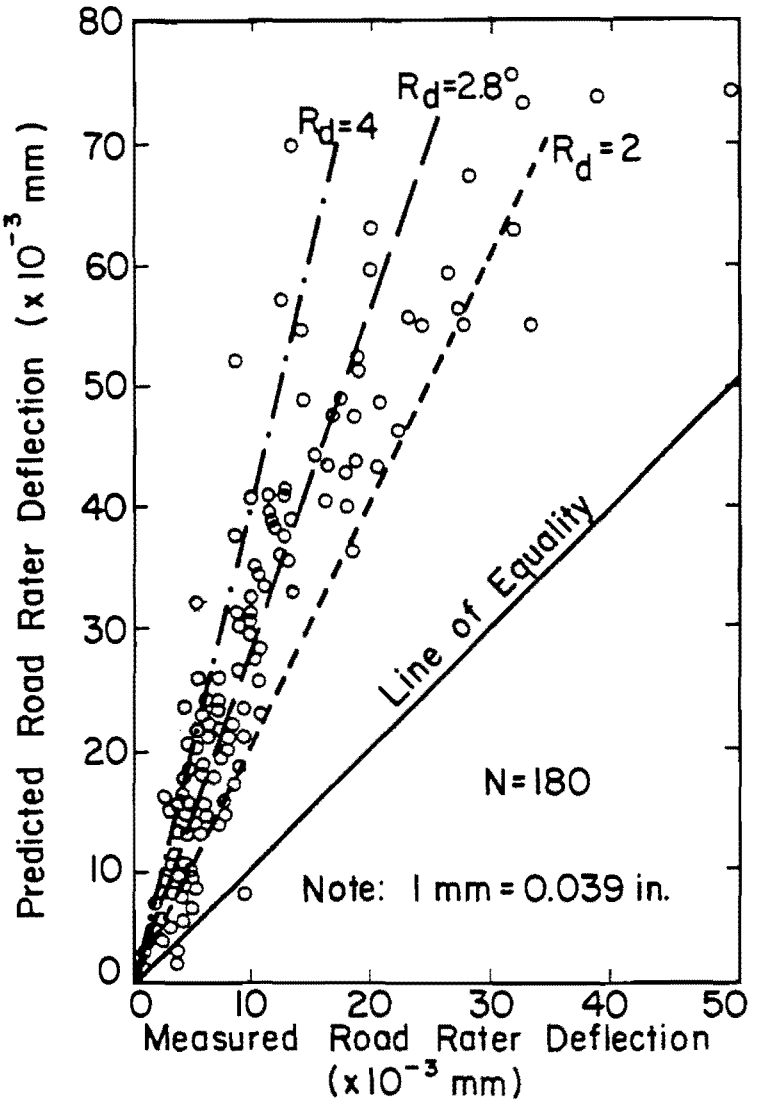

Fig 5.10. Comparison of predicted to measured deflections (Ref 78).

EQUIVALENT LINEAR ANALYSIS

In this section, a relatively new approach to evaluate non-linear moduli of unbound layers and subgrade soil is presented. Basic concepts used in this approach are drawn from recent advances in dynamic/seismic response analysis of soil deposits.

Influence of Shear Strain Amplitude on Deformation and Stress-Strain Behavior

Concepts from Soil Dynamics. In dynamic/seismic analysis, the dynamic shear modulus, G, is of primary importance. Comprehensive research efforts by different investigators (Refs 57, 82, 83, 84, and 85) on laboratory and field determination of dynamic shear modulus have been made within the past two decades. Some of the concepts from these research efforts are presented below. They will be later used in developing a rational approach to determine nonlinear dynamic Young's moduli of unbound pavement layers.

(1) G is a function of shear strain amplitude, γ.

(2) There are several other parameters which affect G. The primary parameters which affect G at all levels of are listed in the following expression:

$$G = f\left[\bar{\sigma}_m, e, N, S, \ldots\right] \qquad (5.15)$$

where

$\bar{\sigma}_m$ = mean effective principal stress,
e = void ratio,
N = number of cycles of loading, and
S = degree of saturation of cohesive soils.

(3) There is a "threshold" strain amplitude (Fig 5.11) below which th dynamic shear modulus is strain-independent and is referred to as the low amplitude strain-modulus (G_{max}). Moduli obtained at higher strain amplitude are nonlinear or "strain sensitive".

(4) Shear modulus and confining pressure (for sands) are related by the following expression (Ref 82):

$$G = 1000\ k_2\ (\bar{\sigma}_m)^{\frac{1}{2}} \qquad (5.16)$$

The K_2 factor has earlier been mentioned in the review of D'Amato and Witczak's study (Ref 78). This factor represents of the influence of void ratio and strain amplitude (Ref 82) as illustrated in Fig 5.12. Using predictive relationships proposed by Hardin and Drenvich (Refs 83, and 84) as well as work from other researchers, Seed and Idriss (Ref 82) have presented the K_2 versus γ relationship at various void ratios which are reproduced in Fig 5.13. Combining the data on sand related to Figs 5.12 and 5.13, Seed and Idriss (Ref 82) have presented a very useful graphical presentation of dynamic shear moduli and shear strain relationship as illustrated in Fig 5.14. It is a dimensionless plot of G/G_{max} as the ordinate and shear strain, γ, percent, as the abscissa. The most interesting point in this presentation is that all the experimental and theoretically generated data fall in a narrow band, which can be considered "unique". In this plot, G_{max} is the value of G at the 10^{-4} percent shear strain level.

Seed and Idriss (Ref 82) also review various testing techniques to determine dynamic shear modulus. In the laboratory methods, cyclic triaxial tests have been widely used, but in

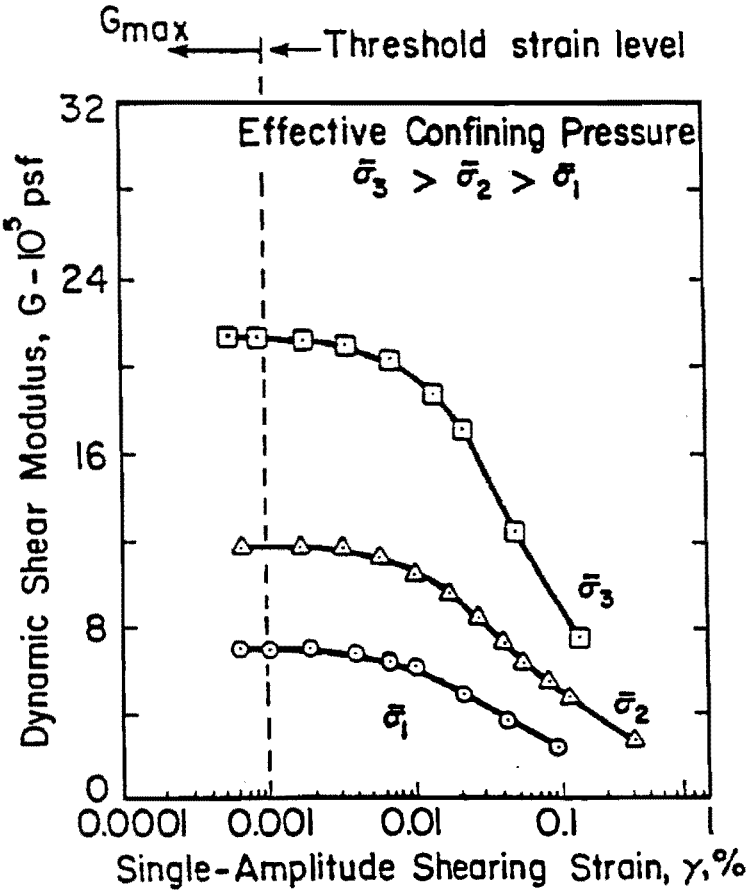

Fig 5.11. Variation of dynamic shear modulus with shearing strain.

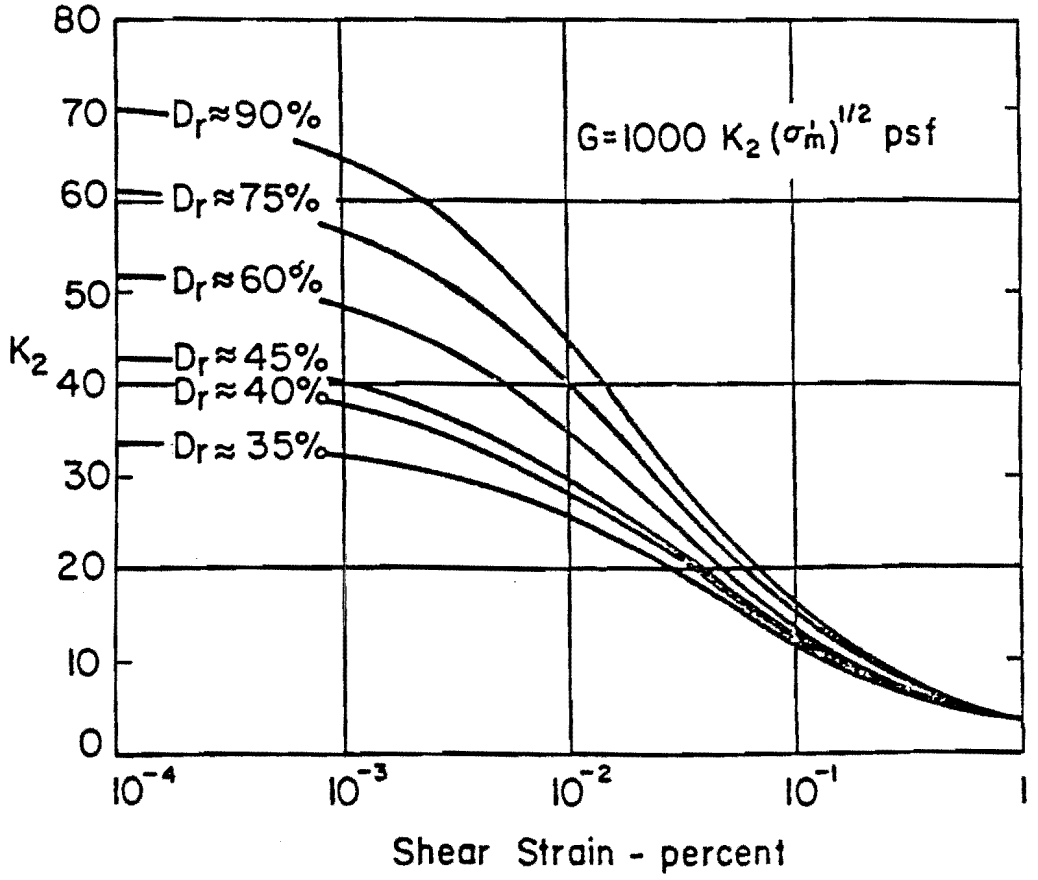

Fig 5.12. Shear moduli of sands at different relative densities (Ref 82).

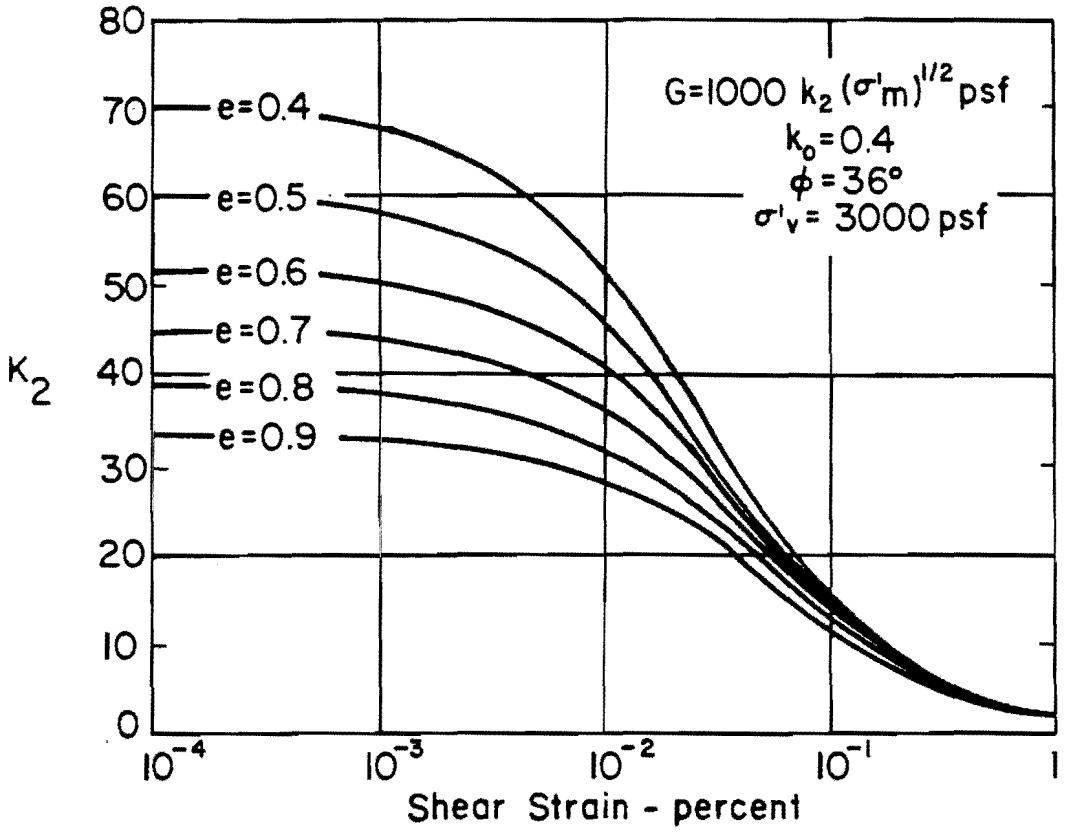

Fig 5.13. Shear moduli of sands at different void ratios (based on Hardin-Drnevich expressions) (Ref 82).

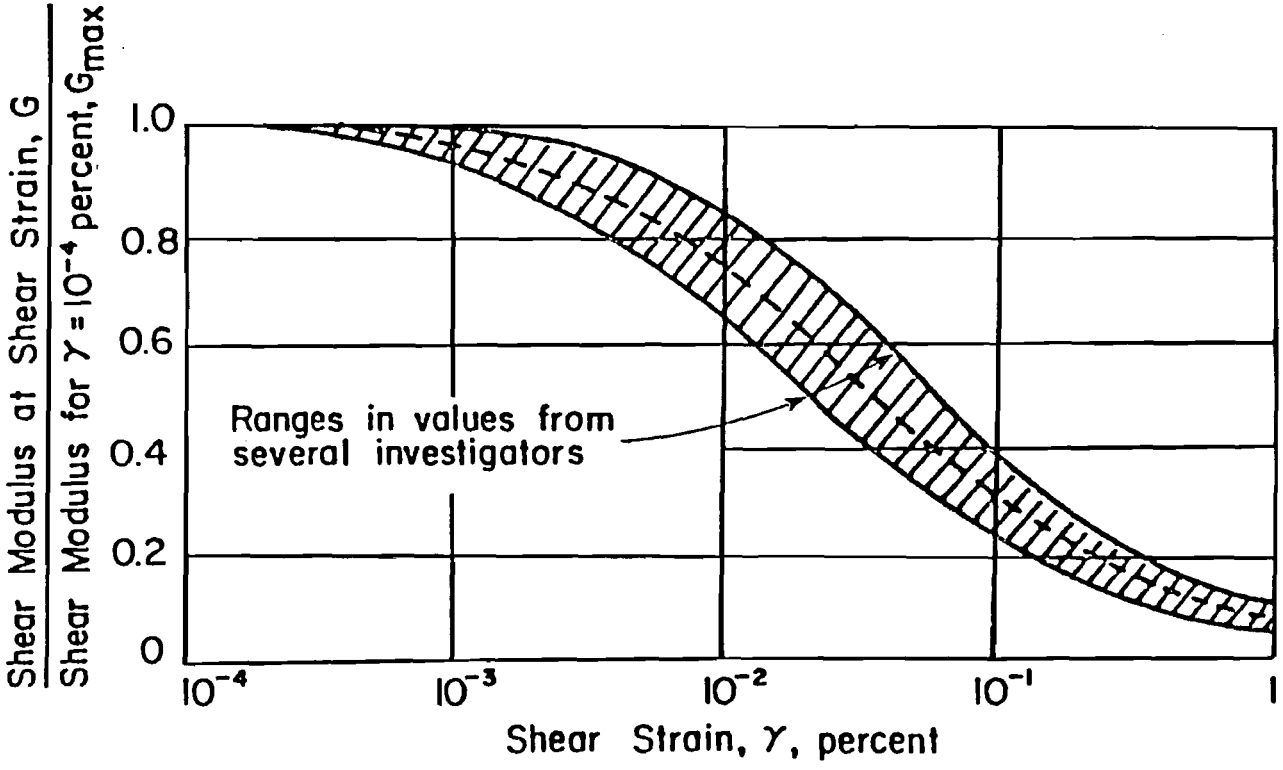

Fig 5.14. Typical reduction of normalized shear modulus with shearing strain amplitude (Ref 82).

general the results will be reliable under moderate (1×10^{-2} percent) to relatively high strains (5 percent) according to Ref 82. Other testing techniques of interest are forced and free vibration methods, which are useful (Ref 82) for determining dynamic properties at relatively low strain to moderately high strain levels (1×10^{-4} to 1 percent). The resonant column test (Refs 57, 83, 86, and 87) comes in the latter category.

(5) Dynamic shear moduli data for gravelly soils which is typical of the unbound bases and subbases of pavements) follow behavior similar to that of sands. Fig 5.15 illustrates such data and Seed and Idriss recommend that the concept of the "unique" G/G_{max} versus γ relationship could be as well applied to gravelly soil (Fig 5.16).

(6) Stokoe and his coworkers (Refs 86, 87, and 88) used the resonant column technique under torsional vibrations to develop G/G_{max} versus γ relationships for a variety of fine-grained soils. A brief description of this technique is presented in Appendix C. Their results are presented in Fig D.1 (Appendix D), which also illustrates the "unique" (mean) curve of Seed and Idriss for sands. These curves indicate that dynamic shear moduli data from different methods when plotted in this non-dimensional way can generate "unique" curves for typical soil types, all of which lie within narrow bands.

(7) If G_{max} is known, then G at any shear strain can be determined using the "unique" curves discussed above. A reliable method for determining G_{max} is use of wave propagation techniques, such as the crosshole test (Refs 56, 58, and 85). A recently developed nondestructive SASW method technique which is based on spectral analysis of surface waves can also provide low-amplitude strain moduli. The SASW method has been used extensively by Stokoe and coresearchers for rigid and flexible pavements as well (Refs 57, 61, 66, 89, and 90).

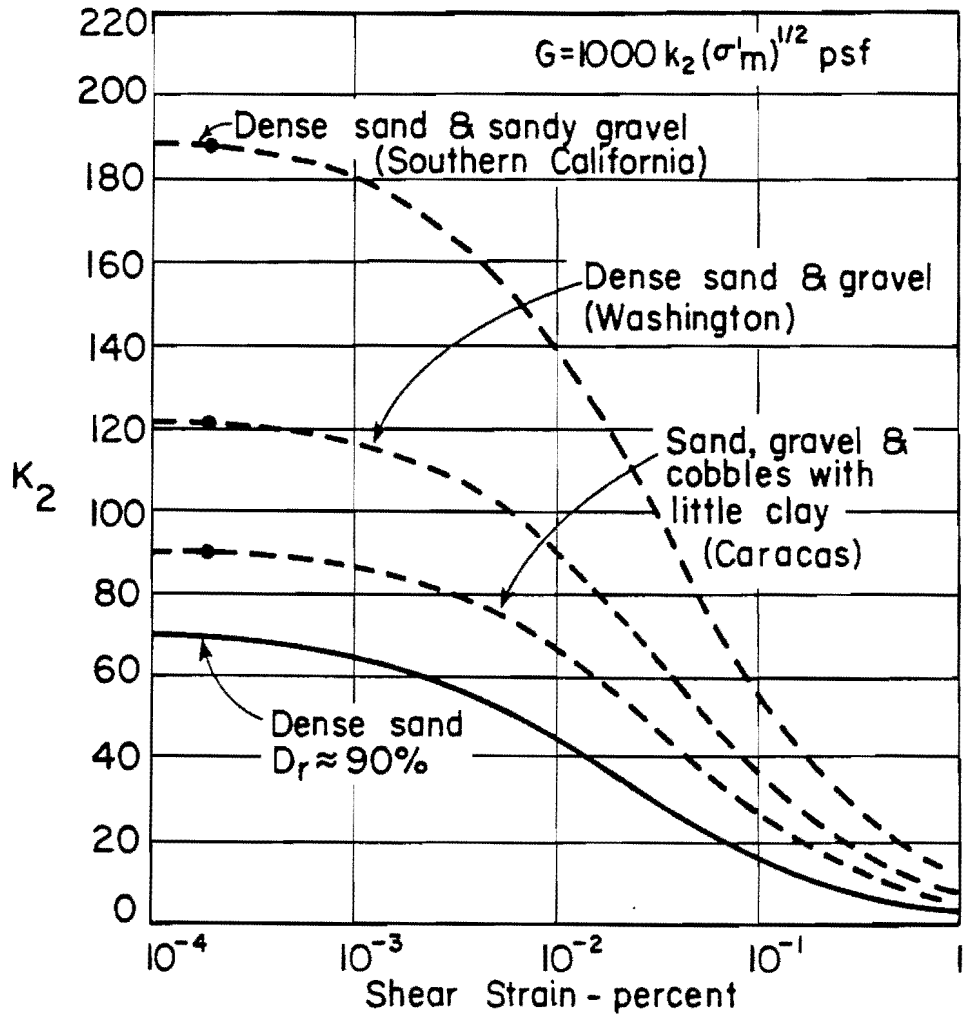

Fig 5.15. Moduli determinations for gravelly soils.

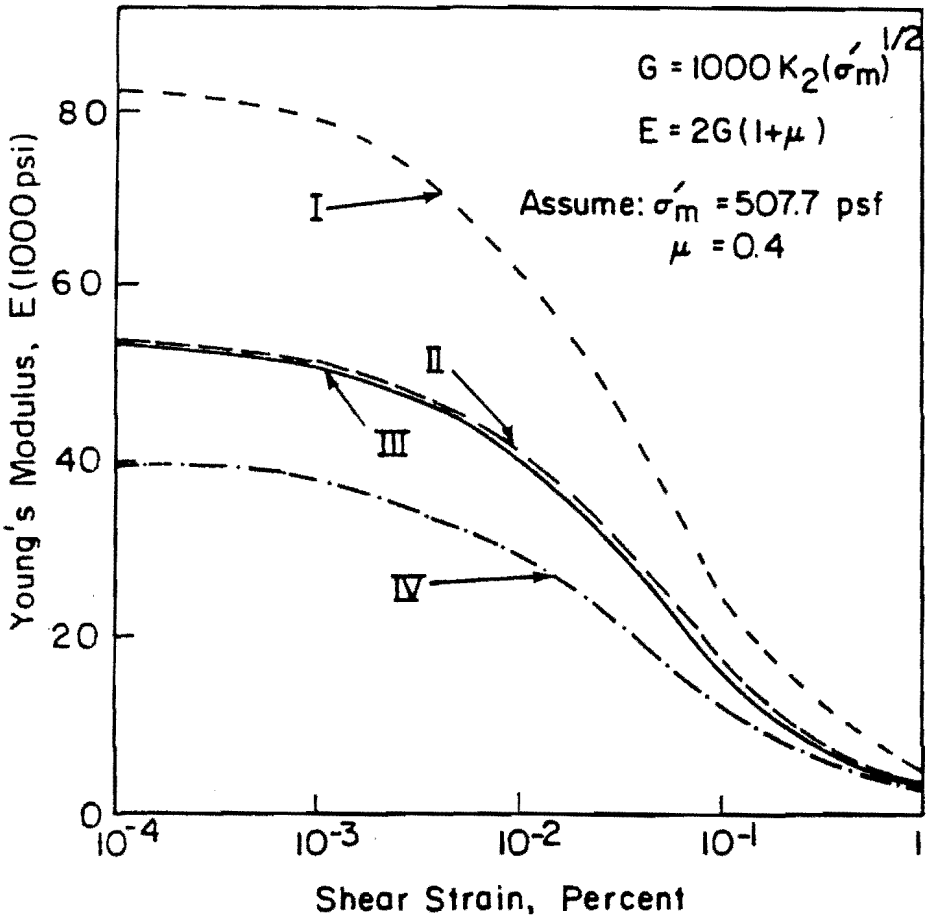

	Soil Type	Origin	K_2 (Corresponding to G_{max})
I.	Dense Sand and Sandy Gravel	Southern California	188
II.	Sand, Gravel and Cobbles with little Clay	Cracas	123
III.	Dense Sand and Gravel	Washington	122
IV.	Sand, Gravel and Cobbles with little Clay	Cracas	90

Fig 5.16. Young's modulus versus shearing strain relationship for gravelly soils (based on data extracted from Ref 82).

005 14

"Strain Sensitivity". The concepts discussed so far are valid when applied in dynamic/seismic response analysis in the geotechnical area. Shear modulus, G, and Young's modulus, E, are interrelated by the following expression:

$$E = 2\,G\,(1 + \mu) \qquad (5.17)$$

where

μ = Poisson's ratio.

Therefore, G/G_{max} data can be translated to E/E_{max} data for a particular soil type. For all practical purposes, the minor effect of Poisson's ratio can be ignored. The "strain softening" behavior exhibited by all types of soils and unbound materials can be examined by using normalized Young's modulus, E/E_{max}, instead of G/G_{max}. Similarly, shear strain amplitude data can be converted to axial strains using Mohr's circle of principal strains. Nazarian and Stokoe (Ref 90) have presented such a nondimensional plot of E/E_{max} versus axial strain in percent from resonant column test data on undisturbed samples of a subgrade soil, as illustrated in Fig 5.17.

Role of Strains in Unbound Layers of Pavements. In the conventional material characterization procedures, the influence of strain amplitudes on M_R measured in laboratory has not been given any emphasis in published research until recently. D'Amato and Witczak (Ref 78) have recognized in print the influence of shear strain amplitude on laboratory M_R relationships of granular materials in base/subbase layers of a pavement by introducing an adjustment factor (the K'_1 factor) in the nonlinear, stress-dependent M_R relationship (Eq 5.14). A strong correlation between shear strain and surface deflection is illustrated in Fig 5.18 (Ref 78). Maree et al (Ref 80) have observed shear failure in base and subbase layers of some of their pavements in heavy-vehicle simulator tests. They indicated that shear stresses and strains in these layers were high and that near failure

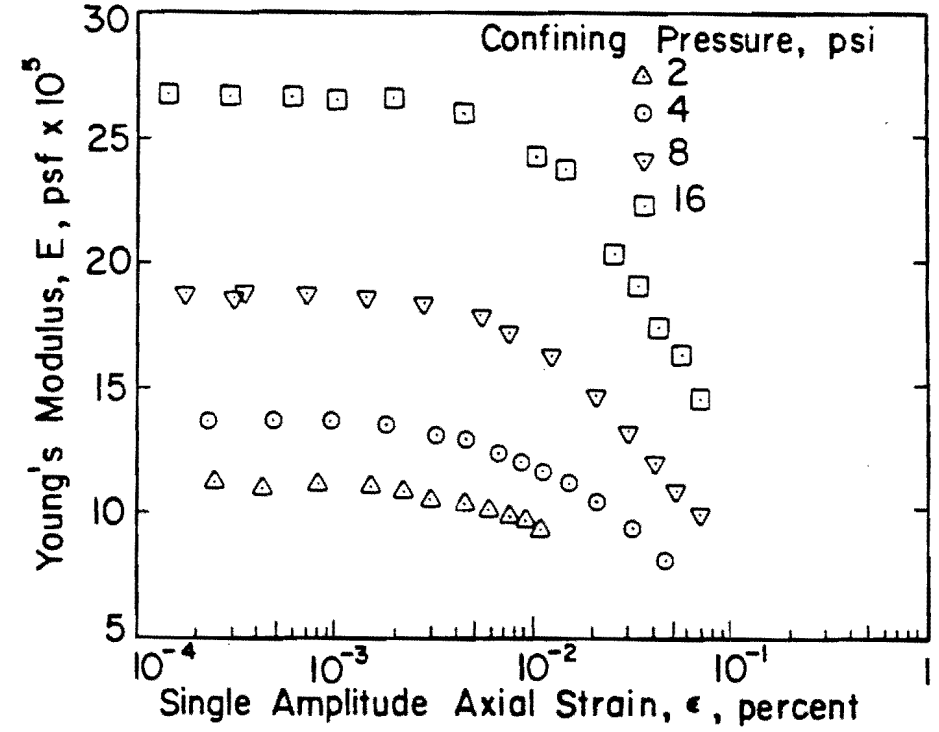

(a) Variation in Young's Modulus with Strain Amplitude at Different Confining Pressure

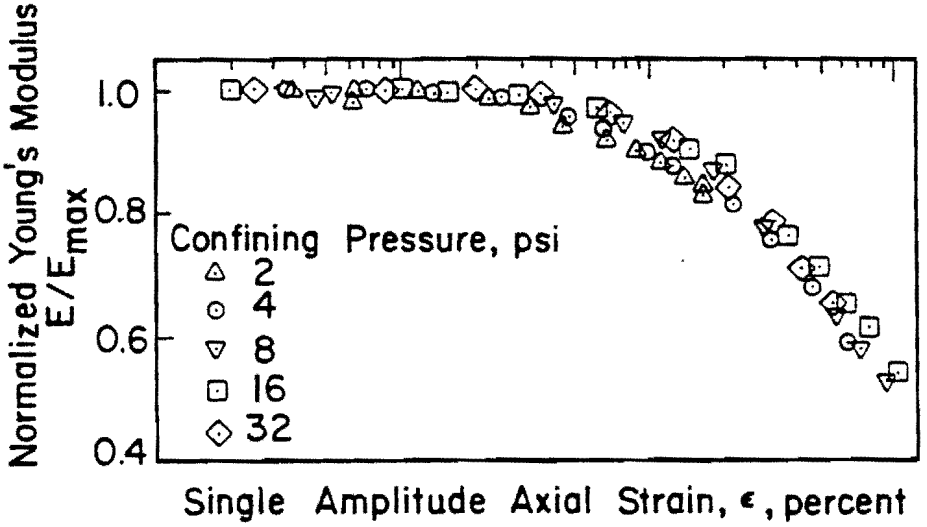

(b) Variation in Normalized Young's Modulus with Strain Amplitude

Fig 5.17. Effect of axial strain amplitude on Young's modulus of an unsaturated clay subgrade (Ref 90).

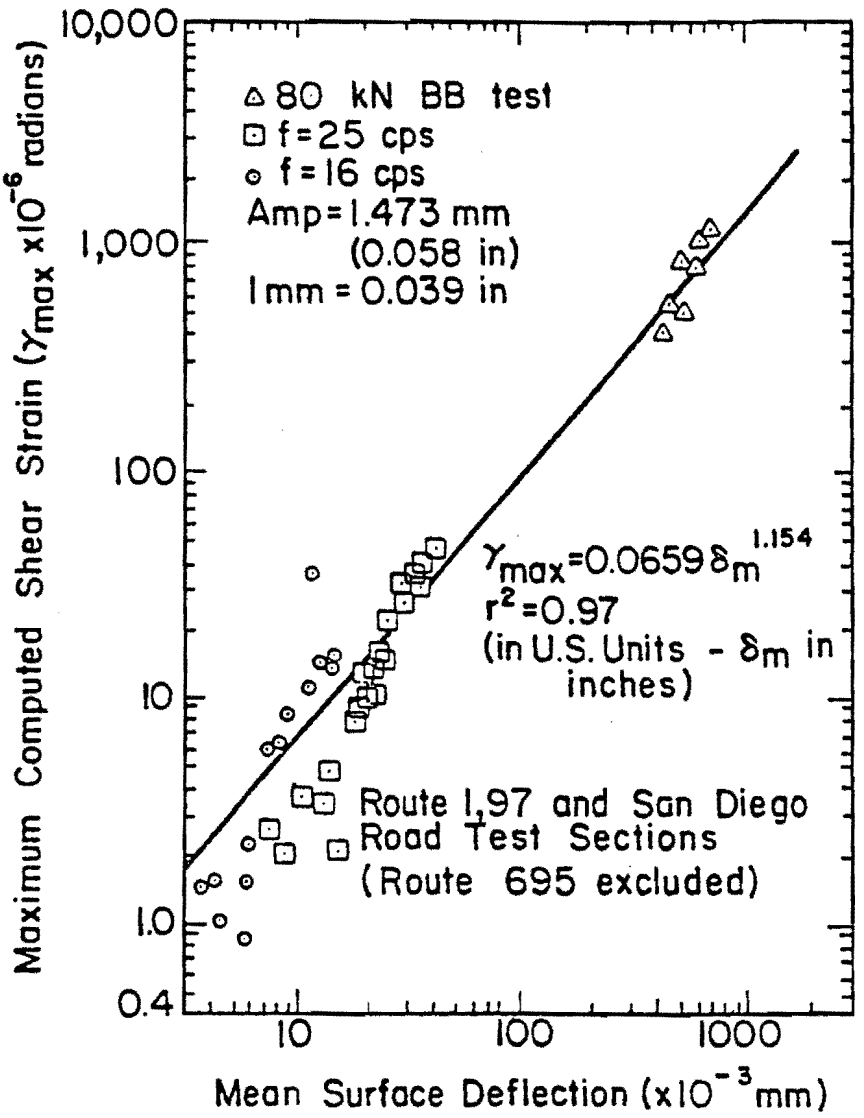

Fig 5.18. Maximum computed shear strain versus mean surface deflection (Ref 78).

conditions existed at the time of measurement. The importance of axial compressive strain on top of a subgrade is realized in current pavement design procedures where a limiting compressive strain is used for thickness design.

Proposed Approach. In the current NDT techniques for pavement evaluation, strain amplitude should be considered in the analysis. Dynamic devices such as the Dynaflect, FWD, and Road Rater will generate different strain amplitudes in pavement layers, which can be associated with the determination of nonlinear moduli using the E/E_{max} versus shear strain relationships. The first step is to determine the threshold strain amplitudes on these curves. Output from ELSYM5 includes maximum shear strain. The maximum shear strain amplitudes predicted by ELSYM5 for NDT loading and for the design wheel load configuration are to be compared. The insitu moduli used in these computations could be the combination derived from the analysis of a dynamic deflection basin. If the strain amplitude under NDT loading in an unbound layer is below the threshold strain level, Young's modulus of that unbound layer is E_{max}. The nonlinear, strain dependent modulus of that layer can be determined by using the unique E/E_{max} versus shear strain curve in an iterative procedure until an acceptable convergence in the computed strain under the design wheel load is achieved.

Determination of Nonlinear Strain Sensitive Insitu Moduli

Insitu moduli of unbound layers and the subgrade determined from the analysis of the dynamic deflection basin (Chapter 4) are to be corrected to reflect nonlinear, strain softening behavior of these materials.

Stress-Strain and Deformation Behavior under Pavement Loading. The NDT loading configuration is therefore an important parameter in applying an equivalent linear analysis.

(1) If the maximum shear strain in the granular layer is below the threshold limit, then the corresponding modulus from the analysis of the deflection basin is E_{max}, which is strain independent. This is the case of the Dynaflect. Therefore, a nonlinear modulus must

be determined corresponding to the shear strain amplitude determined from application of design load. The design load configuration is shown in Fig 5.19.

(2) In those NDT devices, e.g., the FWD, which can apply a peak force equal to design load, the shear strains induced by the two loads will be in close agreement. In that case, there is no need for equivalent linear analysis. The insitu modulus of the granular or subgrade layer used for shear strain calculation already represents a nonlinear modulus and does not require a correction. Examples of these discussions are also illustrated in Fig 5.20.

(3) If the NDT load is heavier than the Dynaflect loading but much less than the design load (e.g., the Road Rater loading or the FWD at smaller peak loads) then the equivalent linear analysis approach cannot be used directly. Conceptually, it is illustrated in Fig 5.21. In this case, the low amplitude modulus, E_{max}, is unknown. One appropriate procedure for determining E_{max} is illustrated in Fig 5.21. In this procedure the input value of E of the unbound layer can be divided by the E/E_{max} ratio obtained from the E/E_{max} versus γ curve (as an appropriate γ was already calculated by ELSYM5). This E_{max} can then be iteratively used to modify E using E/E_{max} and γ values corresponding to the design load.

(4) Low amplitude Young's moduli of unbound layers in a pavement structure can also be determined from the crosshole test, and the SASW method as well as from the Dynaflect deflection basin as discussed in Chapter 4 and above in (1). Yet another approach is to use Hardin and Drnevich's design equation (Ref 84) for G_{max}, which is given below:

$$G_{max} = 1230 \frac{(2{\cdot}973 - e)^2}{(1 + e)} (OCR)^K \bar{\sigma}_m^{\frac{1}{2}} \qquad (5.18)$$

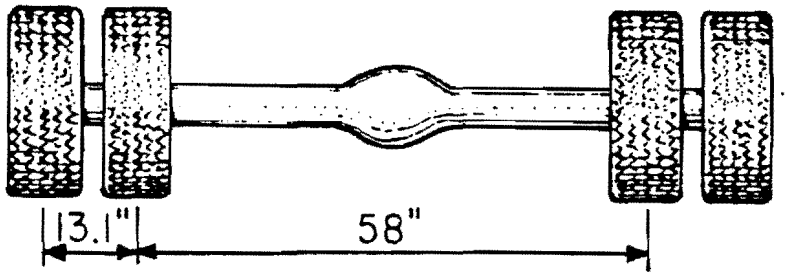

(a) Standard 18-kip single axle: 4 tires, each 5500 lb at 75 psi tire pressure.

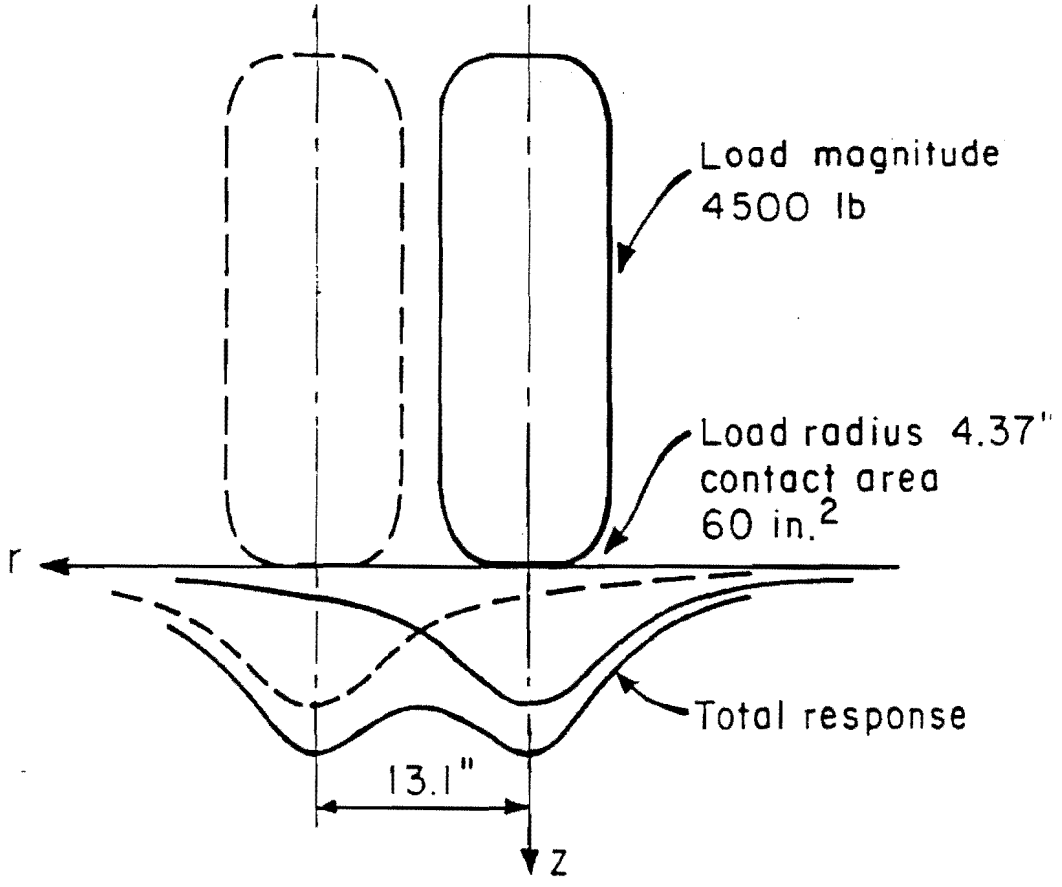

(b) Simulated 18-kip axle load (half the standard axle) and illustration of superposition of responses.

Fig 5.19. Standard 18-kip axle configuration and simulation used in RPRDS-1 (Ref 38).

(a) Rigid pavement structure used in this study

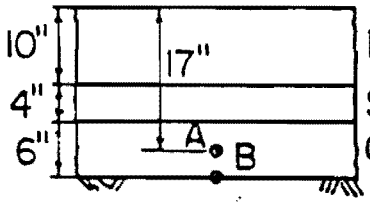

	E (psi)
P.C.Concrete	4,000,000
Stabilized Base	200,000
Granular Subbase	75,000
Semi-infinite Subgrade	30,000

(b) Design Load Configuration (Fig. 5.19)

(c) Computed shear strain data

Loading Conditions	Mid-depth of Subbase (A)		At top of Subgrade (B)	
	γ_{max}[1], %	E/E_{max}[3]	γ_{max}[1], %	E/E_{max}[4]
Single Axle 18 kips - Design Load	5.227×10^{-3}	≈0.83	5.419×10^{-3}	≈0.91
FWD (9000 lbs peak Force Amplitude, Radius of Loading Plate = 5.91 in.)	5.592×10^{-3}	≈0.83	5.683×10^{-3}	≈0.91
Dynaflect[2]	5.381×10^{-4}	≈1.00	5.729×10^{-4}	≈1.00

Notes: 1. Largest of all values of maximum shear strains computed under the loading (from ELSYMS output)

2. For Dynaflect; equivalent single amplitude shear strain amplitude is half of the value shown in the column (E/E_{max} for Dynaflect is based on half of γ_{max} shown in the column)

3. Solid line curve (Fig. 5.22)

4. Broken line curve (Fig. 5.22)

Fig 5.20. Illustration of computed maximum shear strain amplitude variation with loading condition.

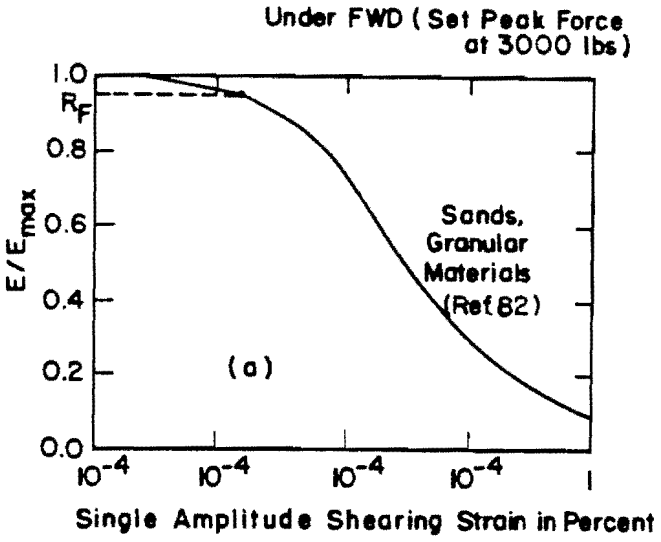

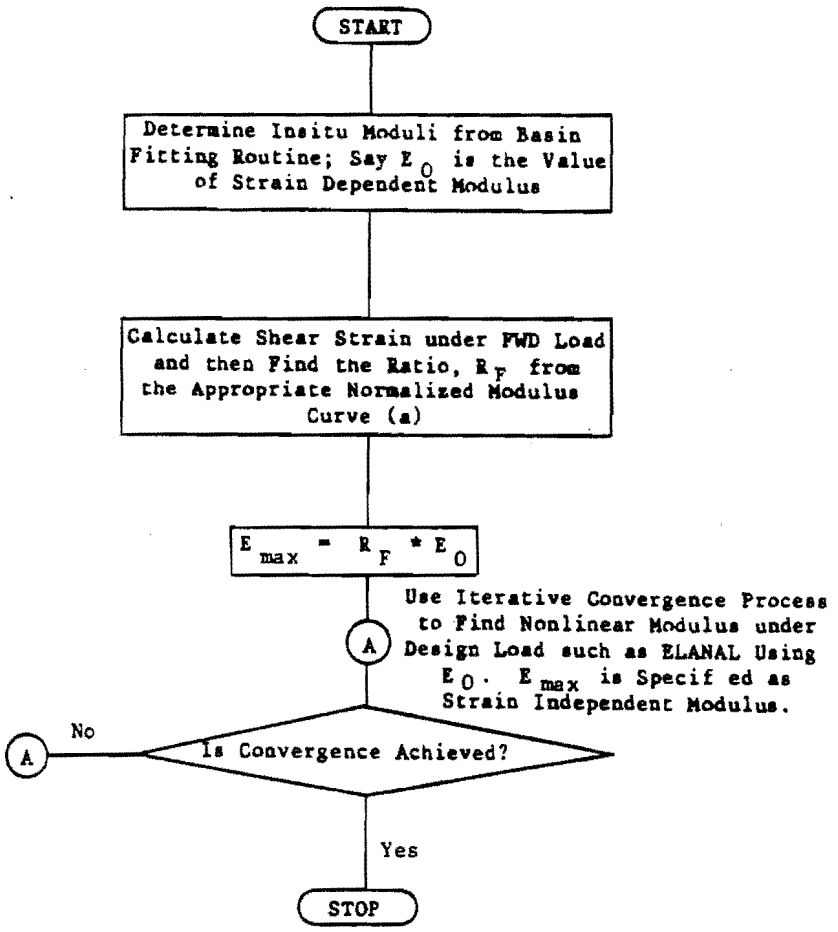

Fig 5.21. Conceptual illustration of an approximate procedure to determine nonlinear moduli when FWD is used at a low amplitude of peak force.

where

e = void ratio,

OCR = overconsolidation ratio,

K = a parameter depending on plasticity index (Table 5.2), and

$\overline{\sigma_m}$ = mean effective principal stress,

$\overline{\sigma_m}$ and G_{max} are in psi.

The above expression has also been used in the analysis of dynamic moduli for an airport pavement by Baird and Nash (Ref 91).

(5) For the purpose of this study, it is concluded that (a) an equivalent linear analysis should be applied to the moduli of unbound layers determined from a dynamic deflection basin measured by the Dynaflect (assumed to be low amplitude strain moduli) in order to derive appropriate insitu nonlinear strain-sensitive moduli of these layers, and (b) the Falling Weight Deflectometer can apply a variable peak force on the pavement surface. Assuming the test force of the FWD chosen is such that its maximum shear strain response is about the same as the design load, then the moduli determined from the deflection basin fitting method are the insitu nonlinear moduli of unbound layers and subgrade. The equivalent linear analysis can therefore be skipped in the case of FWD dynamic deflection data.

Mathematical Modelling of Normalized Moduli versus Shearing Strain Curves. The basis of the equivalent linear analysis discussed until now is the normalized moduli versus shearing strain relationship such as shown in Fig 5.22. As compared to the large scatter in laboratory M_R data (Fig 5.1 and Table 5.1), E/E_{max} versus shear strain data always lie within a very narrow band for different types of soil and sand and gravelly material. Part of the data in the low amplitude strain range can be obtained in field tests (crosshole, SASW, Dynaflect). For the purpose of this study, two unique curves have been selected to use with an equivalent linear analysis. One

TABLE 5.2. VALUES OF K FOR HARDIN AND DRENEVICH'S EQUATION (REF 84)

PI	K
0	0
20	0.18
40	0.41
60	0.41
80	0.48
≥100	0.50

curve is for granular layers (shown in solid lines) and the other is for fine-grained soil (typical of subgrade, shown in broken lines) as illustrated in Fig 5.22.

Mathematical relationships are needed to define these curves. There are several approaches to developing predictive equations by which the E/E_{max} ratio, can be determined corresponding to a known value of shear strain, γ . Ramberg-Osgood curves (Ref 92) have been used by some researchers. The relationship can also be linearlized by transforming γ (e.g., a hyperbolic function) and then fitting a regression line. Another statistical model is a logistical model using the nonlinear regression approach. All these approaches are discussed in detail in Appendix D, where several predictive equations are also developed.

The predictive equations for granular materials and cohesive subgrades based on unique curves in Fig 5.22, which are currently included in this study as default procedures, are shown in Table 5.3. It is noted, however, that these two curves are either a mean curve (Ref 82) or a smoothed curve over experimental data (Ref 87). The statistical fit inherent in the two equations, 5.19 and 5.20 (Table 5.3), are based on unique curves and not actual data points. Actual experimental data were not accessible during the present research. Regression if performed using actual experimental data is always more meaningful and the outcome will certainly be a more reliable predictive relationship. It is recommended that new predictive relationships should be developed as soon as enough experimental data are available on both sands (or gravelly material) and fine-grained (cohesive) type material.

Development of a Self-Iterative Procedure for Equivalent Linear Analysis

A self-iterative procedure has been developed to apply equivalent linear analysis to determine nonlinear strain dependent moduli of the granular base/subbase layers and the subgrade after derivation of insitu linear Young's moduli of these layers from the analysis of the Dynaflect deflection basin. Ideally, the nonlinear modulus should be determined at the top, middle, and bottom of each granular layer, as well as in the middle of subgrade sublayers (two or three layers, each 6 inches to 2 feet thick,

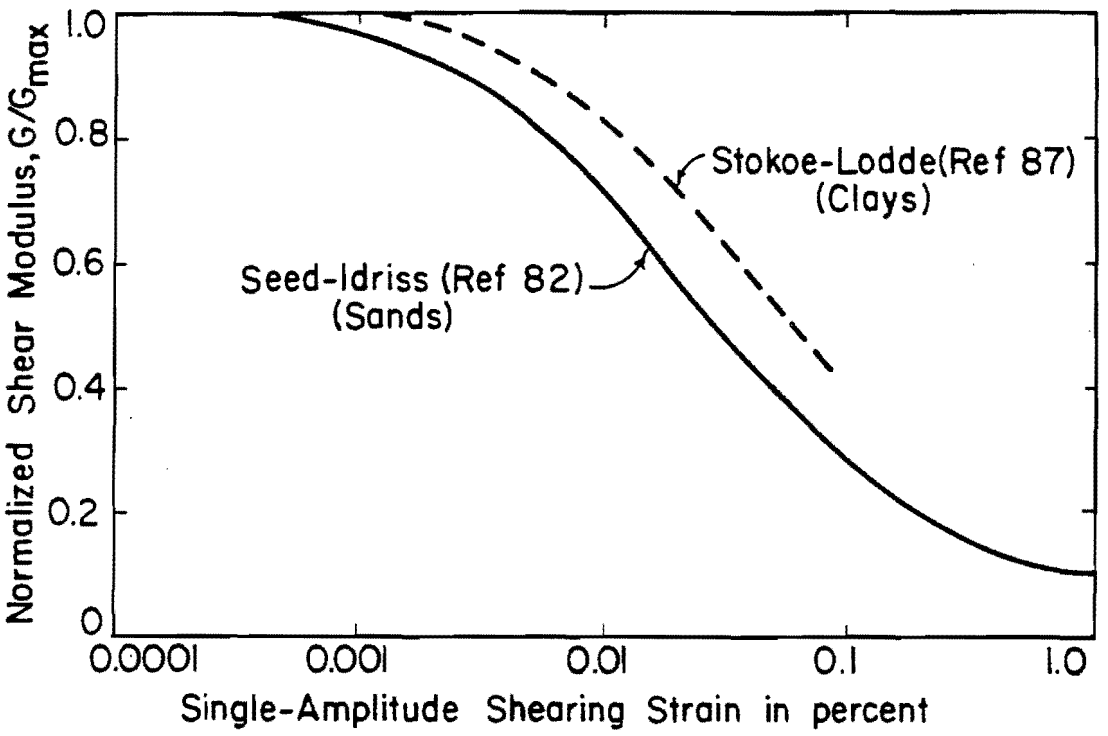

Fig 5.22. Summary of normalized shear modulus variation with shearing strain.

TABLE 5.3. PREDICTIVE EQUATIONS FOR NORMALIZED MODULUS (EQUIVALENT LINEAR ANALYSIS)

MATERIAL	RANGE OF γ (PERCENT)	PREDICTIVE EQUATION	R^2
Granular Soils	> 0.004 ≤ 0.07	$E/E_{max} = 1.2697509 - 1.2072571\ (A)^*$	0.99
	≤ 0.004	$E/E_{max} = 1.0$	
Subgrade (Cohesive Soils)	> 0.001 ≤ 0.07	$E/E_{max} = 1.3760883 - 1.2593853\ (A)^*$	0.99
	≤ 0.001	$E/E_{max} = 1.0$	

* $$A = \frac{2.0}{(2.0)^{\log_{10} \gamma} + \frac{1}{(2.0)^{\log_{10} \gamma}}}$$

where γ = single amplitude shearing strain, percent

created in the original subgrade) and on top of the semi-infinite subgrade. The ideal system is shown in Fig 5.23. Because ELYSM5 is called to calculate the pavement response in each iteration therefore the idealized system will eventually result in a large number of ELSYM5 runs and become prohibitively expensive. Therefore a simplified pavement system is assumed for equivalent linear analysis, as illustrated in Fig 5.24.

Assumptions. There are several simplified assumptions in the equivalent linear analysis adapted in this research.

(1) Any pavement sublayer with stabilized material is assumed to be characterized by a (linear) strain independent modulus which can be derived from the inverse analysis of a Dynaflect/FWD deflection basin. Examples of these materials are asphalt or cement-treated base and subbase material or cement/lime stabilized subgrade materials.

(2) The normalized modulus versus shear strain curves (Fig 5.22) can be uniquely applied to derive nonlinear insitu moduli of granular layers and cohesive subgrade using the pavement model of Fig 5.24.

(3) All the assumptions made to use ELSYM5 for analyzing NDT dynamic deflection data are also applicable to this analysis.

(4) Furthermore, the theoretical responses determined by ELSYM5 under the Dynaflect or design load are analogous to peak-to-peak response due to any steady state or sinusoidal load.

(5) The unique curves for dynamic response analysis (Fig 5.22) were developed by using single amplitude shear strain in percent. In order to ensure compatibility for using the maximum shear strain amplitude predicted by ELYSM5 in the equivalent linear analysis, the predicted shear strain amplitude is to be halved and then multiplied by 100 to convert it into percent single amplitude shear strain.

(6) Equivalent linear analysis is to be commenced from the first strain sensitive layer below the surface asphaltic concrete (flexible pavement) or portland cement concrete layer (rigid pavement).

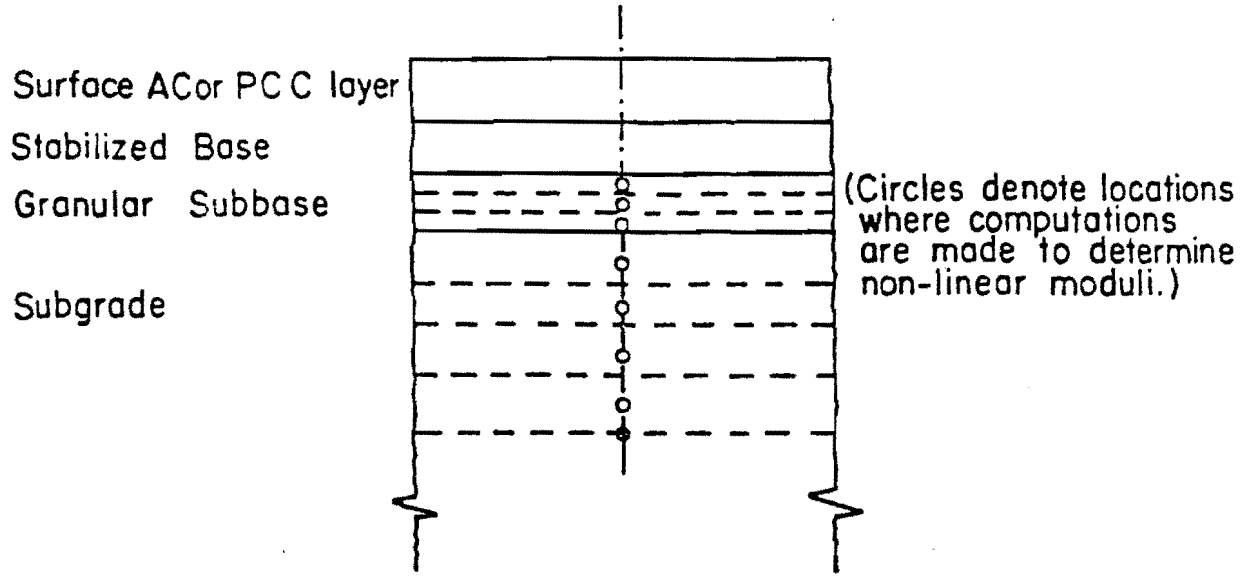

Fig 5.23. An idealized pavement structure for evaluation of strain dependent moduli of granular layers and subgrade.

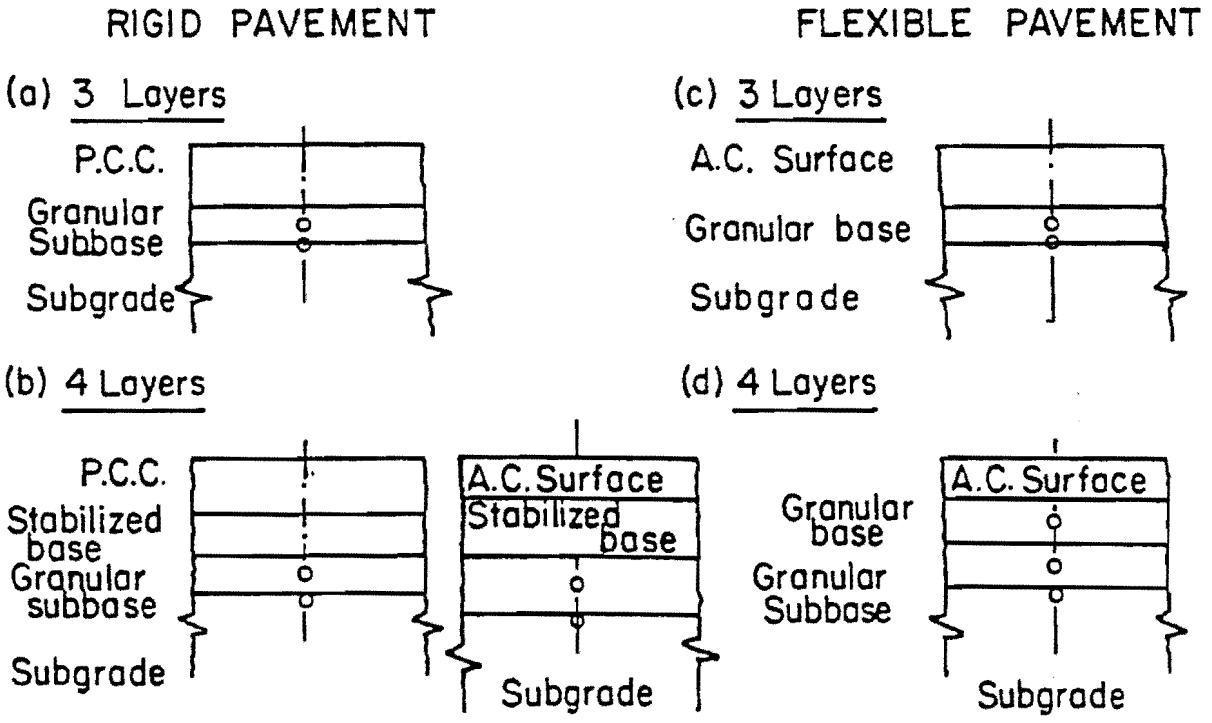

Fig 5.24. Typical pavement configurations adapted in this study.

After obtaining a nonlinear modulus of that layer, this analytical procedure proceeds to the next underlying strain-sensitive layer, until all strain-sensitive layers are characterized by nonlinear moduli. One cycle of equivalent linear analysis is enough for providing acceptable results.

(7) The final combination of moduli is assumed to be correct insitu (strain-dependent) moduli.

(8) Horizontal variability in moduli of any layer is ignored.

Location(s) for Maximum Shear Strain Response. An investigation was made to ascertain the locations in pavement sublayers where maximum shear strain is caused by the design load of Fig 5.19. The locations in the vertical direction will depend on thicknesses of layers, using the guidelines recommended in Fig 5.24. This section is concerned only with the horizontal plane.

To compute pavement response under the design load, ELSYM5 uses the principle of superposition. Therefore, it is necessary to evaluate response to four locations on the pavement. They are (1) at the outside edge of one loaded plate, (2) under the center of one wheel, (3) at the edge of the hypothetical loaded area corresponding to 4500 lb on the wheel and 75 psi tire pressure, and (4) midway between the centers of the dual wheels.

These locations in the (x, y) plane are A(0, 0), B(4.37, 0), C(8.75, 0) and D(1092, 0) respectively, as illustrated in Fig 5.25(a).

Layered theory computations were made using ELYSM5 and assuming different pavement structures. Typical results are shown in Fig 5.25(b). It was found that maximum shear strain generally has the largest amplitude at location C, i.e., at the inner edge of a loading wheel.

Step-by-Step Procedure. A step-by-step procedure for applying equivalent linear analysis to determine nonlinear strain dependent moduli is presented in Fig 5.26 as a simplified flow diagram. An outline of the procedure is described below.

(1) The initial inputs are pavement geometry information, insitu moduli calculated from Dynaflect deflection basin (Chapter 4), type of

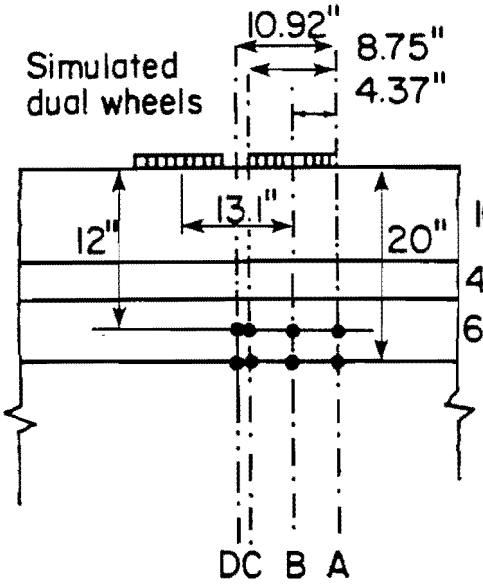

RIGID PAVEMENT CASE

	E (psi)	μ
10 in. P.C. Concrete	4,000,000	0.15
4 in. A.C. Base	200,000	0.35
6 in. Granular Subbase	75,000	0.40
Semi-infinite Subgrade	30,000	0.45

(Dots denote locations where maximum shear strain is computed)

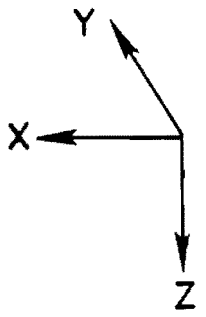

Coordinate system assumed in this figure

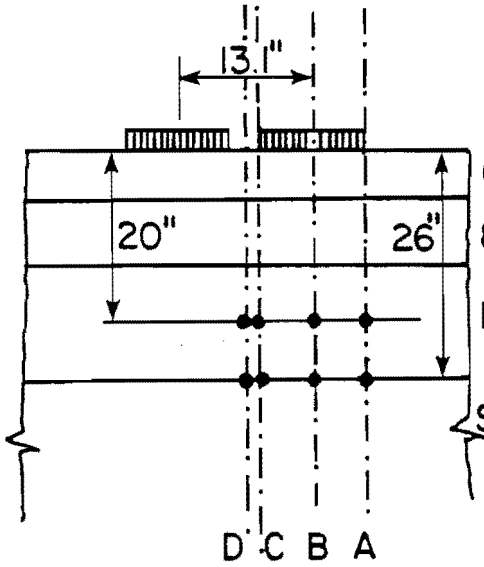

FLEXIBLE PAVEMENT CASE

	E (psi)	μ
6 in. A.C. Surfacing	400,000	0.35
8 in. Stabilized Base	110,000	0.35
12 in. Granular Subbase	45,000	0.40
Semi-infinite Subgrade	20,000	0.45

Fig 5.25(a). Pavement configurations assumed in maximum shear strain study.

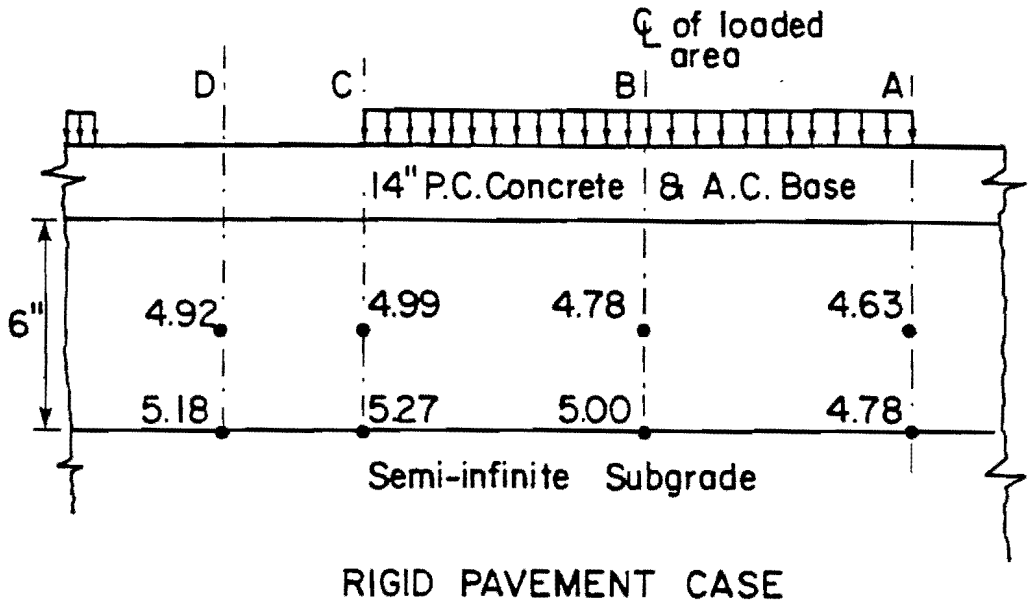

RIGID PAVEMENT CASE

All values printed near dots are maximum shear strains x 10^{-5} in percent

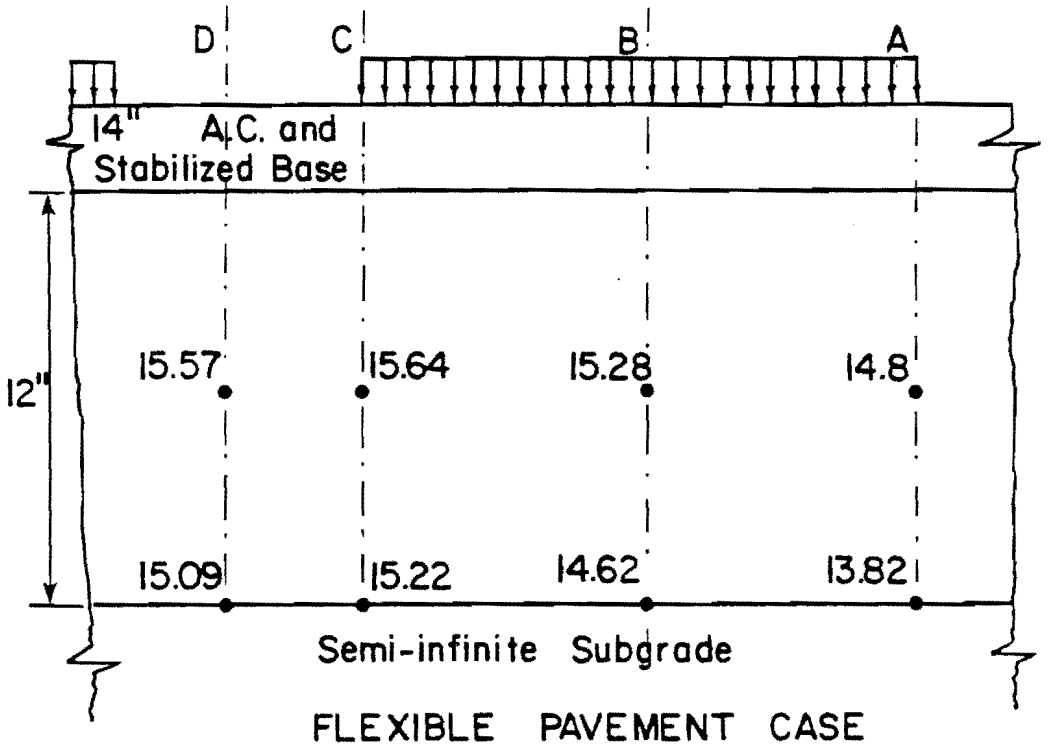

FLEXIBLE PAVEMENT CASE

Fig 5.25(b). Maximum shear strain data under design load configuration.

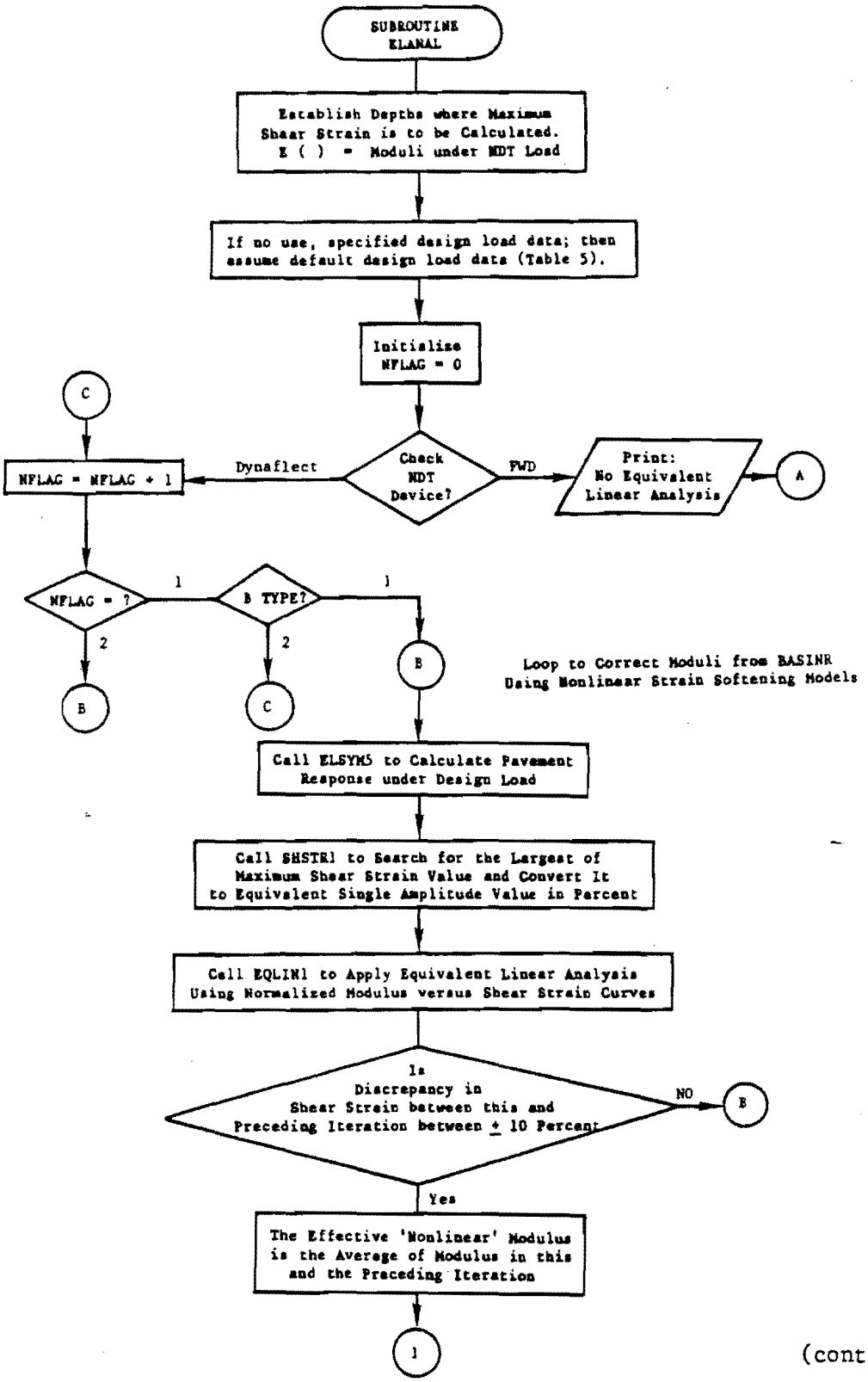

(continued)

Fig 5.26. Simplified flow diagram for equivalent analysis to determine non-linear strain sensitive moduli of granular subbase and subgrade (as used in RPEDD1).

005 332

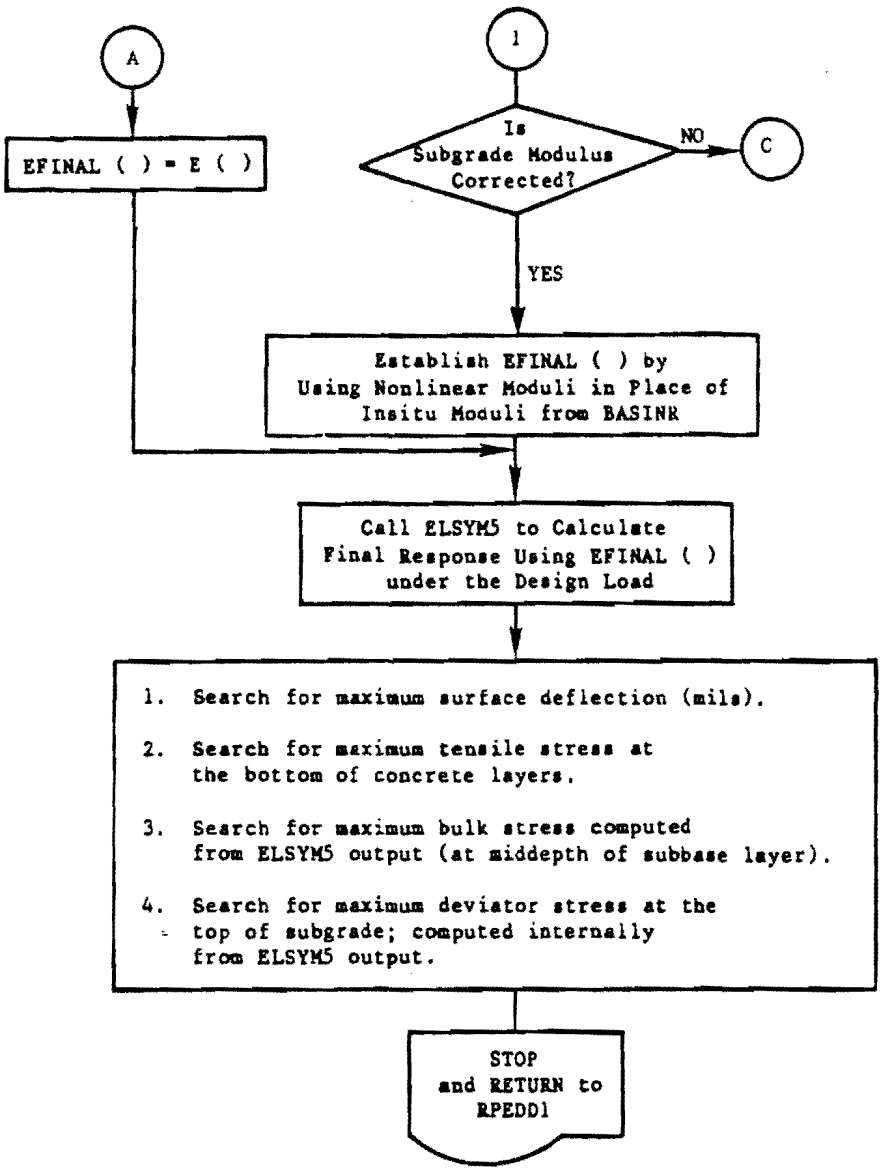

Notes: For use in FPEDD1: following changes were made

1. Value of NFLAG equal to 1 (for 3 layers) or 1 and 2 (for four layer) are used to correct for granular materials.

   Values NFLAG equal to 2 (for 3 layer) and 3 (for four layers) are used to correct subgrade modulus.

2. Search is made for maximum tensile strain at the bottom of AC layer.

3. Finally program is returned to FPEDD1

Fig 5.26 (continued)

base or subbase, design load details, and (x, y) locations where maximum shear strain response is required (midway between wheels).

(2) Locations in z direction where a response is required are computed according to the guidelines of Fig 5.24.

   (a) If the base is stabilized, this step is skipped.
   (b) If the subbase is stabilized, this step is again skipped.
   (c) For the granular base/subbase the desired locations are the middle of the layer under point C of Fig 5.25(a).
   (d) For the subgrade, the desired location to compute response is also under point C of Fig 5.25(a) at the top of the subgrade.

(3) If design load configuration is not entered by the user, default values are assumed (Fig 5.19).

(4) The procedure starts from the top of the first granular layer.

(5) ELSYM5 is called and the computed response is converted into a single amplitude shear strain, in percent, γ (subroutine SHSTR1).

(6) Using the unique relationship of E/E_{max} versus γ for this material (subroutine EQLIN1), ratio EE_1 is obtained; this when multiplied by E_{max} (insitu modulus from the Dynaflect deflection basin for that layer) gives a new value of E' for this layer. If this was the first iteration, the program goes to Step 8.

(7) The computed shear strain is compared with the value in the previous iteration; if the absolute difference is within $\pm$ 10 percent, convergence is achieved and the program proceeds to Step 9.

(8) The old modulus is replaced by E'. This is the second iteration. The program goes to Steps 5, 6, and 7. If convergence is achieved, then the final nonlinear modulus, EFINAL, of that layer is calculated as

$$EFINAL = \frac{E'_1 + E_{i-1}}{2.0} \qquad (5.21)$$

where

i = the i^{th} iteration at which convergence is acnieved.

Equation 5.21 was found reasonable as a large change in E causes a very small change in γ. This nonlinear modulus value is used in further computations. If this was the last strain-sensitive layer (subgrade), the program goes to Step 10.

(9) Equivalent linear analysis is applied to the next underlying strain-sensitive layer. Iteration is initialized and Steps 5 to 8 are followed.

(10) The final combination of pavement moduli includes nonlinear, strain-sensitive moduli for sublayers and subgrade appropriate to design load considerations.

Insitu Moduli from FWD Data. If the dynamic deflection basin data are generated by the Falling Weight Deflectometer, then in the present study the self-iterative procedure for obtaining the nonlinear sensitive modulus is skipped. It is assumed in this study that the FWD is capable of generating a peak force on a pavement surface which is equivalent to the design load. The largest maximum shear strain amplitudes at the appropriate depth in every strain-sensitive layer caused by both of these loading configurations are nearly the same (within $\pm$ 10 percent). Therefore, in this case the equivalent linear analysis is omitted.

However, FWD is capable of applying variable peak forces below the force level discussed in the preceding paragrapn. In these cases, it is necessary to use the equivalent linear analysis. However, an estimate of low amplitude shear strain modulus, E_{max}, will be required for each strain-sensitive layer. The easiest and most reliable method is to obtain a profile of dynamic moduli by performing spectral analysis of surface waves (SASW) tests in each test section (Refs 58, 66, 89, 90). A conceptual flow diagram to

determine nonlinear, strain-sensitive moduli corresponding to the design load conditions is presented in Fig 5.27.

Applications of Self-Iterative Equivalent Linear Analysis

Inservice Pavements. Several problems for insitu nonlinear material characterization have been solved using the procedures discussed up to now. Some examples are presented in Tables 5.4(a) and (b) for typical inservice rigid and flexible pavements. Measured Dynaflect deflection basins were analyzed in all cases.

This approach of insitu, nonlinear, strain-sensitive material characterization of unbound granular layers of pavement and subgrade is relatively new and according to available state of knowledge has never been applied in NDT evaluation of pavements. Overlay designs should be based on insitu moduli determined using the approach of equivalent linear analysis. Inservice monitoring and performance data of such overlaid pavement, and comparisons with performance of the overlaid pavements designed using current conventional procedures of nonlinear characterization should be used to validate either of these approaches.

Advantages Offered by Equivalent Linear Analysis. There are several obvious advantages with the use of equivalent linear analysis for NDT characterization of nonlinear strain softening granular materials and subgrade as listed below.

(1) The inherent problem of handling tensile stresses or very low compressive stresses (for computation of bulk stress) is eliminated.

(2) Errors due to the assumption of weighless materials in any layered theory computations for use in conventional stress dependent M_R relationships are handled by including gravity (self-weight) or overburden stresses. In the equivalent linear analysis, the critical response (maximum shear strain) to determine nonlinear modulus is required only due to the loading stress.

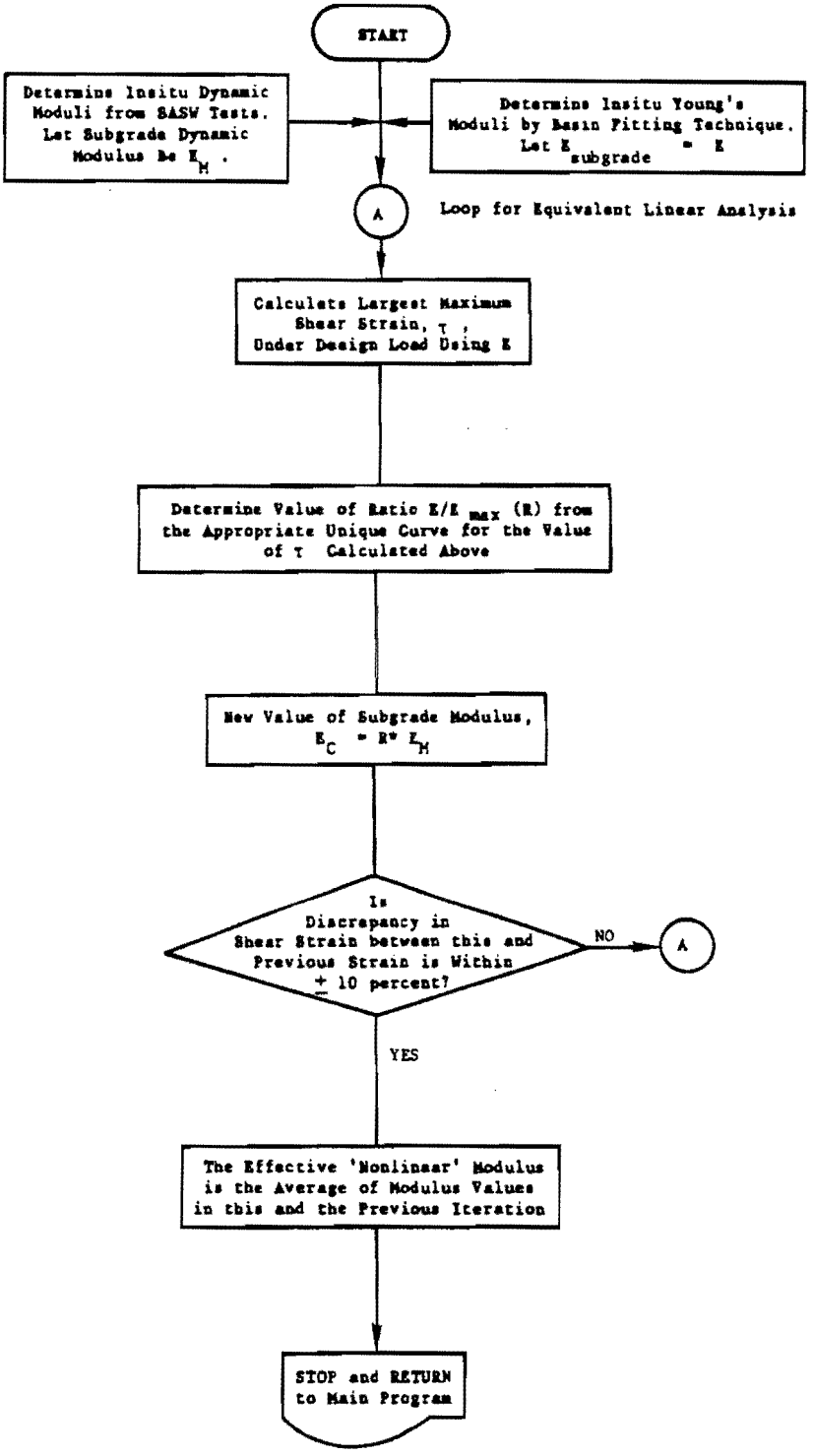

Fig 5.27. A conceptual flow diagram to determine nonlinear strain dependent modulus from the analysis of FWD deflection basin data.

TABLE 5.4(a). EVALUATION OF NONLINEAR STRAIN DEPENDENT MODULI BASED ON DYNAFLECT DEFLECTION BASIN - RIGID PAVEMENTS (RPEDD1)

PAVEMENT	YOUNG'S MODULI PREDICTED FROM DEFLECTION BASIN FITTING (PSI)	YOUNG'S MODULI CORRECTED FOR NONLINEAR BEHAVIOR (PSI)
(1) Fig 4.23 (JRCP)		
10 in. PC Concrete	5,398,000	
6 in. Cement Treated Base	500,000	
Semi-infinite Subgrade	31,030	30,480
(2) CRCP		
10 in. PC Concrete	4,451,501	
4 in. AC Base	457,180	
6 in. Lime Treated Subbase	348,192	
Semi-infinite Subgrade	23,288	22,854

(2) SH-71 (SB), Columbus Bypass, Texas

Measured Deflections (mils):	.33	.32	.29	.25	.23
Computed Deflections (mils):	.333	.321	.290	.256	.224

TABLE 5.4(b). EVALUATION OF NONLINEAR STRAIN DEPENDENT MODULI BASED ON DYNAFLECT DEFLECTION BASIN - FLEXIBLE PAVEMENTS (FPEDD1)

PAVEMENT	YOUNG'S MODULI PREDICTED FROM DEFLECTION BASIN FITTING (PSI)	YOUNG'S MODULI CORRECTED FOR NONLINEAR BEHAVIOR (PSI)
Fig 4.24		
4.5 in. AC Surface	292,900	--
8.0 in. Bituminous Base	112,900	--
Semi-infinite Subgrade	28,280	18,460

(3) Two different types of stress sensitive models are used in the conventional approach. The proposed approach uses only one type of strain sensitive model for all unbound materials.

(4) Maximum shear strain amplitudes generated in pavement layers by NDT tests or actual traffic conditions are generally in low to moderately high levels. These levels of maximum shear strains (γ) and their influence on M_R are not addressed in the conventional approach, although γ is the most important parameter to influence dynamic moduli (G or E).

(5) Use of effective or total stresses is a debatable question in the use of laboratory M_R relationships which correct insitu moduli. This dilemma is not present in the proposed equivalent linear analysis approach.

(6) Tremendous variations in nonlinear moduli based on laboratory M_R relationships may arise due to characteristics of material, experimental scatter, and method of computing stresses. The experimental scatter in developing G (E) versus γ relationships seems to be relatively very low and E/E_{max} versus γ relationships can be approximated as nearly unique curves for all practical purposes.

(7) To determine insitu stress dependent moduli, in the conventional approach, either appropriate M_R relationships are to be developed by extracting samples from sites and performing laboratory M_R tests; or approximate M_R relationship from experience (historical record) are assumed. In both cases, time and money and risk of uncertainty are involved. Moreover, the validity of applying laboratory M relationships in the field for NDT evaluation is open to question.

In using the proposed iterative approach of E/E_{max} versus shear strain curves, which can be safely considered unique, any unnecessary voluminous laboratory work is eliminated without an appreciable risk of uncertainty. This will result in savings of time and money, along with an increased efficiency and confidence in the desired nonlinear moduli. Furthermore, an important

parameter used in the iterative procedure is low amplitude-strain-modulus E_{max} (or G_{max}), which is determined as the insitu modulus from a Dynaflect deflection basin measured in the field or from a non-destructive surface wave test such as the SASW test; E_{max} can also be computed for the analysis of a FWD deflection basin measured at the lowest level of its peak force amplitude.

VALIDITY OF ASSUMING PAVEMENT AS A LINEAR ELASTIC SYSTEM

In the structural design of a new pavement the final design is built upon the assumption that the pavement behaves as a linearly elastic system. It is generally known that a newly built pavement, particularly with stiff layers, does behave linearly. The proposed approach of strain sensitivity can be used to make a theoretically based judgement on the validity of linear behavior.

Examples

Figure 5.28 illustrates the example of determining insitu moduli of pavement layers using the iterative application of layered theory computations to match the measured Dynaflect deflection basin. Equivalent linear analyses were subsequently made to determine nonlinear strain-dependent subgrade modulus. The CRC pavement was recently built with 10 inches of concrete overlying 4 inches of asphaltic concrete base and 6 inches of lime-treated sublayer. The equivalent single amplitude shear strain computed for this pavement under (default) design load is very close to the threshold limit for this material, which implies that the subgrade is almost in the strain-independent range. In other words, the pavement behaves as a linear system.

An older pavement does not behave as a linear system. Analysis of a deflection basin is still carried out assuming a linear system, but equivalent linear analysis results in nonlinear strain dependent moduli, as illustrated in Fig 5.29. The nonlinear behavior of an old pavement is

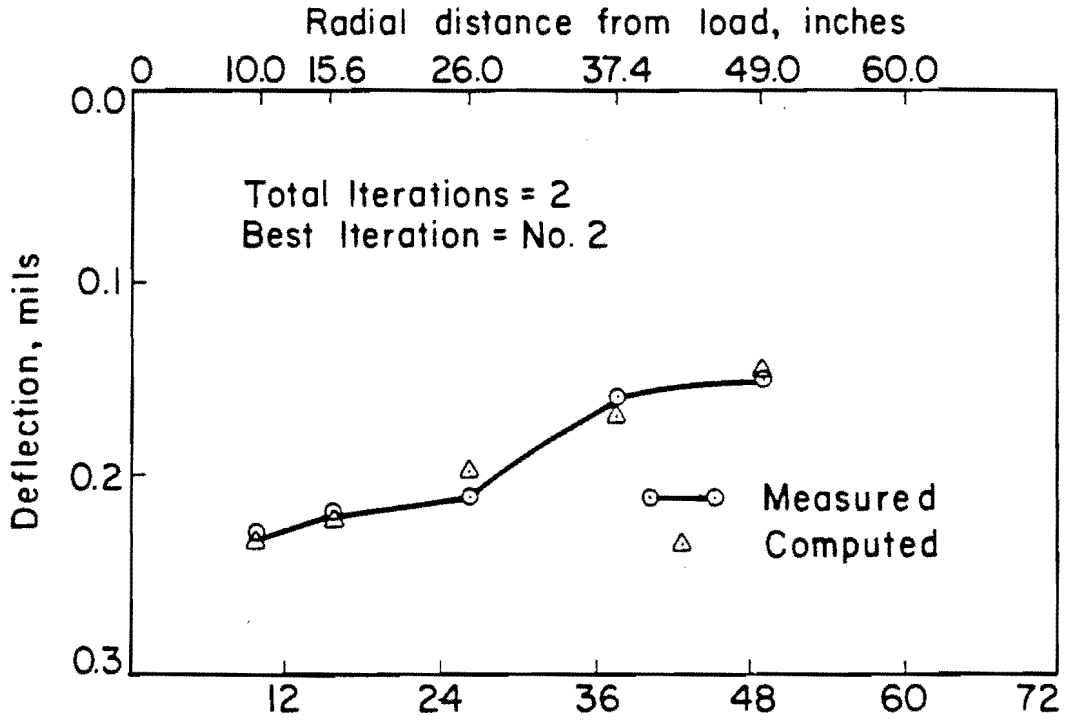

SH-71, Texas, 7 Aug.81
Columbus Bypass (Section 1)
Wheel path/Outside lane

	Young's Modulus (psi) Input Seed	Insitu (1)	Corrected (2)*	%Difference (1) & (2)
10 in. P.C. Concrete	0	6,000,000		
4 in. A.C. Base	0	479,800		
6 in. Lime treated Subbase	0	291,500		
Semi-infinite Subgrade	0	37,140	36,960	0.5%

(* Strain dependent non-linear modulus)

Fig 5.28. Analysis of a Dynaflect deflection basin measured on a newly constructed CRC pavement (prior opening to traffic).

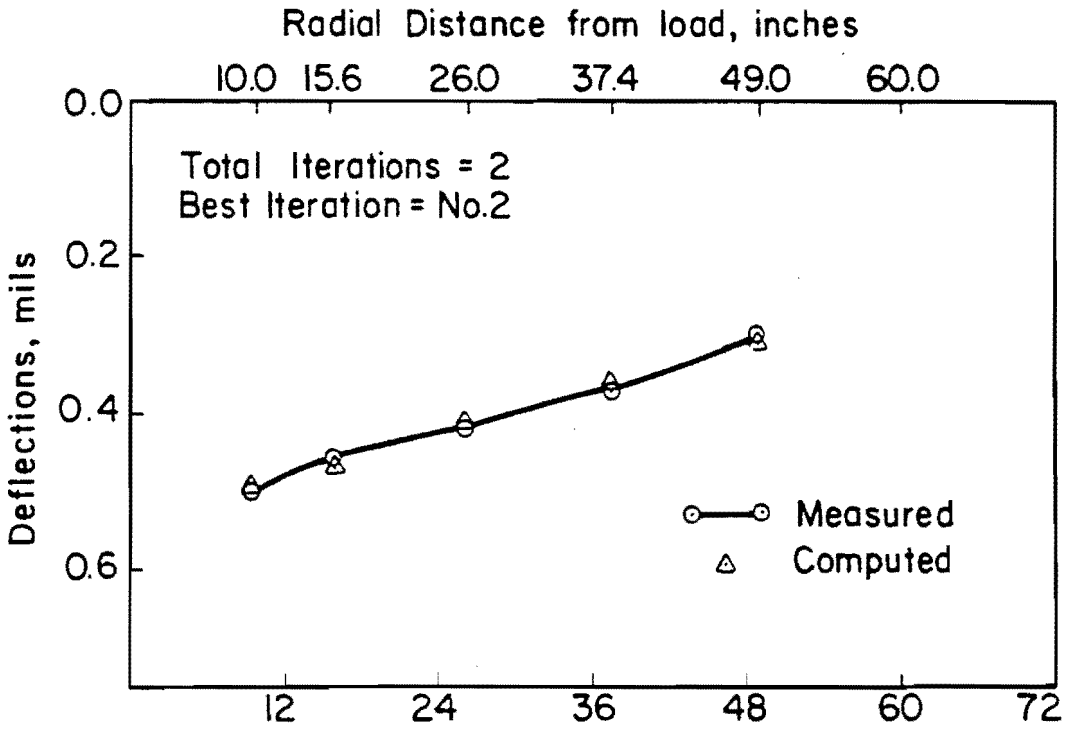

IH-10, East of Columbus,
Texas. 23 Aug.84 EB.,
St.1352+22
Centerline, Outside lane

	Input Seed	Young's Modulus (psi) Insitu (1)	Corrected (2)	% difference between (1) and (2)
10 in JRCP	0	3,515,000		
6 in Cement treated base	0	118,400		
Semi-infinite Subgrade	0	18,490	17,530	5.2%

Fig 5.29. Analysis of a Dynaflect deflection basin measured on an old (around 20 years) JRC pavement.

possible due to one or more reasons, such as discontinuities, creation of voids, and pumping in base/subbase, etc. The strain softening approach does provide an explanation of the nonlinear behavior of the pavement system.

SUMMARY

This chapter has dealt with nonlinear behavior of granular layers and subgrade in pavements. The current practices in the use of stress dependent nonlinear laboratory M_R relationships were reviewed. Results of published research in recent years on improving nonlinear stress dependent material characterization procedures for granular layers were also presented. A brief discussion of strain dependent dynamic shear moduli used in dynamic/seismic response analysis was also presented. The concept of equivalent linear analysis for nonlinear strain dependent moduli is also discussed which is based on normalized modulus E/E_{max} (or G/G_{max}) versus shear strain relationships. Default curves based on these relationships were presented for granular and cohesive materials. A self-iterative procedure is described to determine insitu moduli of nonlinear strain softening materials using the concept of an equivalent linear analysis. The procedure has been designed mainly for NDT evaluation with the Dynaflect because back-calculated moduli from the Dynaflect deflection basins can be treated as low-amplitude moduli (E_{max}). Values of E_{max} are then used in the equivalent linear analysis to converge to a corrected nonlinear modulus corresponding to the shear strain amplitude under the design load condition. For the FWD, the equivalent linear analysis is presently omitted in this study assuming a peak force can be generated by the FWD which results in shear strains in the granular layer or the subgrade comparable to that under the design load. However, if FWD is used at small loads, then the use of an equivalent linear analysis is warranted.

Several advantages of the equivalent linear analysis and discrepancies in the currently used M_R procedures were also presented and discussed. The self-iterative procedure for equivalent linear analysis for nonlinear,

strain-sensitive moduli of sublayers has been implemented in the dynamic-deflections-based structural evaluation system presented in Chapter 6.

CHAPTER 6. DEVELOPMENT OF COMPUTERIZED STRUCTURAL EVALUATION SYSTEMS FOR PAVEMENTS

This chapter presents the comprehensive framework for the development of structural evaluation systems for pavements. The self-iterative procedures developed in Chapters 4 and 5 are the two important stepping stones in this framework. Structural evaluations of pavements based on dynamic deflection will be extended to include the estimate of fatigue life and remaining life.

FRAMEWORK FOR STRUCTURAL EVALUATION SYSTEM

Background

Most of the existing structural evaluation methods based on insitu moduli derived from deflection basins fall in the first of the following categories.

Average Deflection-Basin-Based Evaluation. In this method, an average deflection basin is computed by computing the mean of the deflections measured at each sensor of the NDT device in a test section. Insitu effective moduli are determined by using deflection basin parameters, graphical procedures, or basin fitting procedures (the inverse application of layered theory) which may be user-iterative or self-iterative (Chapter 3). Third, some methods allow correction of moduli of granular layers and subgrade by using nonlinear stress-dependent laboratory M_R relationships. Temperature correction is also made for the modulus of the asphaltic concrete layer in the case of flexible pavements. The final combination of moduli represents effective insitu moduli for the whole section, which are subsequently used for overlay design. Use of an average deflection basin raises the question of ignoring the primary theoretical considerations on which the iterative use of inverse applications of layered elastic theory is based.

Individual Deflection Basin Category. In this approach each deflection basin is analyzed on an individual basin. Insitu moduli are then determined following the procedures outlined above. Uddin et al (Ref 62) have recommended this approach. Design moduli for each design section then can be based on the summary statistic of moduli determined at each Dynaflect test location in that section. This approach is more rational as the user is analyzing each measured basin and not a hypothetical average basin. The variations of moduli in each section represent the in-place variability in each pavement layer.

In the above two approaches, a design (test) section is preselected and after the analysis of deflection basins the next step is to determine design moduli.

Determination of Overlay Thickness at Individual Location of Deflection Basin. This is the approach employed in the recently developed FHWA-overlay design procedures (e.g., Ref 19). Each deflection basin is analyzed individually to determine insitu moduli which are corrected for temperature (for asphalt concrete modulus) and for nonlinear stress sensitive behavior of granular layers and subgrade. The final moduli at the test location are then used for the design of the overlay thickness.

The direct use of insitu moduli for overlay design of each test location results in prohibitively expensive computation at a cost which may be unnecessary in certain instances, especially when the life of an existing pavement can be considerably extended by routine maintenance measures instead of embarking on sophisticated rehabilitation programs involving overlays.

Alternatives for stage construction will also be difficult to design for the strengthening/upgrading of existing pavement.

Proposed Approach

The framework proposed in this study for a structural evaluation system using dynamic deflection basins is comprised of several stages, as summarized below.

(1) The measured deflection basin is analyzed on an individual basis.

(2) Insitu moduli are determined using the self-iterative inverse application of layered theory. The asphalt concrete modulus (for flexible pavement) is to be corrected for temperature effect. This stage has been covered in detail in Chapter 4.

(3) Insitu moduli are then corrected by equivalent linear analysis to take into account nonlinear, strain-softening behavior of granular layers and conesive subgrade as discussed in Chapter 5.

(4) The final combination of corrected insitu moduli are then to be used to predict critical responses under a given design load configuration to make a remaining life analysis as discussed in detail in this chapter.

(5) The final output from the use of the computerized structural evaluation system is a table which summarizes the results of critical responses, fatigue life, remaining life and final combination of corrected insitu moduli with respect to each test location along the roadway.

(6) Separate computer programs are to be developed for rigid and flexible pavements. In the implementation/application phase of these computerized evaluation systems, plots of remaining life, subgrade modulus, and moduli of other layers with distance along the pavement are to be used to delineate areas in need of major rehabilitation for overlay design. Detailed discussions on implementation are included in the latter part of this chapter.

COMPUTERIZED STRUCTURAL EVALUATION SYSTEM

Different features considered for developing a computerized structural evaluation system are described in the following sections.

Simplified Flow Diagram

As outlined earlier, separate computer programs based on the proposed approach are to be developed for structural evaluation of rigid and flexible

pavements. A simplified flow diagram of the framework adapted in the later development of the computer programs is presented in Fig 6.1 and discussed in these sections.

Basic Input Data

Design load specifications and configuration (see Fig 5.19 for default specifications) are required for nonlinear characterization, as discussed in Chapter 5. Additionally, past traffic data in terms of cumulative 18-kip equivalent single axle loads are required. Specific guidelines practiced by different user agencies or AASHTO Interim Guides (Ref 20) can be used for this purpose.

Analysis of Deflection Basin

Determination of Insitu Moduli. Insitu moduli of pavement layers are determined by the self-iterative inverse application of ELSYM5 as discussed in detail in Chapter 4. Separate routines have been developed for rigid and flexible pavements. Except for minor differences, the algorithms used in these routines are based on the procedure described in Chapter 4. The salient features of the self-iterative procedure are briefly repeated here.

(1) Handling the finite thickness of the subgrade layer (including a default procedure for consideration of a rigid bottom).
(2) Capability to analyze dynamic deflection basins measured either by the Dynaflect (standard configuration of five sensors) or by a Falling Weight Deflectometer (not more than seven or less than six sensors with one sensor under the center of load and the remaining placed one foot apart on a line extending outwards in perpendicular direction.
(3) Handling a three or four-layered pavement model.
(4) Capability to determine a unique set of insitu moduli by generating initial seed moduli through a default procedure. The predictive equations developed for this purpose are presented in Appendix B.

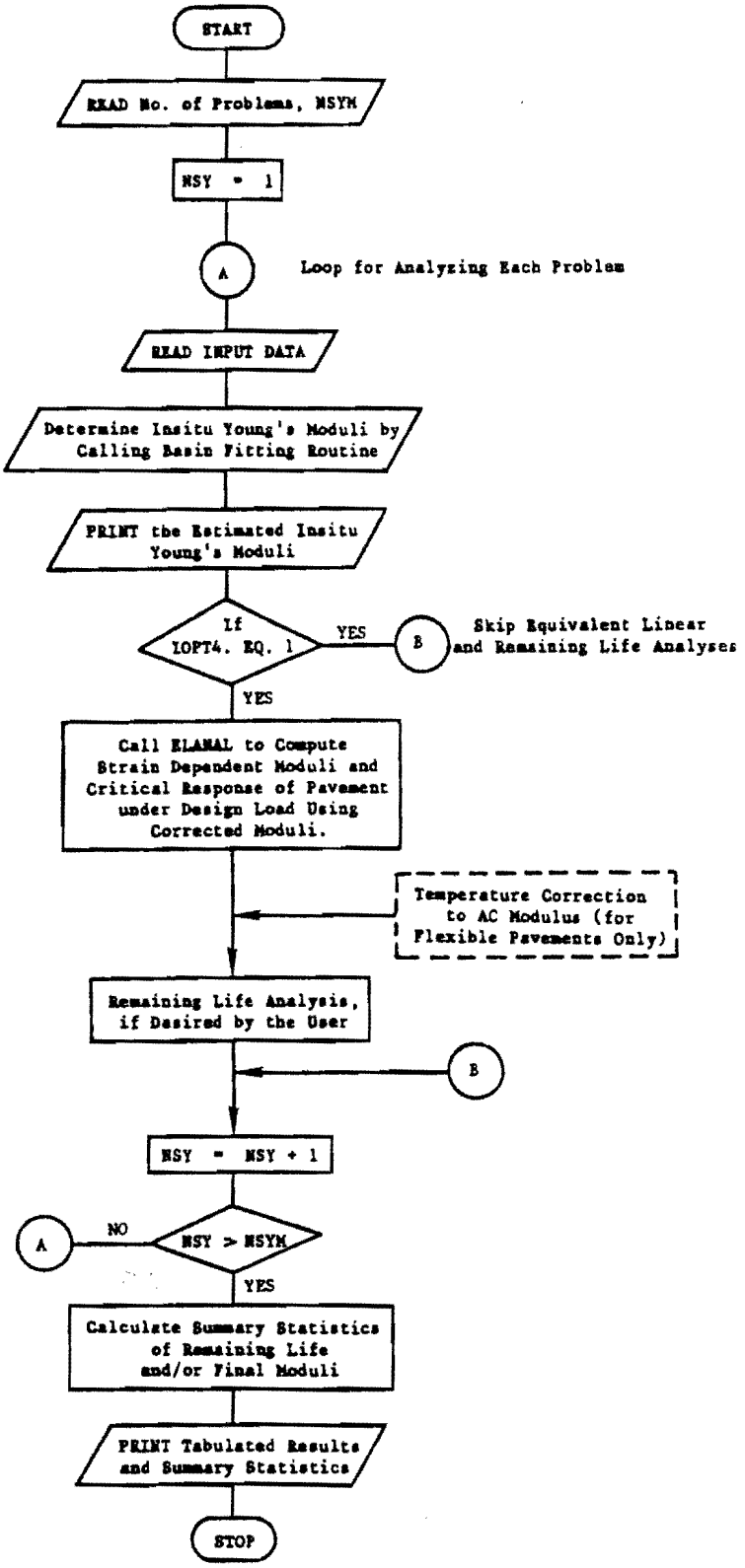

Fig 6.1. Simplified flow diagram of the proposed structural evaluation program based on dynamic deflection.

(5) Better efficiency and using a lesser number of iterations to keep the computational cost to a minimum are the over-riding criteria which are in some instances possible only at the expense of less precision in the convergence process of measured and theoretical deflections. Improvements can be achieved by calibrating the procedure of successive corrections. However, at present it is recommended that the calibration of this model not be improved unless enough experience is gained through a large number of applications of the computer programs.

Temperature Correction. The insitu asphaltic concrete modulus determined from the analysis of the deflection basin measured on a flexible pavement is corrected for temperature sensitivity using the procedure described in the latter part of Chapter 4. The corrected modulus corresponds to asphaltic concrete stiffness at the design temperature. This step is performed after correcting the strain-dependent nonlinear moduli.

Corrections for Nonlinear Behavior of Pavement Sublayers

The self-iterature procedure for equivalent linear analysis developed in Chapter 5 is basically the same for rigid and flexible pavements.

Nonlinear, Strain-Sensitive Moduli. The equivalent linear analysis approach is based on an iterative use of ELSYM5 and "unique" curves of E/E_{max} versus shear strain curves developed using the concept of nonlinear strain softening materials when the shear strain induced by the design load in these layers exceeds certain threshold strain values. This approach is drawn from the dynamic/seismic response analysis procedure well accepted in the field of geotechnical engineering.

Insitu Moduli of Stabilized Layers. The insitu moduli determined for granular materials and cohesive soils which have been stabilized by asphaltic materials, cement, or lime are considered to be insensitive to shear strain and not to exhibit nonlinear behavior. Therefore no corrections are applied to the insitu moduli of such pavement layers.

Results. A print out of all results is generated at this step after the completion of all analyses related to each deflection basin.

Remaining Life Analysis

The final combinations of (corrected) insitu pavement moduli is assumed to represent effective insitu stiffnesses (Young's moduli) under the design load. The existing pavement at this test location is again modelled as a layered "linearly" elastic system for further evaluation. At this stage of structural evaluation existing pavement is analyzed for its remaining life at each test location. A simplified flow diagram of the remaining life analysis is illustrated in Fig 6.2.

Fatigue Life Prediction. The first step in the subroutines developed for the remaining life analysis is to predict the fatigue life of the existing pavement. The fatigue life of a pavement can simply be defined as the maximum number of repetitions of a standard load a pavement can sustain, associated with certain critical response parameters. Detailed treatment of the application of fatigue concepts to pavement analysis can be found in Refs 19, 36, 68, 69 (for flexible pavements) and Refs 23, 38, and 93 (for rigid pavements). Conceptually a predictive relationship for fatigue life is expressed in the following form:

$$N_f = A\left[f\,(C_R)\right]^B \qquad (6.1)$$

where

N_f = maximum allowable number of repetitions of a standard load,

C_R = critical response parameter (either tensile stress or tensile strain),

and A and B are estimates of regression coefficients.

There is a limiting value associated with the critical response parameter which when exceeded can trigger fatigue cracking. Fatigue cracking

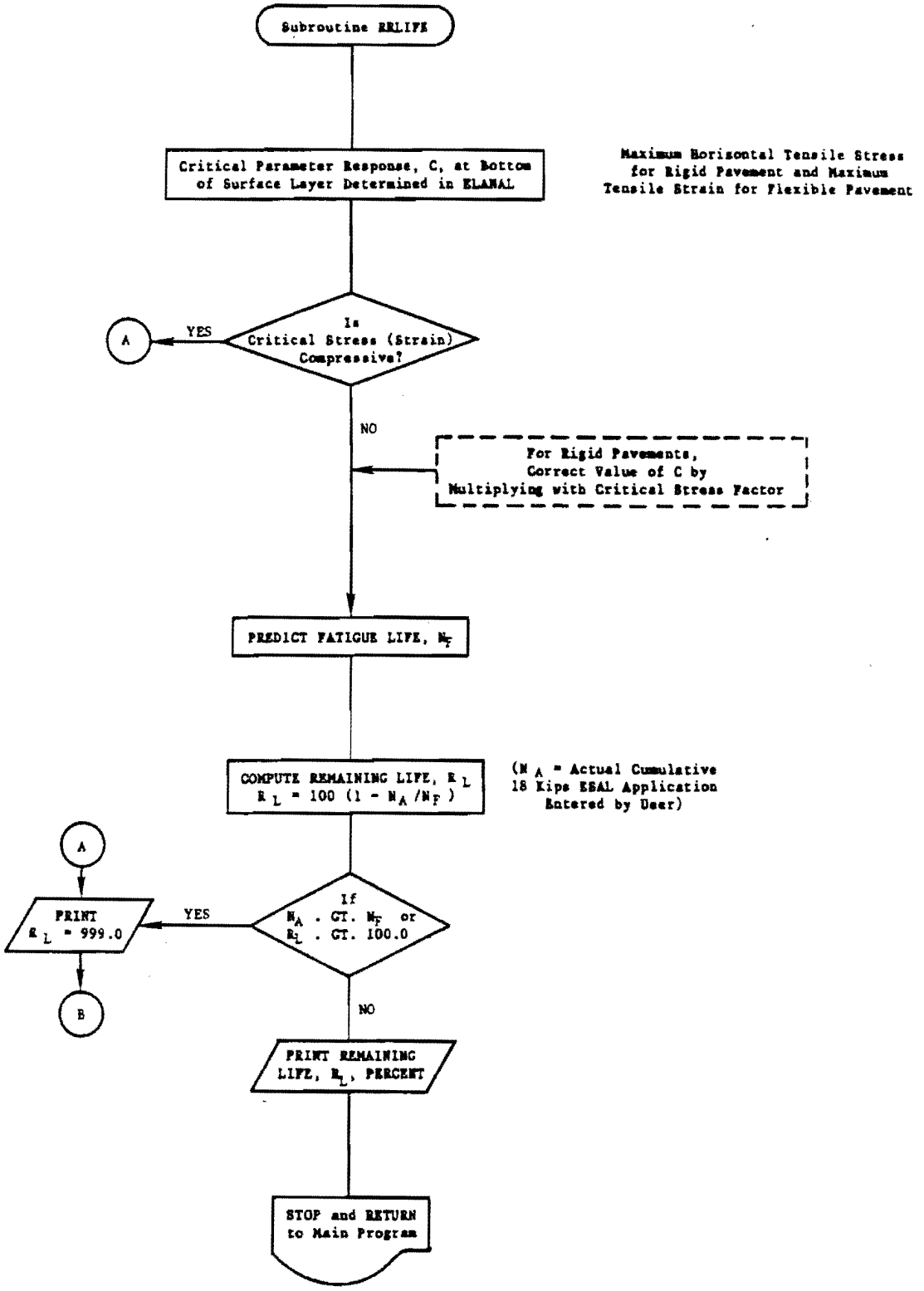

Fig 6.2. A simplified flow diagram of remaining life analysis.

initiates at the bottom of either the asphaltic concrete layer (in flexible pavements) or the surface concrete layer (in rigid pavements) and later appears on the pavement surface. It should be emphasized that a cracked pavement can still carry axle applications without reaching "failure". Here "failure" is referring to functional failure of pavement (Ref 36). For this reason, the fatigue equations developed from the analysis of field data generated at the AASHO Road Test (Ref 94) have been selected for use in this study. A more thorough discussion on the development of the selected fatigue equations is out of the scope of this study. Readers can consult the references cited above for details.

Rigid Pavements

Figure 6.3 illustrates different fatigue equations considered for use in the development of a Design System for Rigid Pavement Rehabilitation (RPRDS), for use in Texas (Ref 38). The fatigue equation selected for use in this study is expressed as:

$$N_{18} = 46000 \left(\frac{S}{\sigma_c} \right)^{3.0} \qquad (6.2)$$

where

N_{18} = maximum number of 18-kip equivalent single axle load (ESAL) applications,

S = flexural strength of pavement quality concrete, in psi (included in the input data for rigid pavements) and,

σ_c = critical tensile stress at the bottom of the concrete layer, in psi (Fig 6.4).

Taute et al (Ref 23) have developed Eq 6.2 from the analysis of AASHO Road Test data (Ref 94) and a study of statewide condition survey data in Texas (Ref 95). This equation presents several improvements over the ARE

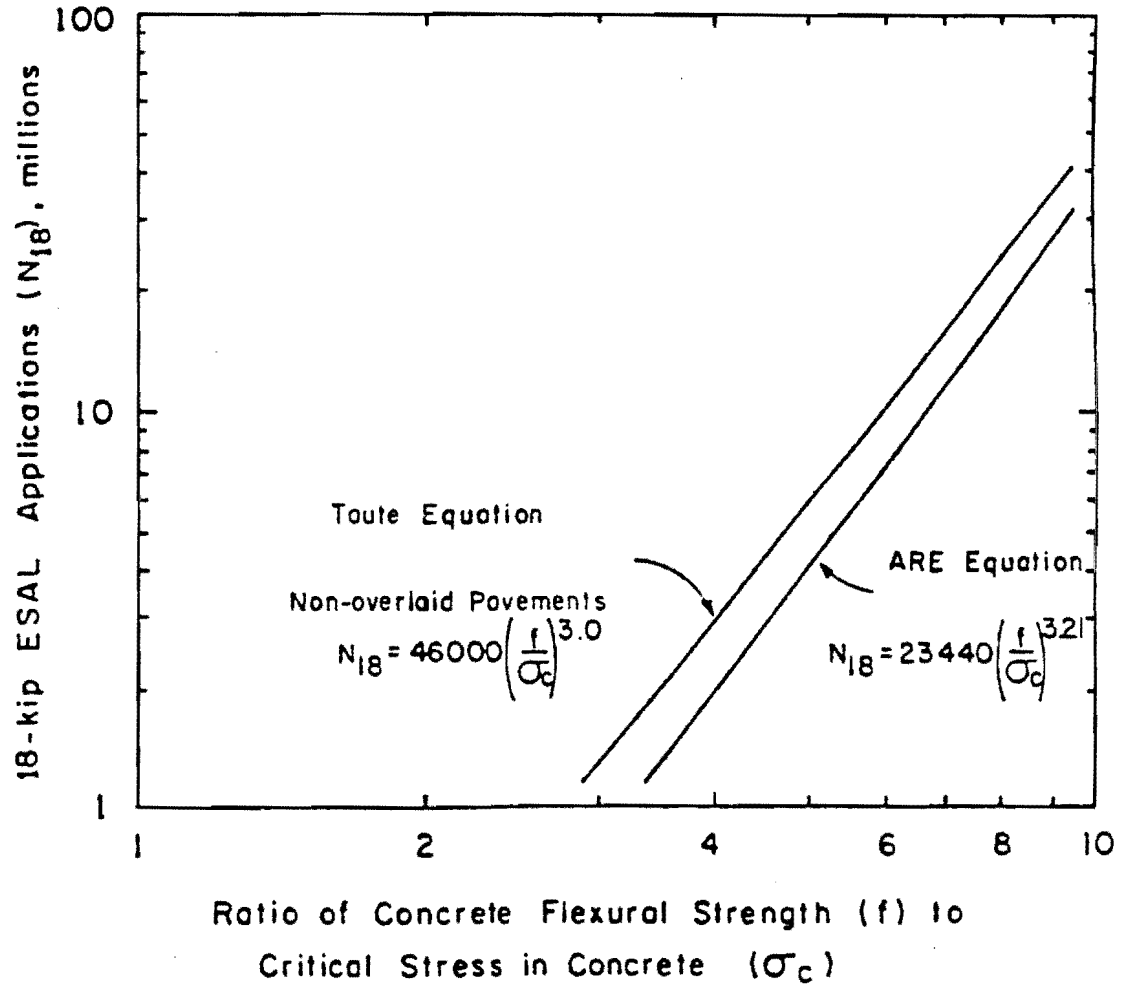

Fig 6.3. PCC fatigue equations.

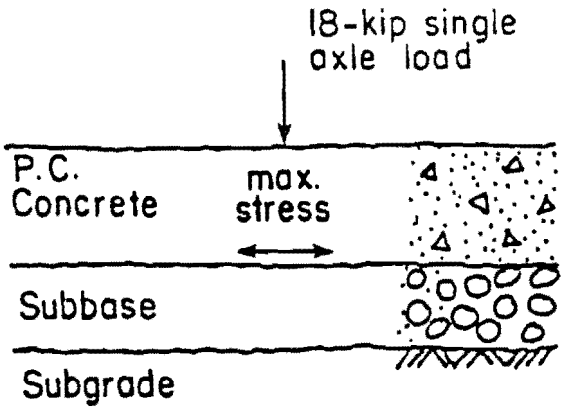

Fig 6.4. Illustration of maximum tensile stress in a rigid pavement.

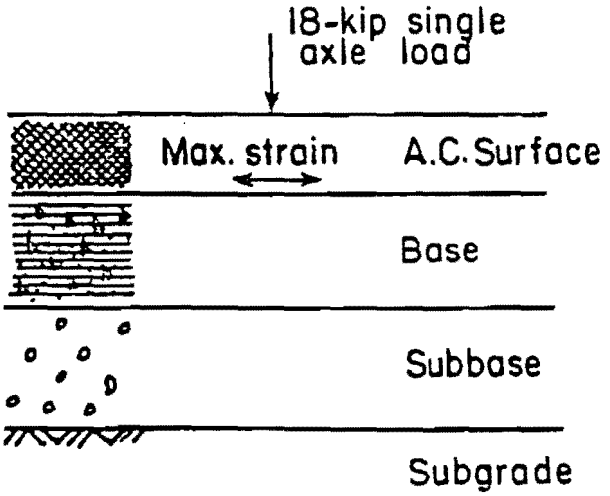

Fig 6.5. Illustration of the maximum tensile strain in a flexible pavement.

equation (Ref 93), which is also shown in Fig 6.3. ELSYM5 was used for layered theory computations in the development of these fatigue equations. Details of the assumptions involved and the derivation of this equation are presented in Refs 23 and 38.

In the subroutine of the remaining life analysis developed in this study, ELSYM5 is used to predict critical tensile stress at the bottom of the concrete layer. Recognizing that a pavement model based on layered theory does not take into account the influence of discontinuities, such as cracks, joints, edges, etc., Seeds et al (Ref 38) recommend critical stress factors to adjust the critical tensile stress computed by layered theory before computing N_{18} from Eq 6.2. These adjustment factors are based on computations based on finite element modelling and their derivation is described in Ref 38. To ensure compatibility with RPRDS, the same approach is incorporated in this study. Therefore, critical tensile stress, σ_c , for use in Eq 6.2 is computed by the following expression:

$$\sigma_c = C_p \cdot \sigma_c' \qquad (6.3)$$

where

σ_c' = critical tensile stress computed by ELSYM5 and

C_p = critical stress factor.

Values of C_p recommended by Seeds et al (Ref 38), are presented in Table 6.1 together with the default values assumed in the present study.

Flexible Pavements. The critical response parameter used in the prediction of the fatigue life of an existing flexible pavement is the critical tensile strain (ε) at the bottom of the asphaltic concrete (AC) layer, as illustrated in Fig 6.5. The FHWA-ARE's fatigue equation (Eq 6.4 in Fig 6.6) was developed from an analysis of data from the AASHO Road Test (Ref 94).

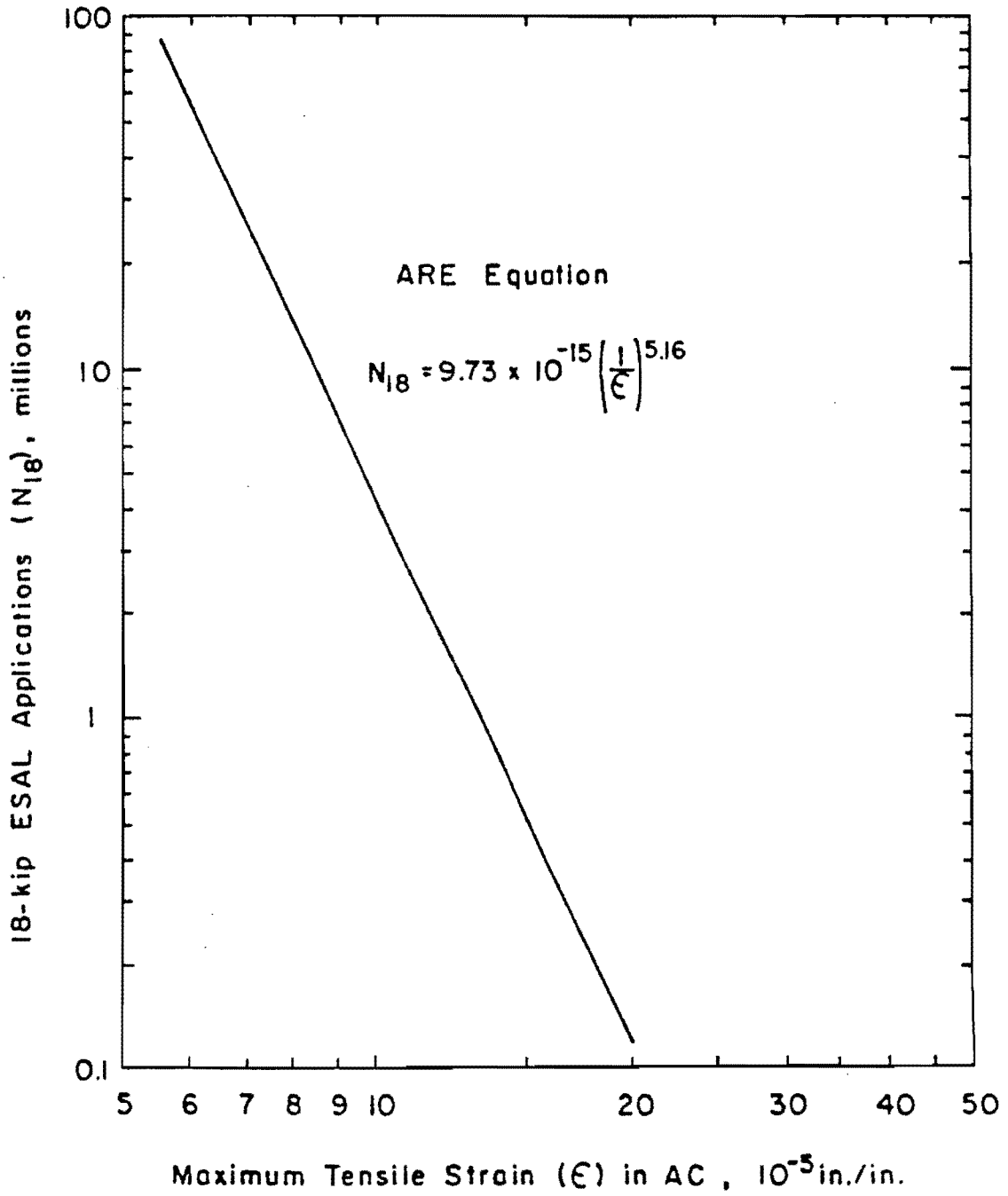

Fig 6.6. AC fatigue equation used in FPEDD1.

TABLE 6.1 EXISTING PAVEMENT CRITICAL STRESS FACTORS

Existing Pavement Type	Existing PCC Shoulders	Range of Critical Stress Factor*	Value Used in RPEDD1
CRCP	No	1.20 - 1.25	1.22
	Yes	1.05 - 1.10	1.08
JCP (with load transfer)	No	1.25 - 1.30	1.27
	Yes	1.10 - 1.20	1.15

*(Ref. 38)

Computation of Critical Response Parameter. In the subroutines developed for fatigue life predictions in the present study, critical response parameters (maximum values of σ_c' or ε as discussed in the preceding sections) are computed at two locations at appropriate depths. As noted in Fig 6.7 (design load configuration), the responses are computed by ELSYM5 (1) at a point directly under the center of the hypothetical circular area representing a wheel, (2) at the inside edge of the loaded area, and (3) beneath the point midway between the wheels. A search is made to find the largest of the three responses for assigning to σ_c' or ε. For some pavements no critical (tensile) response is predicted (e.g., no tensile strain in a thin AC layer over a stiff base). In such a case the fatigue life computation is simply skipped, as indicated by a message in the final output.

Remaining Life Estimate. If fatigue life has been computed in terms of the allowable number of 18-kip ESAL, N_{18}, then an estimate of the remaining life of the existing pavement is determined using the following expression:

$$R_L = \left(1.0 - \frac{n_{18}}{N_{18}}\right) \times 100 \qquad (6.5)$$

where

R_L = predicted remaining life of the existing pavement in percent,
N_{18} = predicted fatigue life in 18-kip ESAL, and
n_{18} = past cumulative 18-kip ESAL (entered in the input data).

In Eq 6.5, n_{18}/N_{18}, represents theoretical damage to the existing pavement, which is an indication of pavement deterioration due to past repetitions of traffic, n_{18}. Equation 6.5 is based on the validity of applying Miner's linear damage hypothesis to estimate fatigue damage in pavements. Thorough discussions of the applicability of this approach in

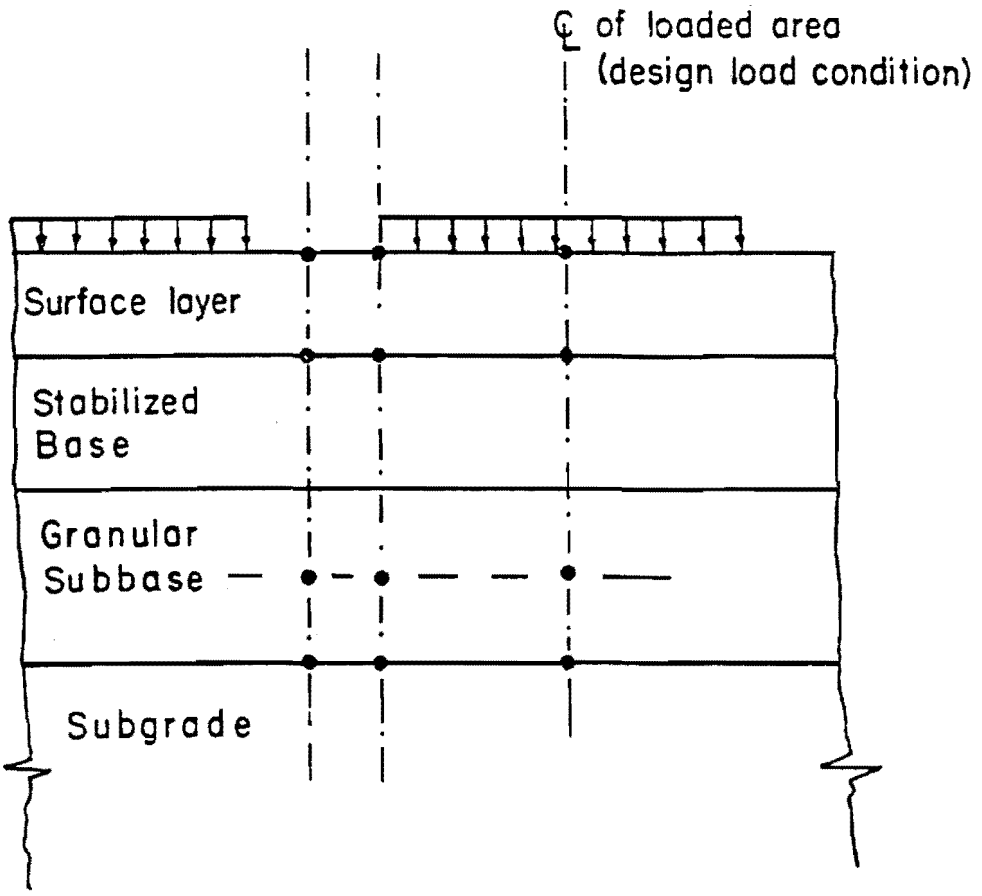

Note: Dots show locations where appropriate pavement responses are computed and the largest value is selected for inclusion in the final output

1. Surface deflections: on pavement surface
2. Tensile stress (strain): At the bottom of surface layer
3. Bulk stress: At the mid-depth of granular subbase layer
4. Deviator stress: At the top of subgrade

Fig 6.7. Configuration of locations for computation of pavement responses.

the analysis and for overlay design of pavements are presented elsewhere (Refs 37, 38, 68, and 93).

Special Considerations. For the purpose of this study, a very detailed and refined type of remaining life analysis is neither necessary nor sought. Therefore the final output is generated using special provisions indicating that remaining life analysis at that test location was either not possible or skipped due to one or a combination of the following reasons.

(1) Accumulated past traffic data, n_{18} in 18-kip ESAL was not entered in the input. The output will show 999 in tne R column if the output is in the detailed format.

(2) Fatigue life, N_{18}, could not be predicted or set to zero. The remaining life analysis is skipped in this case and only a summarized version of the output is printed.

(3) If the option for making a remaining life analysis is not entered by the user, then the default option is to omit the remaining life analysis and generate only summary output.

(4) If R_L is zero, it indicates that the pavement is in badly cracked condition (as specified by the user in an input option about pavement condition). In such cases, the program internally assumes zero remaining life without attempting any remaining life analysis.

Final Output

Final output from the computer programs for structural evaluation is in tabular form. The programs are designed to generate output in either a detailed format or a short format, as dictated by the type of analysis discussed earlier in special considerations. The programs can handle 50 deflection basins in one batch at present, but the capability can be increased by adapting ELSYM5 to handle more than 50 problems.

Table 6.2 presents a list of important output variables in the detailed format. Output variables included in the short form are listed in Table 6.3. In summary, the short format is without the data related to the remaining life analysis. In both cases the moduli are the final combination corrected

TABLE 6.2. SUMMARY OF DETAILED OUTPUT

OUTPUT VARIABLES	DESCRIPTION
Identification and Initial Information	Problem No., Title, NDT Device (FWD/Dynaflect); Station, Test Date; No. of Layers; Type of Layer Above Subgrade (for Rigid Pavements); Type of Base and Subbase Layers (for Flexible Pavements).
Input System Parameters	Maximum No. of Iterations; Tolerances for Discrepency in Deflections (TOLR1 and TOLR2); Tolerances for Change in Moduli (TOLR31, TOLR32, TOLR33).
Layering Information	(Repeated for each layer, starting from the surface layer.) Layer No.; Thickness (Inches); Poisson's Ratio (No value in thickness indicates semi-infinite subgrade).
	Input Seed Modulus in psi (if input is zero, then default seed modulus is printed).
E(MAX)	Maximum allowable value of modulus in psi (default value is printed if there is no input).
E(MIN)	Minimum allowable value of modulus in psi (default value is printed if there is no input).
UNWTI	Unit weight of subgrade soil (lbs./cu. ft.)
Sensor No.	Sensor no. 1 assigned to the first sensor closest to the test load (5 sensors for Dynaflect and 6 or 7 sensors for FWD).
Measured Deflection	At each sensor in mils.
Calculated Deflection	At each sensor in mils.
HERRP (Based on Seed Moduli)	Largest absolute discrepency in measured and calculated deflections (in percent).
ITERATIONS BEGIN	Message when further iterations are stopped; also total number of iterations attempted in this run.

(continued)

TABLE 6.2. (CONTINUED)

OUTPUT VARIABLES	DESCRIPTION
Results of Iterations	Message about skipping results of each iteration if IOPT1 is zero. In that case, only summary of best iteration is printed. If IOPT1 was 1, then summary of each iteration and finally of best iteration are presented.
Young's Moduli	For each layer (in psi).
Measured Deflections	In mils.
Calculated Deflections	In mils.
HERRP	The largest discrepency in percent.
Design Single Axle-Load Data	Load per tire (lbs.); Tire pressure (psi).
Other Pavement Data	For Rigid Pavements: flexural strength; rigid pavement type; shoulder type. For Flexible Pavements: test temperature and design temperature (^{o}F)
RESULTS OF EQUIVALENT LINEAR ANALYSIS	Corrected values of Young's moduli.
TEMPERATURE CORRECTION (Only for Flexible Pavements)	Corrected value of Young's modulus of AC surface.
REMAINING LIFE	Printed in percent (only when IOPT2 was entered as 1). A value of 999.0 is printed if no positive value of remaining life could be determined.
NEXT PROBLEM	All the above output repeated for each successive problem.
SUMMARY OF STRUCTURAL EVALUATION	Following summary outputs printed for each deflection basin analyzed. (1) Station (2) Maximum Deflection (in mils; under design load) (3) Maximum critical response at bottom of surface layer (a) Tensile Stress (for rigid pavements) (b) Tensile Strain (for flexible pavements) (4) Deviator stress on top of subgrade, psi

(continued)

TABLE 6.2. (CONTINUED)

OUTPUT VARIABLES	DESCRIPTION
	(5) Bulk stress in middle of subbase layer (psi) (6) Past traffic in 18 kips ESAL (as entered in input) (7) Maximum theoretical 18 kips ESAL applications (8) Remaining life, percent (9) Final values of Young's Moduli
Summary Statistics	Mean, standard deviation and coefficient of variation (percent) for remaining life, and final moduli

TABLE 6.3. SUMMARY OF SHORT OUTPUT

OUTPUT VARIABLES	DESCRIPTION
Identification and Initial Information	Problem No., Title, NDT Device (FWD/Dynaflect); Station, Test Date; No. of Layers; Type of Layer Above Subgrade (for Rigid Pavements); Type of Base and Subbase Layers (for Flexible Pavements).
Input System Parameters	Maximum No. of Iterations; Tolerances for Discrepency in Deflections (TOLR1 and TOLR2); Tolerances for Change in Moduli (TOLR31, TOLR32, TOLR33).
Layering Information	(Repeated for each layer, starting from the surface layer.) Layer No.; Thickness (Inches); Poisson's Ratio (No value in thickness indicates semi-infinite subgrade).
ESEED	Input Seed Modulus in psi (if input is zero, then default seed modulus is printed).
E(MAX)	Maximum allowable value of modulus in psi (default value is printed if there is no input).
UNWTI	Unit weight of subgrade soil (lbs./cu. ft.)
Sensor No.	Sensor no. 1 assigned to the first sensor closest to the test load (5 sensors for Dynaflect and 6 or 7 sensors for FWD).
Measured Deflection	At each sensor in mils.
Calculated Deflection	At each sensor in mils.
HERRP (Based on Seed Moduli)	Largest absolute discrepency in measured and calculated deflections (in percent).
ITERATIONS BEGIN	Message when further iterations are stopped; also total number of iterations attempted in this run.
Results of Iterations	Message about skipping results of each iteration if IOPT1 is zero. In that case, only summary of best iteration is printed. If IOPT1 was 1, then summary of each iteration and finally of best iteration are presented.

(continued)

TABLE 6.3. (CONTINUED)

OUTPUT VARIABLES	DESCRIPTION
Young's Moduli	For each layer (in psi).
Measured Deflections	In mils.
Calculated Deflections	In mils.
HERRP	The largest discrepency in percent.
Design Single Axle-Load Date	Load per tire (lbs.); Tire pressure (psi).
Other Pavement Data	For Rigid Pavements: flexural strength; rigid pavement type; shoulder type. For Flexible Pavements: test temperature and design temperature (^{o}F)
RESULTS OF EQUIVALENT LINEAR ANALYSIS	Corrected values of Young's moduli.
TEMPERATURE CORRECTION (Only for Flexible Pavements)	Corrected value of Young's modulus of AC surface.
REMAINING LIFE	Printed in percent (only when IOPT2 was entered as 1). A value of 999.0 is printed if no positive value of remaining life could be determined.
NEXT PROBLEM	All the above output repeated for each successive problem.
SUMMARY OF STRUCTURAL EVALUATION	Following summary outputs printed for each deflection basin analyzed. (1) Station (2) Maximum Deflection (under design load) (3) Maximum Critical Response (4) Deviator Stress, psi (5) Bulk Stress, psi (6) Final Values of Young's Moduli
SUMMARY STATISTICS	Mean, standard deviation and coefficient variation (percent) for final moduli.

for nonlinear behavior and temperature sensitivity, if necessary. The generation of results in tabular form facilitates plotting of the following output against the distance along the pavement (the test number or location) on the abscissa.

(1) remaining life, R_L, percent, and

(2) Young's moduli, E's, of pavement layers.

APPLICATIONS/IMPLEMENTATION

The final stage in a structural evaluation system is to identify the sections of the tested pavement for potential problems, to help in delineating areas in need of maintenance and/or rehabilitation, and to provide essential inputs for comprehensive thickness design for overlay. It is not desirable that a computer-generated output should provide all the information for pavement management at the project level. The engineering experience and judgement should play a vital role for the decision making process at the project level. A computerized structural evaluation system such as described in this chapter is designed to provide all the necessary information to the user/engineer. This section provides guidelines to processing and managing the information generated by the computer program for useful applications and implementation by the user/engineer.

Application Areas

The plotted output (as described earlier) can provide a visual diagnostic chart of the structural condition of the whole length of pavement on which the dynamic deflection basins were collected. A conceptual illustration of these plots is presented in Fig 6.8. Examples of some specific applications are discussed below.

Identification of Localized Problem Areas. Visual inspection of the remaining life profile can help to identify localized problem areas along the stretch of tested pavement. The final measures for rectification of these local areas should be based on a study of summary statistics of condition survey data corresponding to these locations. For example, certain measures

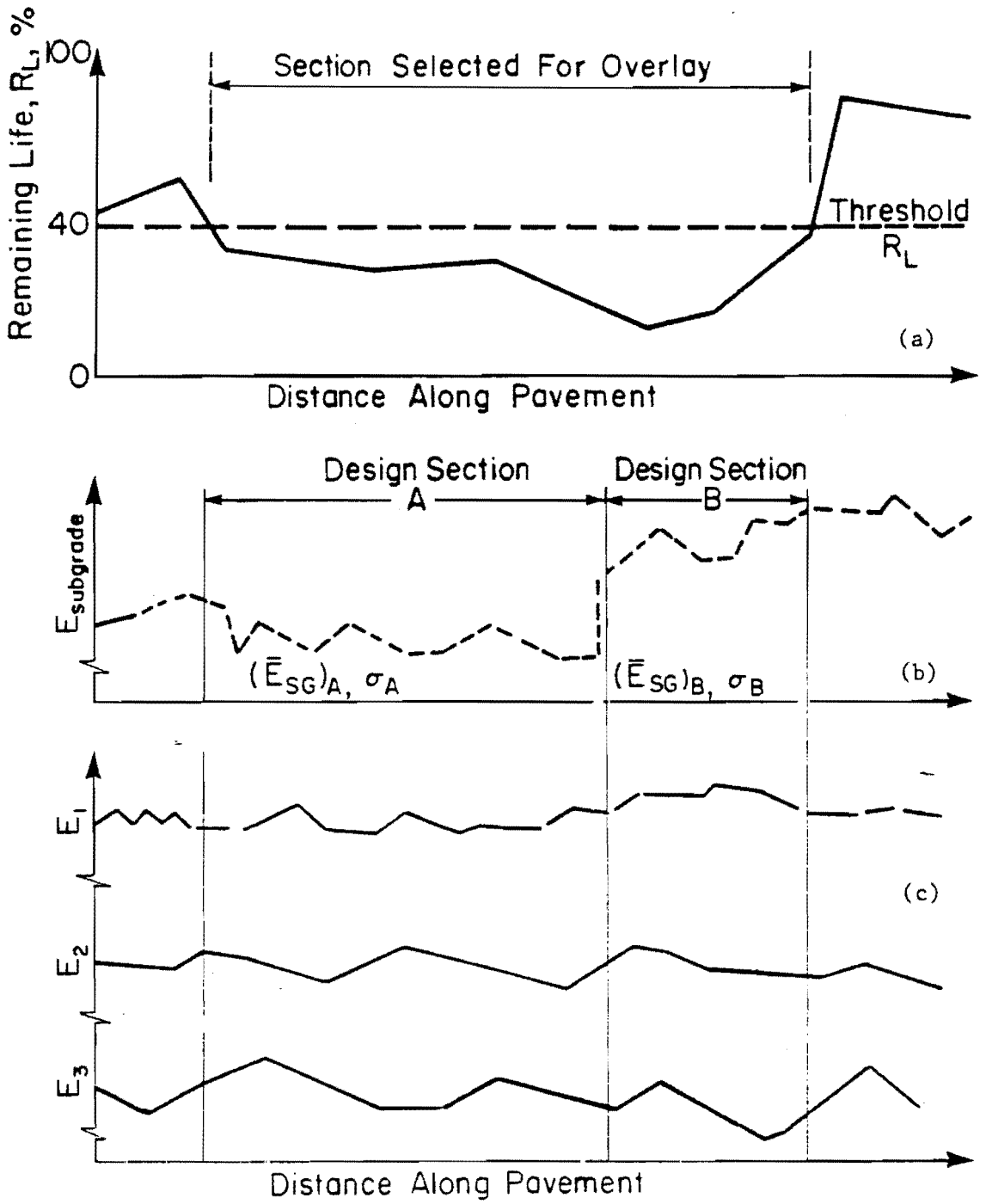

Design Moduli (In Each Design Section)

$$= f\left[\bar{E}_i \ , \ \sigma_i\right]$$

Fig 6.8. Application/implementation of structural evaluation programs.

for correcting existing pavement may be beneficial on these areas before placement an overlay or a seal coat on portions of the pavement which include these localized weak spots.

Assessment of Pavement Maintenance/Rehabilitation Needs. An important decision to be made on the project level has to do with delineating pavement sections according to their maintenance or rehabilitation needs. While maintenance strategies and timing can be based on the results of a condition survey or roughness measurement, assessment of an overlay requirement and other rehabilitation needs is drawn primarily from deflection testing. As noted in Chapter 2, traditionally limiting deflection criteria had been in use to assess the need for an overlay. This procedure is of course based on empirical relationships developed from field performance data. There are obvious limitations to using a similar approach for dynamic deflection data. To provide a rational and mechanistic method for delineation of pavement sections which are to be considered for structural strengthening, the following approach is recommended.

(1) Establish a thresnold value of remaining life (based on structural evaluation) below which consideration must be given to the designing of an overlay thickness. For example, for CRC pavements in Texas, it has been proposed to use 40 percent as the threshold limit of remaining life (Ref 96).

(2) Delineate the sections along the length of the pavement for consideration of overlay design that in general show a computed remaining life equal to or less than the threshold value. This step is illustrated in Fig 6.8(a).

(3) To achieve efficiency and cost reduction in designing overlays, several recently developed procedures rely on dividing the stretch of pavement to be overlaid into several design sections. Then, using the design values of insitu moduli and other parameters representative of each section, the overlay thickness is designed for that section. In general, a deflection parameter is used to identify the design section. For example, tne Dynaflect Sensor 5

deflection profile is recommended in Refs 69 and 93. Use of profiles based on the Dynaflect Sensor 5 deflection and basin slope (SLOP) has been recommended to select design sections for rigid pavements in Texas (Refs 23, 96).

The approach proposed in this study is to use the subgrade modulus, E_{SG} profile, as illustrated in Fig 6.8(b). E_{SG} values in the final output are representative of insitu nonlinear moduli under design load condition. Guidelines in the selection of design sections are briefly described in the following.

(a) Select preliminary design sections for visual examination of the E_{SG} plot along the length of pavement considered for overlay design. This selection is basically based on an approximate graphical contrast observed in the relative stiffness of the subgrade as shown in Fig 6.8(b).

(b) Compute the mean value and standard deviation of E_{SG} for each design section.

(c) Perform hypothesis testing to find if the difference in the means of two adjacent sections is statistically significant. Appropriate statistical tests are to be used, recognizing that the variances of E_{SG} in the two sections may or may not be same. A detailed procedure of hypothesis testing is presented in Appendix E. If the difference in means is not significant, the two sections can be pooled into one combined section and then tested against the next "selected" section.

Once the design sections have been established, the next step is to evaluate design moduli.

Overlay Design-Evaluation of Insitu Design Moduli. Before proceeding to a comprehensive overlay design, design insitu moduli are to be evaluated for each established design section. The design values of insitu moduli are important input for any overlay design and field variability should be taken into account, using known statistical methods. The design modulus of each

layer of existing pavement in a design section can be determined from the mean value, standard deviation, and a preselected value of confidence level (say 95-97 percent). The recommended procedure for computing design moduli is also presented in Appendix E.

Implementation of Structural Evaluation System

The implementation phase of the output generated from the computerized structural evaluation system based on dynamic deflections and their applications warrants special emphasis. All the concepts and recommended procedures have already been discussed in preceding sections of this chapter. A self-explanatory summary is presented in the simplified flow diagram (Fig 6.9).

SUMMARY

A complete framework for structural evaluation of pavements, applicable to both rigid and flexible types, has been presented in this chapter. Procedures are developed here for evaluation of the structural capacity of existing pavement on which dynamic deflection basins are to be measured. Methods for prediction of fatigue life and remaining life analysis have been based on the insitu material characterization developed in Chapters 4 and 5. Guidelines for processing and managing information related to the evaluated pavement are presented so that rational decisions can be made concerning rehabilitation needs. Methodolgies are also recommended for identifying design sections and determining design insitu moduli for subsequent use in comprehensive overlay design.

Two computer programs have been developed which are based on the materials presented in Chapters 4, 5, and 6. Program RPEDD1 is the structural evaluation system for rigid pavements and is described in Chapter 7. A description of FPEDD1, the structural evaluation system for flexible pavements based on dynamic deflections, is presented in Chapter 8.

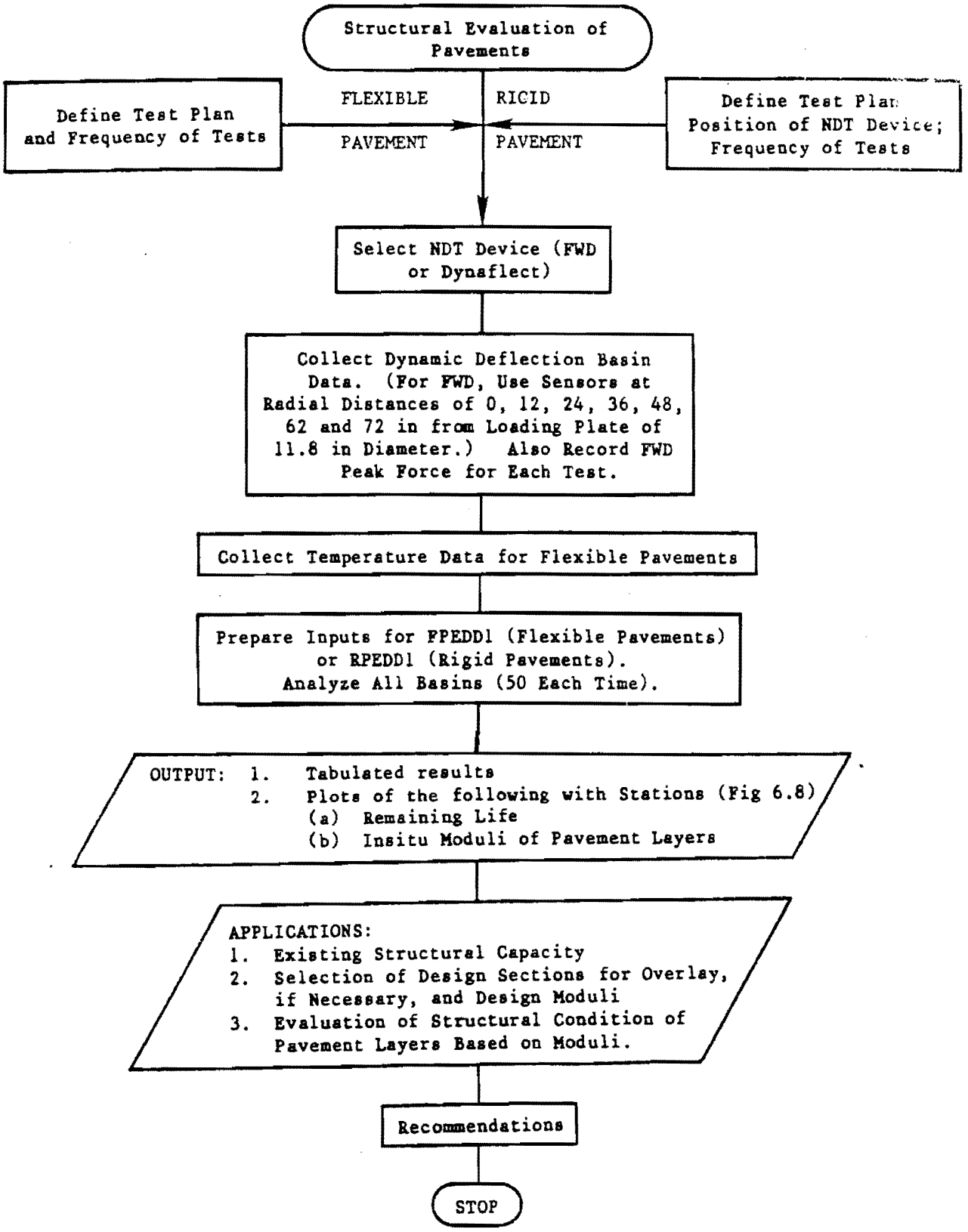

Fig 6.9. A conceptual flow diagram for implementation of the proposed structural evaluation systems.

CHAPTER 7. DESCRIPTION OF RPEDD1

A computer program, RPEDD1, a rigid pavement structural evaluation system based on dynamic deflections, has been developed in this study, based on the analytical models and framework presented in Chapters 4, 5, and 6. This chapter is devoted to a general description of the program in addition to the salient features related only to rigid pavements. Guidelines on application and implementation of the program are also briefly discussed and improvements on the previously proposed evaluation procedures in Texas are presented.

INTRODUCTION

To familiarize the users with the monitoring and evaluation process of rigid pavements, a conceptual flow diagram is presented in Fig 7.1. The computer program RPEDD1 analyzes dynamic deflection basins to generate estimated in-insitu Young's moduli of pavement layers and structural capacity in existing condition. The program is based on the standard American units of measurement. Information required for input to the programs is listed below.

Acquisition of NDT Data

Data Related to NDT Device. Data related to dynamic loading and geophone configuration of a Standard Dynaflect are specified within the program (Fig 2.1). If the FWD is used for NDT evaluation, the configuration illustrated in Fig 2.5 is provided for within the program. However, the radius of the loading plate used in the NDT test should be recorded. The FWD peak force recorded during the measurement of each deflection basin is also required later an an essential input. The number of geophones used with FWD is also required in input.

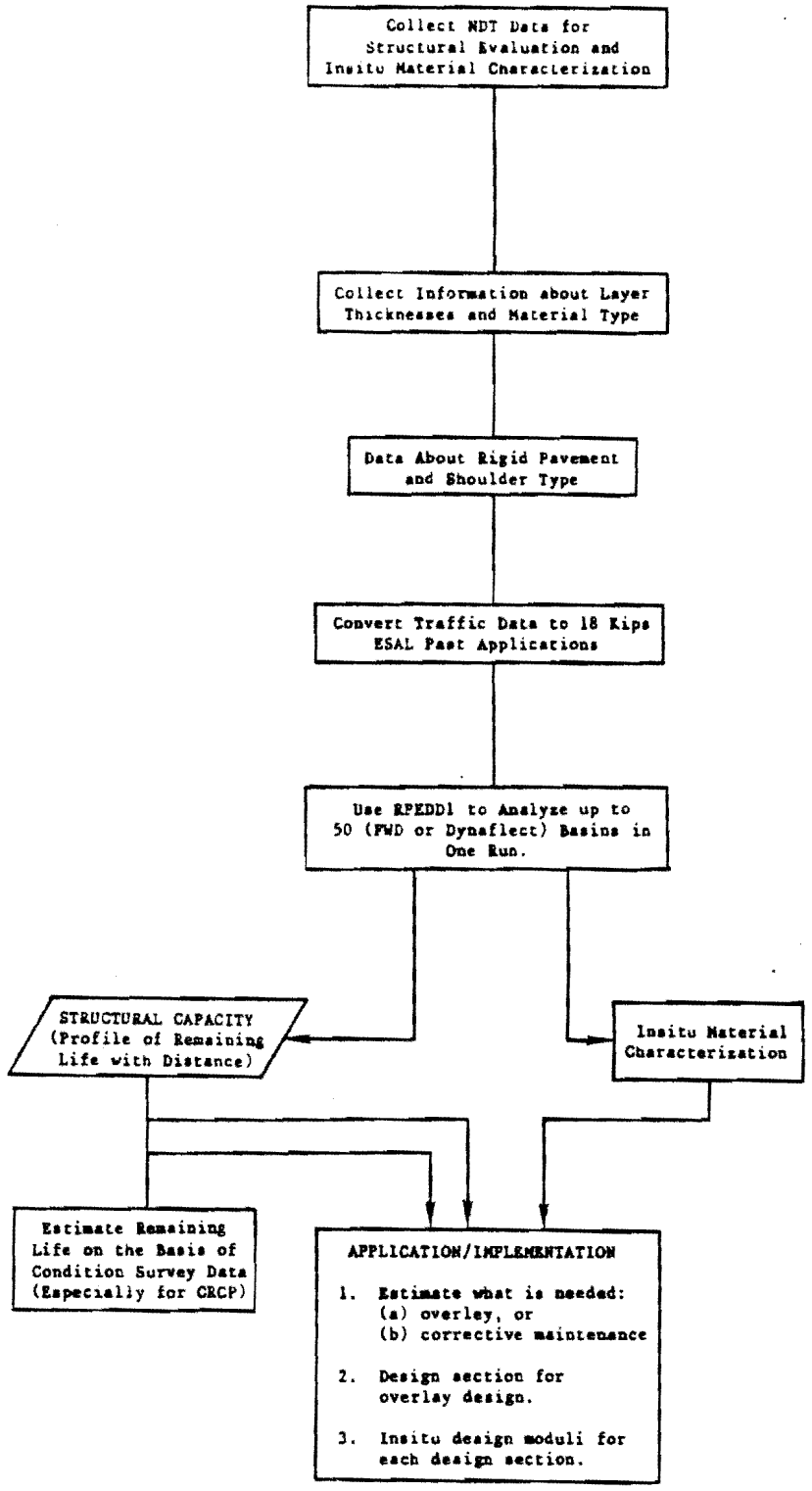

Fig 7.1. A conceptual flow diagram for the proposed framework of structural evaluation and insitu material characterization based on dynamic deflection.

Dynamic Deflection Basins. During each test, dynamic deflections are measured at each geophone in both the Dynaflect and the FWD to define the deflection basin. The programs require deflections to be coded in mils (1/1000's of an inch).

Acquisition of Pavement Data

Pavement Type and Cross Section. This information includes rigid pavement type (jointed concrete pavement, continuously reinforced concrete pavement), shoulder type, and number of layers in the pavement structure. Layering information can be obtained from construction plans and design cross section but preferably should be supported by field evidence, such as from extracted cores. The SASW test is another method for obtaining layering information. If there is any evidence of the existence of a rock layer at a shallow depth (within 20 to 30 feet), then it is important to know the precise depth, for the reasons discussed in Chapter 4.

Pavement Condition Data. Pavement condition should also be recorded at each test location, especially if signs of severe distress are obvious on the pavement surface. Information obtained from a recently performed condition survey can also be utilized for this purpose.

Material Data. Information should be acquired about the type of material used in intermediate layers (base and/or subbase materials). It is essential to know whether these materials are stabilized or can be considered as unbound granular materials. This information is used in the basin fitting routine as well as for nonlinear characterization. Any data available from laboratory characterization of all materials will also be useful later to ascertain allowable ranges of maximum and minimum moduli for each layer.

Overlaid Pavements. The program is basically designed to evaluate non-overlaid pavements. If the deflections test is made on overlaid pavement, it can still be evaluated by specifying the total thickness of concrete layers in the input as the first layer if the overlay is bonded concrete overlay type. In the case of unbonded overlay, the user should provide the initial seed and permissible ranges of moduli for this layer. The ways actual

overlaid pavements are to be idealized for input to the program are illustrated in Fig 7.2. In case of a flexible overlay, the FPEDD1 program (Chapter 8) should be used to analyze measured deflection basins.

Traffic Information

Past traffic data should be converted to 18-kip ESAL. If RPEDD1 is being used only for insitu material characterization, then traffic data are not required and the option for the remaining life analysis need not be used.

Design Load Configuration

If the user wants to specify a design load other than the default configuration (Fig 5.19), that is possible by using the option for user-specified design load. For example, truckers frequently use an inflation pressure higher than 75 psi (Ref 97). The detailed input guide is presented in the User's Manual (Appendix F).

PROGRAM DESCRIPTION

General

RPEDD1, the Rigid Pavement Structural Evaluation System using Dynamic Deflections (version 1.0), analyzes a measured dynamic deflection basin using a self-iterative procedure to derive insitu Young's moduli for a three or four-layer pavement. Nonlinear moduli of granular layers and subgrade are then computed using an equivalent linear analysis based on the strain-sensitivity concept. An option for remaining life analysis is also provided. The program is capable of analyzing up to 50 deflection basins in one run. A user's manual with example application is included in Appendix F.

Input Variables

A maximum of 14 lines (cards) of input must be provided to analyze one deflection basin with RPEDD1. A detailed input guide is presented in

(a) Bonded P.C. Concrete Overlay

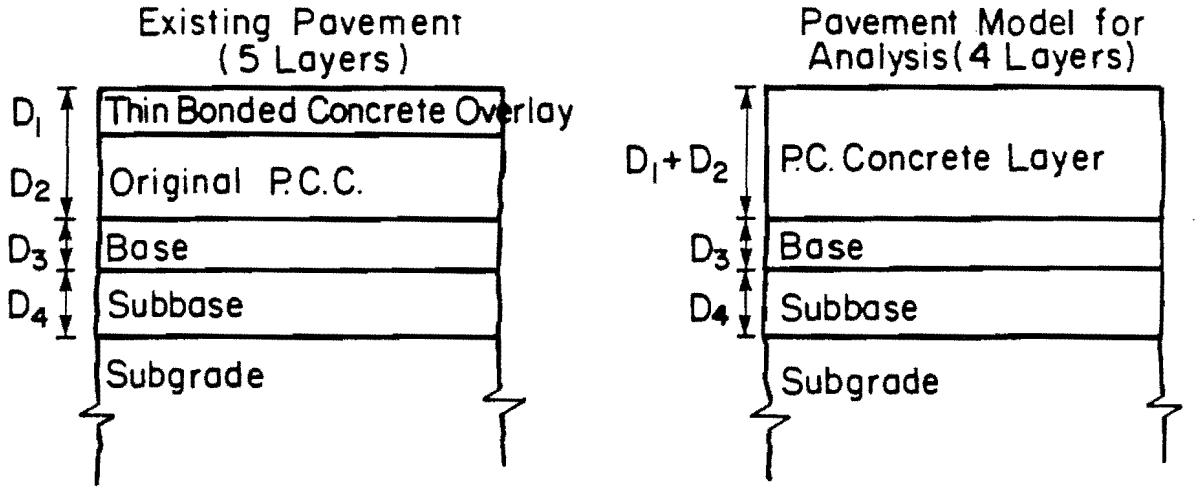

(b) Unbonded P.C. Concrete Overlay

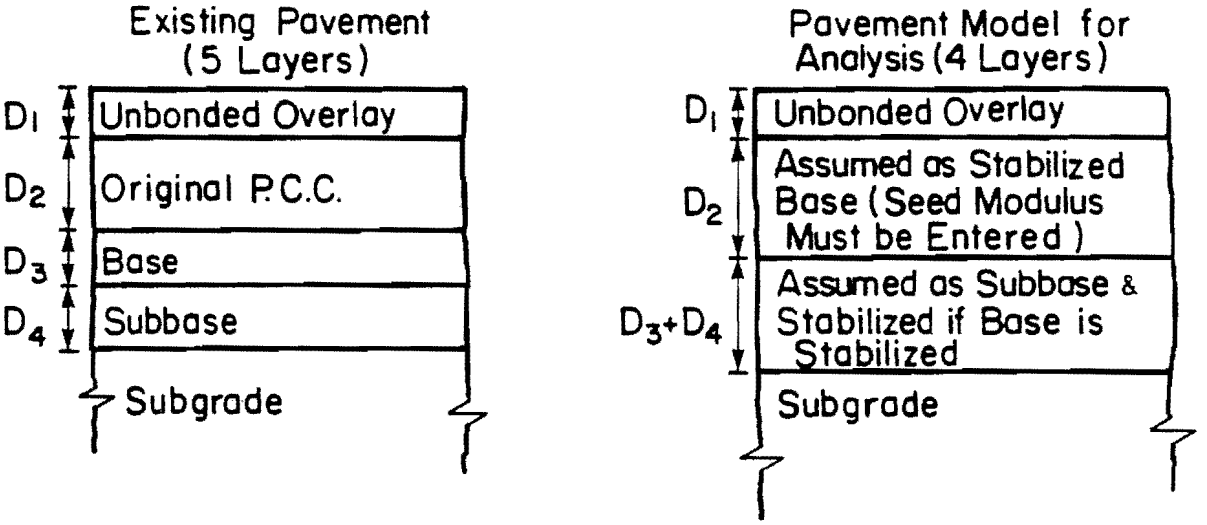

Fig 7.2. Idealized pavement models for rigid pavements overlaid with concrete layer.

Appendix F, which also identifies variables with default values. Only a list of input variables is given here.

(1) Number of total deflection basins to be analyzed.

(2) Test site and date of test.

(3) Station (test location); name of NDT device.

(4) Code for NDT device; number of deflection sensors; peak force, peak stress of FWD and radius of loading plate.

(5) Options for
   (a) summary output,
   (b) remaining life analysis,
   (c) the default procedure for creating a rigid bottom,
   (d) type of rigid pavement,
   (e) type of shoulder,
   (f) type of layer above subgrade,
   (g) unit weight of subgrade soil,
   (h) surface condition, and
   (i) deleting equivalent linear analysis and remaining life analysis.

(6) Measured deflections (in mils).

(7) Number of layers including subgrade layer.

(8) Information about each layer; starting from the top layer (one line/card per layer)

   (a) layer number,
   (b) thickness,
   (c) Poisson's ration,
   (d) initial seed modulus (generally zero should be entered here),
   (e) maximum allowable limit of modulus, and
   (f) minimum permissible value of modulus.

(9) Maximum number of iterations; five types of tolerances for use in the self-iterative basin filling subroutine.

(10) Option for user specified design load configuration; design load per tire and tire pressure, flexural strength of concrete and past 18-kip ESAL applications.

(11) Design load configuration if user specified option is enforced.

All the cards except the first one all other cards are again required for each subsequent problem.

Flow Chart and Analysis Models

The different subroutines used in RPEDD1 are summarized in Table 7.1. Whenever theoretical deflections, stresses, or strains are required in the program, subroutine ELSYM5 (specifically adopted for efficient computations in this program) is called. A simplified flow chart of RPEDD1 is presented in Fig 7.3. Different analytical models used in RPEDD1 are based on materials presented in Chapters 4, 5, and 6. Only primary analysis models are briefly described here to illustrate the sequence in which different analyses are performed in RPEDD1.

BASINR. This subroutine is the focal point of RPEDD1. It is called by RPEDD1 to determine insitu moduli by using a self-iterative procedure of deflection basin fitting based on successive corrections. The basic logic used in BASINR has been discussed in great detail in Chapter 4. The limited experience of using RPEDD1 for evaluation of actually measured deflection basins indicates that not more than eight to ten iterations with ELSYM5 are needed to achieve convergence (most of the time it took less than five iterations to converge).

ELANAL. This subroutine is called by RPEDD1 to correct the insitu moduli determined by BASINR for nonlinear behavior of granular subbase/base and fine-grained subgrade soils. It employs a self-iterative procedure for convergence of nonlinear strain-sensitive moduli under the design load configuration. The approach of equivalent linear analysis employed in this subroutine is discussed in detail in Chapter 5.

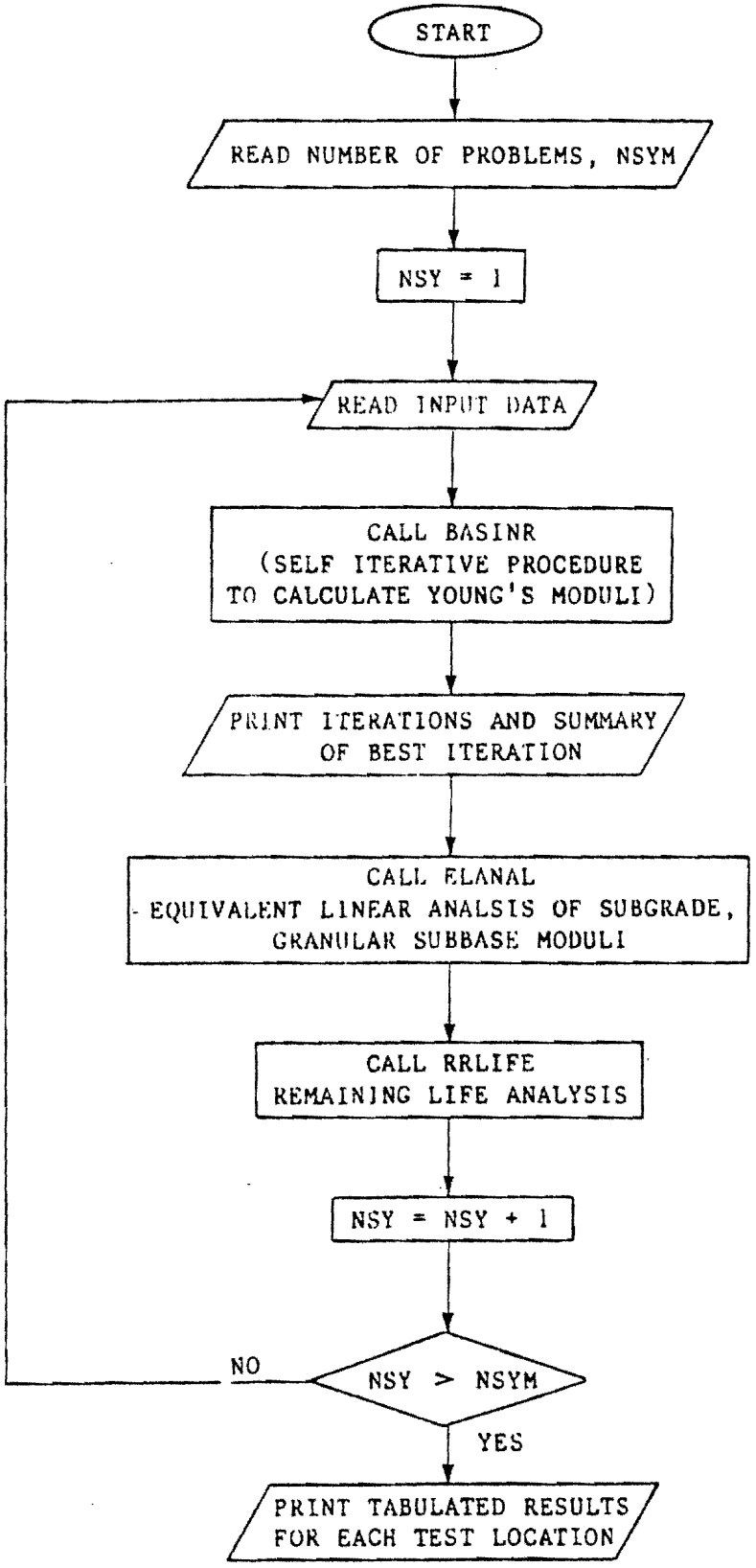

Fig 7.3. Simplified flow chart of RPEDD1.

TABLE 7.1. SUMMARY OF SUBROUTINES USED IN RPEDD1

SUBROUTINE	DESCRIPTION
BASINR	Self-iterative basin fitting model; called by RPEDD1.
EDFALT	Default procedure for maximum and minimum values of pavement moduli; called by BASINR.
ERIGID	Default procedure to generate seed moduli; called by BASINR.
SORTD	Called by BASINR to sort the discrepencies in theoretical and measured deflections in decreasing order.
ELANAL	Self-iterative procedure for equivalent linear analysis; called by RPEDD1.
SHSTR1	Called by ELANAL to search for the largest of maximum shear strains computed by ELSYM5.
EQLIN1	Called by ELANAL to estimate nonlinear modulus of a granular layer or subgrade.
RRLIFE	Called by RPEDD1 for remaining life analysis.
ROUNDM	Called by RPEDD1 to round off values of remaining life and final moduli.
SSTAT	Called by RPEDD1 to calculate summary statistics for remaining life and final Young's moduli.
ELSYM5	This subroutine contains ELSYM5 computer package called by BASINR and ELANAL to compute pavement response.

RRLIFE. Subroutine RRLIFE is called by RPEDD1 to compute fatigue life, and remaining life analysis if the option for remaining life is used. It is described in Chapter 6.

Output

The format of output generated by RPEDD1 is described, in Chapter 6 and example outputs are presented in Appendix F. The sequence in which results are printed is described below.

(1) Initial information based on input data or data generated by default procedures before starting the converge loop for the deflection basin fitting procedure.
(2) Output from BASINR is essentially the results of all iterations made in basin filling loop. In the case of the option used for summarized output, only the summary of tne best iteration (with the least convergence error) will be printed.
(3) Output from ELANAL is the results of nonlinear moduli if equivalent linear analysis has been used.
(4) Output from RRLIFE, remaining life, is also included in the final tabulated output.
(5) The final tabulated summary of output is similar to Table 6.2 or 6.3.

APPLICATION/IMPLEMENTATION

The application and implementation aspects of RPEDD1 are presented in detail in Chapter 6. Fig 7.4 presents a flow diagram of Texas rigid pavement overlay design procedure proposed in earlier reports (Ref 38). Considering the implementation phase of a structural evaluation system (such as RPEDD1) suggested in Chapter 6 (Fig 6.8), an improved framework is proposed in this study for selection of the design section and estimation of design moduli before using an overlay design program, such as RPRDS1 (Ref 38). This proposed framework is illustrated in Fig 7.5.

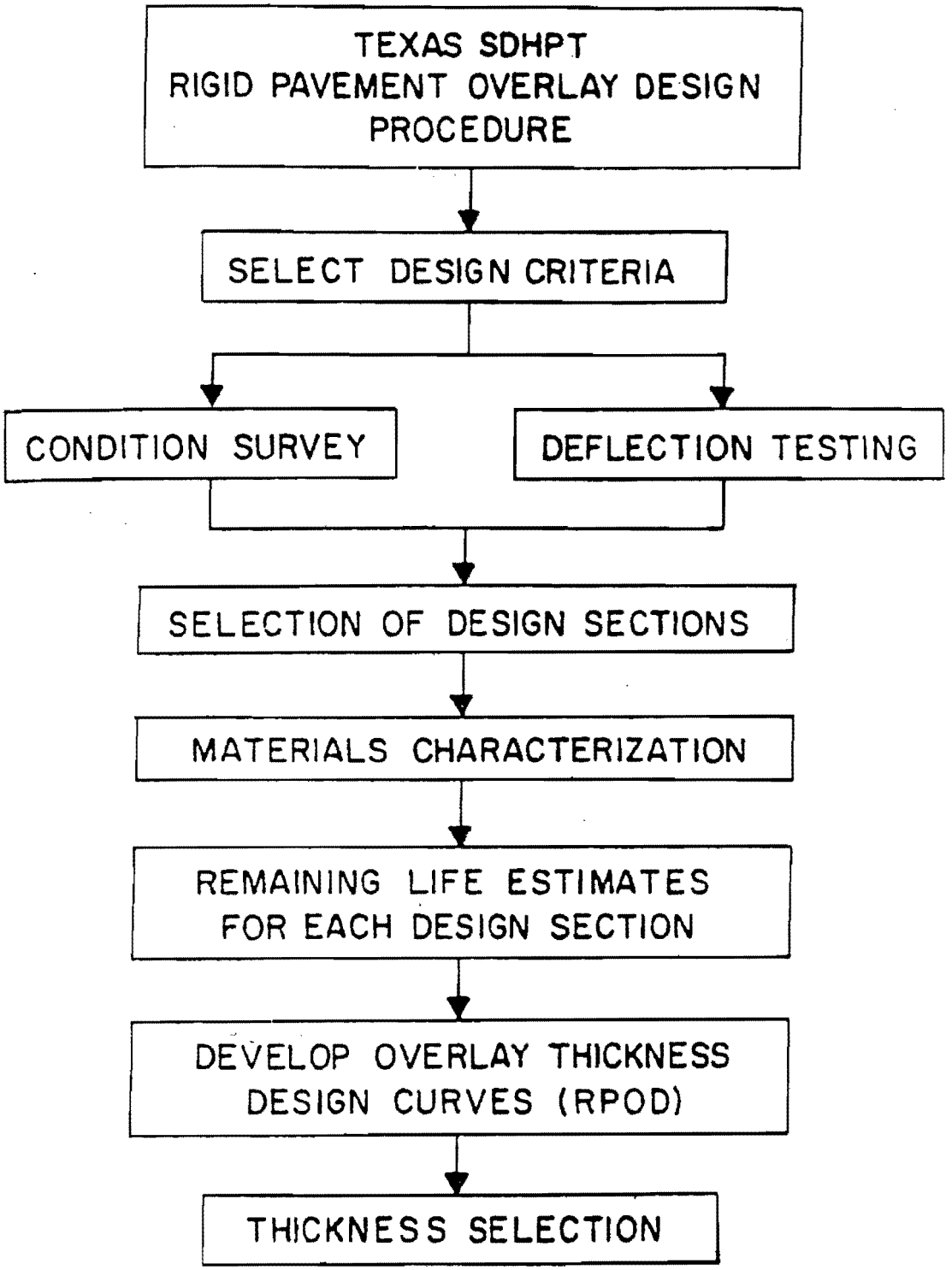

Fig 7.4. Flowchart of the Texas SDHPT rigid pavement overlay design procedure (Ref 38).

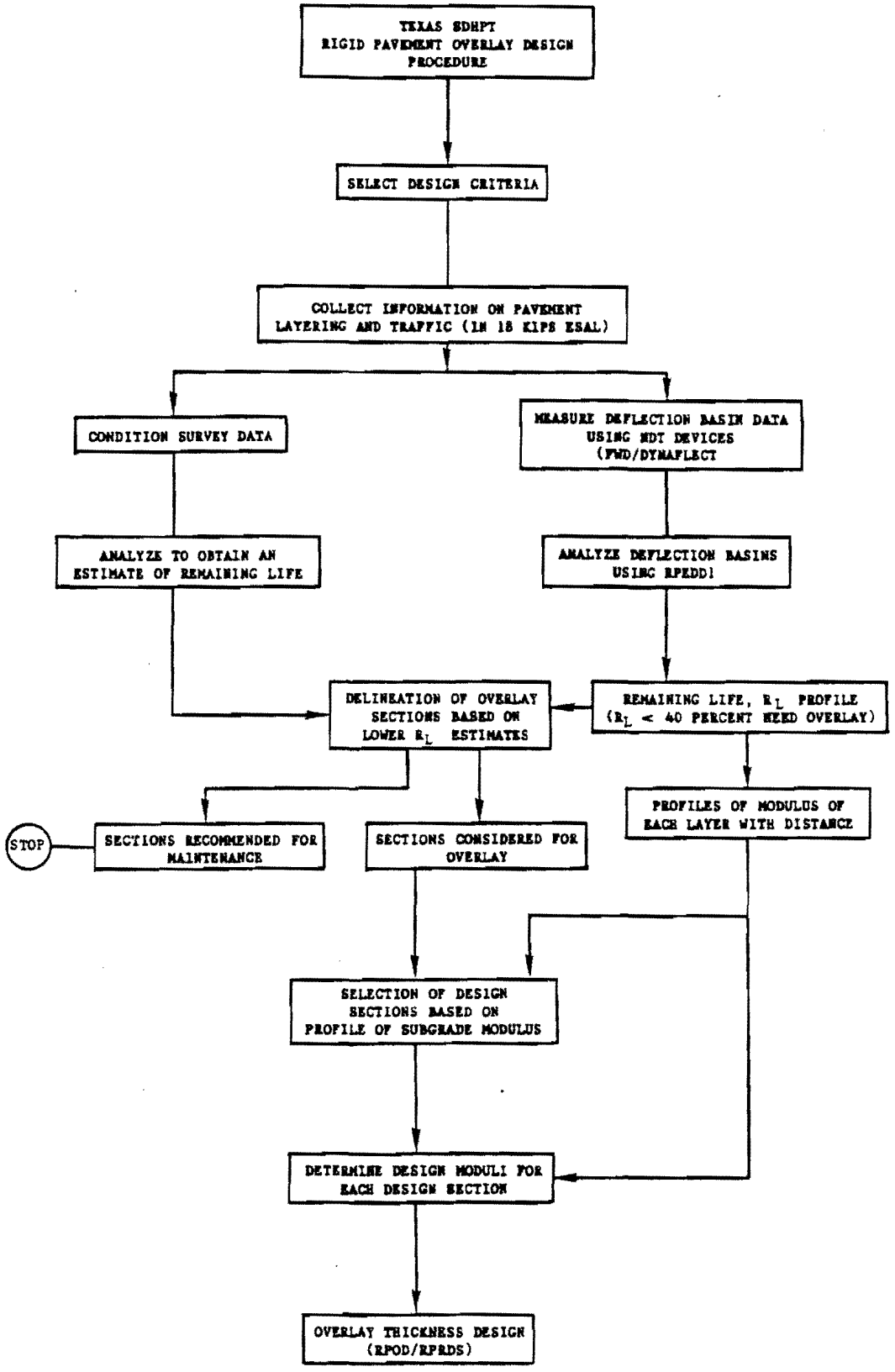

Fig 7.5. A conceptual framework of rigid pavement overlay design procedure proposed for Texas SDHPT.

SUMMARY

This chapter describes computer program RPEDD1, a rigid pavement structural evaluation system based on dynamic deflections. The program has been developed using several evaluation procedures described earlier in detail in Chapters 4, 5, and 6. A list of subroutines used in the program, a simplified flow chart, analysis models, and brief descriptions of input variables and outputs are also presented. A detailed user's manual and an example of RPEDD1 are presented in Appendix F.

CHAPTER 8. DESCRIPTION OF FPEDD1

FPEDD1 is the computer program for flexible pavements and is very similar to RPEDD1. It is based on the evaluation models discussed in Chapters 4, 5, and 6. This chapter presents a general description of FPEDD1, a flexible pavement structural evaluation system based on dynamic deflection.

INTRODUCTION

The conceptual flow diagram shown in Fig 7.1 for monitoring and evaluation purposes is also generally applicable to flexible pavements. FPEDD1 is also designed to analyze dynamic deflection basins measured by either the Dynaflect or FWD for insitu material characterization and structural evaluation. It also employs a self-iterative procedure to derive insitu moduli by fitting a measured deflection basin which is developed based on the discussions of Chapter 4. All input data and output are designed on the basis of standard U. S. units of measurement. FPEDD1 is designed to analyze a three or four-layered pavement model and is applicable to a wide variety of flexible pavement types.

Acquisition of NDT Data

The procedures for the acquisition of data related to the NDT device, (dynamic deflection basin, pavement cross section, layering information, depth of rigid rock, surface condition, and material data) are principally the same as described for RPEDD1 in Chapter 7. However, there is a basic difference in the position of the NDT device relative to the pavement edge. For material characterization in rigid pavements, the NDT device is generally positioned in the interior (away from the edge and midway between transverse cracks or joints), i.e., as recommended in Ref 62. However, for flexible pavements, NDT device is generally positioned in the wheelpath of the outer lane for deflection measurements.

Overlaid Pavements

Overlaid flexible pavements can be handled simply by assuming one combined layer made up of all asphaltic layers, as illustrated in Fig 8.1. Those overlaid rigid pavements in which the cement concrete slab had been broken and seated placing an overlay was placed can also be analyzed using FPEDD1 by considering the original slab as a stabilized layer.

Traffic, Design Load and Design Temperature

The acquisition of past traffic information and specifications of the design load is similar to that discussed for rigid pavements in Chapter 7.

The asphaltic concrete (AC) modulus in flexible pavement is temperature sensitive. The insitu derived AC modulus is based on the test temperature at which deflection basin was measured. For subsequent use in overlay design or even for making comparisons, it is recommended to correct the insitu modulus from test temperature to a design temperature. Therefore, it is necessary to obtain information about the design temperature (70°F is recommended in Ref 68). The test temperature is taken as temperature at the mid-depth of AC layer. It can be estimated from a record of climatological data using computer program FTEMP, which is described in Appendix I.

PROGRAM DESCRIPTION

A description of FPEDD1 is presented in the following sections.

General

FPEDD1, the flexible pavement structural evaluation system using dynamic deflections (version 1.0), evaluates NDT data to determine insitu pavement moduli and applies relevant corrections for the temperature dependency of asphaltic concrete and the nonlinear strain softening behavior of granular layers and subgrade. An option for remaining life analysis is also provided.

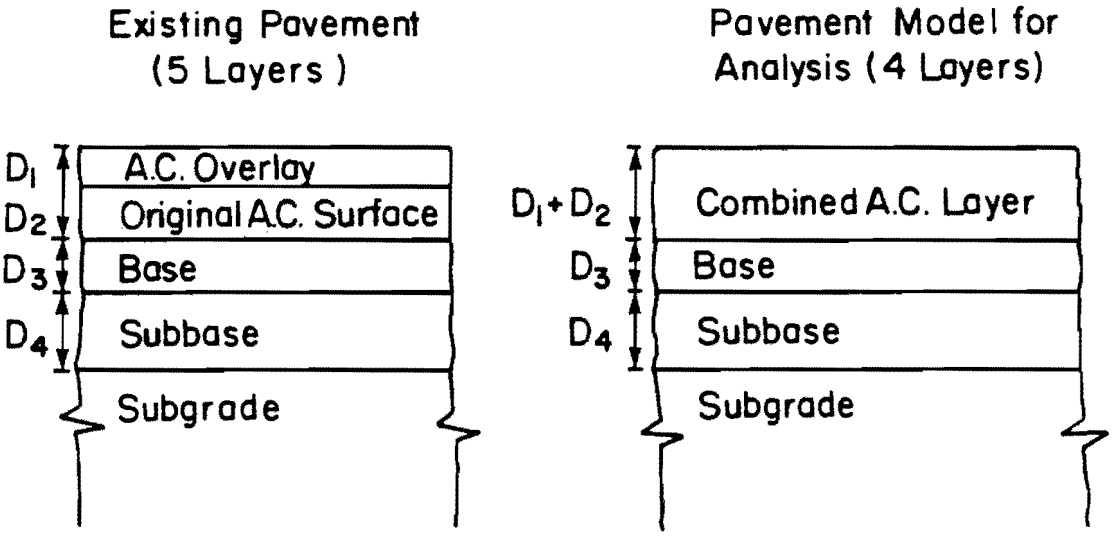

Fig 8.1. Idealized pavement model for a flexible pavement overlaid with one or more AC layers.

The program is capable of analyzing up to fifty deflection basins in one run. A user's manual with example applications is presented in Appendix G.

Input Variables

As many as fourteen lines (cards) with input information are required to analyze and evaluate one deflection basin using FPEDD1. Except for the first card, all the cards are required to analyze each subsequent deflection basin. A detailed input guide is included in Appendix G. A summarized list of input variables is presented in the following.

(1) Number of total deflection basins for analyses.
(2) Test site and date.
(3) Station (test location) and name of NDT device.
(4) Switch for NDT device, number of deflection sensors; peak force, peak stress of FWD, and radius of loading plate.
(5) Options for:
    (a) summary output of basin filling subroutine,
    (b) remaining life analysis,
    (c) default procedure of creating a rigid layer at finite depth of subgrade,
    (d) type of base material,
    (e) type of subbase material,
    (f) average unit weight of subgrade soil,
    (g) surface condition of pavement.
    (h) deleting the equivalent linear and remaining life analyses.

(6) Measured deflections (in mils).
(7) Number of layers including subgrade layer, pavement test temperature (°F), design temperature (°F).
(8) Information about each layer, starting from the top layer (one line/card for each layer). Layer number, thickness, Poisson's ratio, initial seed modulus (generally zero should be entered

here), maximum allowable modulus, and minimum permissible value of modulus.

(9) Maximum allowable number of iterations and five types of tolerances for use in self-iterative basin fitting procedure.

(10) Indicator for user-specified design load configuration, design load per tire, tire pressure, and past traffic in cumulative 18-kip ESAL.

Flow Chart and Analysis Models

Table 8.1 briefly summarizes the different subroutines used in FPEDD1. Subroutine ELSYM5 is called each time for computations of deflections, stresses, and strains. A simplified flow chart of FPEDD1 is presented in Fig 8.2. The detailed discussions related to different analytical models used in FPEDD1 are presented in Chapters 4, 5, and 6. Only the principal analysis models are briefly described here, to illustrate the analysis sequences used in FPEDD1.

BASINF. This subroutine employs a self-iterative procedure to determine insitu Young's moduli of pavement layers by obtaining a best fit of the measured deflection basin. The basic logic used here is discussed in Chapter 4. A simplified flow chart is presented in Fig 8.3. The efficiency of the convergence process is similar to that in BASINR for the rigid pavement program, RPEDD1 (on an average, around five iterations, based on the limited experience in using FPEDD1).

ELANAL. This subroutine is called by FPEDD1 for nonlinear correction of insitu moduli of granular layers and subgrade. It is almost the same for RPEDD1 and FPEDD1. A self-iterative procedure is used in ELANAL for convergence of nonlinear strain-sensitive moduli under the design load using the approach of equivalent linear analysis described in Chapter 5.

TEMPTF. This subroutine is called by FPEDD1 to adjust the insitu AC modulus to the design temperature condition using the logic presented in Chapter 4.

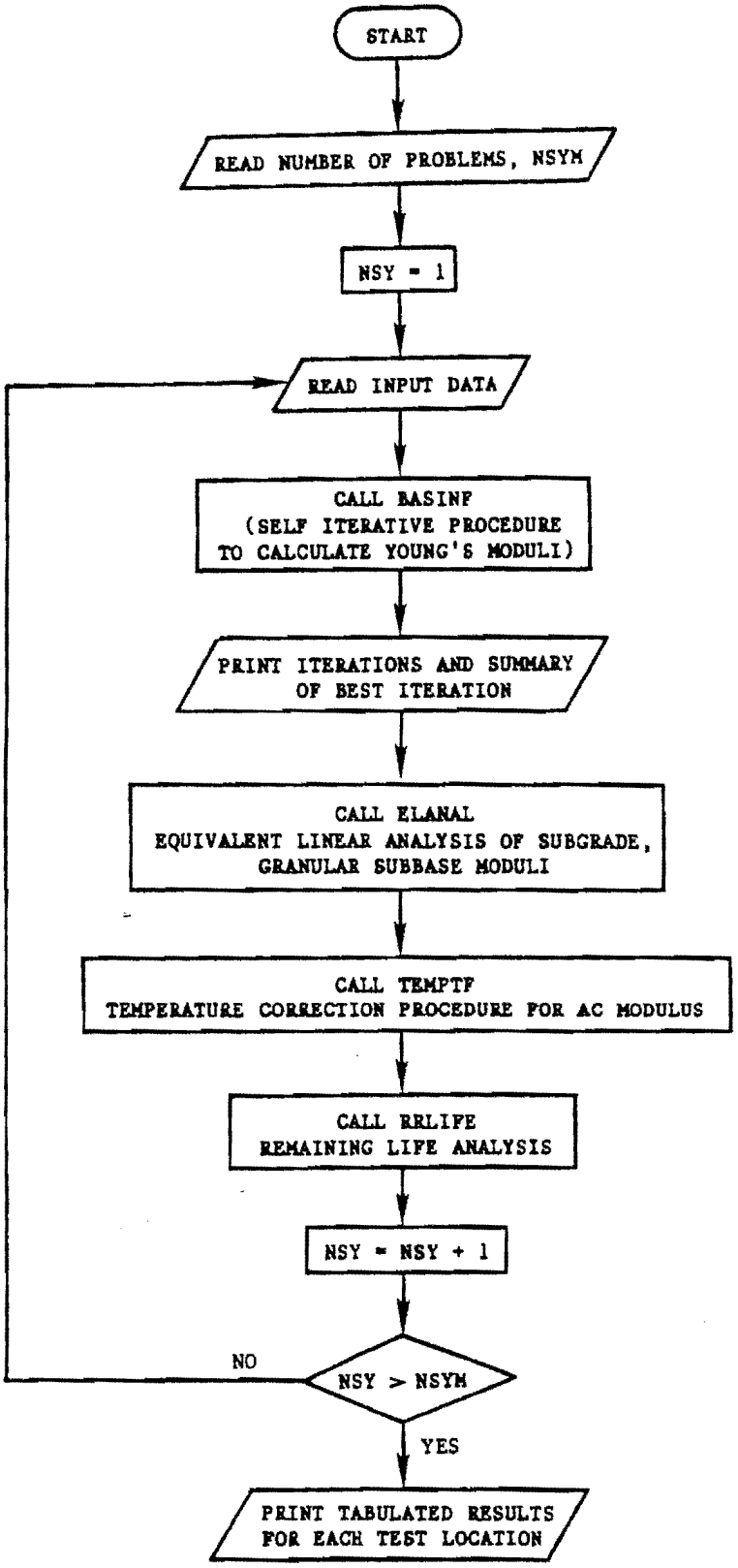

Fig 8.2. Simplified flow chart of FPEDD1.

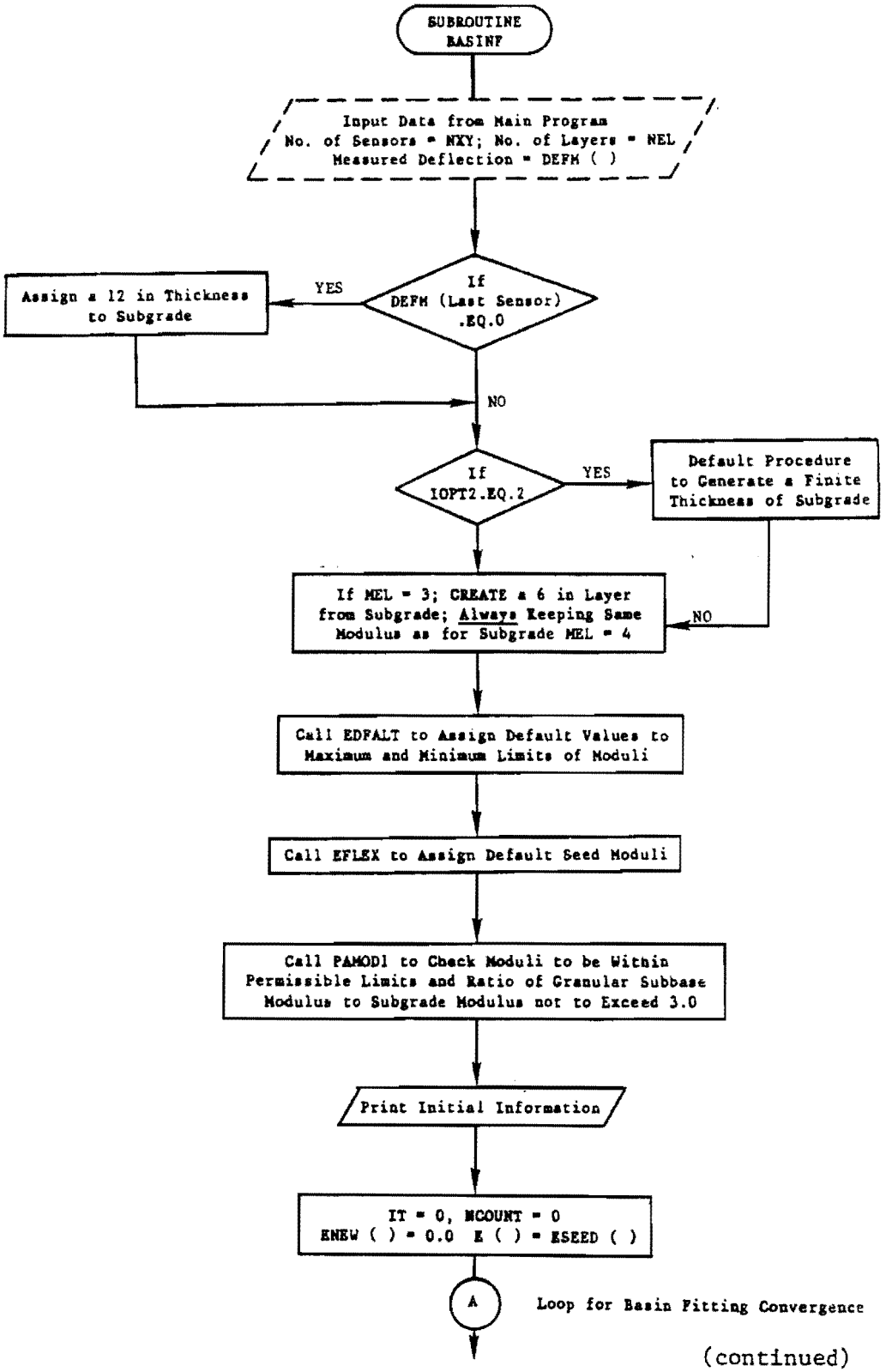

Fig 8.3. Simplified flow diagram of BASINF.

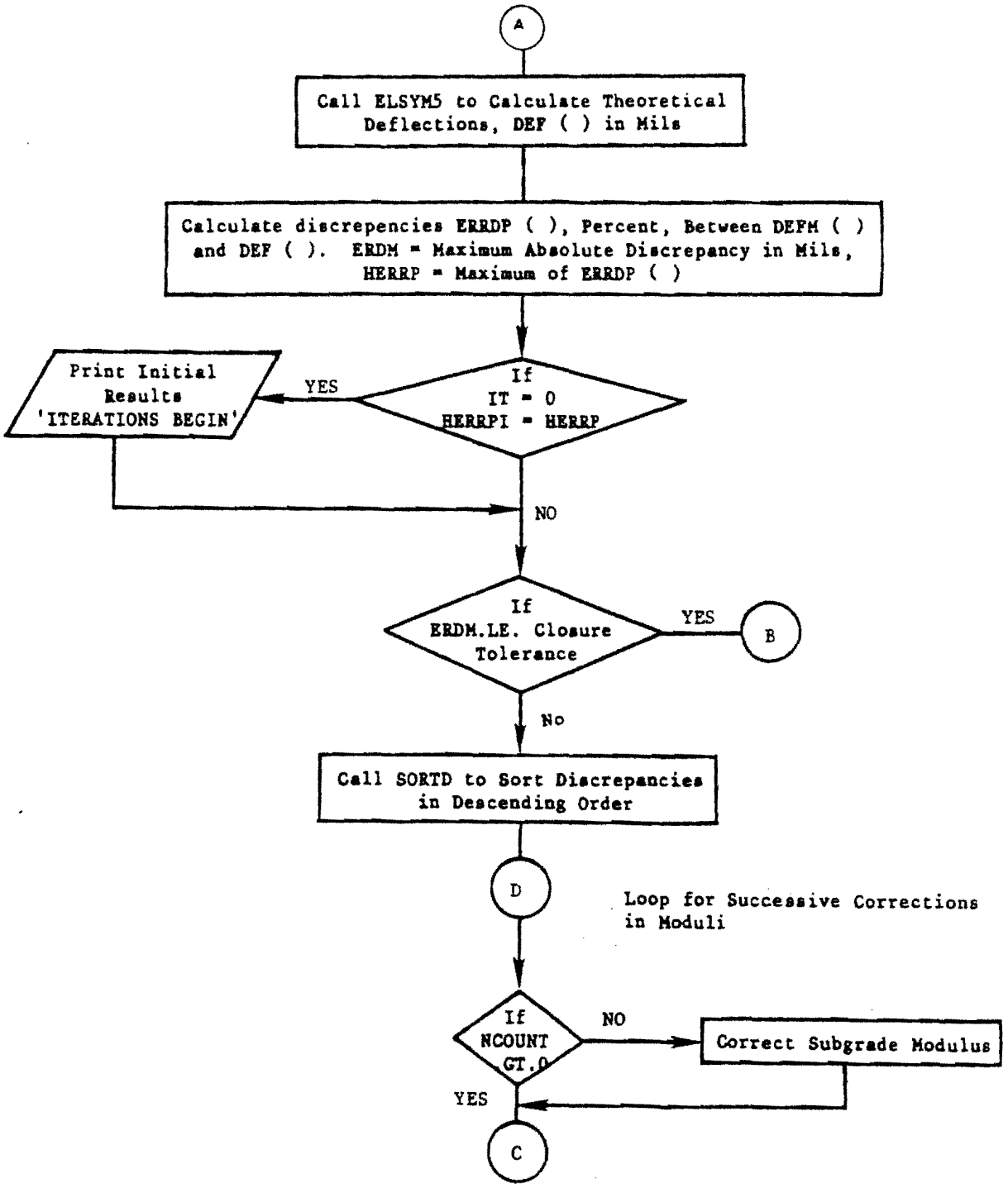

Fig 8.3. (continued)

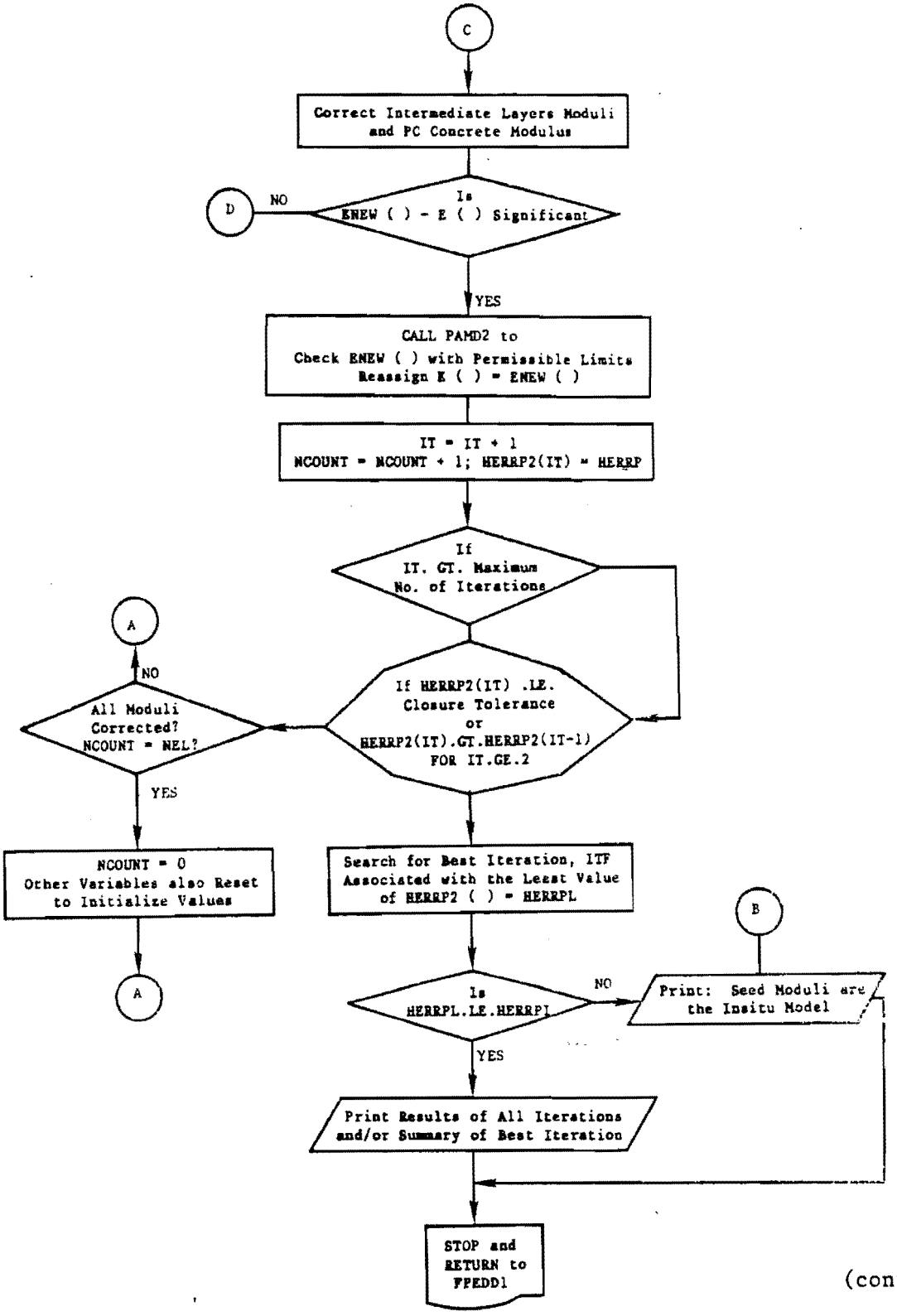

(continued)

Fig 8.3. (continued).

TABLE 8.1. SUMMARY OF SUBROUTINES USED IN FPEDD1

SUBROUTINE	DESCRIPTION
BASINF	Self-iterative basin fitting model; called by FPEDD1.
EDFALT	Default procedure for maximum and minimum values of pavement moduli; called by BASINF.
EFLEX	Default procedure to generate seed moduli; called by BASINF.
PAMOD1	Called by BASINF to check values of moduli ranges and seed moduli.
SORTD	Called by BASINF to sort the discrepencies in theoretical and measured deflections in decreasing order.
PAMOD2	Called by BASINF to check the values of new moduli to make sure that these are within permissible ranges.
ELANAL	Self-iterative procedure for equivalent linear analysis to correct strain dependent moduli of granular layers and subgrade; called by FPEDD1.
SHSTR1	Called by ELANAL to search for the largest of maximum shear strains computed by ELSYM5.
EQLIN1	Called by ELANAL to estimate nonlinear modulus of a granular layer or subgrade.
TEMPTF	Temperature correction procedure for AC modulus; called by FPEDD1.
RRLIFE	Called by FPEDD1 for remaining life analysis.
ROUNDM	Called by FPEDD1 to round off the computed values of remaining life and final Young's moduli.
SSTAT	Called by FPEDD1 to calculate summary statistics for remaining life and final Young's moduli.
ELSYM5	This subroutine contains ELSYM5 computer package called by BASINF and ELANAL to compute pavement responses.

RRLIFE. This subroutine performs the remaining life analysis by predicting AC fatigue life and using past traffic information. The detailed procedure is presented in Chapter 6.

Output

A summary of the output format has been presented in Chapter 6. The outputs generated by the programs are almost the same. An example output of FPEDD1 is included in Appendix G. Following is a presentation of the sequence in which the results of are printed by FPEDD1.

(1) Initial information based on input data or data related to moduli generated by default procedures before the convergence process of BASINF is commenced.
(2) Output from BASINF is essentially the results of all iterations or a summary of the best iteration, as specified by the user.
(3) The output from ELANAL is the moduli corrected for nonlinear strain softening behavior of granular layers and subgrade.
(4) The corrected AC modulus is generated from TEMPTF. The temperature correction is skipped if the pavement is in a severely cracked condition. The final combination of moduli from this step is included in the final tabulated output.
(5) The final tabulated output contains predicted fatigue life and remaining life from RRLIFE, in addition to a summary of final moduli and other results (as shown in Tables 6.2 and 6.3).

APPLICATION/IMPLEMENTATION

The guidelines presented in Chapter 6 are fully applicable for flexible pavements. Flexible pavements can be evaluated by FPEDD1 using the concepts based on Fig 6.8. An arbitrarily selected value for the threshold of remaining life is 40 percent. It is recommended that this value should be based on the judgement and experience of the individual user (or user agency). A framework for use of the output generated by FPEDD1 for overlay

design is presented in Fig 8.4. It is emphasized that the functional failure of a flexible pavement can also be attributed to excessive rutting, which should be given equal consideration in assessing any rehabilitation needs.

SUMMARY

A brief description of computer program FPEDD1, the flexible pavement structural evaluation system based on dynamic deflection, has been presented in this chapter. The program utilizes several analysis models which have been discussed in detail in Chapters 4, 5, and 6. In this chapter, the procedure for acquisition of input information, the list of subroutines used in the program, a simplified flow chart, analysis models, and a list of output variables have been presented. A detailed user's manual and an example output of FPEDD1 are included in Appendix G.

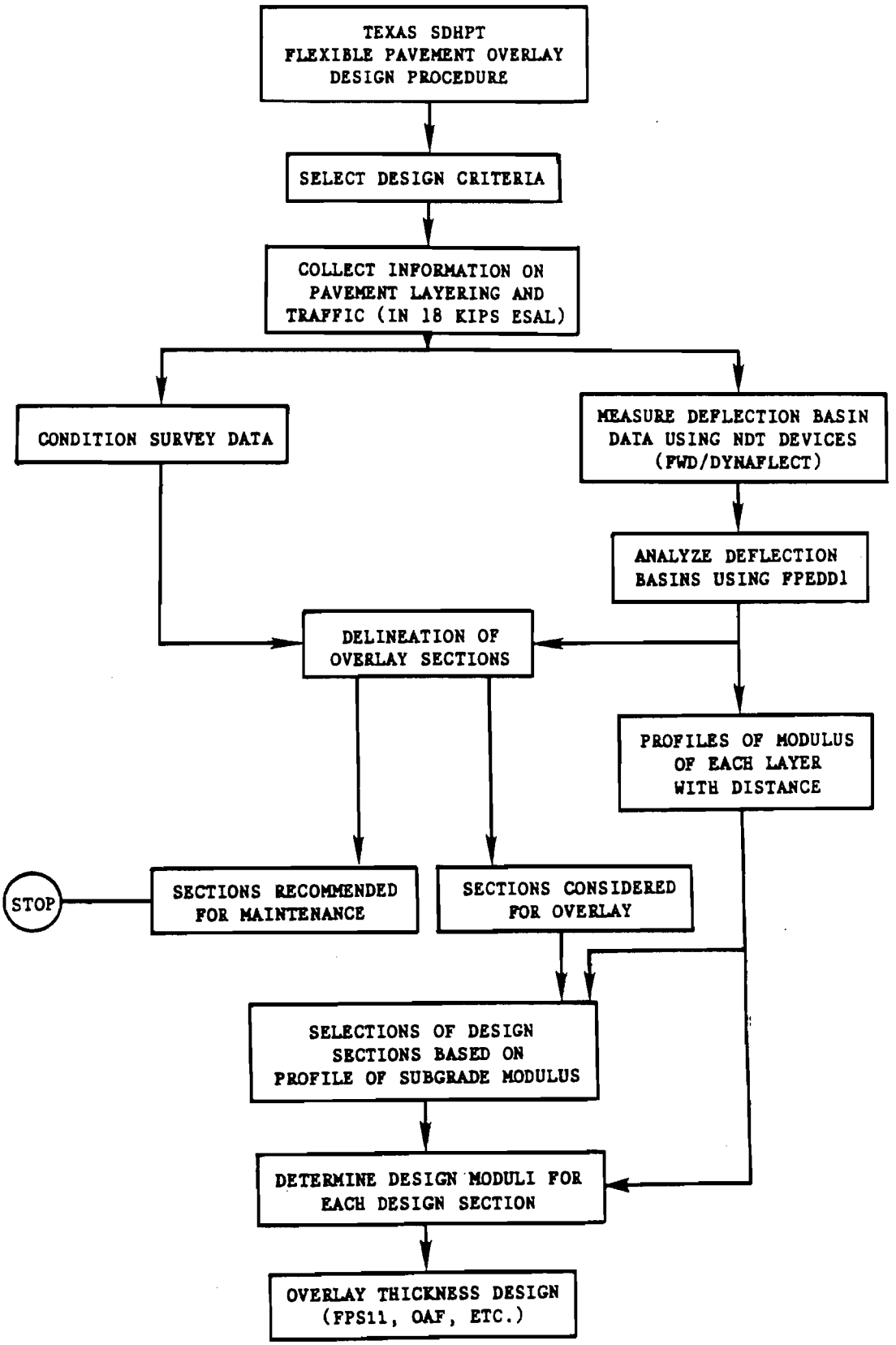

Fig 8.4. A conceptual framework of flexible pavement overlay design procedure proposed for the Texas SDHPT

CHAPTER 9: SUMMARY, CONCLUSIONS, AND RECOMMENDATIONS

SUMMARY

The primary objective of this study was to develop a self iterative computerized structural evaluation system for pavements based on dynamic deflection basins. Research was designed principally to analyze dynamic deflection data measured by the Falling Weight Deflectometer, (FWD), or Dynaflect for NDT evaluation of rigid pavements. A computer program, RPEDD1, a rigid pavement structural evaluation system based on dynamic deflections, was developed. The research work was extended to flexible pavements, using a similar framework resulting in another computer program, FPEDD1, a flexible pavement structural evaluation system based on dynamic deflections. A summary of different evaluation methodologies developed during the course of this research and incorporated in RPEDD1 and FPEDD1 is presented here.

A self-iterative procedure has been developed to analyze deflection basins measured by the Dynaflect or the FWD. The procedure is based on the inverse application of layered elastic theory to estimate insitu moduli of pavement layers. Consideration of a rigid layer and formulation of a methodology to obtain a unique solution are significant contributions to the state of the art. The concept of strain dependent dynamic moduli and its applicability to model nonlinear behavior of granular layers and subgrade have been used to develop a self-iterative procedure of the equivalent linear analysis to make corrections for the nonlinear strain softening behavior of such pavement materials.

CONCLUSIONS

The principal conclusions based on research performed in this study are presented in the following sections.

(1) A self-iterative procedure has been developed to derive insitu Young's moduli by using a multilayered linearly elastic model of the pavement. The procedure has been designed to analyze dynamic deflection basins measured by a FWD or a Dynaflect. Important conclusions are stated below.

(a) The ELYSM5 computer program can be reasonably used for inverse self-iterative applications to determine theoretical response. This is based on comparisons made with the results of the dynamic model at zero frequency and also comparing with the responses computed using the BISAR computer program.

(b) Results of the parametric studies to investigate the influence of thickness and moduli on theoretical deflection basins have been used to develop the procedure of successive corrections for formulation of the convergence methodology.

(c) Different tolerances related to moduli and discrepancies in deflections are used in the procedure to ensure efficiency, accuracy, and reliability of the self-iterative model. Convergence is generally achieved in less than eight iterations.

(d) The methodology used in the procedure to determine a unique set of moduli is based on the default procedure of seed moduli. The predictive equations developed for seed moduli in this study are associated with very high R^2 values (generally ranging between 0.8 and 0.99). The default seed moduli procedure has also resulted generally in reducing the number of iterations and in the elimination of the user dependency on the derived insitu moduli.

(e) The default procedure of creating a rigid layer in the subgrade is also incorporated using concepts from the wave propagation theory. Limited experience with the computer programs developed in this study indicated that consideration

of a rigid layer results in obtaining a better fit of a measured deflection basin.

(2) The strain-dependent models developed in this study to explain the nonlinear behavior of all unbound granular and cohesive materials present a rational approach for use in NDT evaluation of pavements. It is concluded that:

(a) There are threshold limits of shear strain amplitude below which dynamic moduli are strain independent.

(b) Unique relationships of the normalized modulus, (E/E_{max}), versus shear strain amplitude can be found for granular materials and typical subgrade soils.

(c) E_{max} is the maximum dynamic modulus which can be obtained in the field using the surface wave test (SASW) or other wave propagation techniques. The modulus determined from the analysis of a Dynaflect deflection basin falls in the same category, as theoretical shear strains under the Dynaflect loading are below the threshold limits.

(d) An equivalent linear analysis has been used in this study to correct the NDT-based moduli of granular layers and subgrade for nonlinear, strain-softening behavior. A self-iterative model has been developed in this study for this purpose which ensures fast convergence.

(e) It is assumed that the peak load applied by the FWD closely approximates the design load. Therefore the insitu moduli determined from the analysis of a FWD deflection basin represent the appropriate insitu moduli at the strain levels associated with the design load. The procedure of equivalent linear analysis can therefore be omitted for FWD data measured at heavier loads.

(3) The fatigue life prediction and remaining life estimate are also important steps in the structural evaluation methodology developed

in this study. A comprehensive structural evaluation system is rather incomplete without remaining life analysis, as it is an indication of the structural capacity of an existing pavement.

(4) The computer programs RPEDD1 (for rigid pavements) and FPEDD1 (for flexible pavements) can be used on the project level for faster and more reliable analyses of dynamic deflection data of the FWD and Dynaflect. The outputs from these programs provide the user with a global look at the structural capacity of the tested pavements and the variability in insitu moduli.

RECOMMENDATIONS

Computer programs RPEDD1 and FPEDD1 developed in this study for structural evaluation of pavements based on dynamic deflections and the recommended guidelines for their application and implementation should be further evaluated by analyzing extensive field deflection data. Deflection basin data should be measured using both the FWD and Dynaflect on pavement sections based on sound statistical experiment design. Several areas related to the concepts and procedures used in developing the computer models of the structural evaluation system warrant future research, as recommended in the following.

(1) The use of a test pavement with known material properties of the layers can provide the most suitable source of dynamic deflection basins for calibration and validation of the structural evaluation system developed in this study, especially as related to the insitu nonlinear material characterization. A rigid pavement research facility is at present under construction by the Center for Transportation Research, The University of Texas at Austin, as a part of ongoing research programs with the Texas State Department of Highways and Public Transportation (TSDHPT). Deflection data generated from this facility under controlled test conditions should be analyzed by using RPEDD1. These analyses and independent

measurements of deflections under 18 kip-ESAL should then be used to validate, and, if necessary, calibrate, the self-iterative model for determining insitu moduli (BASINR) and the nonlinear strain sensitive models used to correct insitu moduli determined from the Dynaflect deflection basins (ELANAL).

(2) The nonlinear behavior of granular layers and conesive subgrade has been modelled in this study using the strain-sensitivity approach. The E/E_{max} versus shear strain curves used in computer programs RPEDD1 and FPEDD1 were developed using the published research data. The general shape of these curves and most probably the threshold strain levels will not be significantly different if more laboratory tests are performed on local soils and granular materials. However, it is recommended that laboratory research be initiated on samples of subgrade soils and granular materials to validate and develop unique curves related to the strain-softening behavior of these materials.

Another improvement is recommended to the nonlinear correction procedure for the subgrade modulus determined from a Dynaflect deflection basin. The only unique curve used in the present versions of the computer program for the subgrade is based on the assumption of (normally consolidated) cohesive soil. If the subgrade soil is sand, gravelly, or generally classified as coarse-grained, then the nonlinear subgrade modulus may be somewhat overpredicted. It is recommended that in future versions of this program, another option be provided in the input to indicate the type of the subgrade soil. Subroutines ELANAL and EQLIN1 could then be slightly modified so that, if the subgrade soil is not fine-grained, the program can switch to the same nonlinear unique curve as used for granular layers to correct the insitu subgrade modulus.

(3) There are several self-iterative computer programs available to the Texas SDHPT for insitu material characterization of flexible pavements using deflection data. FPEDD1 should be evaluated along

with these programs using dynamic deflection basins measured by the Dynaflect and FWD. A short research study is recommended.

REFERENCES

1. Scrivner, F. H., G. Swift, and W. M. Moore, "A New Research Tool for Measuring Pavement Deflection," Highway Research Record 129, Highway Research Board, Washington, D. C., 1966, pp 1-11.
2. Wang, M. C., T. D. Larson, A. C. Bhajandas, and G. Cumberledge, "Use of Road Rater Deflections in Pavement Evaluation," TRRGG, Transportation Research Board, Washington, D. C., 1978, pp 32-38.
3. Bohn, A., P. Ullidtz, R. Stubstad and A. Sorensen, "Danish Experiments With the French Falling Weight Deflectometer," Proceedings, The University of Michigan Third International Conference on Structural Design of Asphalt Pavements, Volume I, pp 1119-11128, Sept. 1972.
4. The Asphalt Institute, Asphalt Overlays for Highway and Street Rehabilitation, MS-17, June 1983.
5. Lytton, R. L., W. M. Moore, and J. P. Mahoney, "Pavement Evaluation: Phase I, Pavement Evaluation Equipment," Report FHWA-RD-75-78, Federal Highway Administration, Washington, D. C., 1975.
6. Bush A. J. III, "Nondestructive Testing for Light Aircraft Pavement; Phase I, Evaluation on Nondestructive Testing Devices," U. S. Army Engineer Waterways Experiment Station, Vicksburg, January 1980.
7. Uddin, Waheed, Soheil Nazarian, W. Ronald Hudson, Alvin H. Meyer, and K. H. Stokoe II, "Investigations into Dynaflect Deflections in Relation to Location/Temperature Parameters and Insitu Material Characterization of Rigid Pavements," Research Report 256-5, Center for Transportation Research, The University of Texas at Austin, December 1983.
8. Cogill, W. H., "Analytical Methods Applied to the Measurements of Deflections and Wave Velocities on Highway Pavements: Part I, Measurements of Deflections," Research Report 32-14, Texas Transportation Institute, Texas A & M University, College Station, Texas, March 1969.

9. Tholen, Olle, "Falling Weight Deflectometer--A Device for Bearing Capacity Measurement: Properties and Performance," Bulletin 1980:1, Department of Highway Engineering, Royal Institute of Technology, Stockholm, Sweden.

10. Tholen, Olle, J. Sharma, and R. L. Terrel, "Comparison of the Falling Weight Deflectometer with Other Deflection Testing Devices," Presented at 1984 Annual Meeting of Transportation Research Board, Washington, D. C., January 19, 1984.

11. Daleiden, Jerome F., "A Telephone Survey on the Falling Weight Deflectometer," Highway Design Division, Pavement Design Section, State Department of Highways and Public Transportation, Austin, Texas, December 1983.

12. Eagleson, Bary, S. Heisey, W. R. Hudson, A. H. Meyer, and K. H. Stokoe II, "Comparison of the Falling Weight Deflectometer and the Dynaflect for Pavement Evaluation," Research Report 256-1, Center for Transportation Research, The University of Texas at Austin, December 1981.

13. Hoffman, M. S., and M. R. Thompson, "Mechanistic Interpretation of Nondestructive Pavement Testing Deflections," Report No. FHWA/IL/UI-190, University of Illinois, Urbana, Illinois, June 1981.

14. "Dynatest Model 8000 Falling Weight Deflectometer," personal communication with B. Harris and R. Stubstad of Dynatest Consulting, Ojai, California, Fall 1983.

15. "KUAB Falling Weight Deflectometer," personal communication with J. Sharma of Seattle Engineering International, Redmond, Washington, Fall 1983.

16. Michalak, C. H., D. Y. Lu, and G. W. Turman, "Determining Stiffness Coefficients and Elastic Moduli of Pavement Materials from Dynamic Deflections," Research Report 207-1, Texas Transportation Institute, Texas A & M University, College Station, Texas, November 1976.

17. Majidzadeh, Kamran, "Pavement Condition Evaluation Utilizing Dynamic Deflection Measurements," Research Report No. OHIO-DOT-13-77, Federal Highway Administration, Washington, D. C., June 1977.

18. "ELSYM5 3/72 - 3, Elastic Layered System with One to Ten Normal Identical Circular Uniform Loads," Unpublished computer application, by Gale Ahlborn, Institute of Transportation and Traffic Engineering, University of California at Berkeley, 1972.

19. Majidzadeh, K., and G. J. Ilves, "Flexible Pavement Overlay Design Procedures Volume I: Evaluation and Modification of the Design Methods," Report No. FHWA/RD-81/032, Resource International Inc., Ohio, August 1981.

20. "AASHTO Interim Guide for Design of Pavement Structures - 1972, Chapter III Revised, 1981," American Association of State Highway and Transportation Officials, 1981.

21. Kilareski, W. P., and B. A. Anani, "Evaluation of Insitu Moduli and Pavement Life from Deflection Basins," Proceedings, Fifth International Conference on Structural Design of Asphalt Pavements, Volume I, Delft, Holland, 1982, pp 349-366.

22. Vaswani, N. K., "Method for Separately Evaluating Structural Performance of Subgrades and Overlying Flexible Pavements," Highway Research Record 362, Highway Research Board, Washington, D. C., 1971, pp 48-62.

23. Taute, Arthur, B. Frank McCullough, and W. R. Hudson, "Improvements to the Material Characterization and Fatigue Life Prediction Methods of the Texas Rigid Pavement Overlay Design Procedure," Research Report 249-1, Center for Transportation Research, The University of Texas at Austin, March 1981.

24. Miura, Y. and T. Tobe, "Evaluation of Existing Pavement Based on Deflection and Radius of Curvature and Overlay Design," Proceedings, Fourth International Conference on Structural Design of Asphalt Pavements, The University of Michigan, Ann Arbor, 1977, Vol I, pp 862-875.

25. Visser, W., "Pavement Evaluation with the Falling Weight Deflectometer," Special Report 175, Highway Research Board, Washington, D. C., 1978, pp 122-150.

26. Claessen, A. J. M., C. P. Valkering and R. Ditmarsch, Pavement Evaluation with the Falling Weight Deflectometer," Proceedings, Association of Asphalt Paving Technologist, 1976, Vol 45.

27. Wiseman, G., J. Uzan, M. S. Hoffman, I. Isahi, and M. Livneh, "Simple Elastic Models for Pavement Evaluation Using Measured Surface Deflection Bowls," Proceedings, Fourth International Conference on Structural Design of Asphalt Pavements, Vol II, Ann Arbor, Michigan, pp 416-426.

28. Stock, A. F., and J. Yu, "The Use of Surface Deflection for Pavement Design and Evaluation," Paper for Presentation at 63rd Annual Meeting of Transportation Research Board, Washington, D. C., January 1984.

29. Ashton, J. E. and F. Moavenzadeh, "The Analysis of Stresses and Displacements in a Three-Layered Viscoelastic System," Proceedings, International Conference, Structural Design of Asphalt Pavements, 1967.

30. Westergaard, H. M., "Stresses in Concrete Pavements Computed by Theoretical Analysis," Public Roads, Vol. 7, No. 2, April 1962, pp. 25-35.

31. Hudson, W. R., and H. Matlock, "Cracked Slabs with Non-Uniform Support," Journal of the Highway Division, Vol. 93, No. HW1, Proceedings, American Society of Civil Engineers, April 1967.

32. Burmister, D. M., "The Theory of Stresses and Displacements in Layered Systems and Application to the Design of Airport Runways," Proceedings, Highway Research Board, 1943.

33. Foster, C. R., and R. G. Ahlvin, "Stresses and Deflections Induced by a Uniform Circular Load," Proceedings, Highway Research Board, 1954.

34. Ahlvin, R. G., and H. H. Ulery, "Tabulated Values for Determining the Complete Pattern of Stresses, Strains and Deflections Beneath a Uniform Circular Load on a Homogeneous Half Space," HRB Bulletin 342, Highway Research Board, 1962.

35. "BISAR User's Manual," Shell Research, Koninklijke/Shell Laboratorium, Amsterdam, July 1972.

36. Haas, Ralph, and W. Ronald Hudson, Pavement Management Systems, McGraw-Hill, Inc., 1980.

37. McCullough, B. F., "A Pavement Overlay Design System Considering Wheel-Loads, Temperature Changes, and Performance," Institute of Transportation and Traffic Engineering Graduate Report, University of California, Berkeley, July 1969.

38. Seeds, S. B., B. F. McCullough and W. R. Hudson, "A Design System for Rigid Pavement Rehabilitation," Research Report 249-2, Center for Transportation Research, The University of Texas at Austin, Austin, Texas, January 1982.

39. Timoshenko, S., D. H. Young, and W. Weaver, Jr., Vibration Problems in Engineering, John Wiley and Sons, 1974.

40. Weiss, R. A., "Pavement Evaluation and Overlay Design Using Vibratory Nondestructive Testing and Layered Elastic Theory, Volume I: Development of Procedures," Report No. FAA-RD-77-186-I, U. S. Army Engineer Waterways Experiment Station, Vicksburg, March 1980.

41. Yang, Nai C., "Nondestructive Evaluation of Civil Airport Pavements," Report No. FAA-RD-76-83, September 1976.

42. Green, J. L., and Jim W. Hall, "Nondestructive Vibratory Testing of Airport Pavements, Volume I Experimental Test Results and Development of Evaluation Methodology and Procedure," Waterways Experiment Station, Vicksburg, September 1975.

43. Ali, Galal A., W. H. Goetz, and M. E. Harr, "Laboratory Investigation of Flexible-Pavement Response by Using Transfer Functions," TRR 755, Transportation Research Board, Washington, D. C., 1980, pp 36-42.

44. Scrivner, F. H., C. H. Michalak, and W. M. Moore, "Calculation of the Elastic Moduli of a Two Layer Pavement System from Measured Surface Deflections," Research Report 123-6, Center for Highway Research and Texas Transportation Institute, March 1971.

45. Swift, G. "A Graphical Technique for Determining the Elastic Moduli of a Two Layered Structure from Measured Surface Deflections," Research Report 136-3, Texas Transportation Institute, Texas A & M University, College Station, Texas, 1972.

46. Cogill, W. H., "Analytical Methods Applied to the Measurements of Deflections and Wave Velocities on Highway Pavements: Part I, Measurements of Deflections," Research Report 32-14, Texas Transportation Institute, Texas A & M University, College Station, Texas, March 1969.

47. Koole, R. C., "Overlay Design Based on Falling Weight Deflections Measurements," Research Record 700, Transportation Research Board, Washington, D. C., 1979.

48. Irwin, L. H., "Determination of Pavement Layer Moduli from Surface Deflection Data for Pavement Performance Evaluation," Proceedings, Fourth International Conference on Structural Design of Asphalt Pavements, Vol. I, Ann Arbor, Michigan, 1977, pp 831-840.

49. Anani, B. A., and M. C. Wang, "An Evaluation of Insitu Elastic Moduli from Surface Deflection Basins of Multilayer Flexible Pavements," Research Report No. FHWA/PA-80/009, The Pennsylvania Transportation Institute, The Pennsylvania State University, University Park, Pennsylvania, November 1979.

50. Sharma, J., and R. N. Stubstad, "Evaluation of Pavement in Florida by Using the Falling Weight Deflectometer," TRR 755, Transportation Research Board, Washington, D. C., 1980, pp 42-48.

51. Bush, A. J. III, "Nondestructive Testing for Light Aircraft Pavements, Phase II, Development of Nondestructive Evaluation Methodology," Report No. FAA-RD-80-9-II, U. S. Army Engineer, Waterways Experiment Station, Vicksburg, November 1980.

52. Majidzadeh, K., and George Ilves, "Flexible Pavement Overlay Design Procedures, Vol. 2, User Manual," Report No. FHWA/RD-81/033, Resource International Inc., Ohio, August 1981.

53. Majidzaden, K., and George Ilves, "Evaluation of Rigid Pavement Overlay Design Procedures (Development of OAR Procedure)," Report No.

FHWA/RD-83/090, Final Report, Resource International, Inc., Ohio, December 1983.

54. Hou, T. Y., "A Two-Stage Pavement Design Model," Proceedings, Third Conference of Road Engineering Association of Asia and Australia, Vol. I, Taipei, Taiwan,, April 1981, pp 663-676.

55. Tenison, J. H. Jr., "Proposed New Mexico State Highway Department Elastic-Layer Overlay Evaluation and Design Procedures for Asphalt Concrete Pavements," Proceedings, 12th Paving and Transportation Conference, The University of New Mexico, Albuquerque, New Mexico, January 1983, pp 123-146.

56. Ewing, W. M., W. S. Jardetzky, and F. Press, Elastic Waves in Layered Media, McGraw-Hill Book Co., Inc., 1957.

57. Richart, R. F., Jr., J. R. Hall, Jr., and R. D. Woods, Vibration of Soil and Foundations, Prentice-Hall, Englewood Cliffs, New Jersey, 1970.

58. Nazarian, Soheil and K. H. Stokoe II, "Evaluation of Moduli and Thickness of Pavement Systems by Spectral Analysis of Surface Waves Method," Research Report 256-4, Center for Transportation Research, The University of Texas at Austin, December 1983.

59. Henkelom, W. and C. R. Foster, "Dynamic Testing of Pavements," Journal of Soil Mechanics and Foundation Division, Vol. 86, No. SMI, Proceedings, American Society of Civil Engineers, February 1960, pp 2368-2372.

60. Personal Communications with Drs. Jose M. Roesset and K. H. Stokoe II, Professors of Civil Engineering, and K. Shao, Graduate Research Assistant at the University of Texas at Austin, June 1984.

61. Heisey, S., K. H. Stokoe II, W. R. Hudson, and A. H. Meyer, "Determination of Insitu Shear Wave Velocities from Spectral Analysis of Surface Waves," Research Report 256-2, Center for Transportation Research, The University of Texas at Austin, November 1982.

62. Uddin, W., V. Torres-Verdin, W. Ronald Hudson, A. H. Meyer, B. Frank McCullough, and R. B. Rogers, "Dynaflect Testing for Rigid Pavement Evaluation, Vol. 1: Background," Research Report 256-6F, Center

for Transportation Research, The University of Texas at Austin, October 1983.

63. Heukelom, W. and A. J. G. Klomp, "Dynamic Testing as a Means of Controlling Pavements During and After Construction," 1st International Conference on Structural Design of Asphalt Pavements, Ann Arbor, Michigan, 1962, pp 667-679.

64. Connor, W. S., and Marvin Zelen, Fractional Factorial Experiment Designs for Factors at Three Levels, National Bureau of Standards Applied Mathematics Series 54, May 1959.

65. SPSS Update 7-9, Editors: C. H. Hull and N. H. Nie, McGraw-Hill Book Co., 1981.

66. Nazarian, S., Waheed Uddin, K. H. Stokoe II and A. H. Meyer, "Moduli and Thickness of Pavement Systems from Spectral Analysis of Surface Waves", a paper offered for presentation at 10th World Meeting of International Road Federation, Rio de Janeiro, October 1984.

67. Southgate, H. F. and R. C. Deen, "Temperature Distribution Within Asphalt Pavements," TRR 549, Transportation Research Board, Washington, D. C., 1975.

68. Shahin, M. Y. and B. Frank McCullough, "Prediction of Low Temperature and Thermal Fatigue Cracking in Flexible Pavements," Research Report 123-14, Center for Highway Research, The University of Texas at Austin, Austin, Texas, August 1972.

69. Austin Research Engineers, Inc., "Asphalt Concrete Overlays of Flexible Pavements, Volume 2 - Design Procedures," Report FHWA-RD-75-76, August, 1975.

70. Monismith, C. L., R. G. Hicks, and Y. M. Salam, "Basic Properties of Pavement Components," Report No. FHWA-RD-72-19, University of California, Berkeley, California, September 1971.

71. Seed, H. B., F. G. Mitry, C. L. Monismith, and C. K. Chan, "Prediction of Flexible Pavement Deflections from Laboratory Repeated-Load Tests," NCHRP Report No. 35, Highway Research Board, Washington, D. C., 1967.

72. Hicks, R. G., "Factors Influencing the Resilient Properties of Granular Materials," Ph. D. Dissertation, Institute of Transportation and

Traffic Engineering, University of California, Berkeley, California, May 1970.

73. Hicks, R. G., and C. L. Monismith, "Factors Influencing the Resilient Response of Granular Materials," HRR 345, Highway Research Board, Washington, D. C., 1971, pp 15-31.

74. Barksdale, R. D., and R. G. Hicks, "Material Characterization and Layered Theory for Use in Fatigue Analysis," Highway Research Board, Special Report No. 140, Washington, D. C., 1973.

75. Smith, W. S., and K. Nair, "Development of Procedures for Characterization of Untreated Granular Base Course and Asphalt Treated Base Course Materials," Report No. FHWA-RD-7461, Materials Research and Development, Oakland, California, October 1973.

76. Rada, Gonzalo, and M. W. Witczak, "Comprehensive Evaluation of Laboratory Resilient Moduli Results for Granular Material," TRR 810, Transportation Research Board, Washington, D. C., 1981, pp 23-33.

77. Stock, A. F., and S. F. Brown, "Nonlinear Characterization of Granular Materials for Asphalt Pavement Design," TRR 755, Transportation Research Board, Washington, D. C., 1980, pp 14-20.

78. D'Amato, Paul A., and M. W. Witczak, "Analysis of Insitu Granular-Layer Modulus from Dynamic Road-Rater Deflections," TRR 755, Transportation Research Board, Washington, D. C., 1980, pp 20-30.

79. Moossazadeh, J., and M. W. Witczak, "Prediction of Subgrade Moduli for Soil That Exhibits Nonlinear Behavior," TRR 810, Transportation Research Board, Washington, D. C., 1981, pp 9-17.

80. Maree, J. H., N. J. W. Van Zyl, and C. R. Freeme, "Effective Moduli and Stress Dependent of Pavement Materials as Measured in Some Heavy-Vehicle Simulator Tests," TRR 852, Transportation Research Board, Washington, D. C., 1982, pp 52-60.

81. May, R. W., and M. W. Witczak, "Effective Granular Modulus to Model Pavement Responses," TRR 810, Transportation Research Board, Washington, D. C., 1981, pp 1-9.

82. Seed, H. B., and I. M. Idriss, "Soil Moduli and Damping Factors for Dynamic Response Analysis," Report No. EERC 70-10, Earthquake Engineering Research Center, University of California, Berkeley, California, December 1970.

83. Hardin, B. O., and V. P. Drnevich, "Shear Modulus and Damping in Soils: Measurement and Parameter Effects," Journal of Soil Mechanics and Foundations Division, Vol. 98, No. SM6, Proceedings, American Society of Civil Engineers, June 1972, pp 603-624.

84. Hardin, B. O., and V. P. Drnevich, "Shear Modulus and Damping in Soils: Design Equations and Curves," Journal of Soil Mechanics and Foundations Division, Vol. 98, No. SM7, Proceedings, American Society of Civil Engineers, July 1972, pp 667-692.

85. Stokoe, K. H. II, and R. D. Woods, "Insitu Shear Wave Velocity by Cross-Hole Method," Journal of Soil Mechanics and Foundations Division, Vol. 98, No. SM5, Proceedings, American Society of Civil Engineers, May 1972, pp 443-460.

86. Stokoe, K. H. II, and E. Turner, "Resonant Column Tests for the University Houston Pile Test Facility," Geotechnical Engineering Report GR 81-15, University of Texas at Austin, 1981.

87. Stokoe, K. H. II, and P. F. Lodde, "Dynamic Response of San Francisco Bay Mud," Proceedings, Earthquake Engineering and Soil Dynamics Conference, ASCE, 1978, Vol. II, pp 940-959.

88. Turner, E., and K. H. Stokoe II, "Static and Dynamic Properties of Clayey Soils Subjected to 1979 Imperial Valley Earthquake," Geotechnical Engineering Report GR 82-26, University of Texas at Austin, 1982.

89. Nazarian, S., K. H. Stokoe II, and W. Ronald Hudson, "Use of Spectral Analysis of Surface Waves Method for Determination of Moduli and Thickness of Pavement Systems," TRR 930, Transportation Research Board, Washington, D. C., 1983, pp 38-45.

90. Nazarian, S., and K. H. Stokoe II, "Nondestructive Testing of Pavements Using Surface Waves," paper presented at the 63rd Annual Meeting of Transportation Research Board, Washington, D. C., January 1984.

91. Baird, G. T., and Phillip Nash, "Soil Pressures Due to Aircraft Loads," Journal of Transportation Engineering Division, Vol. 108, No. TE6, American Proceedings, Society of Civil Engineers, November 1982, pp 618-631.

92. Treybig, Harvey J., B. F. McCullough, Phil Smith, and Harold von Quintus, "Overlay Design and Reflection Cracking Analysis for Rigid Pavements, Volume 1 - Development of New Design Criteria," Research Report FHWA-RD-77-66, Federal Highway Administration, Washington, D. C., August 1977.

93. "The AASHO Road Test, Report 5, Pavement Research," Special Report 61E, Highway Research Board, 1962.

94. Gutierrez de Velasco, Manuel, and B. F. McCullough, "Summary Report for 1978 CRCP Condition Survey in Texas," Research Report 177-20, Center for Transportation Research, The University of Texas at Austin, January 1981.

95. McCullough, B. F., Victor Torres-Verdin, "Summary and Recommendations of a Rigid Pavement Overlay and Design System," Preliminary Review Copy, Research Report 249-8F, Center for Transportation Research, The University of Texas at Austin, November 1983.

96. Texas Department of Public Safety, "Texas Regulations Governing the Size and Weight of Commercial Vehicles," 1979.

97. Box, G. E. P., W. G. Hunter, and J. S. Hunter, Statistics for Experimenters: An Introduction to Design, Data Analysis, and Model Building, John Wiley and Sons, New York, 1978.

98. Uddin, Waheed, A Structural Evaluation Methodology for Pavements Based on Dynamic Deflections, Ph.D. Dissertation, The University of Texas at Austin, December 1984.

APPENDIX A

A SIMPLIFIED DYNAMIC MODEL OF FWD

APPENDIX A. A SIMPLIFIED DYNAMIC MODEL OF FWD

This appendix presents a very simplified approach for dynamic analysis of FWD tests using the concepts based on the theory of wave propagation in a semi-infinite elastic medium.

BASIC CONSIDERATIONS

Idealized Presentation of FWD Tests

The basic principle of FWD testing is described in Chapter 2, and the generation of the FWD impulse is illustrated in Fig 2.3. Examples of measured deflection-time histories and stress-time histories are presented in Fig 2.4(a) and (b) using the published data (Ref 3). In this analysis, the FWD loading plate is assumed to be resting on the surface of a semi-infinite elastic subgrade. The material under the loading plate is assumed to be a hypothetical column, as illustrated in Fig A.1. The same figure also shows the idealized stress-time history of the impulse generated by the FWD. In this study a parabolic shape has been assumed. A triangular wave pattern could also have been used as idealized representation of the FWD force signal. A peak stress, P_m, of 100 psi is assumed to be applied on the surface. The duration of the stress is assumed to be 0.033 second (based on Ref 3). In addition, the following assumptions are made:

(1) Homogeneous, isotropic elastic half space.
(2) No consideration is given to rebound after the transient signal dies out.
(3) The duration of the FWD stress signal remains constant with depth.
(4) The half space responds as a linearly elastic material.
(5) Shearing stresses on the sides of the vertical soil column can be neglected.

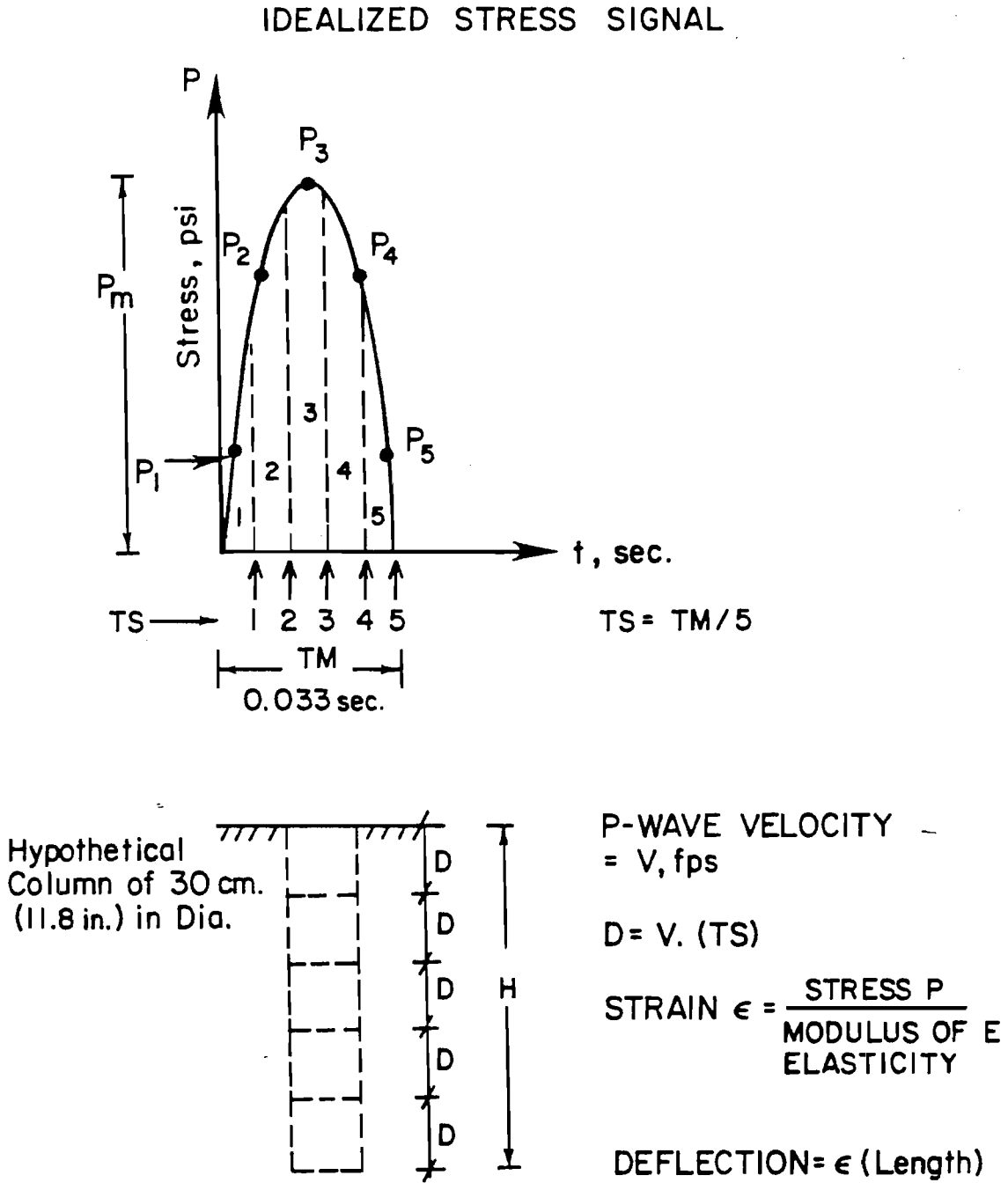

Fig A.1. Stress wave propagation through a homogeneous elastic medium.

(6) In the case assuming no attenuation of stresses, stress levels at each time increment remain constant with depth.

DEVELOPMENT OF THE DYNAMIC MODEL

The propagation of elastic waves in an elastic half space is briefly discussed in Chapter 3. The generation and propagation of compression waves (P-waves) through this column of soil is the basis of the simplified dynamic model described in this section. The basic principle is to divide the idealized stress-time history signal into time increments (Fig A.1) and to study the propagation of the stress wave with time during the duration of the signal as well as after the signal dies out. Basic relationships used in the analysis are also presented in Fig A.1.

No Stress Attenuation

In the first phase of developing the model, stress attenuation with depth was neglected. In Fig A.1, the stress, P_3, at time interval 3 equals the peak vertical stress, P_M. Figure A.2 illustrates the propagation of waves in the hypothetical column during the duration of the force (stress) signal, i.e., 0.033 second. Equal time steps are used. At the end of time step 5, the wave has travelled a distance of H in the half space. The calculation of surface deflections is also shown in Fig A.2. At 0.033 second the stress of the surface will be zero and the wave will have propagated to a depth, H, as illustrated in Fig A.3. An idealized peak stress versus depth relationship at 0.033 second is shown in Fig A.4.

Consideration of Stress Attenuation

Fig A.5(a) illustrates the situation in which stress attenuation is neglected. However, it is important to consider stress attenuation. The approach adopted in this study is to use a hypothetical cone as illustrated in Fig A.5(b). Angle θ can be altered to change the rate of attenuation. For θ equal to 15 degrees, examples of attenuated stress signals at

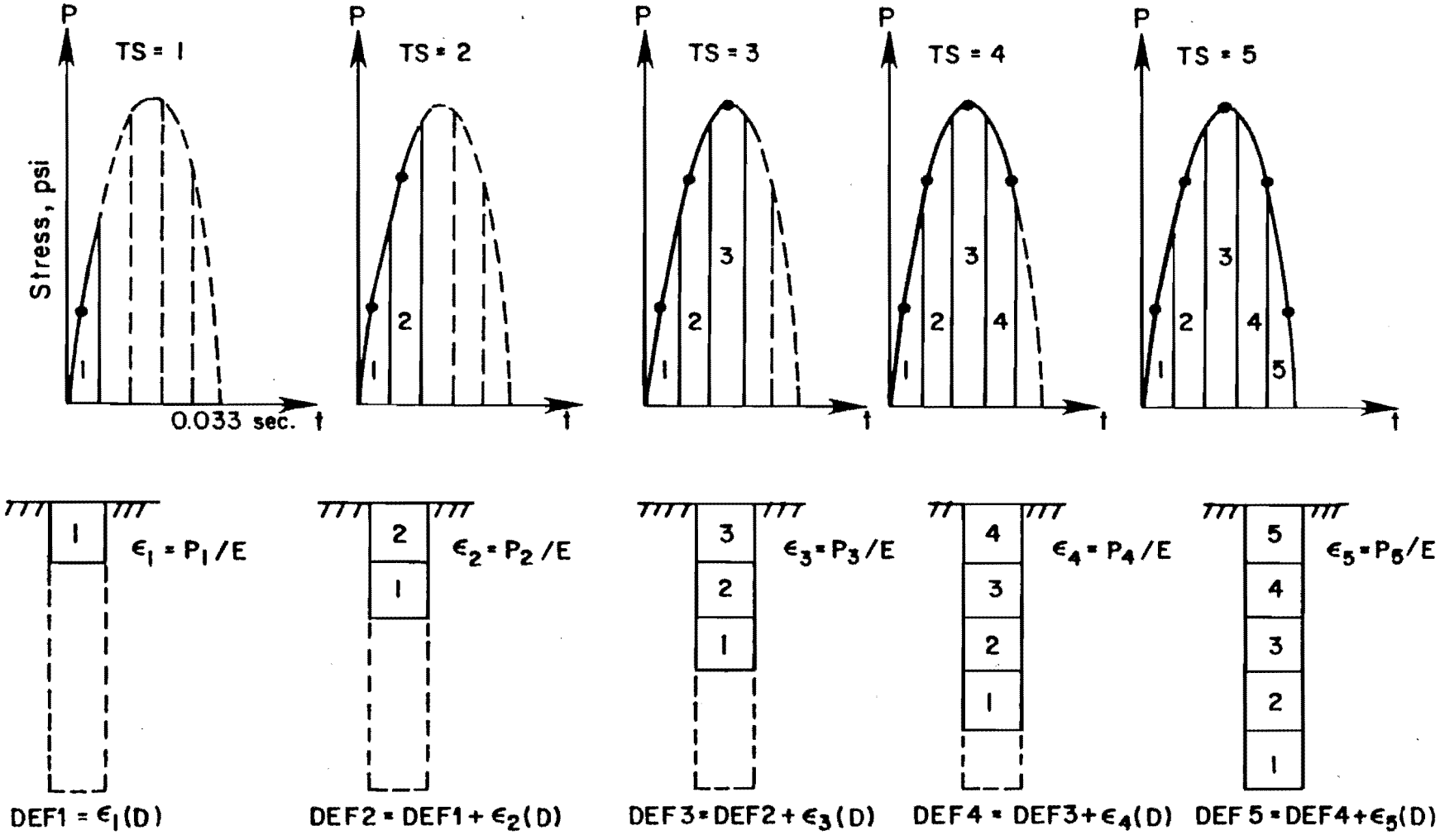

Fig A.2. Stress wave propagation through a hypothetical column under FWD plate.

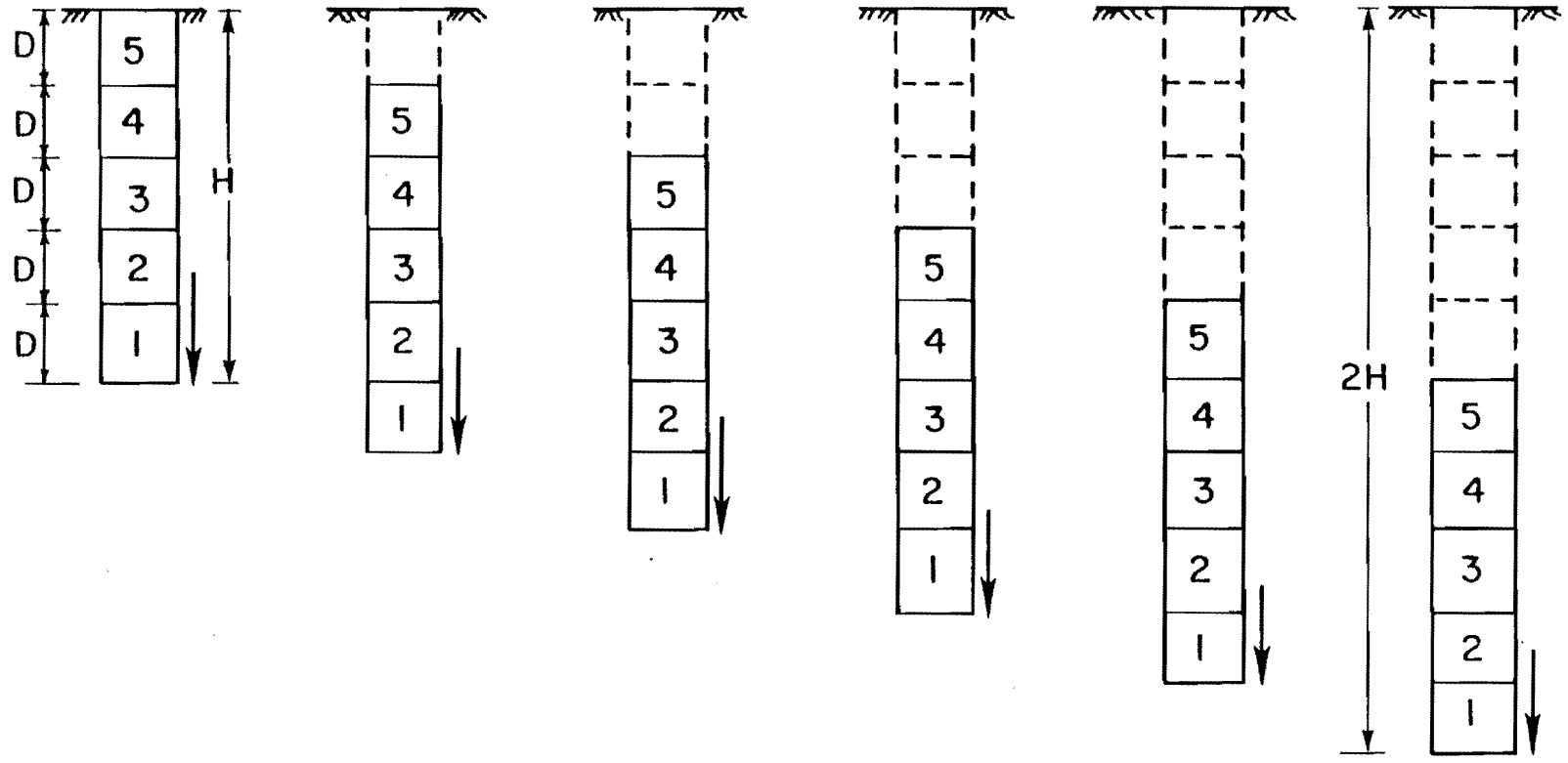

Fig A.3. Stress wave propagation at time intervals after the FWD impulse duration.

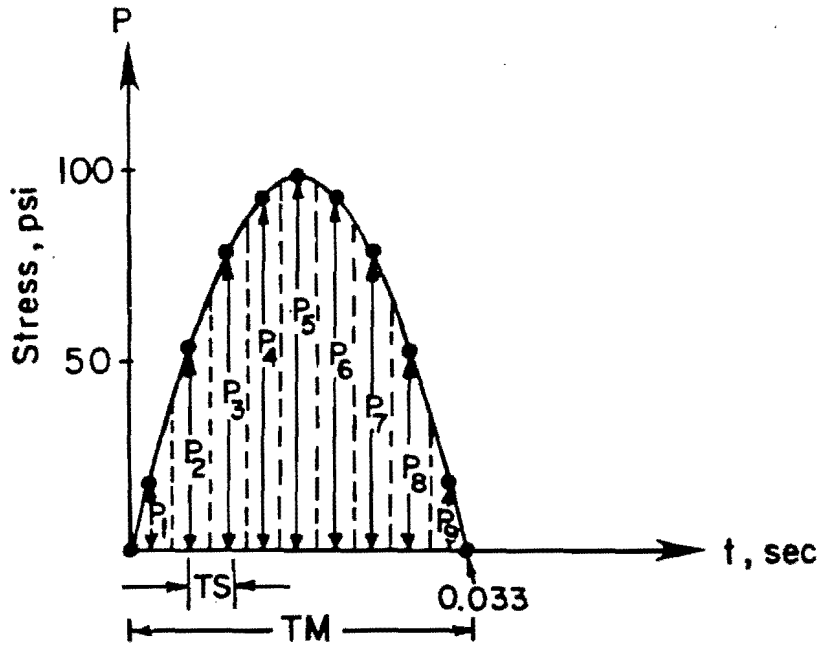

(a) Idealized FWD stress signal on surface.

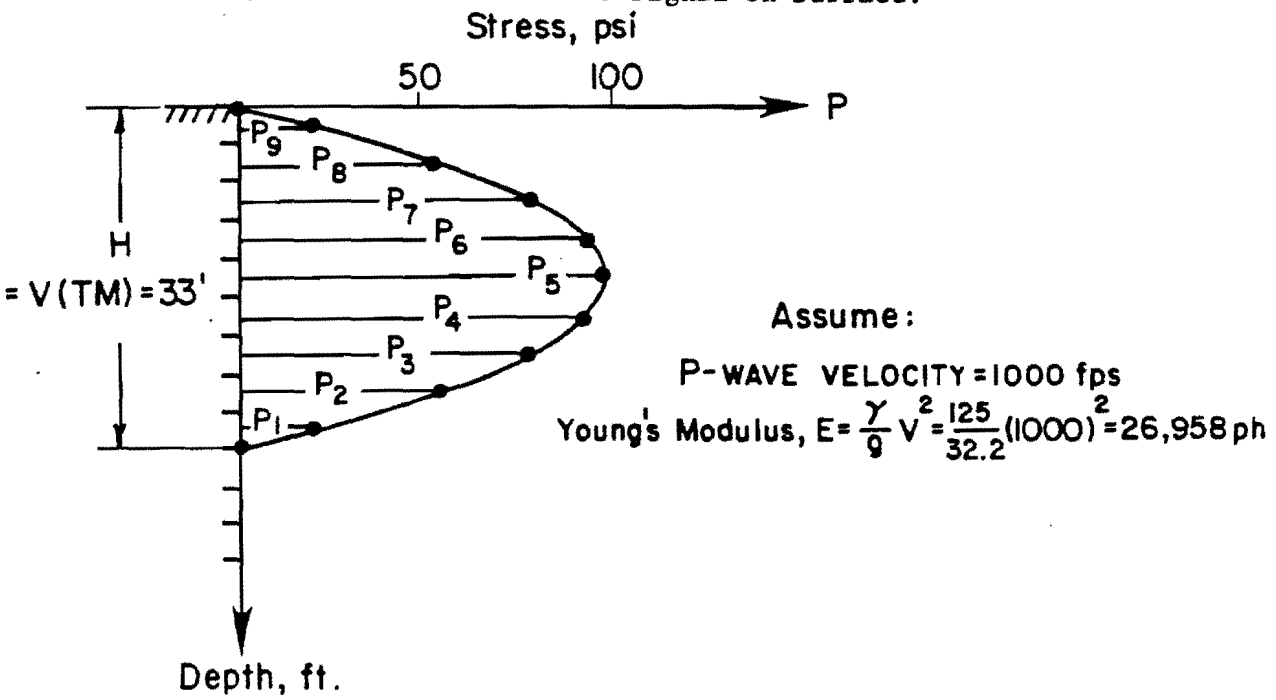

(b) Stress distribution at 0.033 sec. (no attenuation).

Fig A.4. Propagation of stress wave with no attenuation.

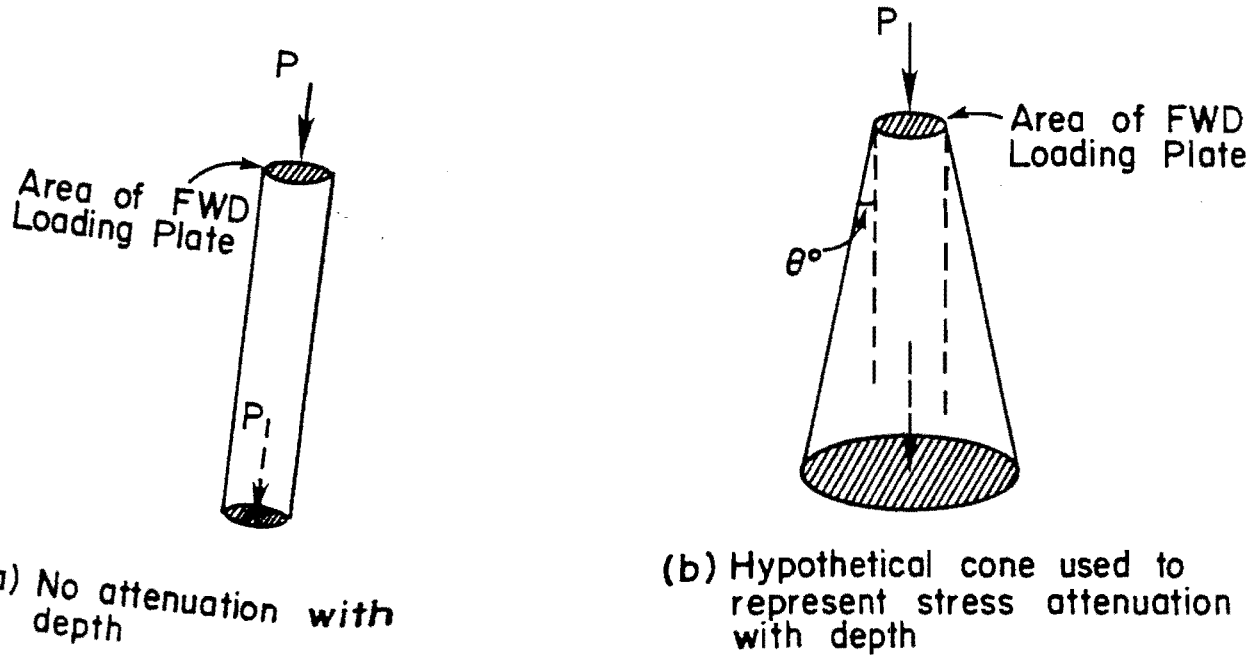

Fig A.5. Attenuation of stress wave with depth.

different depths are presented in Fig A.6. The resulting deflection-time history at the surface is shown in Fig A.7. Note that the peak deflection does not occur at the same time as the peak stress; rather the peak deflection lags behind the peak stress (or peak force). This finding is very interesting, because in the current FWD models only peak force at the surface and "peak" deflections are recorded. And the criterion on which "peak" values are sampled becomes very important. Figure A.8 illustrates variations in peak stress distribution at different time intervals.

Figure A.9 illustrates a comparison of stress attenuation at of 11.6 degrees to geometrical and material damping. There is a loss of energy by radiation of elastic waves from the loading plate. This loss of energy through propagation of elastic waves is dependent on geometric damping. Amplitudes of body waves decrease in proportion to the ratio 1/r, as expressed in the following (Ref 57):

$$w = w_1 \sqrt{\frac{r_1}{r}} \qquad (A.1)$$

where

r_1 = distance from source to point of known amplitude,
r = distance from source to point in question,
w_1 = amplitude at distance r_1 from source, and
w = amplitude at distance r from source.

Because soil is not perfectly elastic, there is also internal damping within the mass. It has been found by field measurement that attenuation is greater than would be predicted by geometrical damping alone (Ref 357). Both geometrical and material damping can be expressed by the following expression:

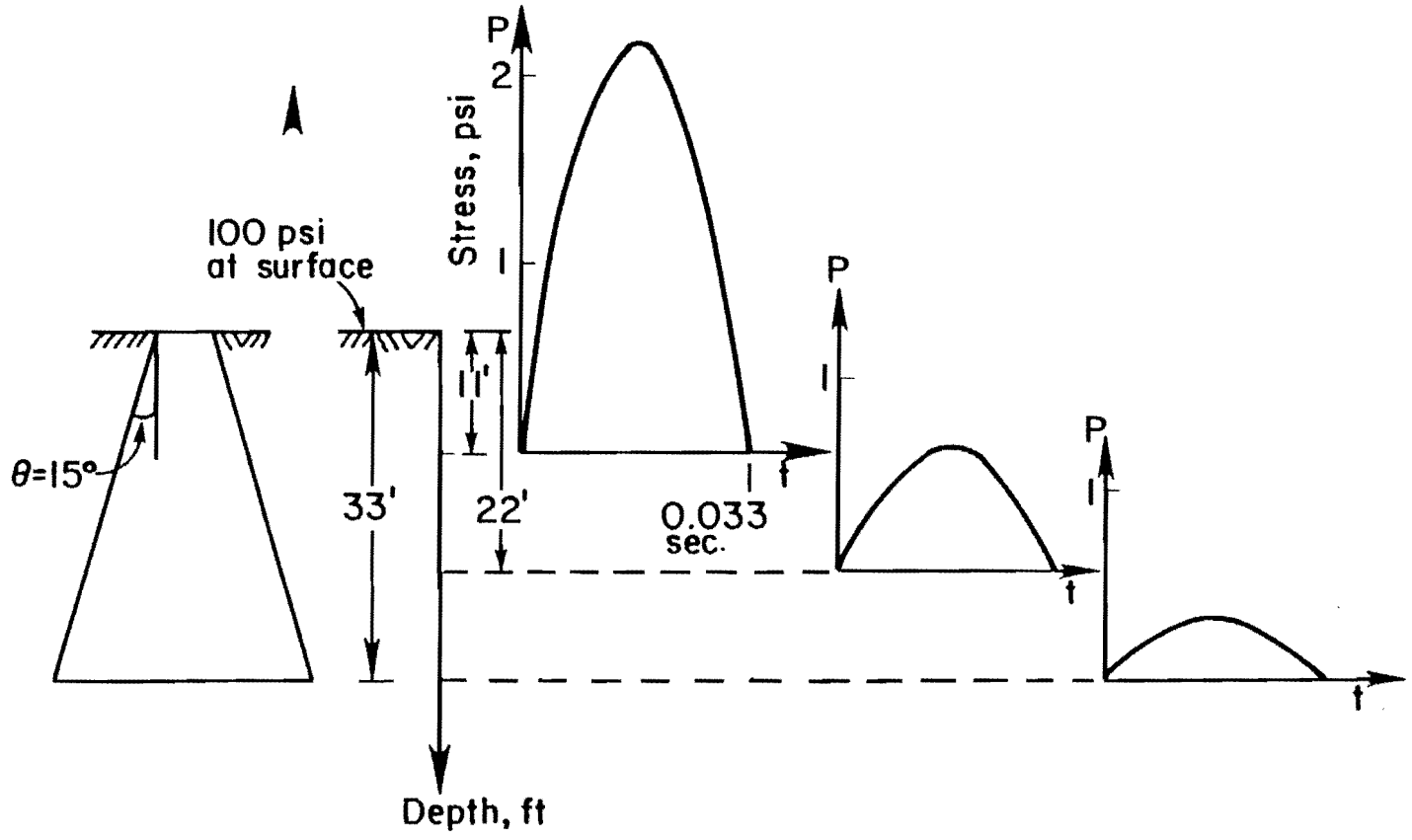

Fig A.6. FWD stress - time histories at different depths.

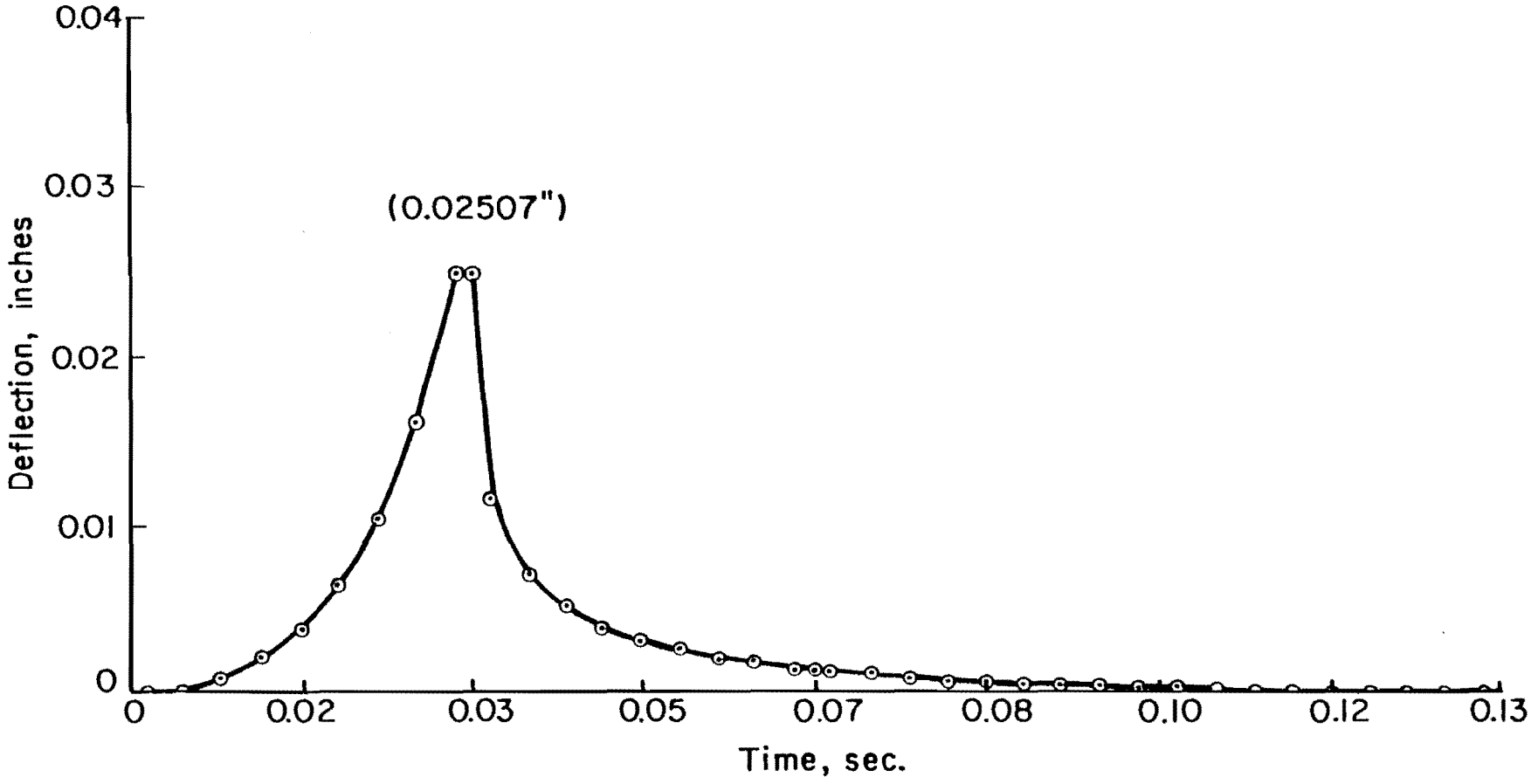

Fig A.7. Deflection-time history at surface.

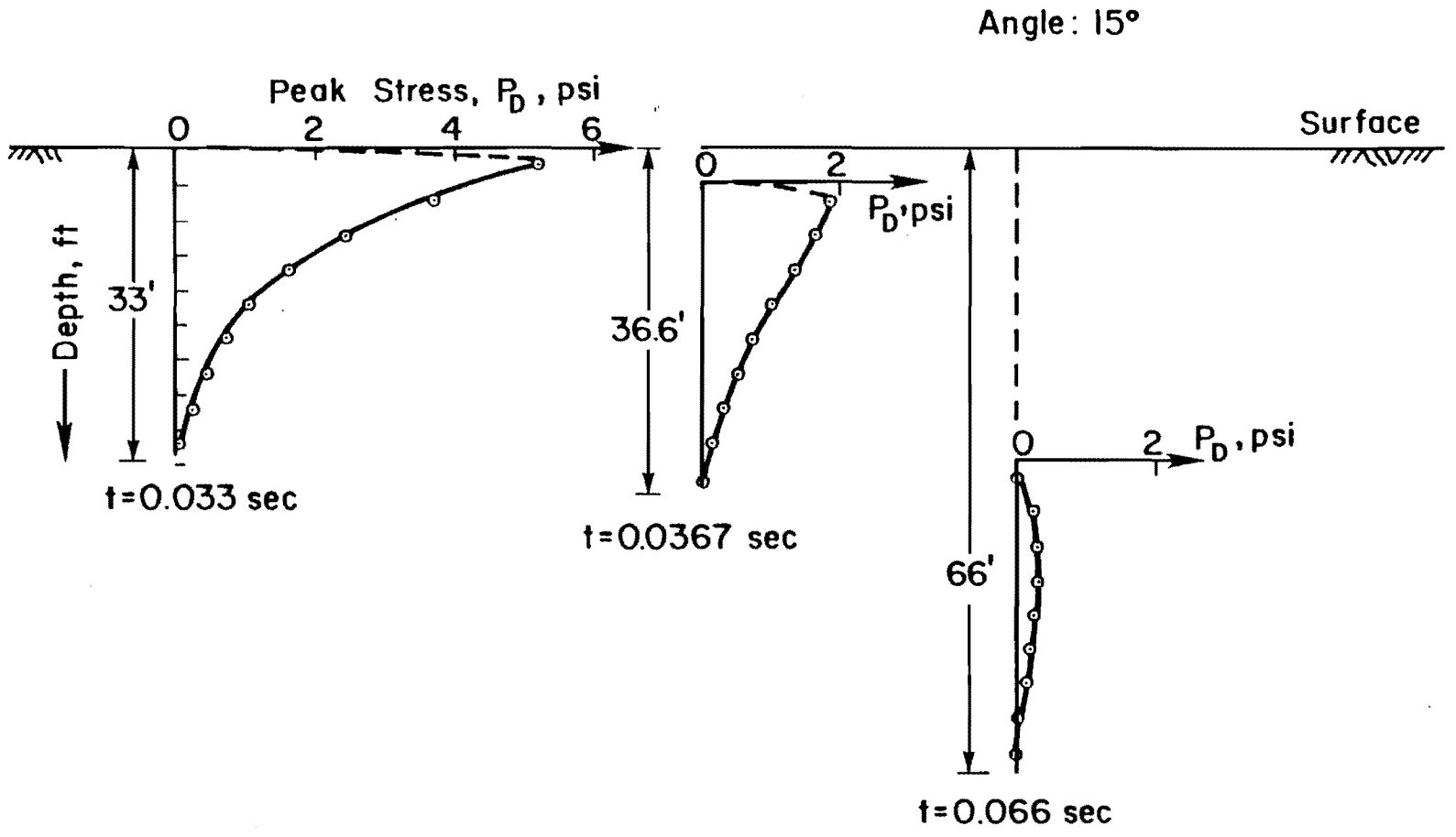

Fig A.8. Peak stress distribution at different time intervals.

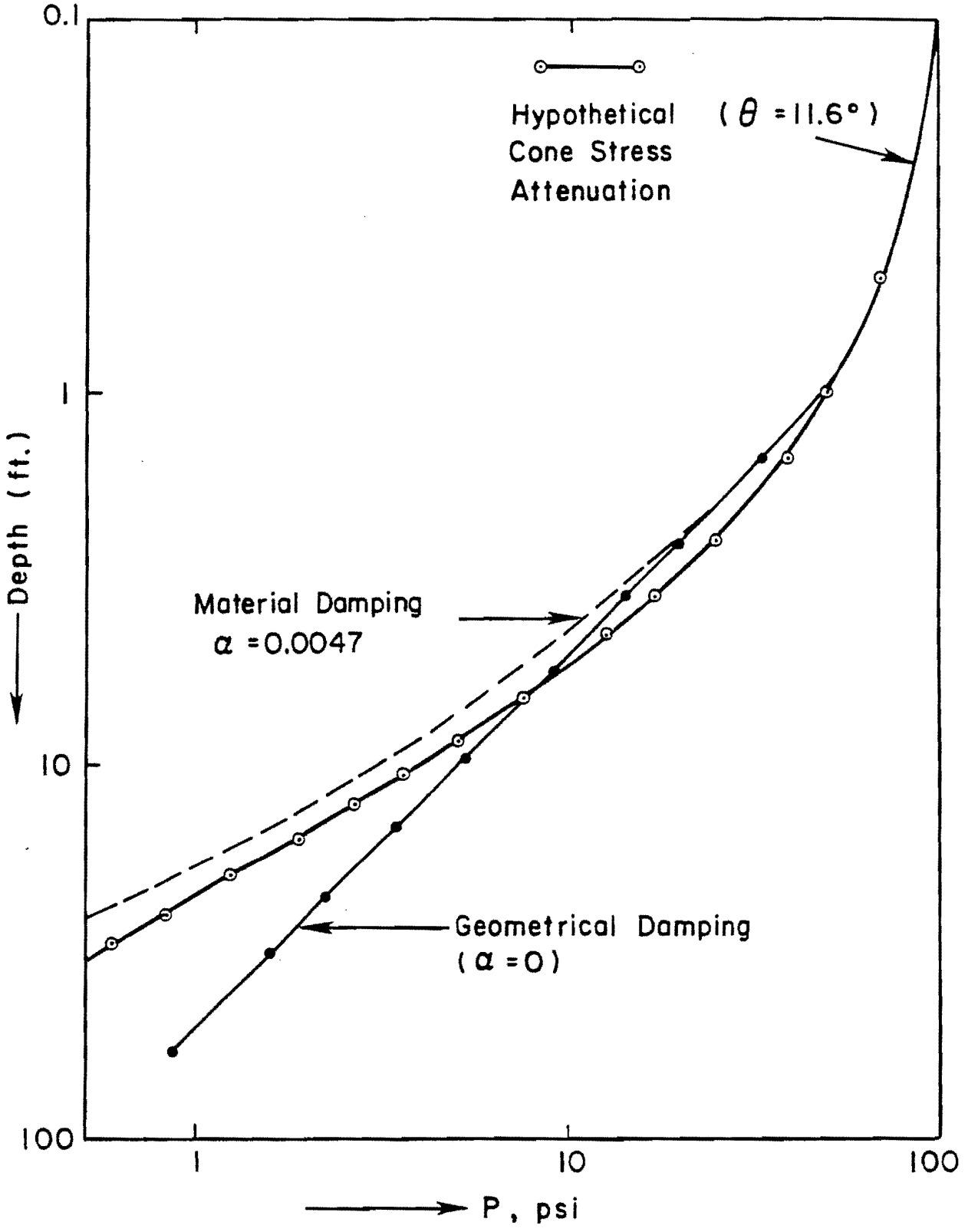

Fig A.9. Comparison of procedures for stress attenuation.

$$w = w_1\sqrt{\frac{r_1}{r}} \exp\left(-\alpha\,(r - r_1)\right) \qquad (A.2)$$

where

α = coefficient of attenuation (1/ft).

Peak stress distributions using equations A.1 and A.2 are shown in Fig A.9. Different values of α were used in this study. It appears that an α value of 0.0047 produces a curve of stress distribution which is similar to the stresses computed by assuming a value of 11.6 degrees for θ .

SUMMARY

The study described above is by no means the only approach to the dynamic analysis of the FWD. However, it demonstrates that concepts from elastic wave propagation theory can be effectively used to predict the response under an FWD impulse. The analysis described above can be easily extended to layered elastic media.

APPENDIX B

DEVELOPMENT OF PREDICTIVE EQUATIONS FOR DEFAULT SEED MODULI

APPENDIX B. DEVELOPMENT OF PREDICTIVE EQUATIONS FOR DEFAULT SEED MODULI

This appendix presents methodology used in developing predictive equations for use in the default procedure for generating seed moduli. All predictive equations developed for programs RPEDD1 and FPEDD1 are also included here.

FRACTIONAL FACTORIAL DESIGN

As explained in Chapter 4, it is known from Burmister's layered theory that thicknesses of pavement layers and Young's moduli are the most important variables to influence surface deflections at known radial distances from the center of load (assuming that load and Poisson's ratios are held at fixed values). Burmister's layered theory presents a mechanistic model for structural response analysis of pavements. Another class of mathematical models is the empirical model, which can be very useful and economical if it is desired to approximate the response only over certain ranges of these variables. One methodology commonly used for this purpose involves the development of a regression equation empirically from experimental data (or, in this case, data generated from layered theory computations).

Factorial designs facilitate generation of useful data for later development of an appropriate model. Such a factorial design is illustrated in Fig B.1. The seven factors selected for this factorial are the thicknesses of pavement layers (excluding the bottom layer, which is kept fixed as a semi-infinite layer) and Young's moduli of each layer. All other factors are kept at fixed levels. The seven factors are assigned three levels. The resulting arrangement is a 3^7 factorial design, which requires 2187 computational runs. For this study, it turned out that six such factorial designs will be required, resulting eventually in a very large number of computational runs. A full factorial arrangement is therefore prohibitively expensive and it is worthwhile to consider a fractional

FACTORS		LEVELS	TOTAL BASINS
E_j	i = 1,2,3,4	3 (Low, Medium, High	$3^7 = 2187$
T_j	j = 1,2,3	3 (Low, Medium, High	

$\frac{1}{9}\ \pi$ Fraction = 243 Deflection Basins

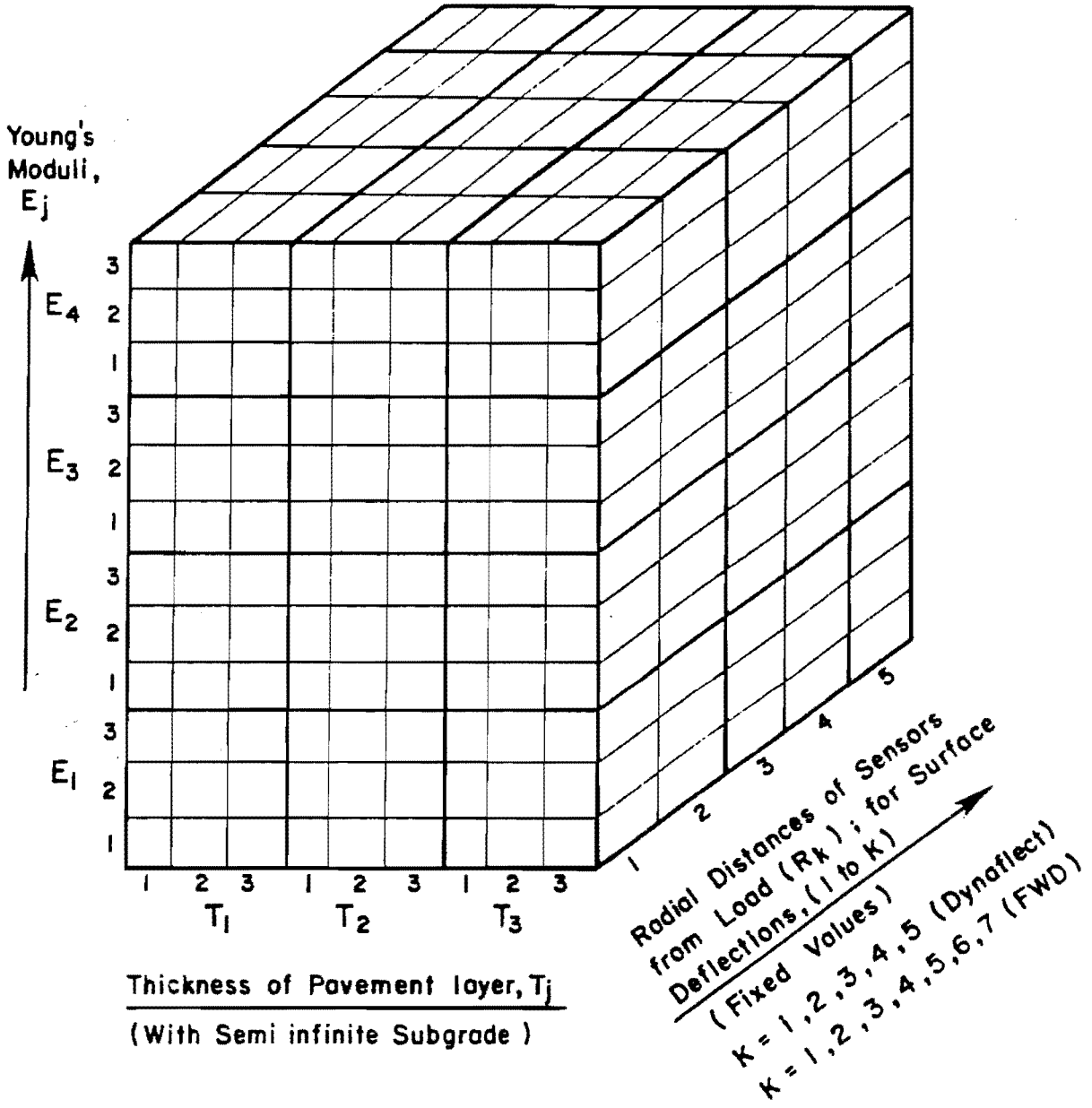

Fig B.1. Graphical illustration of factorial arrangement.

factorial design. It turns out that the desired information can still be obtained by performing only a fraction of the full factorial if the number of factors is not small (Ref 98). A one-ninths replicate fraction of a 3^7 factorial was selected in this study (in other words, 243 runs).

In order to generate deflection basins, pavement responses were calculated at five (Dynaflect) or seven (FWD) locations, as illustrated in Fig B.2. The values of thicknesses and moduli at low, medium, and high levels were selected on the basis of engineering judgement and experience. Selected values for rigid pavements are presented in Table 4.8. For flexible pavements, pavements with stabilized bases were treated separately from those with granular bases. Tables B.1(a) and (b) present selected values of these factors for the FWD and the Dynaflect. The fractional factorial arrangement recommended in Ref 64 has been adopted in this study. The combinations of levels of the seven factors are presented in Table B.2. In this table, zero refers to low level, 1 is for medium, and 2 refers to high level. A computer program DBFIT1 was used to facilitate computations, as described in Ref 98. In the input files for this program, 1, 2, and 3 have been used to indicate low, medium, and high levels (as shown in Table B.1 for the 243 runs).

DEVELOPING PREDICTIVE EQUATIONS

The data of deflection basins generated by each fractional factorial (FWD or Dynaflect) were used to build empirical equations. Multiple regression analyses were performed for this purpose. A detailed discussion of this technique and the statistical package used for this purpose has been presented elsewhere (Ref 7).

Predictive Equations for Deflection Basins

The first step in developing regression equations was to use deflection or a function of deflection as a dependent variable. The multivariate regression analysis procedure, MANOVA (Ref 65) was used because a set of 5 or 7 deflection responses was computed in each run of the factorial. Ref 98

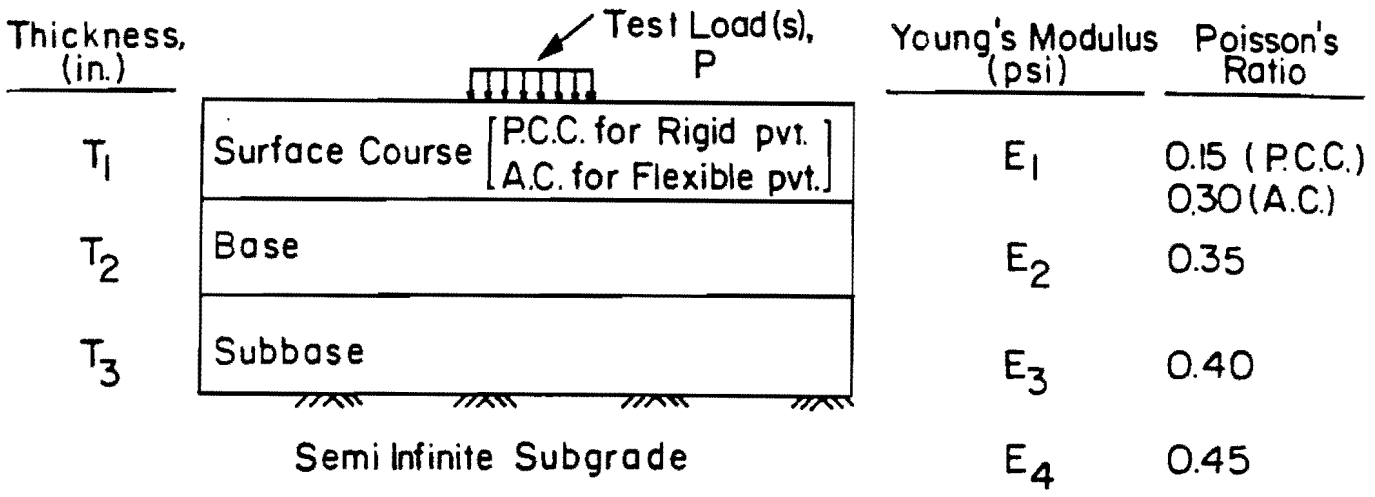

Factors: (a) Thicknesses (3) at 3 levels each.
(b) Young's moduli (4) at 3 levels each.

Control Variables	Dynaflect	FWD
(a) Radial Distances, R_k where surface deflections are to be computed (deflection basin)	(5) 10.0, 15.62, 26.0, 37.36, 49.03 inches	(7) 0, 12, 24, 36, 48, 60, 72 inches
(b) Test Load, P	2 Loads, 500 lb each, 20 inches apart.	1,000 lb on loading plate of 5.91-inch radius.
(c) Poisson's Ratios		
Response Variables		
Surface Deflections, W_k, (mils)	5 locations	7 locations

TABLE B.1(a). FRACTIONAL FACTORIAL DESIGN - FLEXIBLE PAVEMENTS (FOR FWD)

Base Type	Levels	Factors						
		T_1 (in.)	T_2 (in.)	T_3 (in.)	E_4 (psi)	E_3 (psi)	E_2 (psi)	E_1 (psi)
Stabilized Base	(0) Low	2	4	4	10,000	15,000	25,000	100,000
	(1) Medium	4	6.32	6.32	22,000	30,000	225,000	450,000
	(2) High	8	10	10	50,000	60,000	600,000	800,000
	Semi-infinite Subgrade	AC Thickness	Base Thickness	Subbase Thickness	E Subgrade	E Subbase	E Base	E AC
Granular Base	(0) Low	2	4	4	10,000	15,000	22,500	100,000
	(1) Medium	4	6.32	6.32	22,000	30,000	45,000	450,000
	(2) High	8	10	10	50,000	60,000	80,000	800,000
	Semi-infinite Subgrade	AC Thickness	Base Thickness	Subbase Thickness	E Subgrade	E Subbase	E Base	E AC

Stabilized Base: 243 Combinations; Granular Base: 243 combinations

TABLE B.1(b). FRACTIONAL FACTORIAL DESIGN - FLEXIBLE PAVEMENTS (FOR DYNAFLECT)

Base Type	Levels	Factors						
		T_1 (in.)	T_2 (in.)	T_3 (in.)	E_4 (psi)	E_3 (psi)	E_2 (psi)	E_1 (psi)
Stabilized Base	(0) Low	2	4	4	10,000	2,800	25,000	100,000
	(1) Medium	4	6.32	6.32	22,360	13,915	225,000	450,000
	(2) High	8	10	10	50,000	60,000	600,000	800,000
	Semi-infinite Subgrade	AC Thickness	Base Thickness	Subbase Thickness	E Subgrade	E Subbase	E Base	E_{AC}
Granular Base	(0) Low	2	4	4	10,000	2,800	3,920	100,000
	(1) Medium	4	6.32	6.32	22,360	13,915	30,613	450,000
	(2) High	8	10	10	50,000	60,000	180,000	800,000
	Semi-infinite Subgrade	AC Thickness	Base Thickness	Subbase Thickness	E Subgrade	E Subbase	E Base	E AC

Stabilized Base: 243 Combinations; Granular Base: 243 Combinations

TABLE B.2. FRACTIONAL ($1/9^{th}$) FACTORIAL EXPERIMENT DESIGN FOR SEVEN FACTORS AT THREE LEVELS (0, 1, 2) (REF 64)

1	2	3	4	5
0000000	2011202	1022101	0000021	2011220
1212020	0220222	2201121	1212011	0220210
2121010	1102212	0110111	2121001	1102200
2200211	1211110	0222012	2200202	1211101
0112201	2120100	1101002	0112222	2120121
1021221	0002120	2010022	1021212	0002111
1100122	0111021	2122220	1100110	0111012
2012112	1020011	0001210	2012100	1020002
0221102	2202001	1210200	0221120	2202022

6	7	8	9	10
1022122	0000012	2011211	1022110	0122110
2201112	1212002	0220201	2201100	1001100
0110102	2121022	1102221	0110120	2210120
0222000	2200220	1211122	0222021	2022021
1101020	0112210	2120112	1101011	0201011
2010010	1021200	0002102	2010001	1110001
2122211	1100101	0111000	2122202	1222202
0001201	2012121	1020020	0001222	2101222
1210221	0221111	2202010	1210212	0010212

11	12	13	14	15	16
2100012	1111211	0122101	2100000	1111202	0122122
0012002	2020201	1001121	0012020	2020222	1001112
1221022	0202221	2210111	1221010	0202212	2210102
1000220	0011122	2022012	1000211	0011110	2022000
2212210	1220112	0201002	2212201	1220100	0201020
0121200	2102102	1110022	0121221	2102120	1110010
0200101	2211000	1222220	0200122	2211021	1222211
1112121	0120020	2101210	1112112	0120011	2101201
2021111	1002010	0010200	2021102	1002001	0010221

17	18	19	20	21	22
2100021	1111220	0211220	2222122	1200021	0211211
0012011	2020210	1120210	0101112	2112011	1120201
1221001	0202200	2002200	1010102	0021001	2002221
1000202	0011101	2111101	1122000	0100202	2111122
2212222	1220121	0020121	2001020	1012222	0020112
0121212	2102111	1202111	0210010	2221212	1202102
0200110	2211012	1011012	0022211	2000110	1011000
1112100	0120002	2220002	1201201	0212100	2220020
2021120	1002022	0102022	2110221	1121120	0102010

23	24	25	26	27
2222110	1200012	0211202	2222101	1200000
0101100	2112002	1120222	0101121	2112020
1010120	0021022	2002212	1010111	0021010
1122021	0100220	2111110	1122012	0100211
2001011	1012210	0020100	2001002	1012201
0210001	2221200	1202120	0210022	2221221
0022202	2000101	1011021	0022220	2000122
1201222	0212121	2220011	1201210	0212112
2110212	1121111	0102001	2110200	1121102

contains the resulting regression equations for Dynaflect deflection basins (rigid pavements). The generalized form of the equation is:

$$R_k / W_k = f_1 \left[T_1, T_2, T_3, E_4, E_3, E_2, E_1 \right] \qquad (B.1)$$

where

W_k = deflection at the k^{th} sensor (at radial distance R_k)
(Other terms are defined in Fig B.1.)

R^2 values for these equations are well above 0.90.

All other regression equations are also presented by Uddin (Ref 98). All these equations have the following general form:

$$\text{Log}_{10} (R_k \times W_k) = f_2 \left[T_1, T_2, T_3, E_4, E_3, E_2, E_1 \right] \qquad (B.2)$$

It is noted that:

(1) For the pavement type and device type falling in one of the factorial designs, k equations are available for use.

(2) As R_k, T_1, T_2, and T_3 are known quantities, these equations are reduced to k simultaneous equations.

(3) As deflections W_k are also known "measured" values, any four equations can be solved to determine the four unknowns, E_4, E_3, E_2, and E_1.

However, this approach was not successful as the values of moduli are very sensitive to the order in which equations are used in computations. Secondly, moduli were non unique and drastically different. Therefore the attempts to use these equations in inverse order (to predict E's) were abandoned. However, these predictive equations are still valid for predicting deflection responses if thicknesses and moduli are known values. If RPEDD1 and FPEDD1 are to be adapted for field use on microcomputers, then these equations can be used in place of ELSYM5 in the self-iterative deflection basin fitting procedures to predict insitu moduli.

Use of Transformed Variables

Numerous transformations were made in order to develop regression equations showing high R^2 with the modulus (E) or a function of the modulus as a dependent variable and thicknesses and deflections as independent variables. A list of the transformed variables which were found to be significant and appear in the final equations is presented by Uddin (Ref 98).

Moduli Predictive Equations

The regression equations using transformed variables to predict moduli are presented in detail by Uddin (Ref 98). The equation for subgrade modulus takes the general form

$$E_4 \text{ or } \text{Log}_{10} E_4 = f_3 \left[T_1, T_2, T_3, R_k, W_k \right] \qquad (B.3)$$

The generalized form for moduli of upper layers is one of the following two equations.

$$h_1 (E_i, t_i) = f_4 \left[T_1, T_2, T_3, E_4, R_k, W_k \right] \qquad (B.4)$$

or

$$h_2 (E_i, E_4) = f_5 \left[T_1, T_2, T_3, R_k, W_k \right] \qquad (B.5)$$

All these equations are associated with high R^2 values (generally well above 0.80). The prediction of Young's moduli of pavement layers using these equations is based on the assumption of a semi-infinite subgrade.

Influence of Rock Layer on Predicted Subgrade Modulus

This subject is discussed in Chapter 4. If a rock layer exists at considerable depth (say around 100 feet), the resulting deflection basin is not significantly different from the deflection basin in the case of a semi-infinite subgrade. Therefore, a subgrade modulus determined from the predictive equations discussed earlier would not show any appreciable error. On the other hand, in the case of a rock layer existing at a shallow depth, the default seed modulus of a subgrade using these equations may be significantly higher. This problem will become more complex if no information is available on the presence of a rock layer under the subgrade. Experience with the Dynaflect shows that, if the sensor 5 deflection is around or below 0.10 mil, there is probably a very stiff layer (generally rock) at a shallow depth. An appropriate and realistic value for the depth at which the rock layer exists should be determined for proper input in the computer programs RPEDD1 and FPEDD1.

A parametric study was made using different rigid and flexible pavements to investigate the influence of variations in the depth of subgrade on sensor 5 deflection (Ref 98). The ratio of Dynaflect-sensor 5 deflection for D (subgrade thickness) at some finite value to the deflection for a semi-infinite subgrade is defined as RAT5. It is observed that this ratio approaches zero if a rock layer is at one foot or a shallower depth below the pavement. A power function was used to develop a regression equation based on the values of RAT5 and D determined from the parametric study (Ref 98) as presented in the following:

$$\text{Log}_{10}(1.0 + \text{RAT5}) = -0.11430156 + 0.13301293\ \text{Log}_{10} D \qquad (B.6)$$

Where D is in inches.

Subroutines SGRIG (for RPEDD1) and SGFLEX (for RPEDD1) have been written to compute RAT5 if the thickness of the subgrade layer is entered by the user. The equivalent sensor 5 deflection, W_5' for a semi-infinite subgrade case is then calculated using the following relationship:

$$W_5' = W_5/\text{RAT5} \qquad (B.7)$$

where

W_5 = measured sensor 5 deflection (FWD or Dynaflect)

The regression equation developed from the original partial factorial design is then used to predict the subgrade modulus. These equations are based only on sensor 5 deflections, as summarized in Table B.3.

TABLE B.3. PREDICTIVE EQUATIONS FOR SUBGRADE MODULUS, E_4, USED IN DEFAULT SEED MODULUS PROCEDURE IN CASE OF A RIGID LAYER UNDERLYING A KNOWN THICKNESS OF SUBGRADE

(a) Rigid pavement.

Dynaflect	FWD
$\bar{y} = -2637.1187 + 119.6571\ (R_5/W_5)$	$\bar{y} = 5.56172 - 1.1690 \times \text{Log}_{10}\ (R_5 \times W_5)$
$(R^2 = 0.98)$	$(R^2 = 0.97)$
$E_4\ (\text{psi}) = (10.0)^y$	$E_4\ (\text{psi}) = (10.0)^y$

(b) Flexible pavement - stabilized base.

Dynaflect*	FWD
$y = 2.6088 - 0.90216 \times \text{Log}_{10}\ (R_5 \times W_5)$	$y = 5\ 41448 - 0.976 \times \text{Log}_{10}\ (R_5 \times W_5)$
$(R^2 = 0.95)$	$(R^2 = 0.99)$
$E_4\ (\text{psi}) = (10.)^y$	$E_4\ (\text{psi}) = (10.0)^y$

(c) Flexible pavement - granular base

Dynaflect*	FWD
$y = 2.5366 - 0.95488 \times \text{Log}_{10}\ (R_5 \times W_5)$	$y = 5.38724 - 0.96041 \times \text{Log}_{10}\ (R_5 \times W_5)$
$(R^2 = 0.97)$	$(R^2 = 0.997)$
$E_4\ (\text{psi})\ (10.0)^y$	$E_4\ (\text{psi}) = (10.0)^y$

Note: R_i is the radial distance of i^{th} sensor from test load; and W_i is the measured deflection at i^{th} sensor (in mils except where * appears; deflection is in inches).

APPENDIX C

LABORATORY EVALUATION OF DYNAMIC SHEAR MODULUS

APPENDIX C. LABORATORY EVALUATION OF DYNAMIC SHEAR MODULUS

Soils exhibit nonlinear stress-strain behavior under repeated or dynamic loading. Therefore, material characterization using appropriate laboratory tests is very important if a reliable pavement response is to be predicted from mechanistic models based on the assumption of linear elasticity. As discussed in Chapter 5, the stress-strain curve for soils in shear exhibits strain softening behavior, as illustrated in Fig C.1. The initial shear modulus is considered to be the modulus at a low amplitude shearing strain. This modulus represented by the slope of the stress-strain curve at the origin is the tangent shear modulus, G_{max}. At higher levels of shearing strain, the secant shear modulus, G, varies with increasing shearing strain amplitude. As discussed in Chapter 5, the design 18-kip-single-axle loading is associated with low to intermediate amplitude shearing strains and the G/G_{max} versus the shearing strain curve can be used to evaluate the nonlinear (strain softening) modulus, G. Resonant column tests have become standard laboratory devices to evaluate strain softening behavior of dynamic shear moduli for geotechnical and earthquake engineering applications.

RESONANT COLUMN TESTS

Resonant column tests are performed to determine the shear modulus, G, and the damping ratio, D, of soil specimens at low to intermediate shearing strains (strains less than about 0.1 percent). These dynamic properties are found by exciting solid cylindrical specimens in torsion by a constant-force type of excitation. The theory of elasticity is used to calculate shear wave velocities and shearing strain amplitudes from measurements of the resonant frequency, specimen length, and amplitude of drive plate motion. The material damping ratio is calculated from free-vibration-decay-curves that are obtained by suddenly shutting off the power to the drive system at resonance.

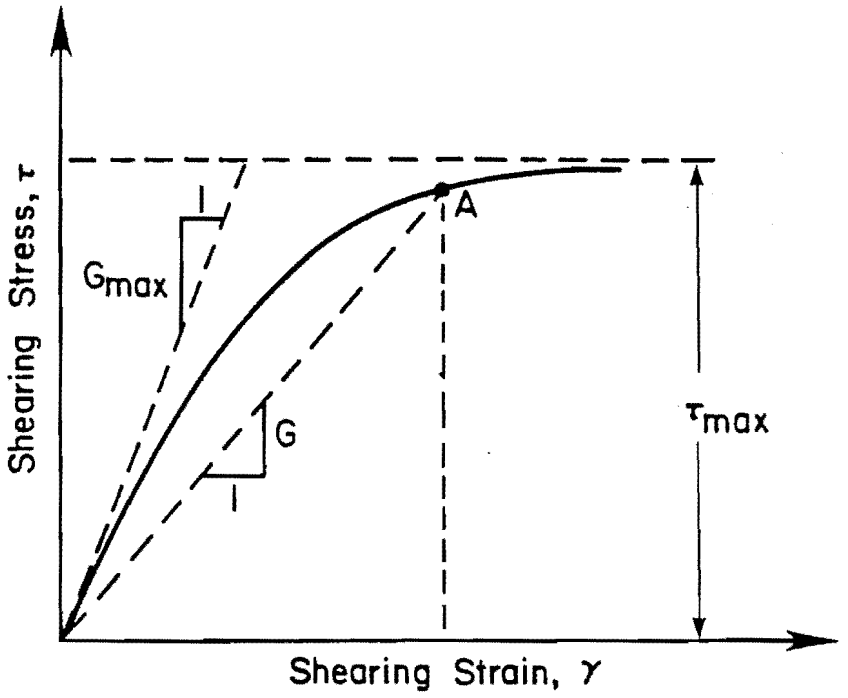

Fig C.1. An illustrative diagram of shearing stress-shearing strain curve and related parameters.

The resonant column configuration described in this appendix consists of a fixed-free column of soil that has a rigid end mass attached to the free end. This arrangement is analyzed as a single-degree-of-freedom system and is illustrated in Fig C.2. Data reduction to determine shear wave velocity is based on the wave equation in torsion.

Resonant Column Equipment

The resonant column device designed by Professor K. H. Stokoe and built at The University of Texas at Austin is described herein. The device consists of a confining pressure system, height-change measurement system, drive system, and frequency measurement system. These systems are shown schematically in Fig C.3. The brief discussion of these systems contained in the following sections is taken from Ref 88.

The confining chamber of the resonant column system is pressurized by compressed air from the building air supply. Before air reaches the cell, it first passes through an air filter to remove any water or oil in the air that could damage the regulator or instrumentation inside the cell. A Kendall Model 30 regulator controls pressure within the cell, and an Ashcroft 100-psi (690-kPa) pressure gage is used to measure it.

If a soil specimen is tested at its natural water contents, it is necessary to cover the sides of the specimen with a membrane and silicon oil bath. To slow air migration into the specimen and keep the specimen from being dried. Air pressure acts on the silicon oil bath, and a hydrostatic state of stress is applied to the specimen.

The height-change measurement system consists of a linear variable differential transformer (LVDT), sine wave generator, fixed-gain amplifier, and digital voltmeter. An excitation frequency of 500 Hz and an LVDT input voltage of 4.77 volts are used to obtain a calibration factor of approximately one volt per 0.1-inch change in height.

The drive system, attached to the top of the specimen, applies shearing stresses to the specimen by oscillating the free end (top) in torsion. The drive system consists of a drive plate, drive coils, sine wave generator, and power amplifier. The drive plate has four arms, each with a magnet attached.

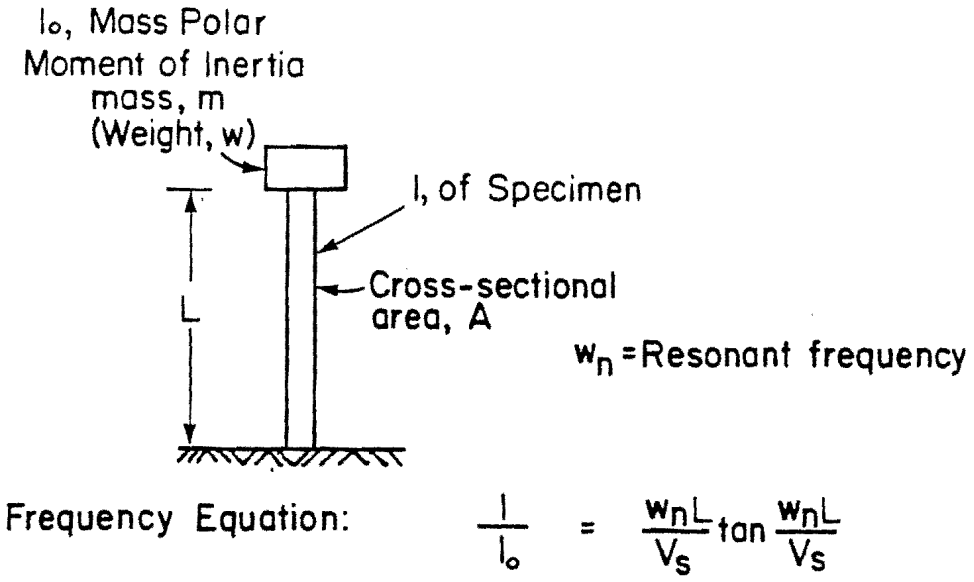

Fig C.2. Basic principle of fixed-free column of soil sample in resonant column test (Ref 82).

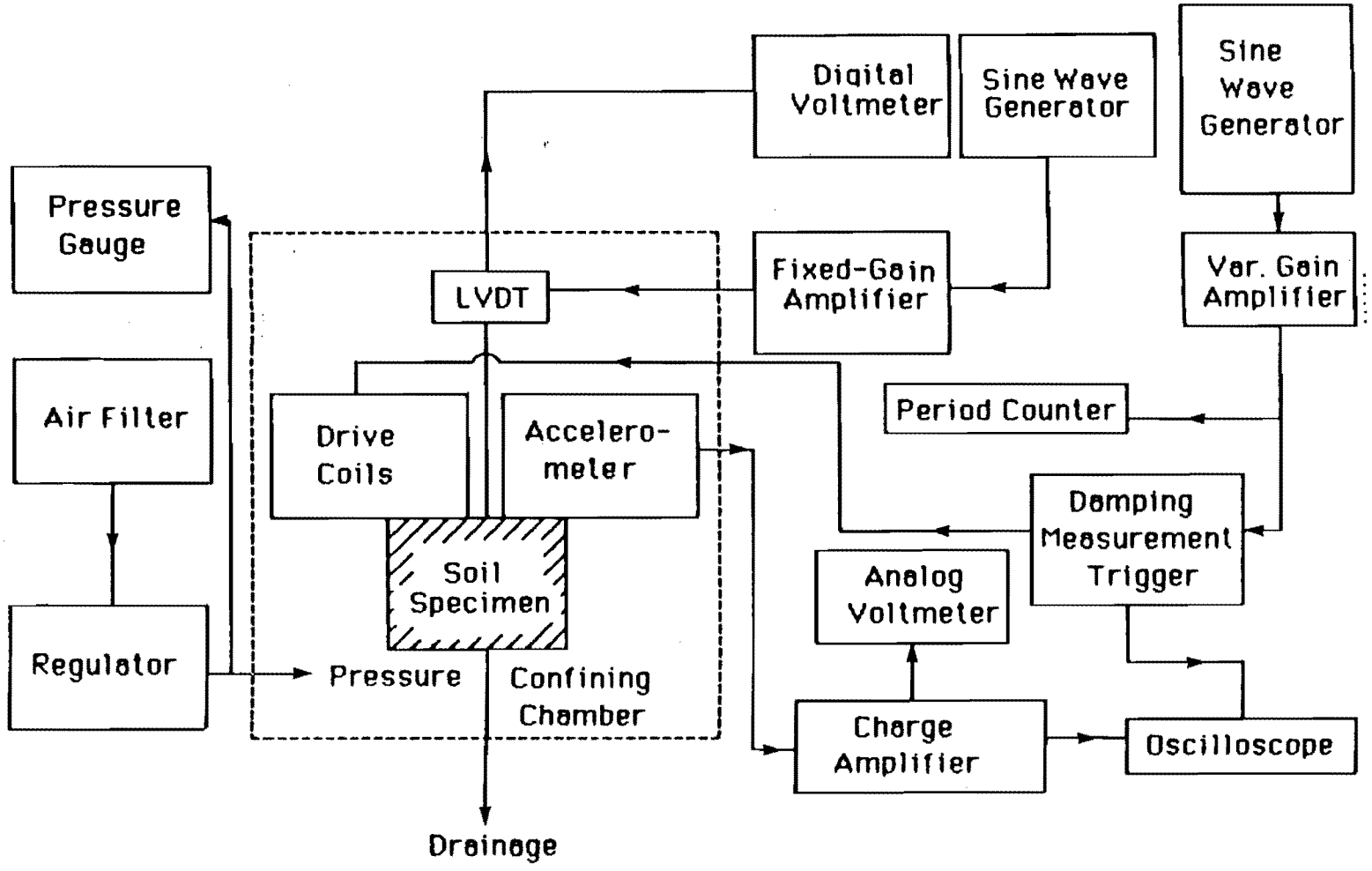

Fig C.3. Schematic diagram of resonant column system (Ref 88).

The ends of the magnets are centered within eight elliptically shaped coils. An elliptical shape prevents the magnets from touching the coils as the specimen consolidates. The coils are wired so that an alternating current passing through them will cause the drive plate to oscillate in pure torsion.

The motion measurement system consists of a piezoelectric accelerometer, charge amplifier, analog root-mean-square (RMS) voltmeter, period counter, and storage oscilloscope. The accelerometer is attached to the drive plate so that it is sensitive to torsional vibrations. Accelerometer output is linearized by the charge conditioner and is read on the analog voltmeter. The RMS voltage measured by the voltmeter is the square root of the average value of the square of the voltage (0.707 times the peak voltage). The storage oscilloscope is used to record the transient decay of free vibrations of the specimen so that an equivalent viscous damping ratio can be determined.

Measurements made with this system are used to calculate the resonant frequency, shearing strain amplitude, and damping ratio of a soil specimen. The resonant frequency of the specimen is found by sweeping through the excitation frequencies with the function generator until the largest accelerometer output is seen on the analog voltmeter. The resonant frequency is calculated from the resonant period, which is accurately measured to 0.01 millisecond. The resonant period is the average of two readings made on each side of the peak accelerometer output of the response curve. The accelerometer output and resonant period are used to calculate the shearing strain amplitude.

An equivalent viscous damping is calculated from measurements of three to six consecutive cycles of the free-vibration-decay curve. At resonance, voltage to the drive coils is suddenly cut off, and the storage oscilloscope is triggered. The accelerometer output of the transient decay curve of free vibration is recorded on the oscilloscope. For low-amplitude resonant column tests, single-amplitude shearing strains below 0.001 percent, three sets of readings are averaged to obtain damping ratio values.

Test Procedure

First, the moisture content cans are weighed and their weights, along with other set-up information, are recorded on a data sheet. The bottom of the base pedestal is greased and then tightened to the base plate. A saturated porous stone is screwed into the top of the base pedestal, and an accumulator is used to saturate the drainage lines in the base and base pedestal. The O-rings and membrane are then fitted to their respective expanders. Filter paper drains are prepared, and high-vacuum silicon grease is applied to the sides of the top cap and base pedestal.

A hydraulic extruder is used to extrude the sample vertically. The sample is then placed on a glass plate and carried to the laboratory to be trimmed. Once the sides are trimmed to the correct diameter, the soil is carefully placed in a mold, and the ends of the specimen are trimmed. While the specimen is being trimmed, water content samples are taken of the sides and ends.

After the specimen is trimmed to its final dimensions, both the weight and length are measured and recorded. The specimen is then placed on the base pedestal, and measurements of the diameter are made. The top cap is set on the specimen, and filter paper strips are placed around the interfaces between the specimen and the top cap and the specimen and the base pedestal to prevent the membrane from being damaged or pinched at these interfaces. Vertical strips are also placed approximately 0.5-inch apart along the sides of the specimen to allow radial drainage. The membrane is placed over the specimen and sealed to the greased top cap and the base pedestal by O-rings.

A 4.0-inch-diameter metal cylinder, to contain the silicon oil bath, is then placed around the specimen and sealed to the base pedestal by an O-ring. Silicon oil is poured into the cylinder until the length of the specimen is covered.

The drive system is then placed over the specimen and the silicon oil bath. As gently as possible, the screws that connect the drive plate to the top cap are tightened. The metal ring, to which the coils are attached, is then leveled and placed so that the magnet ends are evenly surrounded by the

coils. The LVDT is centered around the core at a height within the linear range.

The metal, cylindrical, confining chamber is then placed over the specimen. Connections of the power, LVDT, and accelerometer are made through the bulkhead connectors. The top plate is placed on the cylinder, and the confining chamber is sealed. A seating pressure of one half of the first confining pressure is then applied to the specimen.

DATA REDUCTION OF RESONANT COLUMN TEST

The analysis of the fixed-free resonant column device and calculations of both the shear modulus and the material damping ratio are discussed in this section. The following discussion is applicable to data reduction for both low- and high-amplitude test results.

Dynamic Shear Modulus

Shear modulus can be calculated at any time during consolidation if values of the current unit weight, mass density, void ratio, and mass polar moment of inertia of the specimen are known at that time. These values can be calculated from a measurement of the height change (LVDT output) and known initial properties such as specific gravity, water content, degree of saturation, and specimen diameter, height, and weight. These calculations include a few assumptions: the volume of solids and the degree of saturation remain constant for the entire duration of the test, and the radial strain and the axial strain are equal for hydrostatic loading.

Once these assumptions are made, calculations of void ratio, mass density, volume, and radial strain are elementary. The new void ratio can be determined as soon as the change in the volume of voids is obtained. To calculate this change, it is necessary to know the specimen dimensions so that the new volume can be found. These dimensions are calculated by determining the amount of axial and radial strain the specimen has experienced. The change in volume is then calculated, which equals the change in the volume of voids.

The change in specimen mass (due to expulsion of water) is calculated by multiplying the volume change by the degree of saturation and multiplying this quantity by the mass density of water. This value is then subtracted from the original specimen mass to obtain the new specimen mass. The new specimen mass and diameter are required to calculate a new mass polar moment of inertia of the specimen, I, from the equation

$$I = \int r^2 \, dm \qquad (C.1)$$

where

r = specimen radius and

m = specimen mass.

For a specimen which is a solid, right circular cylinder, Eq C.1 reduces to

$$I = 1/2 \, mr^2 \qquad (C.2)$$

It is obvious that the unit weight and mass density can now be calculated since the new mass and volume are known.

A specimen having the configuration of a fixed end and a free end with a rigid lumped mass attached to the free end is approximated by a single-degree-of-freedom system (SDOF), Ref 82. The equation governing this system is

$$\frac{I}{I_o} = \beta \tan\beta \qquad (C.3)$$

where

I_o = mass polar moment of inertia of the drive plate, attached magnets, and top cap, and

$$\beta = \frac{\omega \ell}{V_s} \qquad (C.4)$$

where

ω = natural circular frequency,

ℓ = specimen length, and

V = shear wave velocity.

This relationship is the solution of the wave equation for an elastic rod excited in torsion for the specified boundary condition. The mass polar moment of inertia of the drive system, I_o, is a previously calibrated constant, and the mass polar moment of inertia of the specimen is easily calculated, as discussed earlier in this section. Shear wave velocity is calculated from the definition of β given by Eq C.4.

Once the shear wave velocity is determined, shear modulus, G, is calculated from

$$G = \frac{\gamma}{g} V_s^2 \qquad (C.5)$$

where

γ = total unit weight of the specimen and

g = gravitational acceleration.

Shearing Strain Amplitude

The amplitude of shearing strain is calculated from the measurements of accelerometer output, resonant period, and specimen height and diameter. Torsional displacement of the drive plate at the position of the accelerometer is calculated by integrating the accelerometer output twice with respect to time. If the angle of twist is small, it can be calculated by dividing the torsional displacement at the periphery of the specimen by the length of the specimen. The shearing strain is calculated at 0.667 of the radius of the specimen and refers to single-amplitude values of shearing strain as shown in Fig C.4. The equation used to calculate shearing strain amplitude of the specimen is

$$\gamma = (9.2204 \times 10^{-10} \cdot A \cdot P \cdot \frac{D}{L}) \qquad (C.6)$$

where

A = accelerometer output voltage in millivolts (rms),
P = resonant period in milliseconds,
D = specimen diameter in inches, and
L = specimen length, in inches.

Damping Ratio

As discussed earlier, damping ratio is calculated from free-vibration-decay curves. These curves are obtained by exciting the specimen at its resonant frequency and suddenly stopping the power to the drive system. The soil specimen and attached drive system, modelled as a freely vibrating SDOF system, are idealized as having linear viscous damping. The differential equation of motion is then solved to determine the damping ratio.

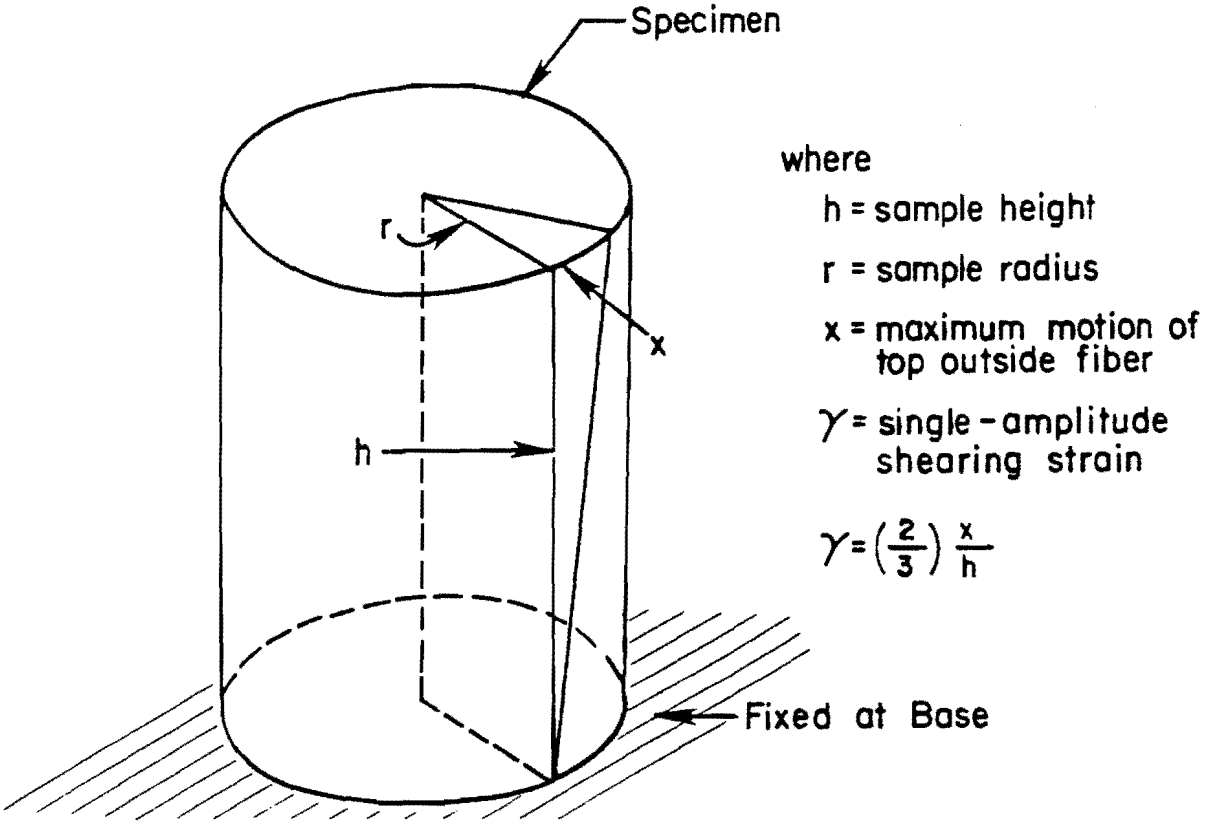

Fig C.4. Single-amplitude shearing strain for a solid specimen (Ref 88).

APPENDIX D

NONLINEAR, STRAIN-SOFTENING MODELS FOR DYNAMIC MODULI OF GRANULAR MATERIALS AND SUBGRADE

APPENDIX D. NONLINEAR, STRAIN-SOFTENING MODELS FOR DYNAMIC MODULI OF GRANULAR MATERIALS AND SUBGRADE

This appendix presents a discussion on different approaches to developing mathematical models for the unique curves of G/G_{max} (or E/E_{max}) versus shearing-strain relationships. The unique relationships (Curve A for clays and Curve B for sands and granular materials) are shown in Fig D.1. At this point, it is emphasized that these are median curves based on a limited amount of data (investigation of actual data was not within the scope of this work).

RAMBERG-OSGOOD CURVES

This class of theoretical curves is discussed by Richart and Wylie (Ref 92) with example applications to actual G/G_{max} versus shearing strain relationships. The decrease in secant shear modulus, G ($= \tau/\gamma$), with an increase in shearing stress ratio, τ/τ_{max} is given by the following expression:

$$\frac{G}{G_{max}} = \frac{1}{1 + \alpha \left[\tau/C_1 \cdot \tau_{max}\right]^{R-1}} \qquad (D.1)$$

where α and R are parameters which adjust the position and shape of the curve, C_1 is a factor related to the yield of the shearing stress, and G, G_{max}, τ and τ_{max} are defined in Fig C.1. Richart and Wylie also present secant modulus curves for the case of R = 3, $\alpha = 1.0$, and $C_1 = 0.4$.

This approach was not utilized in the present research. However, research work in progress at The University of Texas at Austin indicates the

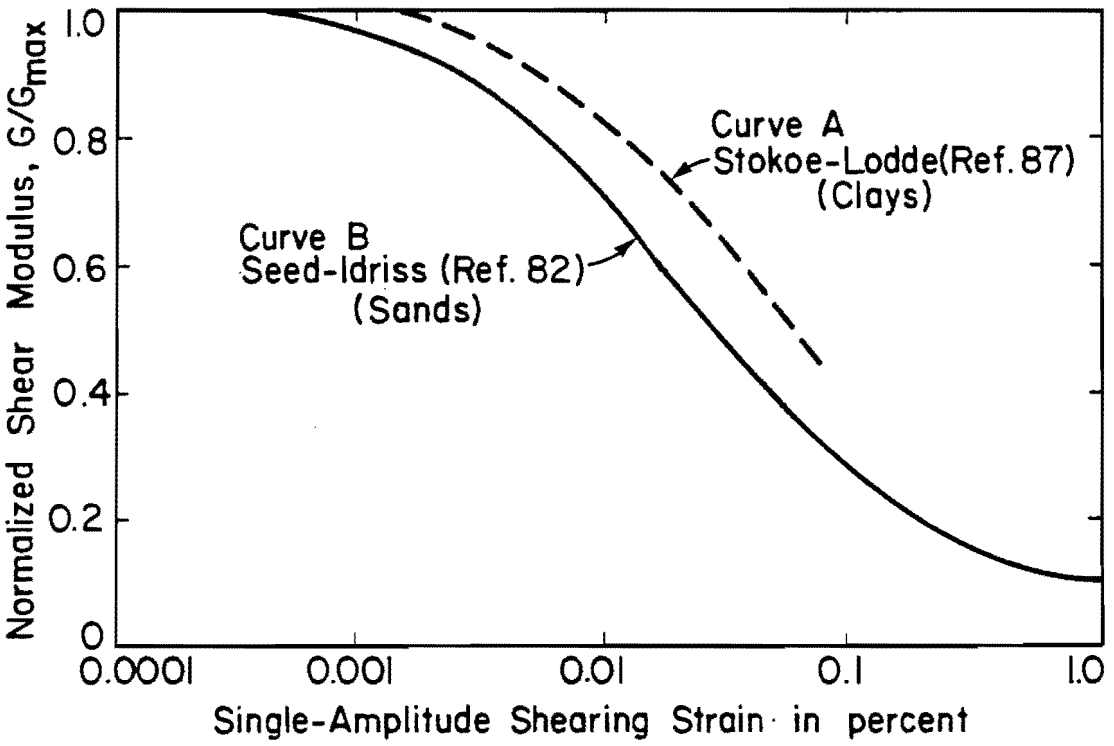

Fig D.1. Summary of normalized shear modulus variation with shearing strain.

approach must be used to characterize different soils with R, α and C_1 parameters.

REGRESSION ANALYSIS

A simpler approach was to use regression analysis to develop predictive equations. The G/G_{max} versus shearing strain values for curves A (for clays) and B (for granular materials) are shown in Table D.1.

Linear Regression Technique

As illustrated in Fig D.1, the generalized curves are plotted with a logrithmic scale as the abscissa (shearing strain). Clearly an appropriate transformation is necessary to linearize these curves. A possible mathematical function to define these curves, Sec h (x), is presented in the following:

$$x_2 = \text{Sec h } (x) = \frac{2.0}{e^x + \frac{1}{e^x}} \qquad (D.2)$$

where

x = $\log_{10}$ (shearing strain in percent) and
x_2 = the transformed (independent) variable.

Using the values in Table D.1, the following regression equations were developed:

$$G/G_{max} = 1.0908788 - 1.0513303\ (x_2) \qquad (D.3)$$

TABLE D.1. G/G_{max} VERSUS SHEARING STRAIN DATA USED TO DEVELOP MATHEMATICAL MODELS (BASED ON FIG D.1.)

	G/G_{max} (or E/E_{max})	
Single Amplitude Shearing Strain, %	Subgrade (Curve A)	Granular Material (Curve B)
0.004	--	1.00
0.0010	1.00	0.98
0.0020	0.98	0.93
0.0030	0.95	0.89
0.0050	0.91	0.83
0.0070	--	0.78
0.010	0.82	0.71
0.020	0.72	0.56
0.030	0.62	0.48
0.050	0 51	0.39
0.800	0.40	--
0.1000	0.35	0.28
0.2000	0.23	0.19
0.3000	--	0.15
0.5000	--	--
0.7000	--	0.11
1.0000	--	0.10

and

$$G/G_{max} = 1.0039127 - 0.99086218\ (x_2) \qquad (D.4)$$

Equation D.3 is for curve A (clays) with an R^2 of 0.98. Equation D.4 represents curve B (sands) with an R^2 value of 0.95. These equations are valid for the ranges of shearing strain shown in Table D.1.

Improvements in these equations were made by modifying the transformation. The generalized form of the final regression equations is expressed in the following:

$$G/G_{max} = \text{constant} + f\left[\frac{2.0}{(2.0)^x + \frac{1}{(2.0)^x}}\right] \qquad (D.5)$$

The equations are presented in Table 5.3 (Chapter 5). Both equations are associated with a (high) R^2 value of 0.99. In programs RPEDD1 and FPEDD1, these final equations are contained in subroutine EQLIN1 for use in the self iterative procedure (subroutine ELANAL) to determine insitu strain-softening nonlinear moduli when the Dynaflect is used to measure dynamic deflection basin.

Nonlinear Regression

The form of the unique curves closely approximates an inverse growth curve. An example of a suitable growth curve is a logistic curve, as expressed below:

$$Y(x) = \frac{A}{1 + B\, e^{-Cx}} \qquad (D.6)$$

where

A, B, C = parameters and

x = independent variable.

Nonlinear regression procedures (included in standard statistical packages) estimate the parameters which appear in the model in nonlinear fashion. Nonlinear estimation procedures require initial estimates of the parameters to achieve faster convergence to the fitted values. Another possible growth model for consideration is Gompertz model which is presented in the following:

$$Y(x) = A.EXP\{-B\, e^{-C\,x}\} \qquad (D.7)$$

DISCUSSION

There are a number of valid approaches to developing predictive equations (based on mechanistic or empirical models) for the G/G_{max} versus shearing strain curves. It is recommended in Chapter 9 that research effort be devoted to performing a large number of tests on samples of subgrade and granular materials for subbase or base to evaluate G/G_{max} versus shearing strain relationships. The resonant column technique would be well suited for these tests. The experimental data collected in this way could be used as the basis for developing appropriate nonlinear models as discussed in this appendix.

APPENDIX E

SELECTION OF DESIGN SECTION AND DESIGN MODULI

APPENDIX E. SELECTION OF DESIGN SECTION AND DESIGN MODULI

Use of Dynaflect sensor 5 or basin slope (SLOP) profiles has been previously recommended for selection of design sections for rigid pavement overlay design (Ref 23). A more direct and appropriate procedure recommended in this study relies on the tabulated outputs generated by computer programs RPEDD1 and FPEDD1. A plot of remaining life (preferably in conjunction with the analysis of condition survey data) versus distance helps the user to identify areas in need of rehabilitation and requiring overlay design. The profile of the subgrade modulus is then used to delineate design sections. An example of such plots is conceptually presented in Fig E.1.

SELECTION OF DESIGN SECTION

Use of the subgrade modulus profile offers a more rational approach for selection of design sections, as compared to the use of the deflection parameter. The procedure for identifying sections for overlay design is similar to that described in Ref 23. The preliminary selection is based on the visual observation of a possible significant difference in the means of subgrade moduli. However, it is pointed out the selection is being made after completion of the structural evaluation of a pavement by analyzing all deflection basins, which could have been measured by either FWD or the Dynaflect.

Adjacent design sections should be checked for statistically significant differences in the means of their subgrade moduli data. A standard hypothesis test for equal means of two samples should be used for this purpose (based on student's t-statistic). A computer program such as TVAL (Ref 69) developed for this test can also be adapted to handle subgrade modulus data. If the difference is statistically not significant then the two sections can be pooled together to determine design moduli.

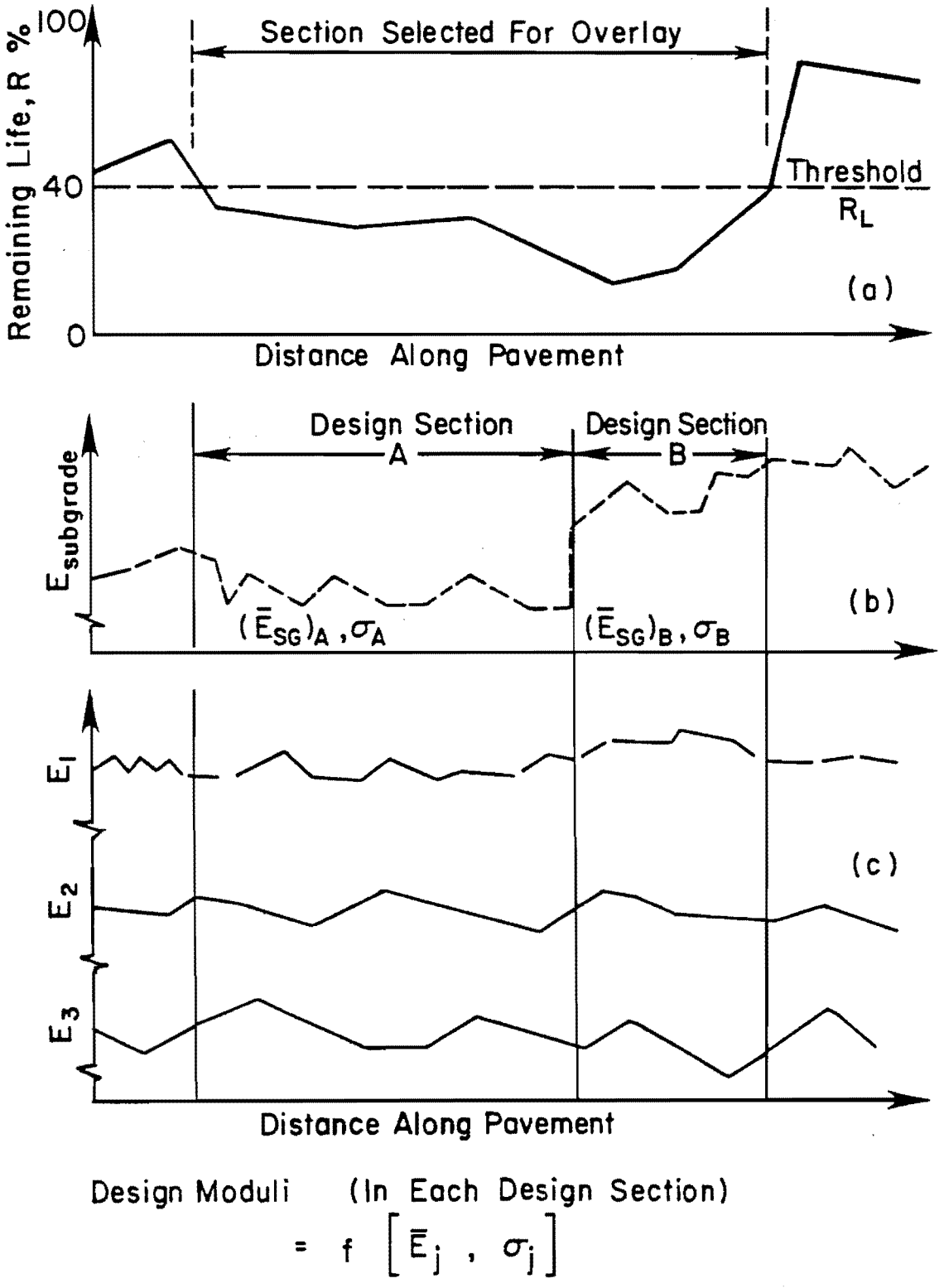

Fig E.1. Application/implementation of structural evaluation programs.

DESIGN MODULI

Once design sections have been delineated and tested for statistical significance, the next step is to determine design moduli in each design section. The rigid pavement overlay design procedure, RPOD, currently used by the Texas SDHPT, recommends that the pavement be designed for a certain confidence limit only with regard to the subgrade modulus. However, in the current study, means and standard deviations of all moduli are readily available. Therefore a confidence limit can be used for the modulus of each layer, using the following relationship, if it is assumed that the data comes from a normally distributed population:

$$(E_i)_\alpha = \overline{E_i} - Z S_i \qquad (E.1)$$

where

$(E_i)_\alpha$ = design modulus value of ith layer,

$\overline{E_i}$ = mean modulus value of ith layer, and

S_i = standard deviation of modulus values for ith layer.

Z values are taken from standard statistical tables, corresponding to the selected significance level. The value of Z is 1.96 corresponding to 95 percent design confidence level (α being 0.05 in this case).

APPENDIX F

USER'S MANUAL OF RPEDD1

APPENDIX F. USER'S MANUAL OF RPEDD1

A detailed input guide, summary formats, and examples of applications are presented in this appendix.

INPUT GUIDE

Input Data

A summary of formats for input data appears in Fig F.1. Several of the input variables have built-in default values in the program. All the input variables are explained in this section. All integers (I-format) must be right justified. F-formats are for real values. Whenever default is mentioned, the user can choose not to enter any value. Input seed moduli should be entered only if the user strongly feels that these values are reliable (based on laboratory or field tests). All card types are explained in the following.

Card 1

NSYM: Total number of deflection basins to be entered for analysis (maximum of 50).

Card 2

NINE: 999 (must be entered). It is a flag to indicate the start of the next problem.

TITLE: Identification information.

KTEST: Date of test.

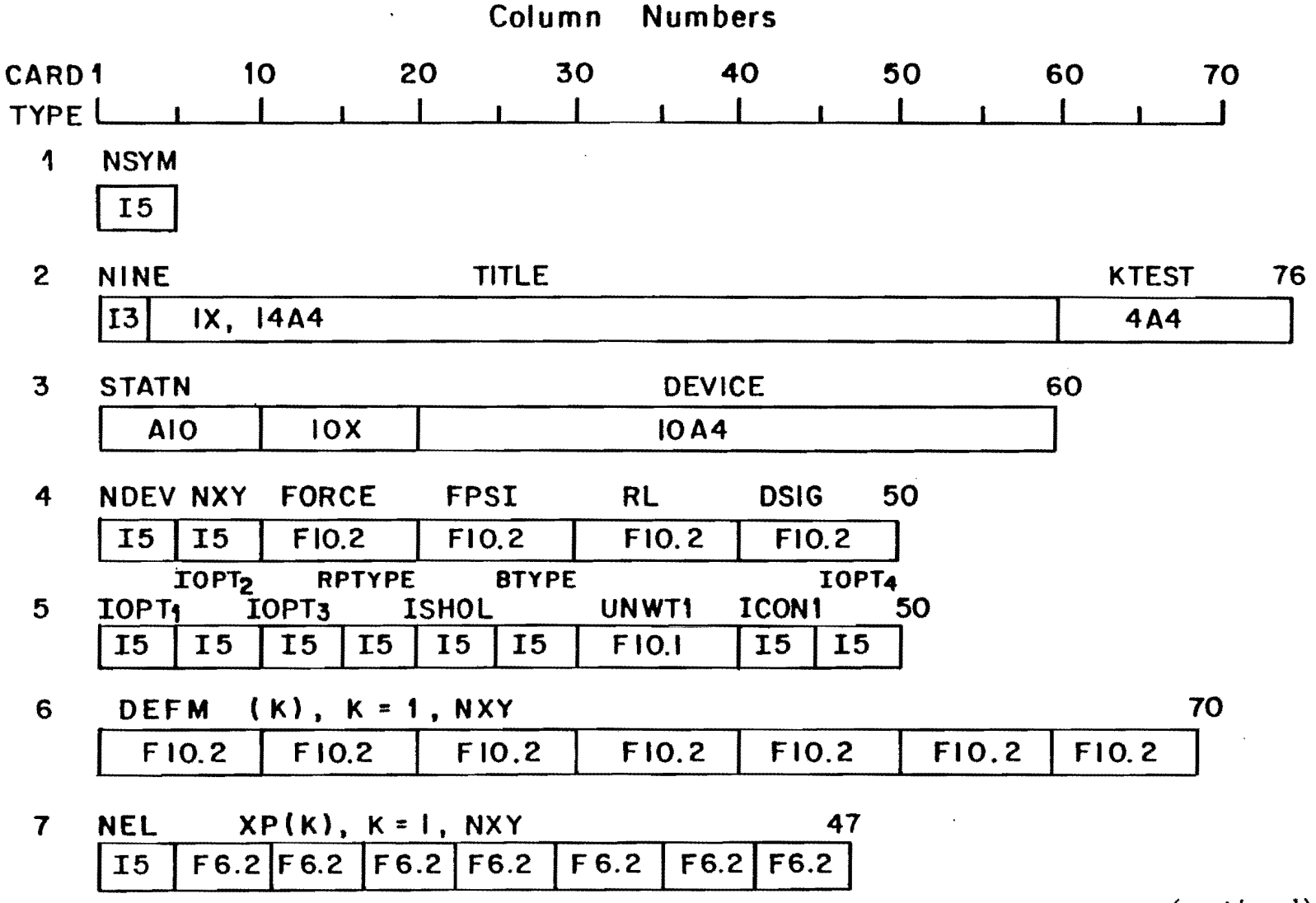

(continued)

Fig F.1. Summary of formats of input data for RPEDD1.

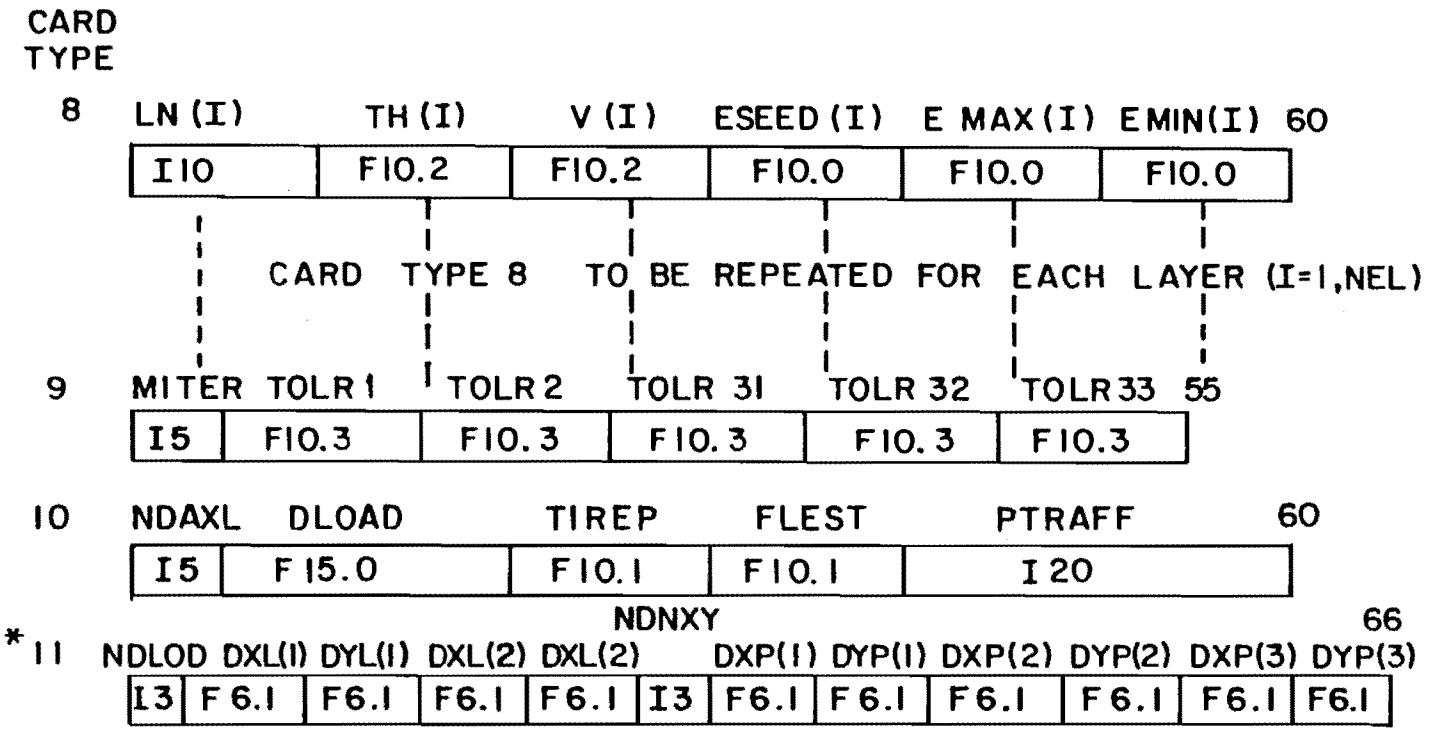

* IF NDAXL ≠ 1 ; SKIP CARD TYPE 11.

(FOR THE NEXT PROBLEM ; REPEAT CARD TYPE 2 TO 11) .

Fig F.1. (continued)

Card 3

STATN: Station at which the deflection basin was measured.

DEVICE: Name of NDT device.

Card 4

NDEV: Code for NDT device
(1 for Dynaflect; 2 for FWD).

NXY: Number of sensors where deflections were measured (it should be entered only for FWD, at least 6).

FORCE: Peak force of FWD-force signal (in lb).

FPSI: Peak stress of FWD at surface (can be left blank if FORCE and RL are entered).

RL: Radius of FWD loading plate (in inches).

DSIG: Duration of FWD force signal (default is 25 msec).

Card 5

IOPT1: Option for output of back-calculated Young's moduli.
(0 for summary only; 1 for detailed output.)

IOPT2: 0 to skip remaining life analysis, 1 to make remaining life analysis.

IOPT3: 0 for ignoring the default procedure to create a rigid layer, 1 to activate the default procedure to create a rigid layer at a finite thickness of subgrade.

RRTYPE: Type of rigid pavement (0 for JCP/JRCP, 1 for CRCP).

ISHOL: Shoulder type (0 for JCP/JRCP, 1 for CRCP).

BTYPE: Type of layer above subgrade (1 for granular, 2 for stabilized).

UNWT1: Unit weight of subgrade soil (lb/cft). An approximate value can be used if no test data are available.

ICON1: Condition of concrete pavement (0 normal, not severely damaged; 1 severely cracked).

IOPT4: 0 for making a complete analysis, 1 to skip equivalent linear analysis as well as remaining life analysis (it overrides IOPT2).

Card 6

DEFM(k): Measured deflections in mils, starting from the first sensor (not exceeding 7 sensors).

Card 7

NEL: Number of layers in the idealized pavement model including subgrade (not less than 2 and not exceeding 4; see additional discussion in the next section).

XP(k): Radial distance of FWD sensors from the center of the loading plate, starting from the first sensor and not exceeding 7 sensors.

Card 8

(Note: Card type 8 is to be repeated for each pavement layer; starting from the surface layer). I ranges from 1 to NEL.

LN(I): Layer number (must be entered).

TH(I): Thickness in inches (must be entered; blank or zero for semi-infinite subgrade).

V(I): Poisson's ratio (must be entered; Table 4.1 can be consulted for guidance).

ESEED(I): Initial estimate (seed value) of Young's modulus in psi. (Generally 0 should be entered here; this will ensure convergence to a unique solution.)

EMAX(I): Maximum allowable value of Young's modulus (see Table 4.5 for default values).

EMIN(I): Minimum allowable value of Young's modulus (see Table 4.5 for default values).

Card 9

(Note: All values in this card can be entered as zero or left blank.)

MITER: Maximum number of iterations for each trial (default is 10). A second trial is activated if the maximum difference is computed and measured deflection is greater than 10 percent.

TOLR1: Tolerance for individual deflections, in mils (default is 0.05 mil).

TOLR2: Tolerance for absolute total error at all sensors is computed and measured deflections (default is 2 percent).

TOLR31: Tolerance for modulus of surface concrete layer (default is 4 percent).

TOLR32: Tolerance for moduli of intermediate layers (default is 3 percent).

TOLR33: Tolerance for subgrade modulus (default is 0.005 percent).

Card 10

NDAXL: Zero or blank for default design load as illustrated in Fig 5.19. (In this case, the next card, type 11, is to be skipped.) Enter 1 for the user specified design load. (Card type 11 must be completed.)

DLOAD: Design load per tire in lb (assuming single axle, dual tires). The default value is 4500 lb.

TIREP: Tire pressure in psi (default value is 75 psi).

FLEST: Flexural strength of concrete in psi (must be entered if remaining life calculation is asked by the user).

PTRAFF: Cumulative past traffic in 18-kip ESAL (must be entered if remaining life is to be computed).

Card 11

NDLOD: Number of loads (e.g., 2 for the default design load simulating dual tires in Fig 5.19).

DXL(1): Position of x-coordinate for first load.

DYL(1): Position of y-coordinate for first load.

DXL(2): Position of x-coordinate for second load.

DYL(2): Position of y-coordinate for second load.

NDNXY: Number of locations where pavement response is to be calculated under the user specified design load (enter 3).

DXP(1): Position of x-coordinate of the nearest location for response.

DYP(1): Position of y-coordinate of the nearest location for response.

DXP(2): Position of x-coordinate of the intermediate location for response.

DYP(2): Position of y-coordinate of the intermediate location for response.

DXP(3): Position of x-coordinate of the farthest location for response.

DYP(3): Position of y-coordinate of the farthest location for response.

(Note: All distances in Card 11 are in inches.)

Idealized Pavement Structure

A major aspect of the RPEDD1 program is that it handles a three or four layer pavement. Therefore, actual pavement structures are to be idealized by an equivalent three or four layered pavement. Examples of some of these cases are illustrated in Fig 7.2. If the actual pavement is of two layers only, then a third layer should be created out of the subgrade and BTYPE should be assigned a value of 1. For pavements of more than four layers, intermediate layers can be combined into one layer so as to make four layered pavements.

APPLICATION OF RPEDD1

An example of input data for four deflection basins is presented in Table F.1. An example of partial output is presented in Table F.2. Results of the analysis of only the first basin are reproduced in this table. Table

TABLE F.1. EXAMPLE INPUT FOR RPEDD1

```
    4
999      JRCP - EAST OF SAN BERNARD RIVER IH10 EB             AUG.1984
              000002          FWD
    2   7   9304.00                   5.91
    0   0     0   1     1   2       115.0      0
     2.30      2.10      1.90      1.60       1.40       1.20       1.00
    3  0.00 12.00 24.00 36.00 48.00 60.00 72.00
        1     10.00       .15          0.   5500000.  2500000.
        2      6.00       .30          0.    500000.    70000.
        3         0       .45          0.          0         0
    6
              4500.       75.0     650.0                  000000
.999     JRCP - EAST OF SAN BERNARD RIVER IH10 EB             AUG.1984
              000003          FWD
    2   7   9206.00                   5.91
    0   0     0   1     1   2       115.0      0
     2.60      2.40      2.20      1.90       1.70       1.40       1.20
    3  0.00 12.00 24.00 36.00 48.00 60.00 72.00
        1     10.00       .15          0.   5500000.  2500000.
        2      6.00       .30          0.    500000.    70000.
        3         0       .45          0.          0         0
    8
              4500.       75.0     650.0                  000000
999      JRCP - EAST OF SAN BERNARD RIVER IH10 EB             AUG.1984
              000004          FWD
    2   7   9192.00                   5.91
    0   0     0   1     1   2       115.0      0
     4.20      4.00      3.50      3.00       2.50       2.00       1.70
    3  0.00 12.00 24.00 36.00 48.00 60.00 72.00
        1     10.00       .15          0.   5500000.  2500000.
        2      6.00       .30          0.    500000.    70000.
        3         0       .45          0.          0         0
    8
              4500.       75.0     650.0                  000000
999      JRCP - EAST OF SAN BERNARD RIVER IH10 EB             AUG.1984
              000005          FWD
    2   7   9152.00                   5.91
    0   0     0   1     1   2       115.0      0
     3.80      3.50      3.10      2.60       2.10       1.70       1.40
    3  0.00 12.00 24.00 36.00 48.00 60.00 72.00
        1     10.00       .15          0.   5500000.  2500000.
        2      6.00       .30          0.    500000.    70000.
        3         0       .45          0.          0         0
    8
              4500.       75.0     650.0                  000000
```

TABLE F.2. EXAMPLE OF PARTIAL OUTPUT FOR RPEDD1

```
1

     ********************************
     *                              *
     *          R P E D D 1         *
     *                              *
     ********************************

     RIGID PAVEMENT EVALLATION PROGRAM
     PROGRAM WRITTEN BY MAHEEL UDDIN
        VERSION : 1.0  APRIL 14,1984
     CENTER FOR TRANSPORTATION RESEARCH
     THE UNIVERSITY OF TEXAS AT AUSTIN


 MEASURED DEFLECTION BASIN (PROBLEM NO.  2 )

     JRCP - EAST OF SAN BERNARD RIVER IH10 EB

         DYNAFLECT              STATION:                    3  AUG.1984

     3   LAYERS SYSTEM        BTYPE =  2  (TYPE OF LAYER ABOVE SUBGRADE :)
                                         ( 1 = GRANULAR ; 2 = STABILIZED )

                    ******** INPUT SYSTEM PARAMETERS ********

 ALLOWABLE NUMBER                                    TOLERANCES
  OF ITERATIONS        TOLR1        TOLR2        TOLR31       TOLR32      TOLR33

         8              .005        1.500        4.000        2.000        .100
                                    PERCENT      PERCENT      PERCENT     PERCENT
                    ***************************************

 LAYER NO.      THICKNESS  POISSONS          ESEED          E(MAX)          E(MIN)
                 (INCHES)   RATIO             (PSI)          (PSI)           (PSI)

    1               10.00       .15       3836251.       6500000.        2000000.
    2                6.00       .30        392638.        500000.          20000.
    3                           .45         28179.         70000.           5000.

      UNIT WEIGHT OF SUBGRADE SOIL     115.0LBS. PER CU. FT.
      ***************************************************

          SENSOR NO.              1      2      3      4      5

     MEASURED DEFLECTIONS
               (MILS)          .280   .260   .230   .220   .180

    CALCULATED DEFLECTIONS
               (MILS)          .336   .318   .278   .238   .202

         MERRP (PERCENT)      22.158
    (BASED ON SEED MODULI VALUES)


    *****                   *****
    ***** ITERATIONS BEGIN *****
    *****                   *****


     STOPPED - NO FURTHER DECREASE IN MAXIMUM PRCENT ERROR IN DEFLECTION

     TOTAL ITERATIONS ATTEMPTED IN THIS RUN ARE    3
        ***************************************

    IOPT1 =    0 ENFORCED ; RESULT OF EACH INDIVIDUAL ITERATION IS NOT PRINTED ***
```

TABLE F.2. (CONTINUED)

```
******* SUMMARY OF BEST ITERATION ( NO. 3 ) *******

 YOUNGS MODULI(PSI)   5398102.1    500000.0     31026.1

  MEASURED DEFLECTIONS
            (MILS)          .280   .260   .230   .220   .180

 CALCULATED DEFLECTIONS
            (MILS)          .284   .272   .241   .209   .179

      MERRP (PERCENT)      4.928


 ************************************************************************
  DESIGN SINGLE AXLE LOAD DATA

  LOAD PER TIRE (LBS.) =     4500.0    FLEX. STRENGTH:   650.0 PSI
  TIRE PRESSURE (PSI)  =       75.0

  RIGID PAVEMENT TYPE :   1            SHOULDER TYPE :   1
   ( 0 = JCP OR JRCP )                  ( 0 = WITHOUT CONCRETE SHOULDER )
   ( 1 = CRCP       )                   ( 1 = WITH CONCRETE SHOULDER )

*********EQUIVALENT LINEAR ANALYSIS FOR CORRECTION OF YOUNGS MODULI*********

  **** SUBGRADE (NATURAL SOIL) MODULUS CORRECTED FOR NON LINEAR BEHAVIOUR ****

      CORRECTED VALUES OF YOUNGS MODULI (PSI)
         5398102.     500000.      30480.

1

******************** SUMMARY OF STRUCTURAL EVALUATION ********************

 STATION DEF.MAX.H. STRESS DEV.STRESS  FINAL VALUES OF YOUNGS MODULI (PSI)

          (MILS)   (PSI)     (PSI)

 1      2  2.7   .641E+02  -.217E+01    4169000.   332506.    36946.
 2      3  2.8   .659E+02  -.173E+01    5398000.   500000.    30480.
 3      4  5.0   .820E+02  -.176E+01    3515006.   118408.    17530.
 4      5  4.3   .796E+02  -.210E+01    3200000.    89500.    22648.

                          *** MEAN :    4070500.   268100.    26898.

                           STD DEV :    972678.3   193198.5   8555.0

                           C V (%) :       23.8       74.3       31.8


  RIGID PAVEMENT EVALUATION PROGRAM
  PROGRAM WRITTEN BY MAHEED UDDIN
     VERSION : 1.0  APRIL 14,1984
  CENTER FOR TRANSPORTATION RESEARCH
  THE UNIVERSITY OF TEXAS AT AUSTIN
```

F.2 also includes the final tabulated summary output. Figure F.2 illustrates plots of moduli along the test section based on the tabulated output. These plots show the analysis of FWD as well as Dynaflect deflection basins measured almost at the same time.

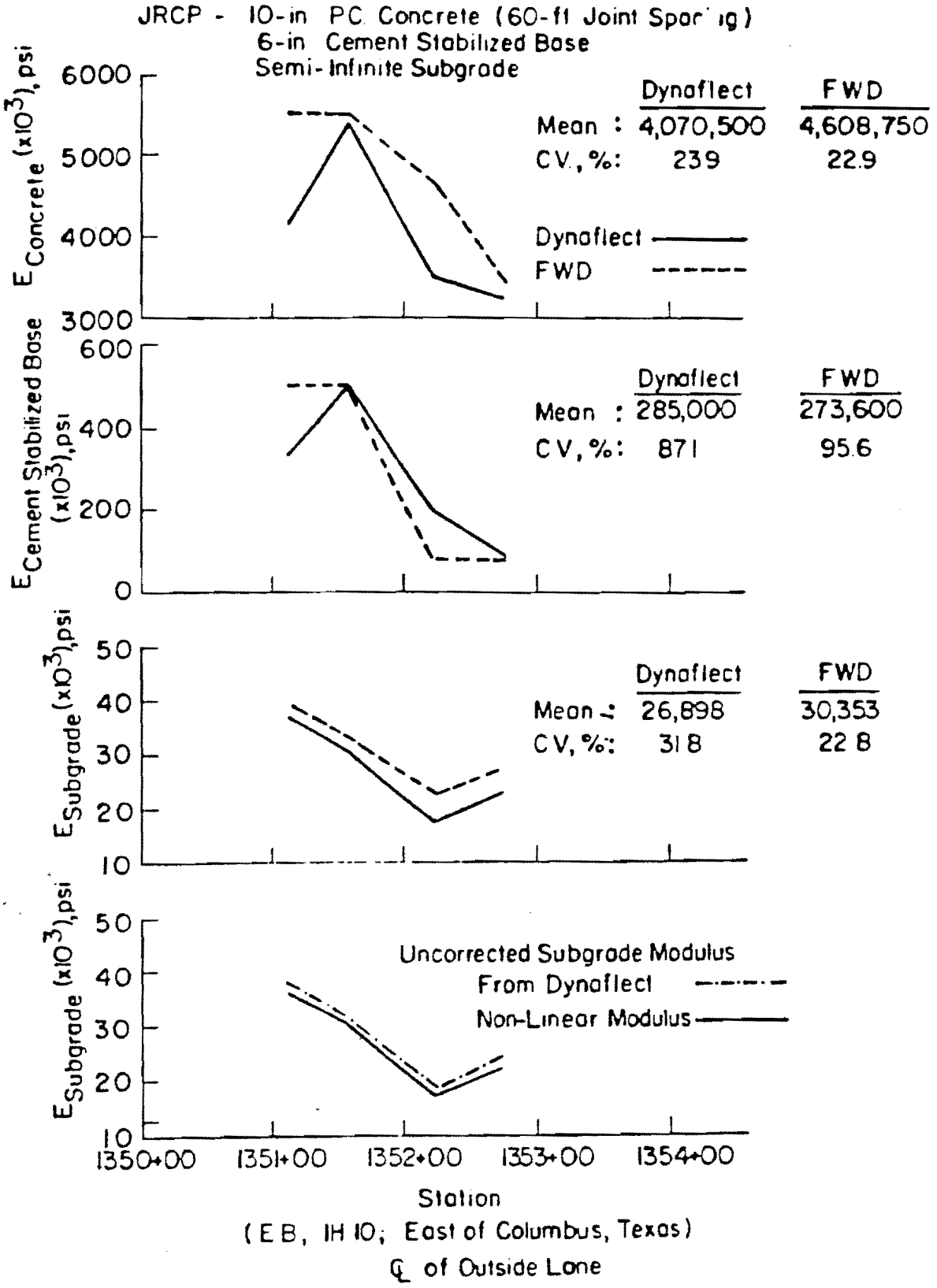

Fig F.2. Example applications of RPEDD1 on a JRC pavement.

APPENDIX G

USER'S MANUAL OF FPEDD1

APPENDIX G. USER'S MANUAL OF FPEDD1

A detailed input guide, summary formats and examples of applications are presented in this appendix.

INPUT GUIDE

Input Data

A summary of formats for input data appears in Fig G.1. Several of the input variables have built-in default values in the program. All the input variables are explained in this section. All integers (I-format) must be right justified. F-formats are for real values. Whenever default is mentioned, the user can choose not to enter any value. Input seed moduli should be entered only if the user strongly feels that these values are reliable (based on laboratory or field tests). All card types are explained in the following.

Card 1

NSYM: Total number of deflection basins to be entered for analysis (maximum of 50).

Card 2

NINE: 999 (must be entered). It is a flag to indicate the start of the next problem.

TITLE: Identification information.

KTEST: Date of test.

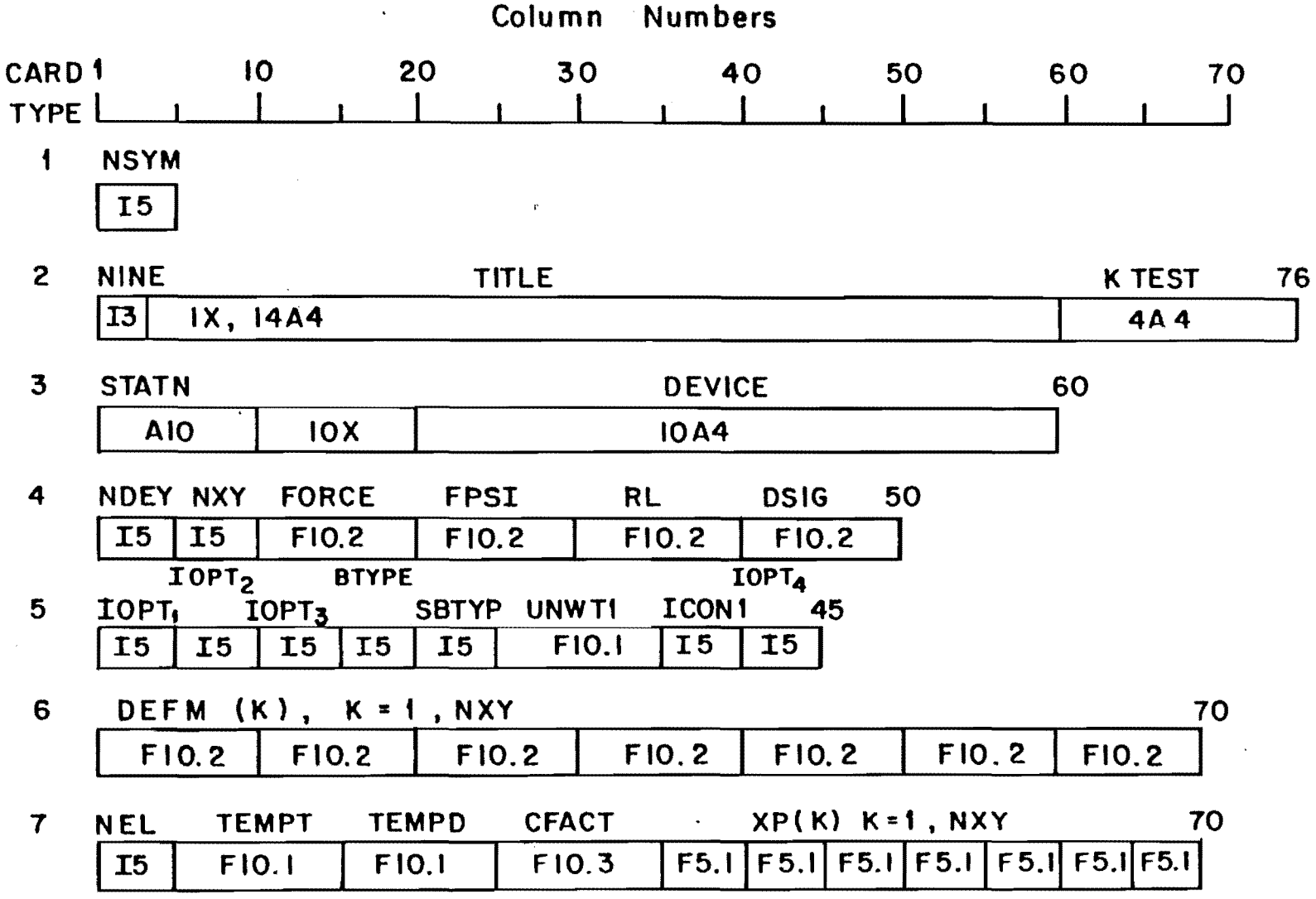

Fig G.1. Summary of formats of input data for FPEDD1.

CARD
TYPE I

8	LN(I)	TH(I)	V(I)	ESEED(I)	E MAX(I)	EMIN(I)	60
	I10	F10.2	F10.2	F10.0	F10.0	F10.0	

CARD TYPE 8 TO BE REPEATED FOR EACH LAYER (I=1,NEL)

9	MITER	TOLR1	TOLR2	TOLR 31	TOLR 32	TOLR33	55
	I5	F10.3	F10.3	F10.3	F10.3	F10.3	

10	NDAXL	DLOAD	TIREP	PTRAFF	50
	I5	F15.0	F10.1	I20	

* 11	NDLOD	DXL(1)	DYL(1)	DXL(2)	DXL(2)	NDNXY	DXP(1)	DYP(1)	DXP(2)	DYP(2)	DXP(3)	DYP(3)	66
	I3	F6.1	F6.1	F6.1	F6.1	I3	F6.1	F6.1	F6.1	F6.1	F6.1	F6.1	

* IF NDAXL ≠ 1 ; SKIP CARD TYPE 11.

(FOR THE NEXT PROBLEM ; REPEAT CARD TYPE 2 TO 11) .

Fig G.1. (continued)

Card 3

STATN: Station at which the deflection basin was measured.

DEVICE: Name of NDT device.

Card 4

NDEV: Code for NDT device (1 for Dynaflect, 2 for FWD).

NXY: Number of sensors where deflections were measured. (It should be entered only for FWD, at least 6.)

FORCE: Peak force of FWD-force signal (in lb).

FPSI: Peak stress of FWD at surface (can be left blank if FORCE and RL are entered).

RL: Radius of FWD loading plate (in inches).

DSIG: Duration of FWD force signal (default is 25 msec).

Card 5

IOPT1: Option for output of back-calculated Young's moduli (0 for summary only, 1 for detailed output).

IOPT2: 0 to skip remaining life analysis, 1 to make remaining life analysis.

IOPT3: 0 for ignoring the default procedure to create a rigid layer, 1 to activate the default procedure to create a rigid layer at a finite thickness of subgrade.

BTYPE: Type of base layer (1 for granular, 2 for stabilized).

SBTYP: Type of subbase layer (above subgrade), (0 for a three layer pavement, 1 for granular, 2 for stabilized).

UWIT1: Unit weight of subgrade soil (lb/cft). An approximate value can be used if no test data are available.

ICON1: Condition of the pavement; (0 for normal, not severely damaged; 1 for severely cracked, class 2 or 3 cracking).

IOPT4: 0 for making a complete analysis, 1 to skip equivalent linear analysis as well as remaining life analysis. (It overrides IOPT2.)

Card 6

DEFM(k): Measured deflections in mils, starting from the first sensor (not exceeding 7 sensors).

Card 7

NEL: Number of layers in the idealized pavement model including subgrade (not less than 2 and not exceeding 4; see additional discussion in the next section).

TEMPT: Test temperature of surface AC layer, °F.

TEMPD: Design temperature of AC pavement, °F (default is 70°F).

CFACT: Ratio of AC stiffness at design temperature to the stiffness at test temperature based on laboratory M vs temperature relationship. If not known, leave blank, the program will activate a default procedure to make the temperature correction.

XP(k): Radial distance of FWD sensors from the center of the loading plate, starting from the first sensor and not exceeding 7 sensors.

Card 8

(Note: Card type 8 is to be repeated for each pavement layer starting from the surface layer.) I ranges from 1 to NEL.

LN(I): Layer number (must be entered).

TH(I): Thickness in inches (must be entered, blank or zero for semi-infinite subgrade).

V(I): Poisson's ratio (must be entered; Table 4.1 can be consulted for guidance.)

ESEED(I): Initial estimate (seed value) of Young's modulus in psi. (Generally 0 should be entered here; this will ensure convergence to a unique solution.)

EMAX(I): Maximum allowable value of Young's modulus (see Table 4.5 for default values).

EMIN(I): Minimum allowable values of Young's modulus (see Table 4.5 for default values).

Card 9

(Note: All values in this card can be entered as zero or left blank.)

MITER: Maximum number of iterations for each trial (default is 10). A second trial is activated if the maximum difference is computed and measured deflections are greater than 10 percent.

TOLR1: Tolerance for individual deflections, in mils (default is 0.05 mils).

TOLR2: Tolerance for the absolute total error at all sensors in computed and measured deflections (default is 2 percent).

TOLR31: Tolerance for the modulus of the surface asphaltic concrete layer (default is 4 percent).

TOLR32: Tolerance for moduli of intermediate layers (default is 3 percent).

TOLR33: Tolerance for the subgrade modulus (default is 0.05 percent).

Card 10

NDAXL: Zero or blank for default design load as illustrated in Fig 5.19. (In this case the next card, type 11, is to be skipped.)

DLOAD: Design load per tire in lb (assuming single axle, dual tires). The default value is 4500 lb.

TIREP: Tire pressure in psi (default value is 75 psi).

PTRAFF: Cumulative past traffic in 18-kip ESAL (must be entered if remaining life is to be computed).

Card 11

NDLOD: Number of loads (e.g., 2 for the default design load simulating dual tires in Fig 5.19).

DXL(1): Position of x-coordinate for first load.

DYL(1): Position of y-coordinate for first load.

DXL(2): Position of x-coordinate for second load.

DYL(2): Position of y-coordinate for second load.

NDNXY: Number of locations where pavement response is to be calculated under the user specified design load (enter 3).

DXP(1): Position of x-coordinate of the nearest location for response.

DYP(1): Position of y-coordinate of the nearest location for response.

DXP(2): Position of x-coordinate of the intermediate location for response.

DYP(2): Position of y-coordinate of the intermediate location for response.

DXP(3): Position of x-coordinate of the farthest location for response.

DYP(3): Position of y-coordinate of the farthest location for response.

(Note: All distances in Card 11 are in inches.)

Idealized Pavement Structure

Pavements with more than four layers can be idealized by a four layered pavement as illustrated in Fig 8.1. In the case of a three layered pavement, the program generates a 6-inch layer from the subgrade but the output gives values of final moduli, only for the three originally specified values. A two layered pavement, should be converted to a three layered pavement using the following strategies.

(1) A thick AC surface (equal to or exceeding 5 inches), can be divided into two layers and the pavement becomes a three layered pavement.

BTYPE in the input must be entered as 2 in card type 5. (SBTYP should be zero.)

(2) For a thin surfacing, one 6-inch layer should be created from the subgrade and BTYPE should be assigned a value of 1. (SBTYP should be zero.

Composite Pavement

For the insitu material characterization only, experience has shown that FPEDD1 can still be successfully used, within the following constraints.

(1) The top layer should be a combined overlaid AC layer.
(2) The second layer is a PC concrete layer. An ESEED value must be assigned for this layer (say 4,000,000 psi). EMAX and EMIN must also be entered by the user.
(3) BTYPE must be assigned a value of 2.
(4) IOPT2 must be zero.

APPLICATION OF FPEDD1

An example of a partial output from FPEDD1 is presented in Table G.1. The basic form of output is similar to the output of RPEDD1. A summary detailed output of FPEDD1 is also printed in Table G.1, which also illustrates summary statistics. The results from this output have been plotted in Fig G.2. This pavement has shown signs of fatigue cracking as observed in condition surveys. Figure G.2(a) shows the remaining life profile. In Fig G.2(b), the ESG symbol is for subgrade moduli obtained after making correction for nonlinear behavior and ESG2 is the symbol for uncorrected moduli. Surface asphaltic concrete moduli are plotted in Fig G.2(c), where broken lines (E12) stand for insitu moduli at the test temperature and full lines (E1) are the estimated moduli at the design temperature of 70°F. Figures G.2(d) and (e) illustrate profiles for selected fill moduli (fill was divided into two layers). Here again broken lines are for uncorrected moduli and full lines for moduli corrected for nonlinear

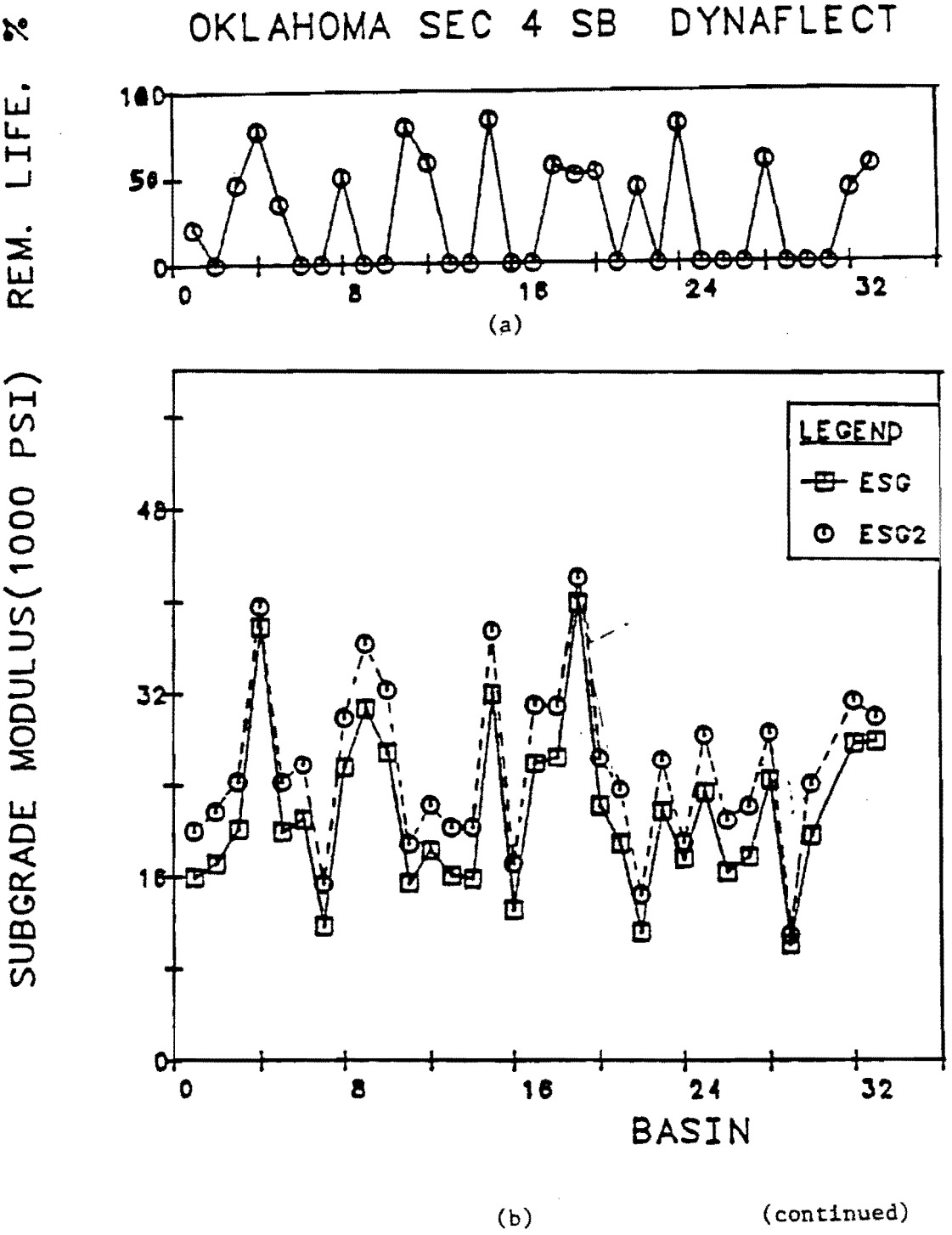

D05 47

Fig G.2. Example of plots based on the output of FPEDD1.

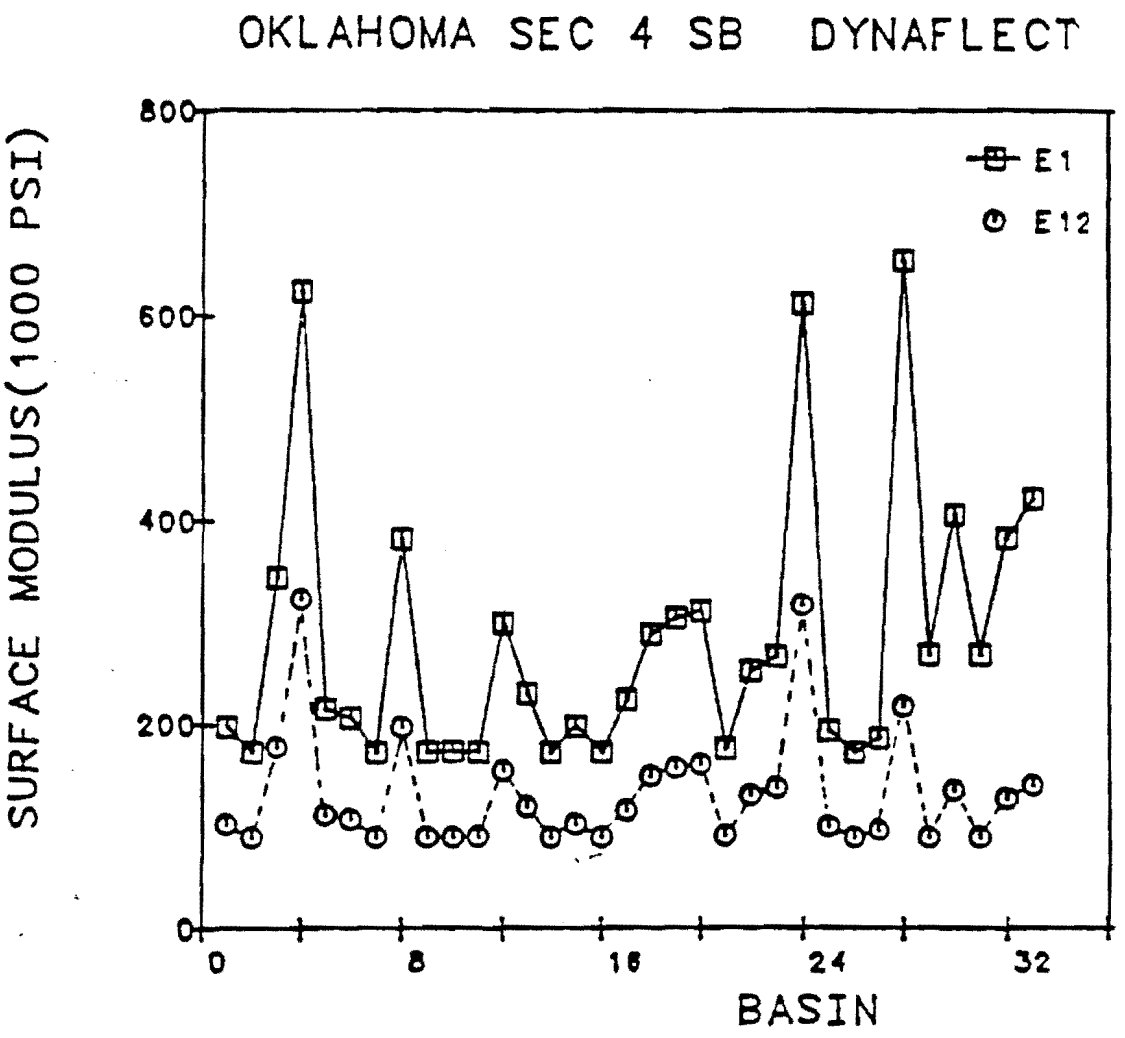

(c)

Fig G.2. (continued)

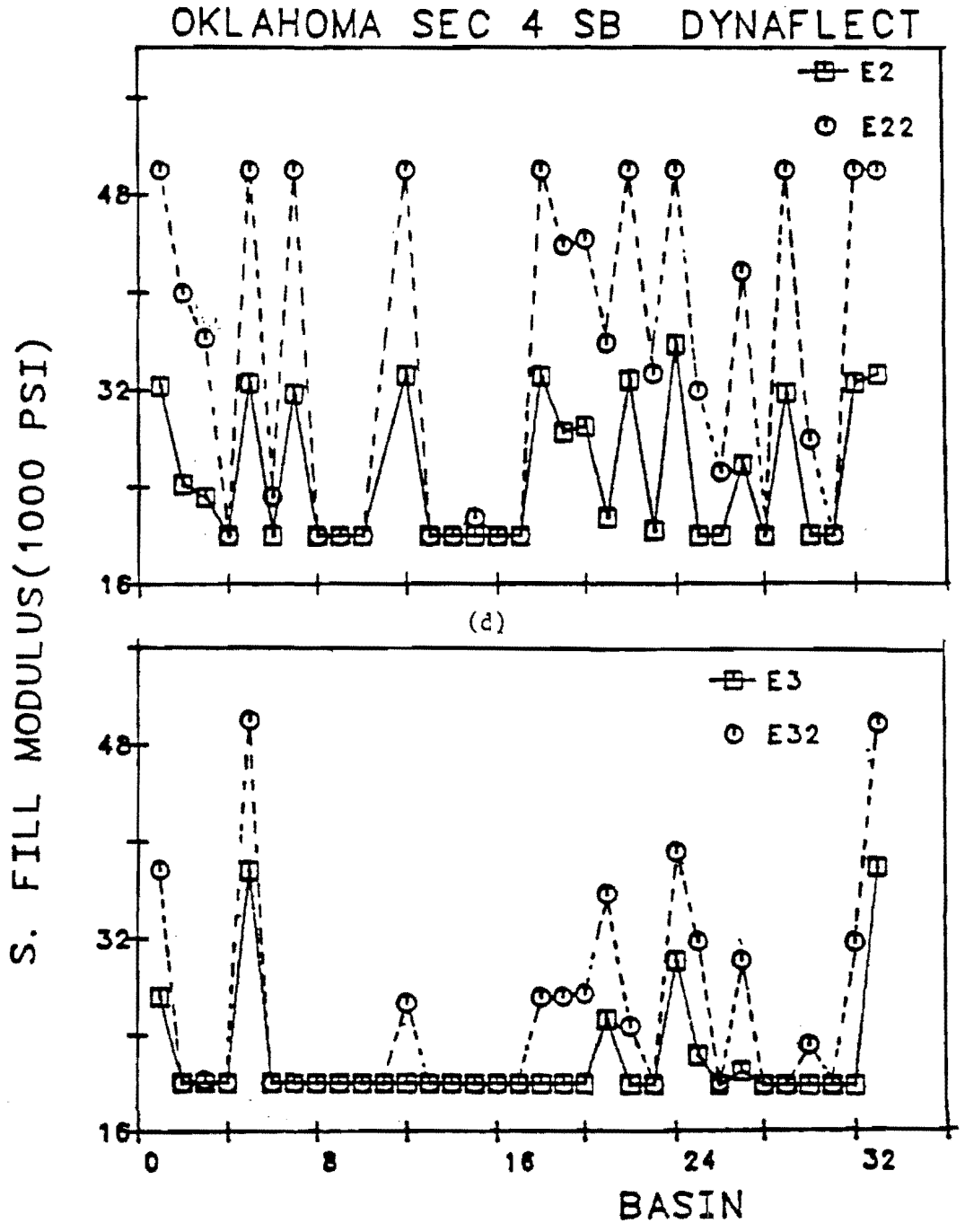

Fig G.2. (continued)

TABLE G.1. EXAMPLE OF PARTIAL OUTPUT FOR FPEDD1

```
1

     ********************************
     *                              *
     *          F P E D D 1         *
     *                              *
     ********************************

     FLEX. PAVEMENT EVALUATION PROGRAM
     PROGRAM WRITTEN BY WAHEED UDDIN
        VERSION : 1.0  APRIL 16,1984
     CENTER FOR TRANSPORTATION RESEARCH
     THE UNIVERSITY OF TEXAS AT AUSTIN


 MEASURED DEFLECTION BASIN (PROBLEM NO.  1 )

 US-69 SB (SITE 4) WP

      DYNAFLECT                STATION:                  9

     4   LAYERS SYSTEM        BTYPE =  1  (TYPE OF BASE MATERIAL    :  )

                              BBTYP =  1  (TYPE OF SUBBASE MATERIAL :  )

                                          ( 1 = GRANULAR ; 2 = STABILIZED )

                  ******** INPUT SYSTEM PARAMETERS ********


 ALLOWABLE NUMBER                                    TOLERANCES
  OF ITERATIONS        TOLR1        TOLR2        TOLR31        TOLR32        TOLR33

         8              .005       1.500         4.000         2.000         .100
                                   PERCENT       PERCENT       PERCENT       PERCENT
                  ****************************************


 LAYER NO.      THICKNESS  POISSONS            ESEED          E(MAX)          E(MIN)
                 (INCHES)   RATIO               (PSI)           (PSI)           (PSI)

    1               10.75      .35          162489.          700000.          90000.
    2               12.00      .45           58300.          90000.           20000.
    3               12.00      .45           50300.          70000.           20000.
    4                          .45           16387.          70000.           10000.

      UNIT WEIGHT OF SUBGRADE SOIL     115.0LBS. PER CU. FT.
      ************************************************


         SENSOR NO.              1      2      3      4      5

     MEASURED DEFLECTIONS
              (MILS)           .800   .640   .510   .350   .270

    CALCULATED DEFLECTIONS
              (MILS)           .794   .655   .499   .395   .322
```

TABLE G.1. (CONTINUED)

```
     HERRP (PERCENT)      19.10A
(BASED ON SEED MODULI VALUES)

*****                    *****
***** ITERATIONS BEGIN    *****
*****                    *****

 STOPPED - NO SIGNIFICANT DICREASE IN MAXIMUM PERCENT ERROR IN DEFLECTION

 TOTAL ITERATIONS ATTEMPTED IN THIS RUN ARE     3
    ****************************************

IOPT1 =   0 ENFORCED ; RESULT OF EACH INDIVIDUAL ITERATION IS NOT PRINTED ***


          ******* SUMMARY OF BEST ITERATION ( NO. 3 ) *******

YOUNGS MODULI(PSI)    103803.9      50189.8.     37632.5      19952.6

 MEASURED DEFLECTIONS
          (MILS)           .800    .640   .518.   .358    .278

CALCULATED DEFLECTIONS
          (MILS)           .803    .631   .460    .352    .279

     HERRP (PERCENT)       3.802

 ************************************************************************
  DESIGN SINGLE AXLE LOAD DATA                  PAVEMENT TEMPERATURE

  LOAD PER TIRE (LBS.)=      9500.)              TEST   88.0 (DEG.F)
  TIRE PRESSURE (PSI)=         75.0             DESIGN  70.0 (DEG.F)

*********EQUIVALENT LINEAR ANALYSIS FOR CORRECTION OF YOUNGS MODULI*********

    **** GRANULAR BASE LAYER MODULUS CORRECTED FOR NON LINEAR BEHAVIOUR ****

    **** GRANULAR SUB BASE MODULUS CORRECTED FOR NON LINEAR BEHAVIOUR ****

    **** SUBGRADE (NATURAL SOIL) MODULUS CORRECTED FOR NON LINEAR BEHAVIOUR ****

       CORRECTED VALUES OF YOUNGS MODULI (PSI)
            19303.       32342.       27133.       15899.


    **** TEMPERATURE CORRECTION APPLIED TO ASPHALT CONCRETE MODULUS ****
    **** THE CORRECTED MODULI (PSI)  ARE : ****

            198597.      32342.       27133.       15899.

    ***** REMAINING LIFE :  25.8 % *****
```

005 45

TABLE G.1. (CONTINUED)

•••••••••••••••••••••••• SUMMARY OF STRUCTURAL EVALUATION ••••••••••••••••••••••••

STATION	DEF.MAX.H. (MILS)	STRAIN DEV. IN./IN.	STRESS (PSI)	R.STRESS (PSI)	CUM.TRAFFIC	MAX.AXLES APP.	REM. LIFE PERCENT	FINAL VALUES OF YOUNGS MODULI(PSI)			
1	0 13.8	.184E-03	-.229E+01	-.811E+01	1366560	1821899	25.0	198600.	32300.	27100.	15900.
2	20 15.4	.231E-03	-.261E+01	-.828E+01	1366560	568830	0	173500.	24200.	20000.	17100.
3	40 11.3	.166E-03	-.249E+01	-.712E+01	1366560	3108395	56.0	344300.	23100.	20000.	27100.
4	60 7.4	.117E-03	-.285E+01	-.729E+01	1366560	19113697	92.9	624700.	23000.	23000.	37800.
5	80 12.0	.175E-03	-.246E+01	-.986E+01	1366560	2371811	42.4	215800.	32600.	37800.	19900.
6	100 14.0	.231E-03	-.286E+01	-.894E+01	1366560	559131	0	207200.	20000.	20000.	21300.
7	120 16.7	.198E-03	-.233E+01	-.640E+01	1366560	1247314	0	173500.	31700.	23000.	11700.
8	140 13.3	.162E-03	-.275E+01	-.779E+01	1366560	3476030	63.7	382700.	20000.	20000.	25600.
9	160 13.7	.252E-03	-.336E+01	-.999E+01	1366560	357521	0	173500.	20000.	20000.	30700.
10	180 14.1	.252E-03	-.321E+01	-.978E+01	1366560	358236	0	174000.	23000.	20000.	26900.
11	200 13.3	.199E-03	-.235E+01	-.339E+01	1366560	26751064	94.9	173500.	70000.	20000.	15400.
12	220 11.5	.154E-03	-.227E+01	-.574E+01	1366560	9567191	78.1	299800.	33230.	20000.	18300.
13	240 14.6	.221E-03	-.231E+01	-.819E+01	1366560	734632	0	231000.	20000.	20000.	16100.
14	260 16.4	.254E-03	-.263E+01	-.898E+01	1366560	348318	0	173500.	20000.	20000.	15800.
15	280 9.8	.595E-04	-.232E+01	-.426E+01	1366560	618936896	99.8	103112.	21800.	20000.	32129.
16	300 17.4	.254E-03	-.292E+01	-.855E+01	1366560	345584	0	173500.	20000.	20000.	13100.
17	320 12.7	.221E-03	-.335E+01	-.910E+01	1366560	710663	0	225100.	20000.	20000.	26700.
18	340 11.3	.156E-03	-.271E+01	-.658E+01	1366560	4239412	67.8	289007.	33130.	20070.	24500.
19	360 9.3	.162E-03	-.322E+01	-.782E+01	1366560	3546579	61.5	305000.	28500.	20000.	97500.
20	380 10.9	.160E-03	-.254E+01	-.665E+01	1366560	3730328	63.4	311700.	29000.	20000.	22200.
21	400 14.8	.241E-03	-.276E+01	-.997E+01	1366560	458132	0	176600.	21500.	25400.	18900.
22	420 14.9	.168E-03	-.197E+01	-.520E+01	1366560	2899804	52.8	252800.	32800.	20000.	11187.
23	460 12.4	.200E-03	-.276E+01	-.830E+01	1366560	1183032	0	267100.	20430.	23020.	21700.
24	480 8.8	.101E-03	-.186E+01	-.561E+01	1366568	40575094	96.6	612400.	35780.	30380.	17600.
25	500 13.7	.237E-03	-.299E+01	-.976E+01	1366560	490349	0	195000.	20000.	22400.	23400.
26	540 16.2	.254E-03	-.267E+01	-.896E+01	1366560	34,095	0	173500.	20000.	20030.	16400.
27	560 14.5	.215E-03	-.257E+01	-.815E+01	1366560	810445	0	187200.	25809.	21100.	17780.
28	580 10.0	.153E-03	-.265E+01	-.748E+01	1366560	4752422	71.2	654700.	20000.	20000.	24500.
29	600 17.8	.198E-03	-.193E+01	-.610E+01	1366560	1251476	0	268000.	31700.	20000.	10000.
30	620 13.0	.204E-03	-.267E+01	-.824E+01	1366560	1069415	0	405700.	20000.	20000.	19600.
31	640 11.9	.252E-03	-.419E+01	-.109E+02	1366560	363798	0	268000.	21800.	23020.	67400.
32	660 10.9	.169E-03	-.283E+01	-.787E+01	1366560	2810998	51.4	382600.	32500.	20000.	27700.
33	680 9.8	.156E-03	-.271E+01	-.978E+01	1366560	4257798	67.9	420900.	33230.	30180.	27900.
						• MEAN :	32.6	297436.	26959.	21883.	23257.
						STD DEV :	36.9	151894.9	9880.0	4732.6	11171.7
						C VE R :	113.4	51.1	36.6	21.6	48.0

•••• PLEASE RECALCULATE SUMMARY STATISTICS FOR REMAINING LIFE IF 999.0 APPEARS IN THE OUTPUT ••••

FLEX, PAVEMENT EVALUATION PROGRAM
PROGRAM WRITTEN BY WAHEED UDDIN
VERSION : 1.0 APRIL 16,1989
CENTER FOR TRANSPORTATION RESEARCH
THE UNIVERSITY OF TEXAS AT AUSTIN

behavior. This pavement has a combined thickness of 10.75 inches of asphaltic material, 24.0 inches of selected fill (divided into two layers of 12 inches), and semi-infinite subgrade.

APPENDIX H

DESCRIPTION OF FTEMP,
FLEXIBLE PAVEMENT TEMPERATURE PREDICTION PROGRAM

APPENDIX H. DESCRIPTION OF FTEMP

The FTEMP computer program can be used to predict temperatures within an asphaltic concrete pavement. The program was originally written by Shahin and McCullough (Ref 68). It is based on the prediction of temperatures in a 24-hour cycle using climatological data. The same program has been adapted here to predict the test temperature of AC surfacing. The theoretical background and other details are presented elsewhere (7, 62, 68). Formats for input data are shown in Fig H.1, which also illustrates the needed information. The program predicts temperature at the surface, mid-depth, and bottom. The average of these three computed temperatures is printed in output as the estimated test temperature.

A listing of the FORTRAN source of FTEMP is also included in this appendix.

NTOT

15	One Card

NTOT = Total number of problems (maximum of 5 problems)

FOR EACH PROBLEM

NPROB

15	5 x	5 A 10	One Card

NPROB = Problem number for identification

TITLE(I) = Date and Location (I = 1 to NTOT).

TA	TR	One Card
F10.3	F10.3	

TA = Average air temperature (°F): (From weather record)

TR = Daily temperature range (°F): (From weather record)

V	W	S	AK	B	AL	X	
F10.3	F10.3	F10.3	F10.3	F10.3	F10.3	F10.3	One Card

V = Wind speed (mph): (From weather record)

W = Mix density (lb/cu.ft):

S = Specific heat (BTU/lg/°F):

AK = Thermal conductivity (BTU/sq. ft./hour/°F/ft):

B = Absorptivity:

AL = Solar radiation (Langley's/day): (From weather record)

X = Depth (inches): (Equal to thickness of asphaltic concrete layer)

Fig H.1. Input guide.